REFERENCE ONLY

CONTROL OF SOUNDNESS AND MECHANICAL PROPERTIES IN ALUMINIUM-SILICON-MAGNESIUM ALLOYS

by

D. S. EDWARDS, B.Sc.(Hons.), M.Sc., A.I.M.

Thesis submitted to the University of Aston in Birmingham in part fulfilment of the requirements for the degree of Doctor of Philosophy

June 1973

SYNOPSIS

Previously, specifications for mechanical properties of casting alloys were based on separately cast test bars. This practice provided consistently reproducible results; thus, any change in conditions was reflected in changes in the mechanical properties of the test coupons. These test specimens, however, did not necessarily reflect the actual mechanical properties of the castings they were supposed to represent[1]. Factors such as section thickness and casting configuration affect the solidification rate and soundness of the casting thereby raising or lowering its mechanical properties in comparison with separately cast test specimens.

In the work now reported, casting shapes were developed to investigate the variations of section thickness, chemical analysis and heat treatment on the mechanical properties of a high strength Aluminium alloy under varying chilling conditions. In addition, an insight was sought into the behaviour of chills under more practical conditions. Finally, it was demonstrated that additional information could be derived from the radiographs which form an essential part of the quality control of premium quality castings.

As a result of the work, it is now possible to select analysis and chilling conditions to optimize the as cast and the heat treated mechanical properties of Aluminum 7% Silicon 0.3% Magnesium alloy.

AIM OF THE INTERDISCIPLINARY HIGHER DEGREE SCHEME

The scheme formed in 1968, is a new venture in postgraduate education. It enables those students, who are qualified to carry out research work but who do not wish to become highly specialized, to tackle problems encountered within an industrial or commercial sphere. With the collaboration of his Sponsoring Organization the student can attempt to solve a particular problem in its industrial context and at the same time gather experience and confidence essential for a career in industry. This plan, therefore, broadens the concept of traditional higher degree studies which tend to restrict the holder to academic or research interests.

THESIS LAYOUT

The research project was carried out to determine the effects that directional solidification, produced by different chilling techniques, have upon the soundness and mechanical properties of Aluminium 7% Silicon 0.3% Magnesium alloy.

The Thesis is divided into the following major sections:

(1) A Literature Survey which includes the state of the art in the U.S.A. regarding the production of premium quality castings.

(2) Experimental details defining the lines of investigation adopted and from the results the reasons why particular variables were either introduced to or deleted from the final experimental plan.

(3) A feasibility study of additional information derived from X-ray radiographs which form an important part of the quality control of premium quality castings.

(4) An extension to the understanding of chill behaviour by investigating various chill shapes using quantitative thermal measurements.

CONTENTS

1. INTRODUCTION

The term premium quality castings refers not only to the improved internal quality of a particular casting but also to describe castings with resultant higher mechanical properties reliably reproduced in designated areas of each casting produced from a given pattern and confidently guaranteed by the foundry.

Generally, it is accepted that Aluminium alloys are characterised by relatively low strength and ductility compared to similar alloys in wrought conditions. The low strength and ductility are associated with defects present in the cast alloy. These defects fall into two categories; voids due to shrinkage or gas inclusions and large particles of intermetallic phases formed from impurity elements or oxide inclusions trapped in the casting and manifesting themselves in greatly reduced mechanical properties.

As a result many factors have been considered as essential in the production of premium quality castings[2]. They include:-

(a) higher purity metals and closer alloy composition limits,

(b) stricter quality control of each melting, casting and heat treating stage,

(c) determination of proper mould designs to produce the optimum solidification rates in the designated areas of the casting configuration,

(d) careful evaluation of the properties of the castings.

The major influence for this change to the concept of premium quality castings was the insistence by designers and engineers on castings with guaranteed quality. Previously, if castings were used as mechanically stressed components a casting safety factor had to be employed which jeopardised its chances when strength-to-weight ratios were the primary consideration. The inability of foundries to produce castings of guaranteed quality forced the designers to utilise forgings and fabrications produced from wrought products. The repercussions were considerable; cost and time penalties were accrued due to additional machining and joining operations involved and in many instances increased weight was also incurred.

In the U.S.A. the reluctance of the foundry industry to change its basic philosophy of quantity production to guaranteed casting properties prevented a rapid development of the idea. However, adoption of scientific improvements became a necessity for the financial survival of the foundry industry, although some industries still showed a certain hesitancy in employing skilled personnel for the production of a few high integrity castings.

As a result of increasing interest in premium quality castings in the United Kingdom, foundries are beginning to realise the inevitability of producing guaranteed quality. The present work is concerned with the investigation into foundry factors which could produce improvements in the mechanical properties of Aluminium - Silicon - Magnesium castings in accordance with Specification D.T.D. 5028. (This has now been superseded by B.S.S. 2L99). The work is part of a broader exercise being carried out at Sterling Metals Ltd., Nuneaton, in advance of the expected demand for high integrity castings. The aim of the project is to quantify the factors affecting mechanical properties within castings. On a more fundamental basis it is hoped that an extension to our knowledge of heat flow and solidification under critical casting conditions will also result.

2. LITERATURE REVIEW

2.1 Physical Metallurgy

Alloys rarely reach the ideal state of equilibrium. Non-equilibrium or metastable structures result from the inability of metallurgical processes such as nucleation and growth to achieve completion in the time permitted. Equilibrium phase diagrams can, however, be utilised to predict metastable structures and their characteristics.

Rates of diffusion in the solid state are considerably lower than in the liquid state. Thus equilibrium phase boundaries such as liquidus, secondary and solidus boundaries may be displaced by varying degrees, depending upon the rate of solidification encountered, resulting in non-equilibrium solid structures. These structures may include cored solid solutions and intermetallic compounds not transformed or only partially transformed by a peritectic reaction. In Aluminium alloy castings metastable conditions may be equilibrated by heating slightly below the solidus temperature for periods ranging from hours to months. Dislocations produced during cold working encourage nucleation and diffusion thereby decreasing the time to approach equilibrium. Equilibrium may be more rapidly approached with increase in the amount of cold work and elevation of the temperature. Use of lower temperatures may result in several cycles of cold working and reheating being necessary to achieve near equilibrium structures.

The equilibrium condition is not always desirable and the metastable characteristics may be those that are preferred.

Finally, it must be borne in mind that constituent diagrams may differ from equilibrium phase diagrams not only in the displacement and distortion of phase boundaries but also in the forms and composition of the constituents.

2.1.1. General Survey of Commercial Aluminium-Silicon-Magnesium Alloys[3]

CEH, the binary valley, separating the primary Aluminium and Mg_2Si fields reaches a ridged maximum at 595°C, point "E" in Figure 1. This maximum appears to coincide with the intersection of the quasi-binary section AEK. The composition of the Aluminium, Silicon and Mg_2Si ternary eutectic at point "C" has been determined and is given in Table I. The ternary of Aluminium, Mg_2Si and Mg_2Al_3 is also given together with the quasi-binary analysis.

In the alloys lying in the area LCB, the secondary separation is that of the Aluminium-Silicon binary eutectic. LC is linear and corresponds to the position where the secondary surface meets the ternary eutectic plane. In the region LCEHJ, Figure 1, the secondary separation is that of the Aluminium, Mg_2Si binary. This secondary surface

TABLE I.—*Invariant Points of the Liquidus and Solidus Surfaces*[4].

Description	Solid phases present	Temp. °C	Composition of participating Liquid		Al-rich solid	
			Mg%	Si%	Mg%	Si%
Quasi-binary eutectic	Al, Mg_2Si	595	8.15	4.75	1.13	0.67
Ternary eutectic	Al, Mg_2Si, Si	555	4.97	12.95	0.85	1.10
Ternary eutectic	Al, Mg_2Si, Mg_2Al_3	451	33.20	0.37	15.30	0.10

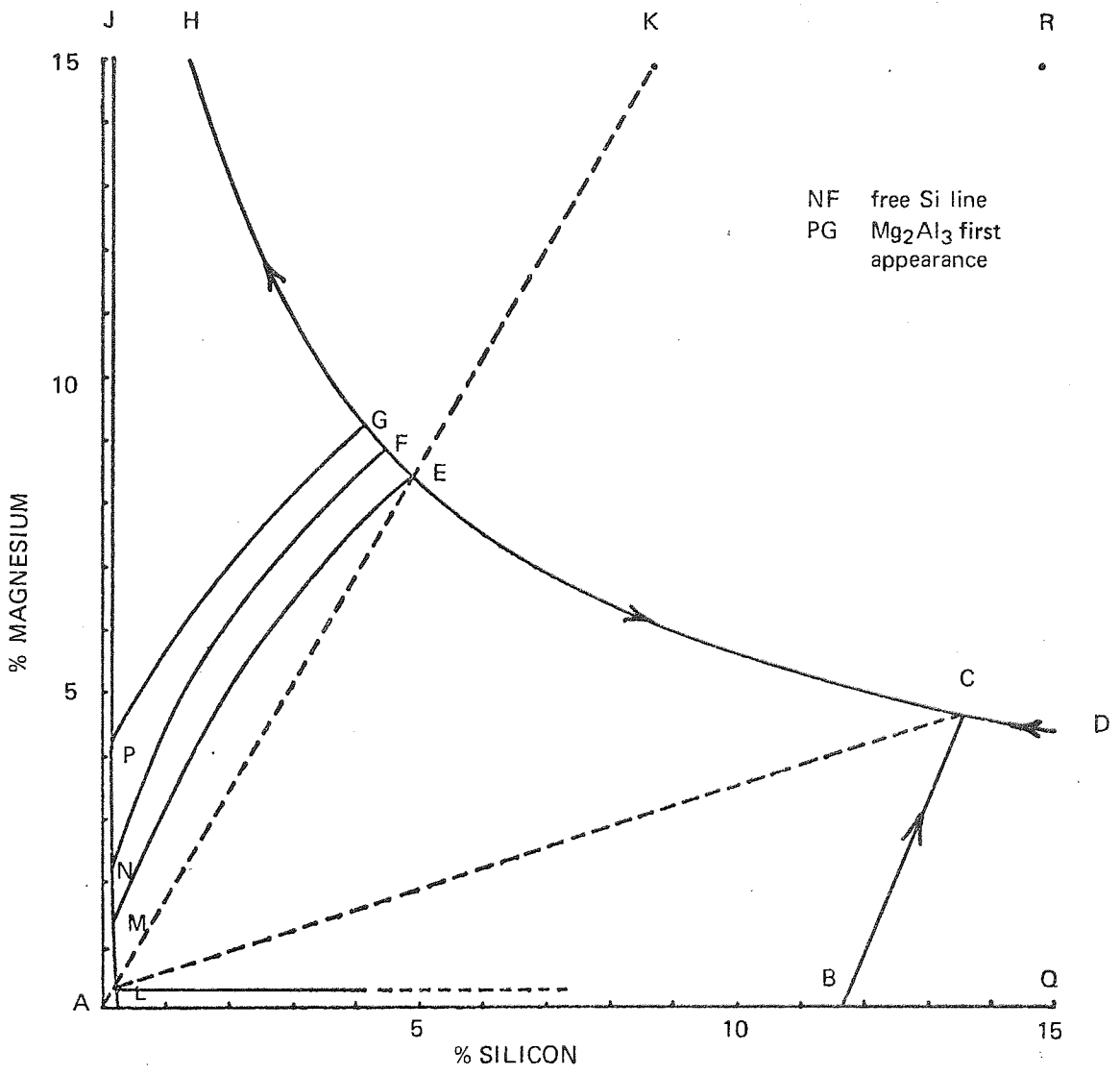

Figure 1.—*General Survey of the Commercial End of the Aluminium - Silicon - Magnesium system*[3].

is also ridge shaped with a maximum ME at 595°C; it does not coincide with the quasi-binary nor is it straight. This curvature in ME indicates that the primary Aluminium takes increasing quantities of Magnesium into solid solution as solidification proceeds. In equilibrium this ridge of maximum temperatures coincides with the quasi-binary line.

In the region BLNFC the solidus coincides with the separation of the ternary eutectic Aluminium, Mg_2Si and Silicon, in the region PGHJ it coincides with that of the ternary eutectic Aluminium, Mg_2Si and Mg_2Al_3.

The primary phase fields are simply: for Aluminium ABCEHJ, Silicon BCDQ and Mg_2Si DCEHR.

In sand cast binary alloys of Aluminium and Magnesium failure of the Aluminium-rich solid solution to absorb sufficient Magnesium results in coring and the appearance, prematurely, of Mg_2Al_3. This appearance of Mg_2Al_3 can occur in alloys with Magnesium contents as low as 3 - 4% Magnesium compared to 15.35% at equilibrium. In ternary alloys the same thing occurs with Magnesium contents larger than those required to form Mg_2Si.

The appearance of free Silicon in the alloys on the Magnesium side of the quasi-binary line AEK indicates that the supposedly balanced reaction between Magnesium and Silicon has not proceeded to completion. Magnesium is preferentially taken into solid solution thus reducing the amount available for chemical reaction. The first appearance line of Silicon, NF, is curved and merges with the quasi-binary line at approximately 9.0% Magnesium.

Under conditions of slow cooling Aluminium is incapable of dissolving more than 0.2% Silicon and 4.25% Magnesium in the solid state. The solid solubility for Mg_2Si is very small, since the addition of 0.1% Mg to Aluminium/Silicon alloys or 0.1% Si to Aluminium/Magnesium alloys is sufficient to produce precipitation of Mg_2Si.

Failure to reach equilibrium during casting results in much lower solidus temperatures than expected. When Silicon is in excess, solidification does not cease until the ternary eutectic temperature of 555°C is reached; with Magnesium in excess, Mg_2Al_3 occurs and this separates out at the ternary eutectic temperature of 451°C. In the quasi-binary alloy non-equilibrium conditions can lead to solidification at 555°C instead of 595°C. Heat treatment may be used to attain equilibrium; the metastable Mg_2Al_3 and excess Silicon disappear, consequently the solidus rises and removes the possibility of hot shortness.

2.1.2 *The Effect of Iron as an Impurity*

In the ternary system Aluminium - Silicon - Magnesium the series of alloys in which the atomic ratio of Magnesium to Silicon is 2 : 1 is quasi-binary. A similar situation is found in the quaternary system where here the system Aluminium - Mg_2Si – $FeAl_3$ is quasi-ternary. Under equilibrium conditions on the Magnesium side of the quasi-ternary plane the alloys form a sub-system in which the components are Aluminium, Mg_2Si, $FeAl_3$ and Mg_2Al_3. No others occur in this region. On the other side of the quasi-ternary the structures are more complex and Aluminium, Mg_2Si, Si, $FeAl_3$, α, β and π may be found.

In fact on the Magnesium side, with excess Magnesium to form Mg_2Si, Iron should occur as $FeAl_3$, but this is not the case until the alloy lies above the Mg_2Al_3 line. Below this line the complex constituents α (FeSi) and β (FeSi) separate during solidification and are unaffected by heat treatment. They are not converted to $FeAl_3$ with liberation of free Silicon and thence formation of Mg_2Si. On the Silicon side: α and β are equilibrium constituents and undergo a peritectic reaction to form the quaternary π based on the formula $Al_8\ Mg_3\ Si_6\ Fe$. Peritectic reactions are sluggish so all three constituents are detected in microstructure.

Of the three forms of Iron in the Aluminium - Silicon - Magnesium alloys, β is the most harmful as it tends to crystallize in thin platelets or needles, forming localised planes of weakness. The α body, formation of which is favoured when Manganese impurities are present, occurs in globular or script form while π tends to occur in dendrites similar in habit to Mg_2Si. The latter two constituents are tougher than β and have less pronounced cleavage.

2.1.3 *Heat Treatment of Aluminium Alloys*

The main purpose for heat treating alloys is to change the form and distribution of the soluble elements present. The control of solution treatment and precipitation of these soluble elements can improve mechanical properties considerably. Whether an alloy lends itself to heat treatment depends upon the solid state relationships of the element species present. The most important factor is the variation in solid solubility of elements with temperature. Considerable use has been made of equilibrium diagrams as they reveal the general directions to which solid state reactions should proceed at a given composition, temperature and structure. They do not, however, show the actual structures formed at low temperatures and the reasons for hardening,

Equilibrium diagrams are therefore useful in the formulation of a satisfactory thermal processing cycle.

A major fundamental factor not provided by equilibrium diagrams is the influence of heat treatment on kinetics. Equilibrium diagrams may show whether a particular element will dissolve or precipitate at a particular temperature, but not the diffusion rate of an element through the Aluminium solid solution at that temperature which may be so slow as to suppress the reaction. Specific reaction rates also depend upon alloying species, solute concentration, energy changes and nucleation rate.

In the Aluminium alloys there are wide variations in holding times and temperatures caused by differences in the solid solubility/temperature relationships and diffusion rates of the individual solutes. Aluminium alloys may contain elements that possess solubility and precipitation characteristics for precipitation at high temperatures as well as those elements characterised by low temperature precipitation trends. As a result a high heat treatment temperature may produce precipitation of Chromium or Manganese and simultaneously take Copper, Magnesium, Silicon and Zinc into solid solution.

Complex intermetallic phases containing two or more soluble elements, in addition to Aluminium, may be precipitated and may be forecasted from the relevant ternary or quaternary equilibrium diagram. To obtain specific mechanical properties precise combinations of temperature and time are required for heat treatment operations.

2.1.4 Hardening Mechanisms in Aluminium-Silicon-Magnesium Alloys[5]

This system includes a quasi-binary eutectic (Figure 2) between Aluminium solid solution and the intermetallic compound Mg_2Si. The solubility of Mg_2Si decreases from 1.85% at the eutectic temperature to 0.1% at room temperature and thus alloys with more than 0.6% Mg_2Si show extensive precipitation hardening. Figure 2 illustrates the two conditions where the fundamental solution-precipitation relationship exists. The diagram indicates that holding the alloy with 0.47% Mg_2Si (equivalent to alloy A356) at approximately 540°C for a sufficient period of time results in the Mg_2Si going totally into solution. This stage is referred to as solution heat-treating. When the temperature falls to the region of 450°C the solid solution becomes supersaturated and that solute in excess of the equilibrium amount retainable in the solid solution precipitates out. The driving force for precipitation increases with the degree of supersaturation which is promoted by decrease in temperature but the rate of precipitation relies upon atom mobility and this decreases with falling temperature.

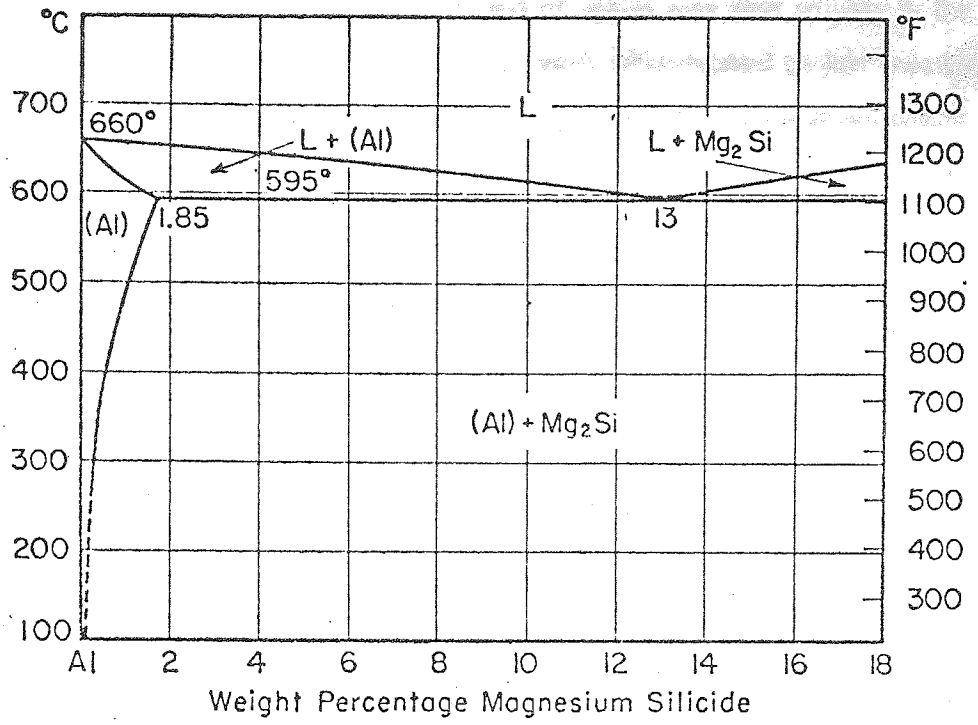

Figure 2.—*Quasi-Binary Section Aluminium - Mg_2Si*[6].

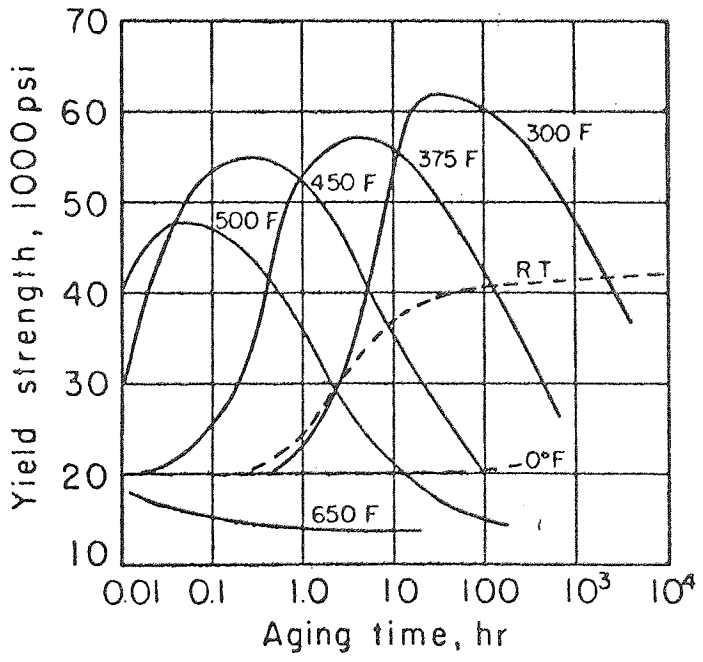

Figure 3.—*Characteristic Aging Curves for an Aluminium/Copper Alloy*[5].

The alloy containing 3% Mg_2Si has an excess of solute over that soluble in the solvent even at the eutectic temperature and as a result when heated to just below the eutectic temperature, the alloy contains undissolved Mg_2Si. The undissolved solute remains unchanged during a cycle of heating and cooling but it does contribute to the overall strength of the alloy.

Quenching the saturated solutions from high temperature retains the solute in a supersaturated state by preventing precipitation at intermediate temperatures. Heat treatment of these quenched alloys has pronounced effects on their mechanical properties attributable to controlled precipitation. (Figure 3).

Considerable strengthening occurs with prolonged natural aging and it is assumed to be due to the formation of zones although none have been positively identified. Electron microscopy has detected definite subgrain structures but no general precipitate is detected until maximum strength at aging temperatures of 320°C - 340°C.

After short aging times at temperatures up to 200°C, the X-ray and electron diffraction patterns indicate the presence of very fine needle shaped zones orientated to the <001> direction of the matrix. Continued aging causes the needle or stringlet to grow laterally to produce a platelet with its maximum dimension being no greater than 100 Å. Electron microscopy indicates the zones to be approximately 60 Å in diameter and 200 Å to 1000 Å in length. It has been suggested[7] that the zones are initially spherical and transform to a needle shape near the maximum strength positions on the aging curves. Further aging causes three dimensional development of the zones to rod-shaped particles with structures corresponding to a highly ordered Mg_2Si. At higher temperatures this transition phase, designated β', undergoes a diffusionless transformation to the equilibrium Mg_2Si. There has been no direct evidence of coherency strain in either zone or transition precipitate stage and the increased resistance to mobile dislocations in these structures is attributed to the increased energy required to sever the Magnesium - Silicon bonds.

The precipitation sequence may be expressed as:
.... supersaturated solid solution - Guinier-Preston Zones $\{100\}_{AL}$ - β' (Mg_2Si) - β (Mg_2Si).

The excess Silicon, above that required to form Mg_2Si, is precipitated as a separate phase in the early states of aging within the grain boundaries. The Magnesium in excess reduces the solubility of Mg_2Si in the Aluminium thereby impairing the hardening characteristics of the alloys.

2.2 Foundry Practice

Production of high quality castings requires great care in melting and foundry practice albeit with conventional equipment and manufacturing techniques[2]. Any practice must ensure that:-

(a) During melting, impurities are not included in the melt and chemical analysis remains within specified limits;

(b) After melting the metal is free from inclusions and dissolved gases which will cause porosity;

(c) Grain refinement is promoted.

2.2.1 Melting Practice

Before melting can be satisfactorily carried out control must be exercised over the raw materials entering the melting furnace[8]. Control covers the storage, identification and chemical analysis of the materials to be melted. Initially, ingots should be stored in a manner that prevents them suffering excessive corrosion, due to weathering, which leads to oxide andHydrogen pick-up.

To ensure reliable analysis control over melts no raw ingots should be employed until chemical analyses have been verified. Suitable samples should also be taken before the melt is finally cast[9]. Lack of control over recirculated scrap can raise considerable problems of gas pick-up. This is illustrated in Table II. Many investigators have considered the implications of variation in chemical composition[8,11,12,13,14], however, all agree the most important element to be controlled is Iron and consequently melting, where possible, must be performed in silicon carbide crucibles. Skimming tools, for dross removal, should also be thoroughly coated with a refractory wash of clay, lime or alumina.

2.2.2 Degassing and Fluxing

During the melting sequence Aluminium tends to absorb gases forming oxides, nitrides and other intermetallic compounds all of which are detrimental to the mechanical properties and soundness of the final casting.

Of the gases absorbed Hydrogen is the most troublesome. Figure 4 indicates the increase of Hydrogen dissolution in molten Aluminium. On cooling and solidification there is a rapid rejection of the Hydrogen resulting in porosity within the casting. The voids produced by Hydrogen evolution reduce the effective cross section of the casting, hence reducing its load bearing ability. Thus, if one wishes to produce castings of a premium quality, attention must be paid to processes which reduce Hydrogen absorption during melting and remove it before solidification.

TABLE II.—*Effect of Charge components on Hydrogen content of an Aluminium/ Copper alloy showing three levels of Hydrogen contents originating from different types of scrap charges*[10].

Charge Components	No. of Tests	Density Determinations (Vacuum Density Test) 2-5mm	50mm	Hydrogen Content Ml/100gms
Primary Ingot and Alloy	1	2.5	2.6	0.28
½ R.S.I.* and ½ Ingot butt end scrap	3	2.3	2.5	0.30
*Remelted Secondary Ingot	9	2.3	2.4	0.34
R.S.I.* and chips	12	2.2	2.4	0.32
Chips into molten heel	2	2.3	2.5	0.32
1/3 Oily tube scrap to heel	3	2.1	2.4	0.35
2/3 Oily tube scrap to heel	2	2.3	2.4	0.32
1/3 Bailed lacquered foil scrap to heel	4	2.2	2.2	0.48

The main sources of Hydrogen[15] are:-

(1) Steam from combustion,

(2) Atmospheric moisture,

(3) Gas included in the ingots,

(4) Moisture on tools, ingots and refractories.

Many of these sources may be reduced to a minimum by ensuring proper furnace control[8] and preheating of ingots, scrap, crucibles and tools. Chemical composition may be related to gas absorption since alloys with higher Magnesium contents tend to absorb more Hydrogen[16].

Many techniques have been established for removing Hydrogen from molten Aluminium alloys, they include:-

(a) the introduction of inert gases into the melt such as Nitrogen and Chlorine;

(b) vacuum degassing[17,18];

(c) the addition of decomposable solid degassers;

(d) vibration[15].

The techniques[8,15,16,19,20,21] most commonly practiced in foundries fall into the first and third categories, namely the use of pure dry Nitrogen or Chlorine (and in some cases a mixture of the two) and solid degassers containing Chlorine compounds.

The mechanism of Chlorine and Chlorine-containing solid degassers is such that, as well as removing the gas from the melt, the melt is flushed of suspended oxides and dross. This is in contrast to the plain mechanical action of Nitrogen on the melt which proves less effective. Chlorine reacts with Magnesium within the melt to

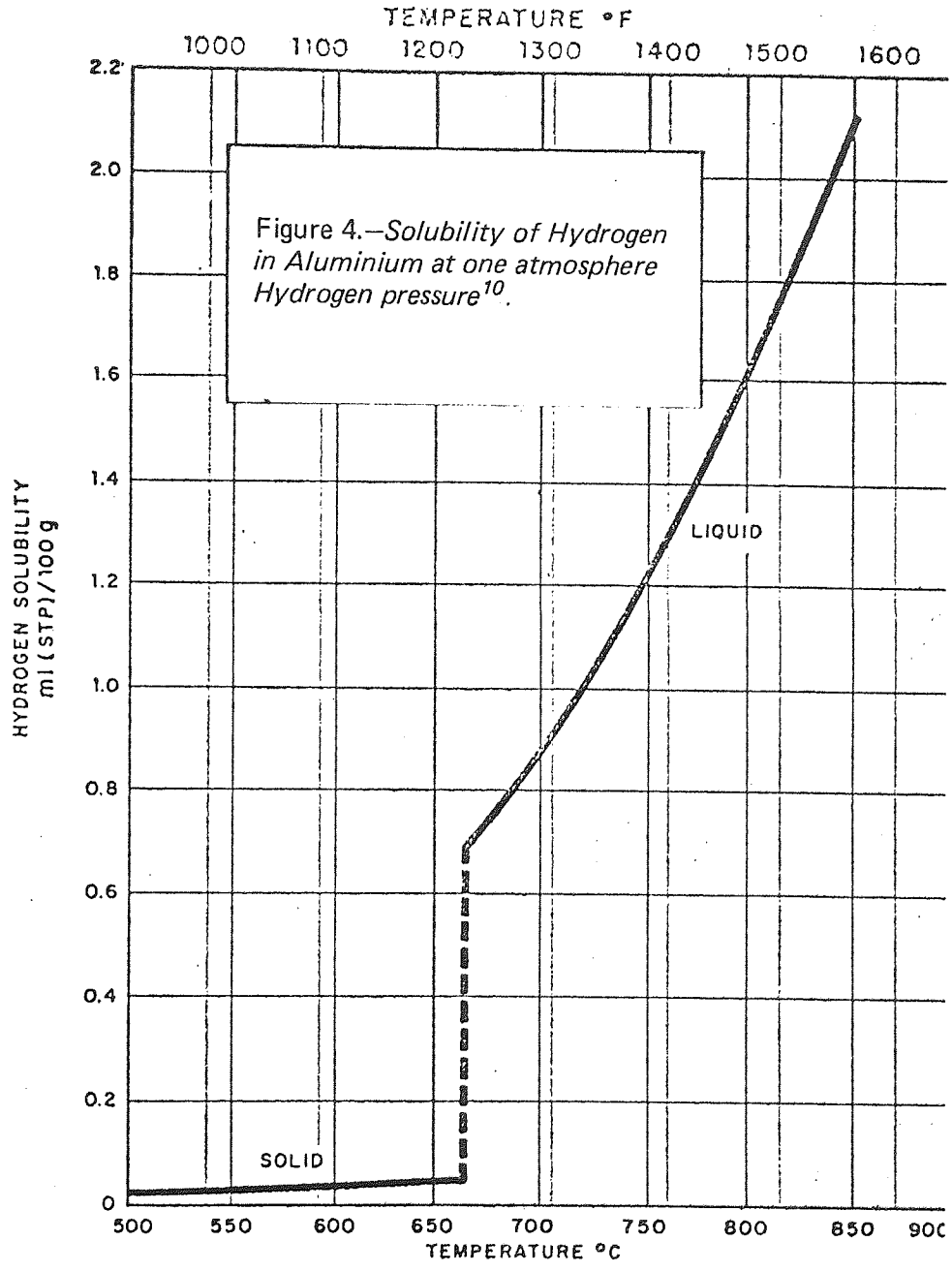

Figure 4.—*Solubility of Hydrogen in Aluminium at one atmosphere Hydrogen pressure*[10].

produce Magnesium Chloride hence some compensation is required since with repeated melts and degassings the Magnesium content decreases[21] as shown in Table III. One foundry has found that the mixture of 90% Nitrogen and 10% Chlorine[19] reduces the problem of Magnesium loss and also combines the advantages of mechanical agitation required for Nitrogen with the chemical reactivity of Chlorine. There is no toxicity or corrosion problem since all the Chlorine reacts with the melt. The results obtained are comparable to 100% Chlorine.

It is essential that some method [22,23] must be adopted for degassing to produce castings, not only of a premium quality but of a quality suitable for normal service. Nitrogen can be used provided that it is oil pumped and possesses a dew point below -59°C (-75°F) to prevent the formation of Aluminium Nitride[20].

TABLE III.—*Effect of Fluxing on Magnesium Content*[15].

No. of Remelts	Al-4% Cu Alloy		Al - 12% Si Alloy	
	With flux	No flux	With flux	No flux
1	0.10	0.12	0.33	0.42
2	0.08	0.12	0.20	0.41
3	0.08	0.11	0.19	0.38
4	0.06	0.10	0.10	0.35

2.2.3 Modification

Modification is essential for alloys containing 7% Silicon or more and produces marked changes in the microstructure. Under equilibrium conditions the microstructure of a hypoeutectic alloy would consist, at room temperature, of primary Aluminium dendrites plus the eutectic. The Silicon in the eutectic normally appears in the form of needles or platelets. When Sodium is added to the alloy there is a change in appearance of the Silicon; the structure of the hypoeutectic alloy again contains primary Aluminium dendrites but the eutectic Silicon is in the form of globules. Slighly hypereutectic alloys, up to approximately 14.5% Silicon, also exhibit this structure indicating a movement in the eutectic composition. Additions of Sodium result in a remarkable refinement of the structure accompanied by an improvement in mechanical properties[24]. These additions have an effect on the microstructure similar to that produced by undercooling.

As a consequence of considerable experimental work several theories to explain the modification mechanism have been developed [25,26,27,28,29,30]. Thall and Chalmers[31] suggest that Sodium additions alter the relative interfacial energies between alpha Aluminium, Silicon and the melt. Mascre[32] suggested that Sodium changes the viscosity

of the liquid and, as a result, the deposition of Silicon atoms. A similar conclusion by Kondic and Kozlunski[33] was derived from observations that Sodium additions reduce casting fluidity in Aluminium/Silicon eutectic alloys.

Sodium may be added as the pure metal[34], but fluxes containing the modifying agent[20] are more common. The amount of Sodium added and the holding time after additions are inter-related when considering the structure. The optimum amount of Sodium added to a particular alloy would be the least amount which would permit a holding time while retaining a modified structure. Zuech[35] indicates a maximum level of mechanical properties produced by the inclusion of a Sodium addition in the region of 0.02%. However, Harris *et al*[34] recommend that for melts degassed with Chlorine 0.03% Sodium is the least amount that will retain modification effects for up to 10 minutes holding time. For metal degassed with Nitrogen additions of 0.01% Sodium are sufficient. Modification is carried out after degassing since chlorination of a melt containing Sodium promotes Sodium loss caused by the formation of Sodium Chloride.

Harris's approach was to assume that the primary cause of increased tensile properties in binary Aluminium/Silicon alloys was the form of the Silicon constituent in the eutectic areas. If this had been the case it would have been logical to assume that over extended holding times there would have been gradual degradation of mechanical properties as the microstructure reverted to its original form. This did not happen and the microstructure was completely changed without loss in mechanical properties.

2.2.4 Grain Refinement

It is essential for the production of premium quality castings that they are grain refined to attain the optimum mechanical properties. The original work[36] performed on Aluminium 4.9% Copper alloys indicated that Boron additions singularly or with Titanium, Niobium or Vanadium were all potential grain refiners. However, a combination of Titanium and Boron proved the most successful, Figure 5.

These observations have been confirmed by other researchers[37,38] and all agree that a boride is produced with similar lattice dimensions to Aluminium Boride, presumably Titanium Boride containing Aluminium Boride in solid solution. Kissling and Wallace also include many alternative mechanisms[38] for grain refining including: mechanical vibration, alloying to provide constitutional super-cooling and nucleation of high melting point intermetallics.

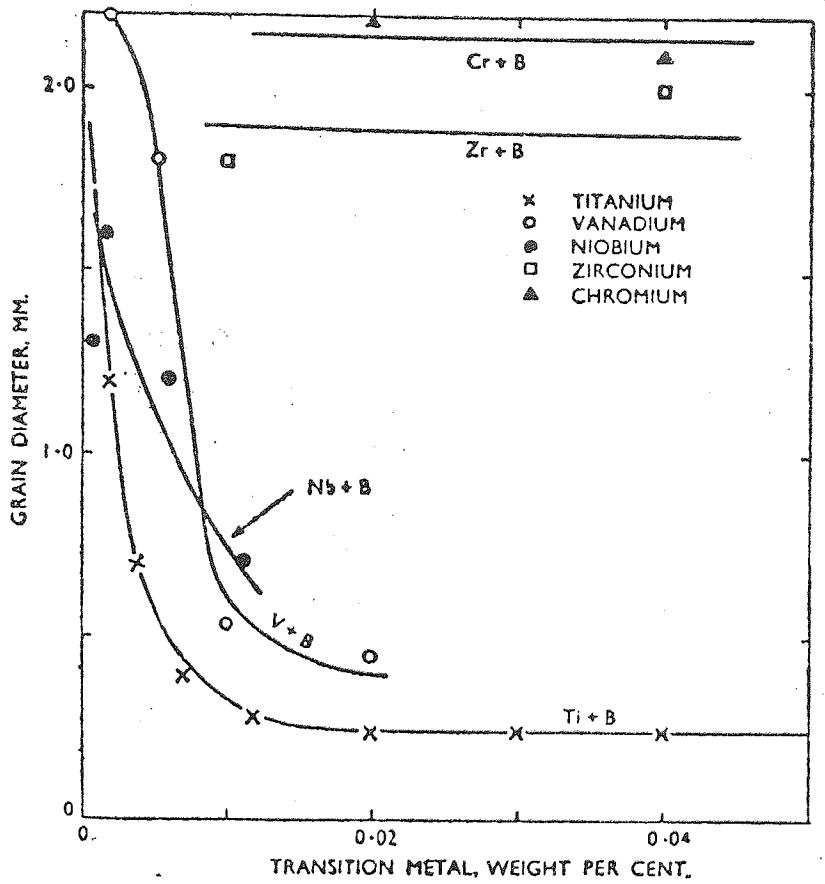

Figure 5.—*Grain Size in test bars in Al 4.9%Cu containing 0.01%B plus small quantities of various transition elements, cast at 800°C*[36].

During subsequent remelting the effect of the grain refiner diminishes resulting in an increase in the grain size[38]. As a result the usual practice is to purchase the basic ingots and add the hardeners during process melting. Under normal foundry conditions these additions are:-

(a) 0.10-0.15% Ti; (b) 0.04% B or (c) 0.01% Ti plus 0.003% B.

Control must be exercised over the pouring temperature because experimental observations indicate that as the pouring temperature increases so does the grain size[39]; consequently one must adjust the pouring temperature to suit the casting configuration and the final grain size. It was concluded that the decrease in grain size, with increased pouring temperatures, Figure 6, was attributable to reactions involving trace elements, or impurities producing, or eliminating, compounds not present in melts cast at lower temperatures.

2.2.5 Gating

The production of gas free, inclusion free, metal would be of little consequence unless the system delivering the metal to the mould cavity obeyed some basic principles of gating[40,41]. As a result the gating system must:

(a) fill the mould cavity, with as little turbulence as possible in order to minimise gas absorption, mould erosion and oxide formation;

(b) introduce adequate skimming action on the metal as it flows through the gating system;

(c) regulate the rate of entry of molten metal into the mould cavity;

(d) produce the optimum temperature gradients within the casting;

(e) perform the above functions efficiently but contain the minimum of excess metal.

The gating system begins with a pouring basin which possesses the distinct advantage of allowing the operator to reach his maximum rate of pouring before any metal enters the sprue. Information on basin designs is available in the literature[41,42].

Blending with the bottom of the pouring basin is the sprue which should be tapered to prevent aspiration during pouring. The aspiration of air promotes oxide formation and is produced by the acceleration of molten metal causing constriction of the metal column. This phenomenon is well established[41,42,43]. The downward motion of the molten metal has to be transformed into horizontal flow along the running system. Considerable turbulence accompanies this directional change and has led to the introduction of sprue sumps or wells. One observer[42] suggested the sump diameter should

be 1½ times the runner width and 1½ times the runner depth. This suggestion enables a pool of relatively motionless metal to exist at the bottom of the sprue thus reducing the erosion of the mould material at this point[43]. A further technique[40] to dissipate some of the kinetic energy of the metal entering the runner is to enlarge the area at the base of the sprue by some 2 to 2½ times and to make the depth at least similar to the depth of the runner. The metal flow is also reduced by a constriction in the runner bar.

The velocity of the metal passing from the sprue well into the runner should be as low as possible to reduce the likelihood of turbulence, however, every precaution must be made to ensure that no other regions of turbulence exist. Runners should not contain severe changes in direction as these cause aspiration of gases. The metal flow may be regulated by means of adjusting the ratios of the areas of the sprue bases and runners and gates. In an unpressurised system the flow is controlled by the sprue and ratios of sprue area to total running and gating areas of 1:2:2 and 1:3:3[42,43] have been recommended for light alloys.

Streamlining the system entails a reduction of the runner bar area after each gate, in order to reduce energy losses and maintain the proper metal flow. Streamlining reduces turbulence and permits oxide and air free metal to enter the mould. It is quite common for the runner to extend beyond the final gate to prevent the first metal through the running system, which may be damaged due to turbulence or over-chilling, entering the mould cavity. The technique of runner extensions also tends to prevent sand particles etc. from being washed into the mould, but exerts no influence on the following metal. For this reason strainers or screens are introduced into the running system[42,43,44] to clean the metal. The screens can be made of tinplate, mica or refractory materials. Enlargement of the runner bar area is essential to compensate for the screen which would otherwise act as a choke.

Thinner sections of casting have provided some problems in running and as a result there has been interest shown in mould coatings. Hexachloroethane[45] has been found to be exceedingly effective (Table IV) . Improvements in fluidity have also been examined in relation to pouring temperature, impurities and moulding materials[46].

2.2.6 Risering and Chilling

Solidification is usually accompanied by a volume change. The position of volume change, shrinkage, depends upon the temperature gradients present in the casting. By design considerations such as gate and riser position, it is hoped that the final shrinkage occurs adjacent to the riser.

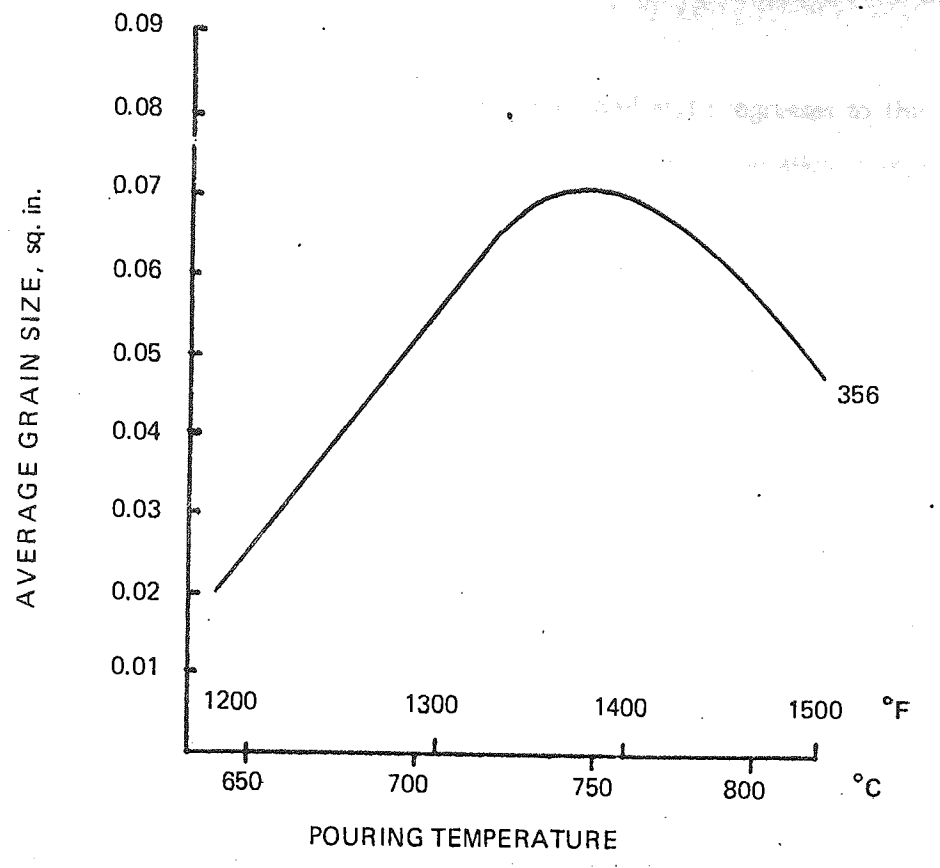

Figure 6.—*Variation in grain size with pouring temperature for Aluminium 7% Silicon 0.3% Magnesium Alloy*[38].

TABLE IV.—*Hexachloroethane Effect on Fluidity of some Commercial Alloys and Pure Aluminium (in the Double Spiral Test)*[45].

Alloy	Pouring temperature °C	Fluidity control spiral, ins.	Fluidity coated spiral, ins.	Fluidity increase due to coating	Percent increase due to coating
195					
Al 4.5 Cu	757	13.0	>28.0	-	-
Al 4.5 Cu	715	6.3	17.9	11.6	184
Al 4.5 Cu	676	3.8	11.0	7.2	190
356	732	15.5	22.1	6.6	43
Al 7 Si	715	11.9	22.1	10.2	86
0.3 Mg	675	7.2	14.1	6.9	96
220	744	17.1	>28.0	-	-
Al 10 Mg	711	10.7	22.9	12.2	114
Al 10 Mg	678	10.3	16.5	6.2	60
40E	732	8.2	13.2	5.0	61
Al 5 Zn	703	7.2	13.2	6.0	83
0.5 Mg 0.5 Cr	676	4.0	6.6	2.6	65
99.9 Al	758	18.7	>28.0	-	-
99.9 Al	715	13.8	20.4	6.6	46
99.9 Al	671	9.9	16.9	7.0	71

Symbol (>) used when the metal ran the complete length of the fluidity spiral (28 in.). These represent minimum values.

Generally, solidification starts at the mould wall and progresses to the centre of the casting. The nature of the solidification depends upon the alloy composition[47] and, hence, gating and risering varies from system to system. In systems with large freezing ranges, the liquid metal must be drawn between the grains to compensate for shrinkage. Progressive solidification reduces the intergranular channels to such an extent as to prevent the liquid metal feeding the shrinkage. Production of deliberate thermal gradients within the casting to cause progressive solidification towards the riser shortens the narrow channels and decreases shrinkage defects.

In casting, the subjects of risering and chilling are so closely linked that detailed consideration of one involves the manipulation of the other. Much emphasis has been placed on chilling in order to produce premium quality castings and two notable contributions are from Johnson *et al*[48] and Flemings *et al* [49].

Johnson made a serious attempt to produce principles governing the location of gates, risers and chills. His attempt was to evolve practical methods of estimating, in advance, riser dimensions to feed casting configurations. By means of "thermal dynamics" it was hoped to determine how thermal gradients in castings originated and progressed and how they are affected by controlled changes in gate, riser and chill locations. The starting point for his investigation was the work of Bishop *et al*[50] who established an empirical relationship between the shape factor and the ratio of riser volume to casting volume for a low carbon (0.30%) steel and a straight line relationship indicated the demarcation between sound and unsound castings, Figure 7.

In short plates, with side risers, Johnson[48] observed that solidification progressed towards the side riser but decreased with increased length of plate. In long plates solidification developed adjacent to the riser while liquid metal still remained at a point further from the riser. After modifications to the riser volume/casting volume ratio Johnson concluded that the feeding range of a riser increases with increasing thickness and that the feeding of Aluminium alloy plate castings, as a function of thickness, does not follow the general rule for steel castings of the same shape and having the same design of gates and risers.

On 2inch and 1inch plates, Johnson[48] pursued investigations with top, as opposed to side, feeding and with single and multiple gating. Results indicated a maximum width of section after which severe porosity occurred below the riser and this porosity increased with section thickness. Using multiple gates (2 or 4) soundness was improved markedly under the riser in the 1 inch section. Improvements were less spectacular in the 2inch section. Micro-porosity was less noticeable when four gates were used.

Chilling was also investigated on the 1 inch and 2 inch sections. The two techniques worthy of note being end chilling and wedge-shaped chills. In sections of 1 inch, lengths of 3 inches and 5 inches were radiographically sound but in 2 inch sections only the 6 inch plate was satisfactory. The limited effect of end chills was attributed to their short range influence on solidification rate whereby the thermal conductivity of the solidified metal itself becomes the controlling factor for heat dissipation.

Wedge chills were shown to produce a desirable combination of thermal gradients and directional solidification. Real impetus to the optimum thermal gradients were produced by tapering both the thickness and the width of the chill. The following recommendations were made as a result of the work:-

(a) where possible, the riser should be attached to the side of the casting and gating through the riser is also preferable;

(b) if top risers are essential, insulating sleeves and multiple gates should be employed;

(c) to extend feeding, tapered wedge shaped chills or equivalent bar chills should be used. For plate castings, the thicknesses of the taper wedges should decrease from a thickness equal to that of the cast section at the end away from the riser, to half the section thickness at the riser end. In more substantial castings the wedges should be split and placed either side of the casting.

Taylor *et al*[51] clearly showed the mechanisms of feeding for Aluminium castings to be fundamentally different from those of steel. However, whatever the alloy system, the riser should possess certain principles, namely the minimum surface/volume ratio and adequate metal to compensate for shrinkage. Two commercially adopted methods of feeding are referred to in the paper. One relates the riser diameter to the section thickness, the former being 1½ to 2 times the latter. The second, the safer technique, involves yield and is expressed thus:

$$\frac{\text{weight of casting} \times 100}{\text{weight of casting and runners etc.}} < 50\%$$

Design considerations for both top and side risers are also included. Taylor recommends that for wide risers: (a) the riser neck should be heavier than the section to be fed and be smaller in diameter than the riser diameter; (b) the neck should not be so short as to overheat the sand and hence increase shrinkage in the casting.

Taylor[51] points out that chilling does not increase feeding but only promotes directional solidification towards risers. Thus the essential principle of any system to

achieve high properties is that chills and risers are spaced alternatively so that the entire casting freezes directionally towards the risers and the maximum spacing should be 2inches[52].

Flemings *et al*[49] determined the influence that solidification rate exerted on mechanical properties for end-fed plate castings. Considerable improvement in mechanical properties at the chilled ends of the plates were noted. This would be expected as a result of the fine grained structures at the chilled ends. As well as the strength and ductility decreasing towards the riser end mechanical properties became poorer with decreasing section thickness.

With the pattern illustrated in Figure 8, Flemings determined variations in mechanical properties of Aluminium 4.5% Copper 0.8% Silicon, and Aluminium 7% Silicon 0.3% Magnesium alloys, using two techniques of chilling, Figure 9. It was found that substantial improvements in properties were achieved in the chilled castings, Figures 10 to 13. The data produced forms a foundryman's guide to chill placement. By sectioning a casting into a series of plates Flemings[49] states that the data indicates maximum permissible distances, between risers and chills, to obtain given minimum properties permitted by specifications for varying sections.

A certain latitude must be allowed for variations in chemical composition, heat treatment, chill wash thickness, etc.

Chamberlain *et al*[53] investigated the effect of solidification rate and gas content on mechanical properties. Feeding was so arranged that the effect of differing gas contents could be studied independently of shrinkage defects. By using a stepped casting he was able to determine the variation in mechanical properties with solidification rates for a particular gas content. To ensure directional solidification Chamberlain[53] adopted chilling techniques similar to those of Flemings and Johnson.

A similar investigation to those of Flemings[49] and Chamberlain[53] by Murthy *et al*[54] examined the effect chills of varying powers exert on the solidification process and casting soundness for end chilled test castings. Cooling curves were obtained in the test castings when variously chilled by Copper, Cast Iron, anodized Aluminium and Graphite. The curves were used to determine the influence of the end chilling on solidification of the test casting and indicated that the distance to which the chill effect is felt increases with the increase in heat capacity of the chill used. For Copper and Cast Iron chills the chill effect was a full 7 inches along the casting (2in section) and 5 inches for the anodised Aluminium chill. Within the region of the chill influence, solidification time at a particular thermocouple station decreased with an increase in heat capacity of the particular chill.

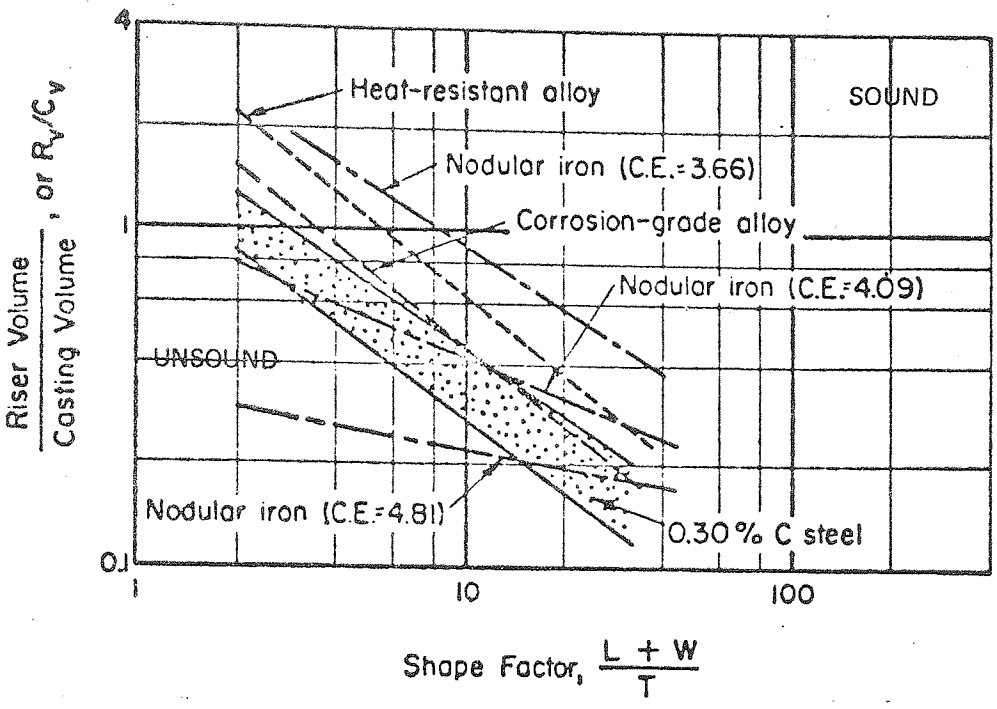

Figure 7.—*Relationship between Shape Factor and the ratio of Riser Volume to Casting Volume*[48].

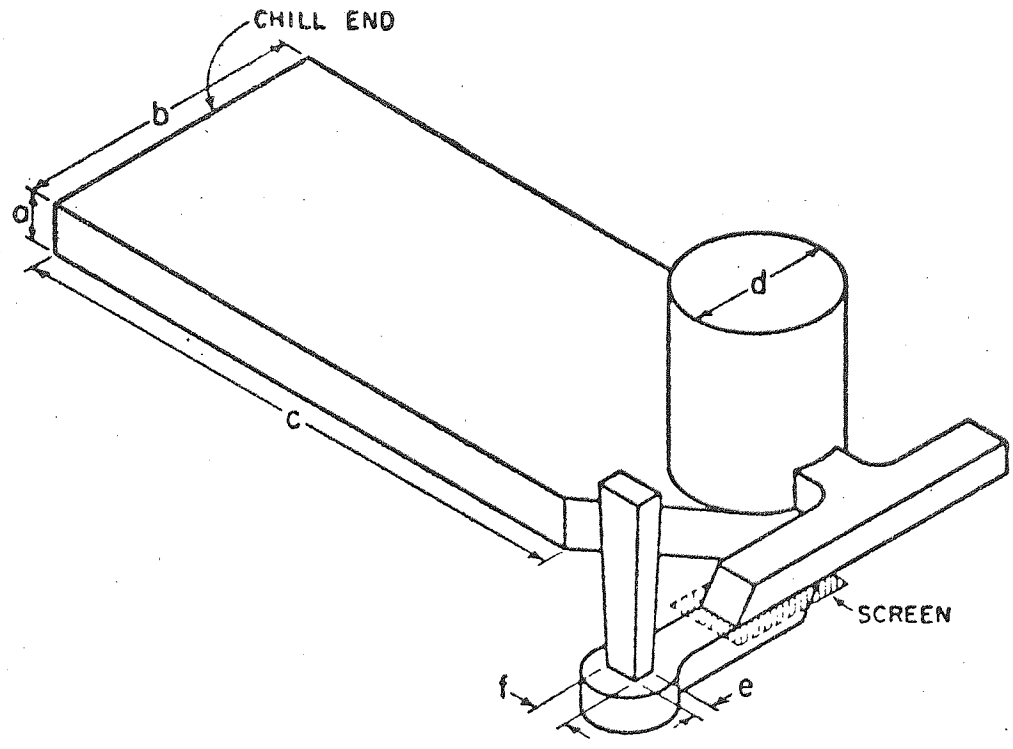

Plate No.	Dimensions, in.					
	a	b	c	d	e	f
1	1½	6	18	4	½	⅝
2	1	6	12	3	½	⅝
3	¾	6	9	3.5	½	½
4	½	5	6	2	½	½
5	⅜	6	8	2	½	½
6	¼	6	8	2	½	½

Gating ratio for all castings, Sprue : Runner : Gate — 1:3:3

Figure 8.—*Sketch of plate pattern for chill depth studies*[49].

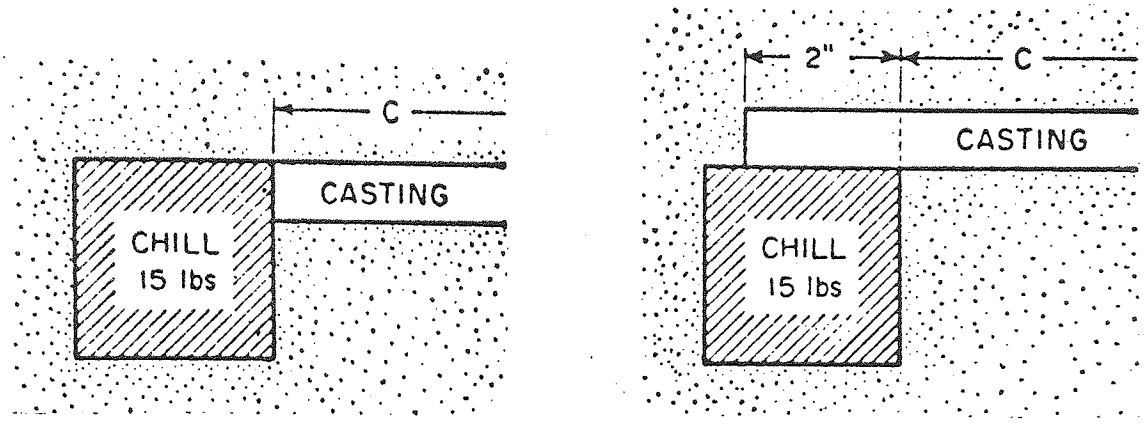

(a) Chill placement used for Heats A and C.

(b) Chill placement used for Heats B and D.

Figure 9.—*Methods of chill placement used in chill distance study*[49].

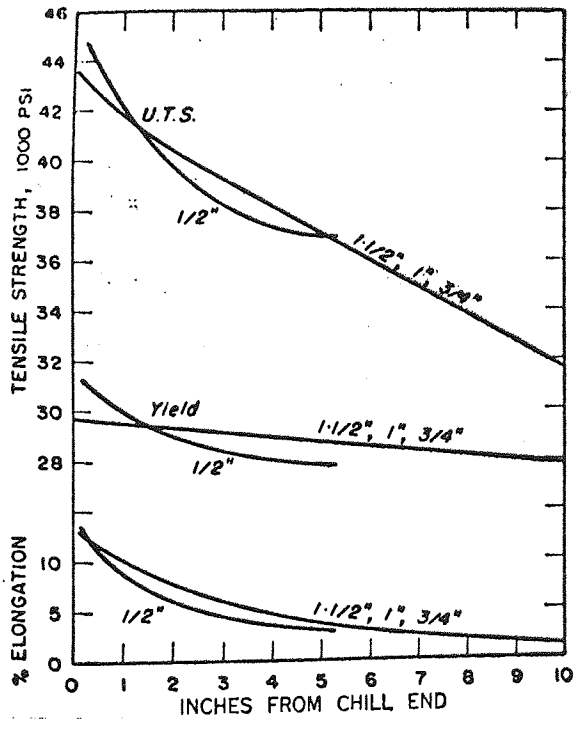

Fig. 10.—*Summary of tensile properties of end-chilled 356 alloy plates. Heat C.*[49]

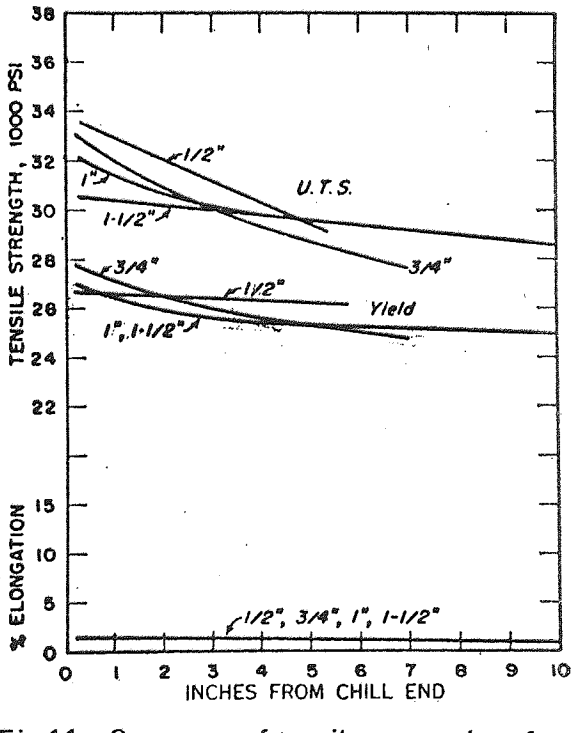

Fig. 11.—*Summary of tensile properties of unchilled 356 alloy plates. Heat C.*[49]

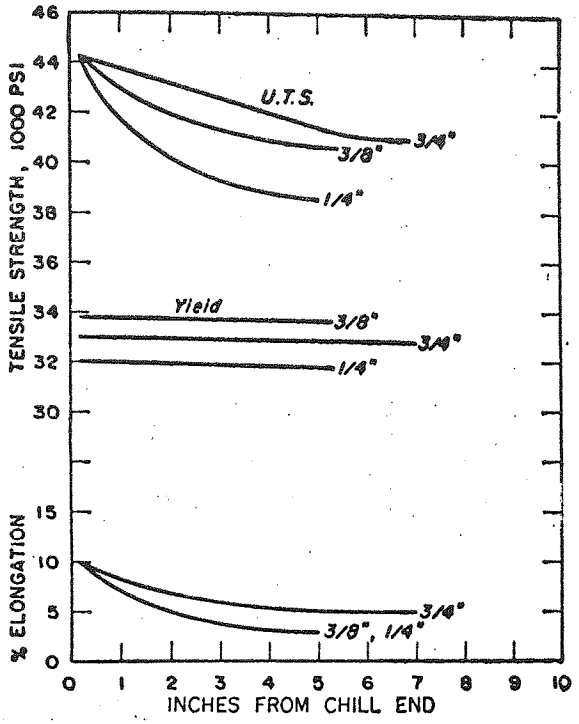

Fig. 12.—*Summary of tensile properties of end-chilled 356 alloy plates. Heat D.*[49]

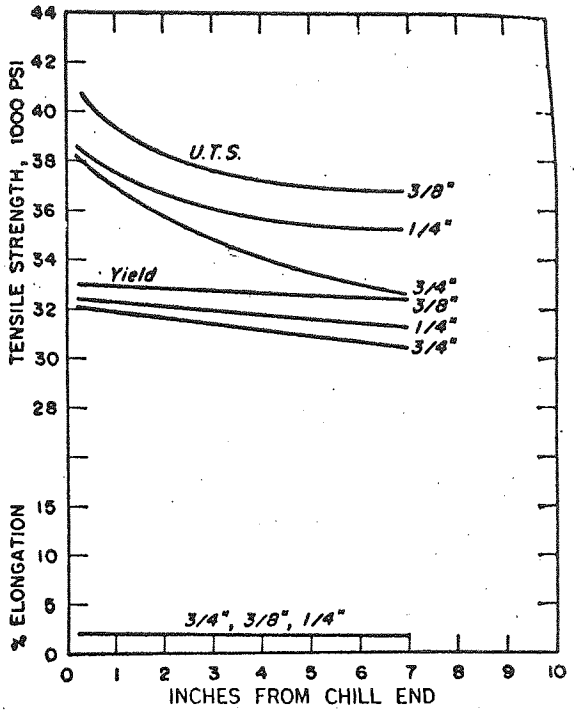

Fig. 13.—*Summary of tensile properties of 356 alloy unchilled plates. Heat D.*[49]

No good correlation was observed between the maximum temperature gradient and percentage porosity or tensile strength but a relationship was formulated between the logarithm of the average cooling rate and percentage porosity or tensile strength. There was some scatter which Murthy[54] attributed to the relative position of the tensile specimens with respect to the chill and, in addition, to the type of chill. Also the nature of the shape of the tensile specimen tended to magnify the problems of pore shape and distribution. Murthy[54] acknowledged that similar scatter was obtained using a combination of end and wedge-shaped chills.

Bailey[55] thought it necessary to study the effect of variations in Beryllium and Magnesium contents on the mechanical properties of high purity Aluminium 7% Silicon 0.3% Magnesium alloy. A casting configuration was adopted with as much complexity as economically feasible in order to determine the mechanical properties of the casting as a whole as well as properties of coupons taken from the casting. It was hoped to directly compare changes in the mechanical properties of complete castings with compositional variations.

The configuration adopted was tee-shaped, two being cast in the form of an "H". The tees thus produced represented test pieces for static loading as well as sources for test coupons. The casting was bisected by an axis of symmetry parallel to the two vertical bars of the "H". One side was chilled, using eitherCast Iron or Aluminium chills depending on the foundry, and the other sand cast.

Metallographic examination indicated finer dendritic structures in the Aluminium chilled castings. Higher tensile and proof strengths were attained in the Aluminium chilled castings but a better ductility was observed with the Iron chills. Increased Magnesium content produced increases in ultimate and yield strength and decreases in ductility.

Finally, there is little information available in the literature on chill size. Flemings[49] indicated that when using Aluminium, the weight of the chill should be of the same order as the weight of the section to be chilled. Taylor[51] suggested large chills should be of Aluminium and one to two times the section weight. When small chills are required to establish temperature gradients Cast Iron is chosen. No adverse effect is recorded by 'overchilling'.

2.2.7 Heat Treatment

Table V gives the specified or recommended heat treatments for premium quality Aluminium 7% Silicon 0.3% Magnesium alloy castings. The American Military specification

TABLE V.—*Specified or recommended heat treatments for Premium Quality A356 and 356 alloys.*

Alloy	Condition Condition	Type of casting	Sol. treatment Temperature °C[3]	Time hrs.	Water quench temperature °C	Delay time hrs.	Temp. °C	Time hrs.	Ref. no.
A356[4]	T6[5]	S.C.[1]	538	14	60 - 100	-	154	5	56
356[4]	T6	S.C.	527 - 543	6 - 18	66 - 100	-	149-160	1-6	
356	T51	S.C.	527 - 543	6 - 18	66 - 100	-	221-232	6-12	
356	T6	P.M[2]	527 - 543	6 - 18	66 - 100	-	149-160	1-6	57
A356	T6	S.C.	527 - 543	6 - 18	66 - 100	-	149-160	1-6	
A356	T61	P.M.	527 - 543	6 - 18	66 - 100	-	149-160	6-10	
356	T51	S.C.	-	-	-	-	221-232	7-9	
356	T6	S.C.	532 - 543	12	66 - 100	-	149-160	3-5	
356	T6	P.M.	532 - 543	8	66 - 100	-	149-160	3-5	
356	T7	S.C.	532 - 543	12	66 - 100	-	199-210	3-5	58
356	T7	P.M.	532 - 543	8	66 - 100	-	221-232	7-9	
356	T71	S.C.	532 - 543	12	66 - 100	-	241-252	2-4	
A356	T61	P.M.	532 - 543	12	66 - 100	-	149-160	6-10	
A356	T6	S.C/P.M.	532	14	hot	24	160	8	53
356	T6	S.C.	538	16	hot	24	154	12	49
A356	T6	S.C.	538	10	82	24	177	2	
A356	T61	S.C.	538	10	82	24	204	2-4	59
A356	T6	P.M.	538	10	82	24	160	3	
A356	T61	P.M.	538	10	82	24	160	8	
356	T51	S.C/P.M		-	100	-	227	7-9	
356	T6	S.C/P.M	558	6 - 12	100	-	154	3-6	
356	T7	S.C/P.M	558	6 - 12	100	-	227	7-9*	
A356	T6	S.C/P.M	558	8 - 12	66 - 100	-	154	2-5	
A356	T61	S.C/P.M	558	8 - 12	66 - 100	-	154	6-12	60
A356	T61(1)	S.C/P.M	558	8 - 12	66 - 100	-	154	6-9	
A356	T62	S.C/P.M	558	8 - 12	66 - 100	-	154	10-12	
A356	T7	S.C/P.M	558	8 - 12	66 - 100	-	227	7-9*	
356	T6	S.C.	538	16	185	Various	154	3-6	61
A356	T6	S.C.	527	-	hot	-	154	3	62

(1) Sand Cast
(2) Permanent Mould
(*) Stabilising Treatment
(3) Temperatures converted from °F quoted in American literature.
(4) A356 and 356 have the same nominal analysis of Aluminium, 7% Silicon and 0.3% Magnesium but the Iron content of A356 is restricted to a maximum of 0.2%.
(5) The conditions tabulated refer to variations of heat treatment in American specifications.

MEL - H - 6088E - allows considerable latitude for temperature control but in practice control is normally much closer. With the higher purity alloys solution treatment at the maximum temperatures is possible because the likelihood of low melting point grain boundary eutectic phases is minimal. Obviously, the maximum solution temperature permits more of the soluble phases to dissolve resulting in an optimum aging response.

Specifications do not dictate the time that elapses between castings being removed from the solution treatment furnace and quenched into the water. Commercially this time may be in the order of minutes. Flemings[52] proposes that in premium quality castings this delay time before quenching be reduced to below 10 seconds. Dump bottom furnaces can reduce this interval to less than a second.

The water temperature into which the castings are quenched has been found to exert an influence on mechanical properties. Reinemann *et al*[56] compared the effect of more rapid quenching, i.e. quenching into water at 60°C as an alternative to boiling water, for A356 alloy. Little increase was noted in elongation but the yield stress showed a 15% improvement and the ultimate strength a 10% improvement.

Distortion produced by high internal residual stresses originating from quenching may not be so critical in alloys with improved ductility since residual stresses would be relieved by service straining without premature failure but difficulty could be encountered during machining. The commercial practice is to have the water temperature in the region of 60°C - 82°C.

The effect that the interval at room temperature between quenching and artificial aging has on mechanical properties has been studied by Quadt[61]. The delay times investigated were 'immediate' (defined as any time up to 30 minutes) one day and one week. For a balance to be struck between elongation and ultimate or yield strength Quadt[61] suggested the one day interval as most advantageous, Figure 14.

DeRoss[59] investigated different aging cycles for 356, A356 and a modified form of A356, including a higher Magnesium content, designated XHP.356. Investigation of the aging curves obtained suggested a wide combination of mechanical properties available in A356 heat treated at 160°C. The range was somewhat narrower for XHP.356. The mechanical properties of the alloys were obtained for different aging cycles and Quadt[61] concluded that the cycle depended primarily upon the design requirement of the material.

A similar investigation[62] involving heat treatment cycles on shell mould cast 356 alloy, concluded that acceptable aging treatments on the basis of processing and chemistry

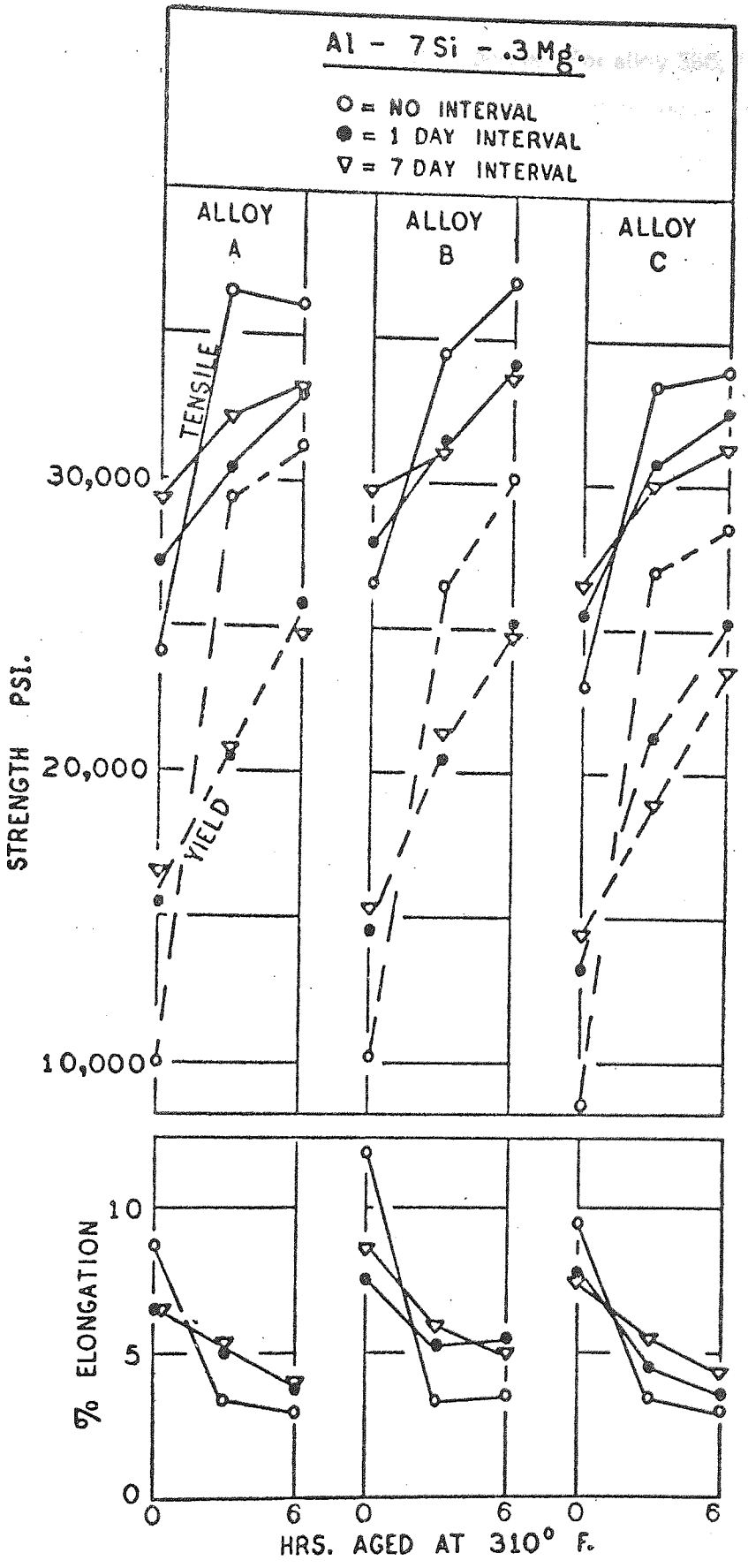

Figure 14.—*Effect of room temperature interval between quenching and artificial aging of Aluminium sand cast alloys*[61].

permitted attainment of still better mechanical properties. For alloy 356, Toledo *et al*[62], indicated that a wide range of aging times and temperatures will produce the best mechanical properties providing the iron content is below 0.03%. However, the acceptable aging cycles, in terms of time and temperature ranges, narrow rapidly when iron increases above 0.04%. It should be noted, however, that data developed in the work was restricted to one casting and one process.

3. FACTORS IN IMPROVING CASTING QUALITY

3.1 Experimental - Casting Series I

It was thought beneficial that, as a starting point in investigating improvements in the quality of castings, the number of process variables investigated, intentionally or otherwise, should be kept to a minimum. This enabled comparisons to be made with existing commercial foundry practices. The variables investigated in this initial series of castings were:

(a) Section thickness,

(b) Chemical analysis,

(c) Chill material,

(d) Chill shapes, and

(e) Distances from the more chilled ends of the cast plates.

The quality of the castings, for the purpose of this investigation, was defined by their mechanical properties. The most important factor examined in the chemical analysis was the Iron content, but because of the limitations of the melting facilities and the extent of the casting series, variations in Silicon and Magnesium contents were also obtained and included in the comparisons.

3.1.1 Melting Practice and Analysis

The alloy (A356, nominal analysis Aluminium 7% Silicon 0.3% Magnesium, see Table VI), was produced using:-

(i) Aluminium Ingot (99.99%),

(ii) Commercial Aluminium/Silicon hardener for the higher Iron content alloys and high purity Aluminium/Silicon (using 99.99% Silicon) for the low Iron alloys.

(iii) Aluminium 10% Magnesium hardener produced from Aluminium Ingot and Magnesium Ingot (99.99%).

(iv) Remelted Secondary Ingot of known analysis having been analysed in order that estimates for the additions of Aluminium 10% Magnesium may be made.

(v) Analysed scrap made up from runner systems from previous melts, shotblasted to remove all surface contamination.

Aluminium/Titanium hardening alloy was not deliberately added as sufficient (referred to previously in the section entitled 'grain refinement') was accumulated from successive remelts of secondary scrap and repeated grain refining.

In the melting procedure the alloy constituents were preheated for 30 minutes. The melting crucible was similarly preheated in a separate gas furnace and the ingot and

TABLE VI.—*Chemical Analysis for castings as specified in D.T.D. 5028.*

Elements	Per Cent Min.	Max.
Copper	-	0.10
Magnesium	0.20	0.45
Silicon	6.50	7.50
Iron	-	0.20
Manganese	-	0.10
Nickel	-	0.10
Zinc	-	0.10
Lead	-	0.05
Tin	-	0.05
Titanium	-	0.20
Aluminium	Remainder	

scrap transferred to this pot. Before melting was completed, the Aluminium 10% Magnesium hardener was added and the remaining solid material introduced to submerge the Aluminium/Magnesium alloy.

The remainder of the melting sequence was as follows:-

(a) Degassification of the melt at 680°C to 700°C,

(b) Nucleation treatment at 700°C to 720°C,

(c) Fluxing and dross flotation at 720°C and

(d) Heating to 735°C, removing the melt from the furnace and cleaning the surface before casting the experimental plates and analysis coupons at 720°C. When 1/8 in (3mm) sections were cast the pouring temperature was raised to 735°C - 740°C.

To avoid deviation from existing commercial foundry practice, degassing and inoculation were performed using tablets.

3.1.2 Iron Content

In view of the importance of Iron content on the mechanical properties of castings, two ranges of Iron content were produced by careful sorting of the commercial Aluminium/Silicon hardening alloy ingots. This required that all the commercial alloys be analysed. An additional Iron content range was developed using the high purity Aluminium and Silicon, thus eliminating the Iron associated with impure Silicon. The ranges investigated were nominally:-

(a) 0.02% Fe; (b) 0.07% Fe and (c) 0.11% Fe.

To provide control over Iron pick-up, foundry tools were coated with aluminia and melting was carried out in silicon carbide crucibles.

3.1.3 *Moulding Practice and Chill Shapes*

The effect that different chilling techniques had on mechanical properties was investigated using the pattern illustrated in Figure 20.

The moulding material was a synthetic green sand comprising of:-

(a) Lynn 60 Silica Sand (90% between 60 and 100 mesh),

(b) 4% Bentonite Clay,

(c) 3% China Clay,

(d) 2½% - 3% Moisture.

A series of plates, 1/8 in (3mm) to ½in (12.5mm) thick in 1/8 in divisions, was cast. Three chilling techniques; end block, single taper and double taper chilling were employed, Figure 15. In addition to investigating the effect that chill configurations have on mechanical properties, comparisons were made by varying the chill material. Thus, two sets of chills were produced, one in Cast Iron and the other in Aluminium. The series was completed by casting an unchilled plate of each section.

Chill sizes were selected after reference to the studies of Flemings[49] and Johnson *et al*[48]. Flemings[49] indicates that an Aluminium chill with comparable weight to the cast section has sufficient chill capacity. Consequently, with a maximum section of ½in (12.5mm) and plate dimensions of 5in (127mm) wide by 7in (178mm) long the end dimensions of a 5in (127mm) wide block chill, calculated from the resultant plate weight, was approximately 2in (51mm) square. The relationships regarding the plate dimensions and taper chill dimensions were derived from the work by Johnson[48]. All the tapers in the horizontal plane were kept constant with 2½in (63.5mm) basesand heights of 7in (178mm). Vertically, sections in half the taper chills produced were either similar to the cast sections, i.e. single taper chills or tapered from the section thickness at the 2½in (63.5mm) base end to half the section at the apex, i.e. double taper chills (Figure 15). Two taper chills were necessary to chill each plate; the bases being furthest from the riser. The main divergence from Johnson's work was in the chill material; Johnson used steel.

3.1.4 *Development of the Mould Design*

A casting configuration was needed to investigate varying sections of sufficiently large surface area to observe cooling rates under conditions approaching unidirectional heat flow. The ideal approach for investigating several section thicknesses is to form a stepped casting similar to that adopted by Chamberlain *et al*[53]. An added advantage of this shape is that, by lining the sections in ascending order, directional solidification can be superimposed upon the casting.

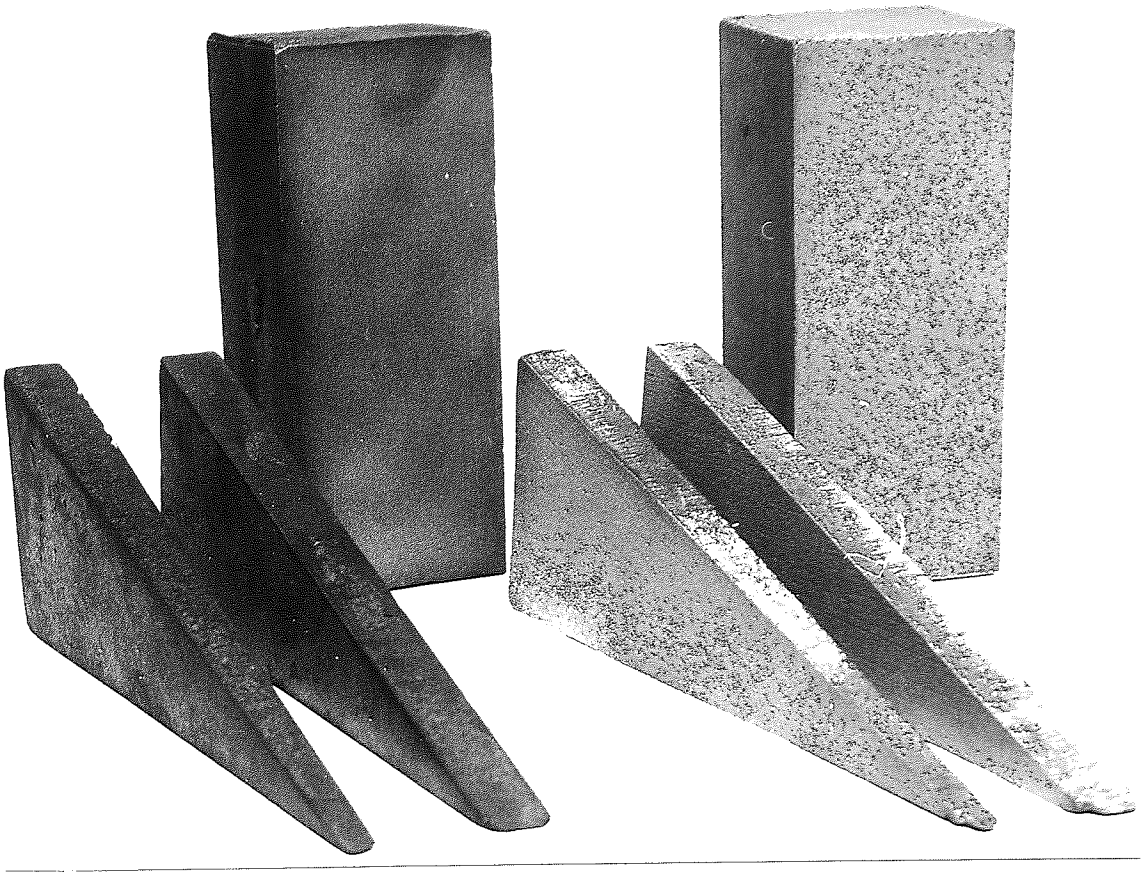

Figure 15.—*Illustrating Series I chilling techniques, from left to right; Cast Iron double taper chill, single taper chill and block chill; similarly in Aluminium.*

Figure 16.—*Showing chill techniques investigated in Series II. These are Cast Iron tapered plate and double thickness single taper chill; similarly in Aluminium.*

The starting point in designing the running system for the stepped casting was the technical file by Latimer[41]. Modification of the casting design was needed because of the limiting size of the moulding boxes available. Apart from an estimate of pouring rate and discharge coefficient, the sizes of the moulding box and pouring basin provided all the information necessary to determine the sprue dimensions using the nomogram in Latimer's work (Appendix I). An estimate of discharge coefficient was made after considering the values of some of the more common Aluminium foundry alloys quoted in the paper. The value obtained was 0.67. An initial pouring rate of 4 lbs/second was proposed. For satisfactory results when casting Aluminium alloys Latimer[41] suggests a divergent series of sprue base,runner and gating area ratios. Latimer[41] also supplies guides as to the ratio of the dimensions of individual runner bars, gates and sumps. The original ratio 1:1:1.5 was the lowest claimed to be successful, but calculations for the runner bar and gate areas, taking into account relationships between runner heights and widths and gate heights and widths, resulted in the restricted gating ratio of 1:2.2:1.5.

Each step was 6in (152.5mm) wide and 3in (76mm) long and increased in thickness from 1/8 in (3mm) in 1/8 in divisions to ½in (12.5mm) and a semi-circular extension of the ½in (12.5mm) section acted as a feeder pad for a 3in (76mm) diameter feeder. The pad and the parallel runner were linked by means of the gate. The runner bar was split between the cope and drag to accommodate a steel screen as an added precaution.

Several melts were carried out using the mould shown in Figure 17. Unfortunately, the mould design proved unsatisfactory as the pouring temperature had to be raised excessively before any fully run castings were produced. Attempts were made to raise the pouring rate by enlarging the sprue area, but the constriction at the gate was highlighted by the failure to produce any good castings.

To reduce the overall distance over which the metal had to travel to the 1/8 in (3mm) section it was decided to split the four sections into two groups. Directional solidification was again assisted by having the thinner sections further from the gates. The sprue base, runner bar and gate ratios were determined by two criteria, (a) the optimum pouring rate, (b) the larger cross-sectional areas adjacent to the runners. The gates were considered as extensions of the larger sections and had areas of $1\frac{1}{2}in^2$ ($970mm^2$) and $3in^2$ ($1940mm^2$) respectively. Flemings[43] considered the minimum satisfactory sprue base, runner and gating area ratio to be 1:3:3 and 1:6:6 was also considered satisfactory. Both these sets of ratios require a sprue base area of $\frac{1}{2}in^2$ ($323mm^2$), which agrees closely with the result obtained for a 2 lb/second pouring

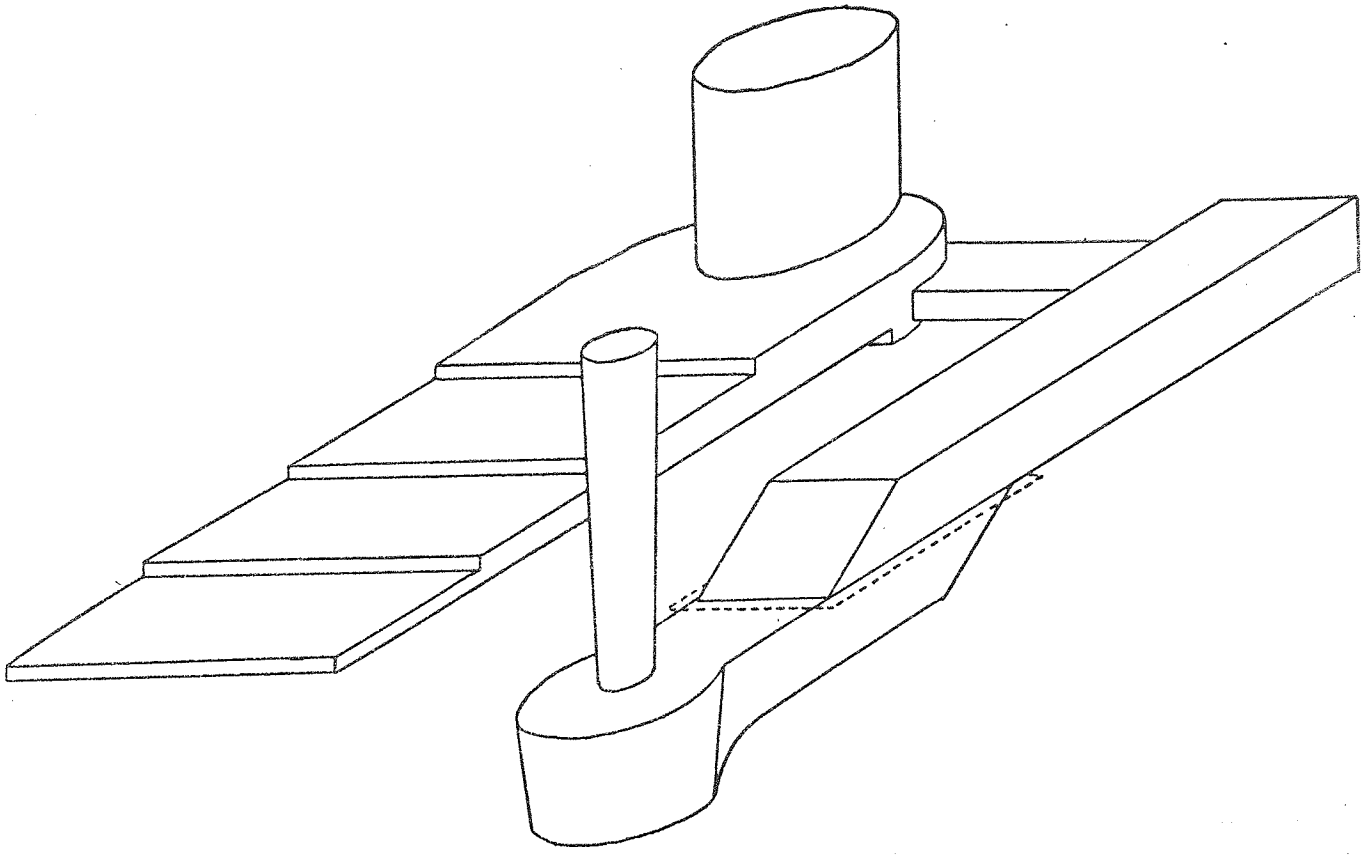

Figure 17.—*Original mould design.*

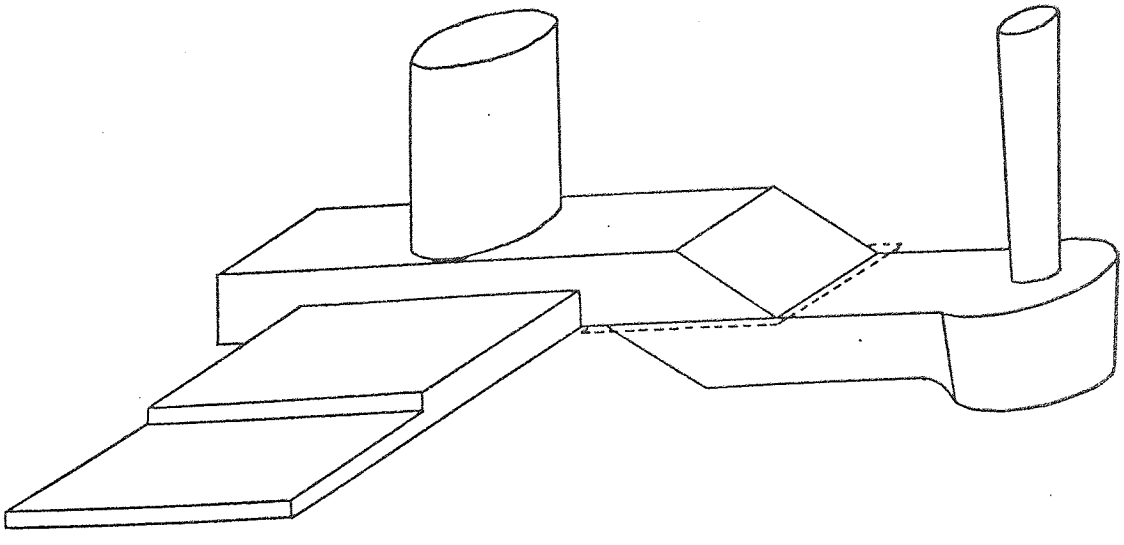

Figure 18.—*First modification to mould design.*

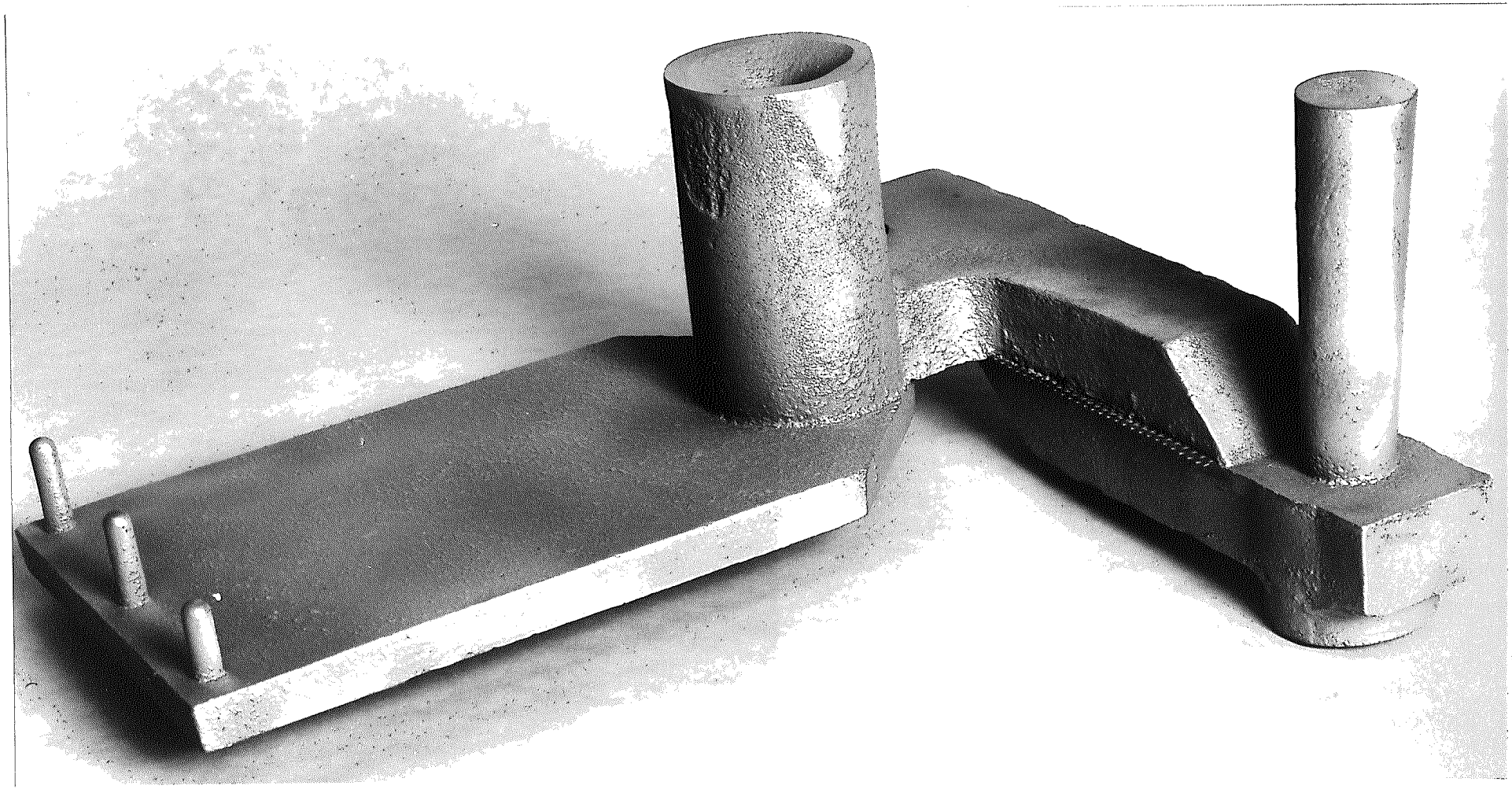

Figure 19.—*Showing the final experimental casting shape developed from the work of Latimer*[41] *and Flemings*[43,49].

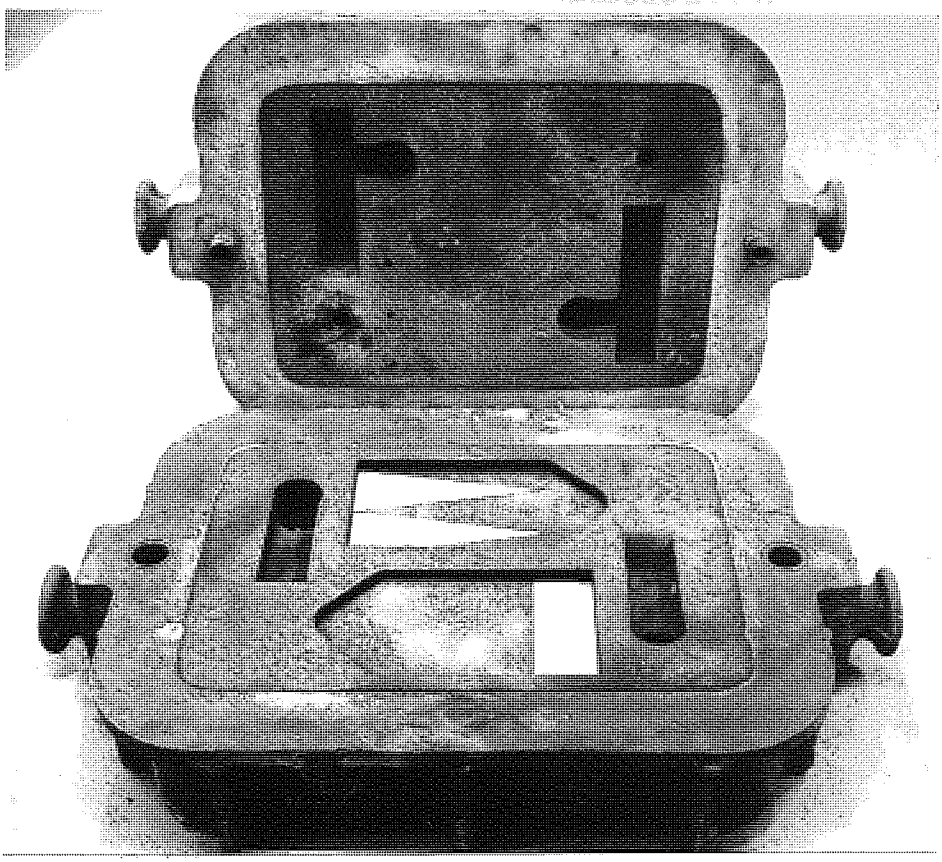

Figure 20.—*The final pattern for investigating chilling techniques on mechanical properties.*

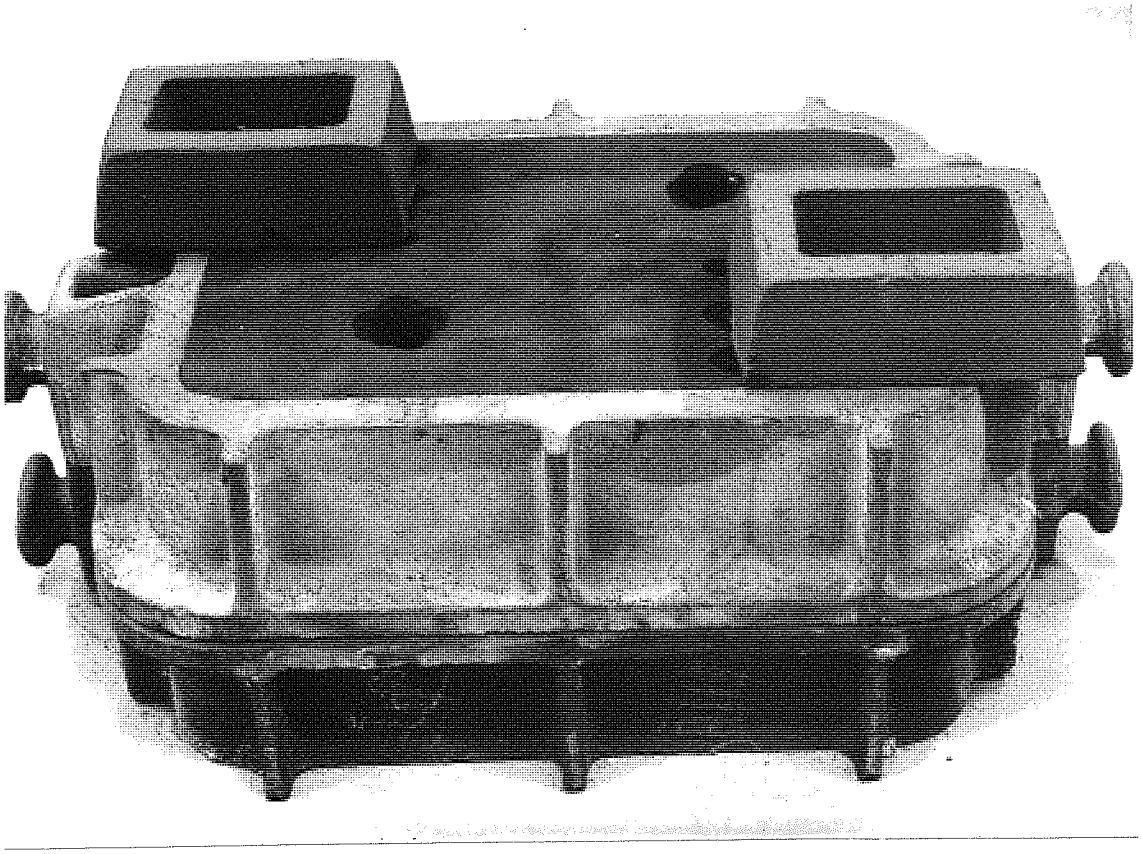

Figure 21.—*Mould closed ready for casting.*

(Figure 23); for example plate Y33 refers to a Cast Iron single taper chilled 3/8 in plate with a nominal analysis of 0.07% Fe.

Specimens for mechanical properties from ½ in, 3/8 in and ¼ in plates were identified by the numbers 1 - 7, starting from the more chilled end. The centre line of the first specimen lay ¾ in from the end of the plate, subsequent specimens had centre lines coinciding with 1¾ in, 2¾ in, 3¾ in, 4¾ in, 5¾ in and 6¾ in from the chill end. It was not possible to machine bars from the 1/8 in plates, consequently, only flat specimens could be produced from each plate with centre lines 0.50 in, 1.63 in, 2.75 in, 3.88 in , 5.00 in and 6.13 in from the chill end. Hence final nomenclatures presented for regression analysis were, for example, Y33001, Y33002, etc.

3.2 Casting Series II

3.2.1 Additional Experimental Details

This series of castings involved two further methods of chilling. For some time there has been industrial interest in the effect tapered chill plates would have on the mechanical properties of plate castings. A series of tapered plate chills were produced in Aluminium and in Cast Iron to extend over the complete face area of the plate casting and varying in thickness from the thickness of the section being cast, to half that thickness (Figure 16). In considering the influence that chill capacity has on mechanical properties it was becoming clear that insufficient chill capacity existed at the narrower end of the taper chills so far investigated and there was insufficient gradient towards the wider ends. As a consequence, it was decided to examine the effect of Aluminium and Cast Iron single taper chills with thicknesses twice that of the section being cast i.e. double thickness single taper chills (Figure 16).

Although the medium level of Iron content in Series I provided information on the effect increasing levels of Iron had on the mechanical properties of the plates, it was decided to investigate only the two extreme ranges viz. nominal Iron contents of 0.02% and 0.11%. The reason was that although the intermediate Iron level could be obtained by careful selection of the commercial Aluminium/Silicon hardener used for laboratory scale alloys, this facility would not be available in a commercial practice using industrial alloy ingot. The minimum Iron content normally obtained, at present, commercially is in the region of 0.10%. To reduce the work load from this second series it was thought sensible to perform a half replica of the complete matrix, which simplified the comparison with results obtained in the previous series. Finally, in order to produce satisfactory castings in contact with such large chilled areas venting was introduced into the taper chill plates by drilling small holes from the back face

		Section			
		1/8 in	1/4 in	3/8 in	1/2 in
IRON CONTENT	0.02%	X11 X12 X13 x X16 X17 x	X21 X22 X23 X24 X26 X27 X28	X31 X32 X33 X34 X36 X37 X38	X41 X42 X43 X44 X46 X47 X48
	0.07%	Y11 Y12 Y13 x Y16 Y17 x	Y21 Y22 Y23 Y24 Y26 Y27 Y28	Y31 Y32 Y33 Y34 Y36 Y37 Y38	Y41 Y42 Y43 Y44 Y46 Y47 Y48
	0.11%	Z11 Z12 Z13 x Z16 Z17 x	Z21 Z22 Z23 Z24 Z26 Z27 Z28	Z31 Z32 Z33 Z34 Z36 Z37 Z38	Z41 Z42 Z43 Z44 Z46 Z47 Z48

Figure 22.—*Complete experimental matrix for Series I castings with plate codings - note no 1/8 in plates were cast with double taper chills.*

Unchilled			Y31
Chill Material	Cast Iron	Chill Technique	Block Y32
			Single Taper Y33
			Double Taper Y34
	Aluminium	Chill Technique	Block Y36
			Single Taper Y37
			Double Taper Y38

Figure 23.—*Unit cell within the matrix.*

of the chill until the drill point just broke the chill/casting surface. This venting permitted the air to be exhausted from the mould cavity once the three vents, normally present, became blocked.

3.2.2 Nomenclature and Matrix used in Series II castings

The system of identification in this series of plates was similar to the previous method; the identity of the section thicknesses and the low and high range Iron contents remaining unaltered; however, a new way of identifying the chill configuration was adopted. This involved the removal of the first numeral in the original identity and its replacement by the letter A, B, C, or D where:-

A represents an Aluminium double thickness single taper chill,

B represents an Aluminium tapered plate,

C represents a Cast Iron double thickness single taper chill,

D represents a Cast Iron tapered plate. Thus, the plate codes took the form XD1 etc.

The experimental matrix is illustrated in Figure 24; again each individual sample from a plate was identified by its original position in that plate using the same method as in Series I, for example, the final code for the 2¾in sample from plate XD1 is XD1003.

% Iron Content	Section		1/8in	1/4in	3/8in	1/2in
0.02	Double Thickness Single Taper	Aluminium	x	XA2	XA3	x
		Cast Iron	XC1	x	x	XC4
	Tapered Plate	Aluminium	x	XB2	XB3	x
		Cast Iron	XD1	x	x	XD4
0.11	Double Thickness Single Taper	Aluminium	ZA1	x	x	ZA4
		Cast Iron	x	ZC2	ZC3	x
	Tapered Plate	Aluminium	ZB1	x	x	ZB4
		Cast Iron	x	ZD2	ZD3	x

Figure 24.—*Illustrates the experimental matrix adopted for Series II castings.*

3.3 Casting Series III

3.3.1 Additional Experimental Details

Although at this stage, the strongest evidence for the improvement in mechanical properties was the reduction in Iron content, the commercial interest was, obviously, still centred on the possibility of improving the properties of the low purity alloys by means of effective chilling and heat treatment, sufficiently to comply with more stringent specifications. Consequently a series of plates was cast in a commercial foundry using foundry practices similar to those adopted in the earlier experimental work. The decision was made to investigate block and single taper versions of both Aluminium

and Cast Iron chills and to omit the double taper chilling technique because it was generally considered to be the least favourable. Unchilled castings of the four sections were also included for comparison. By careful selection of the commercial ingot available it was possible to cast the entire series with one composition:-

7.5% Si; 0.30% Mg; 0.09% Fe; 0.13% Ti.

Before the plates were subjected to X-radiography their faces were machined to reduce those features on the radiographs caused by uneven surfaces. Specimens were then cut from the plates in a similar manner to that previously described, but unfortunately the centre lines of the samples from the ½ in, 3/8 in and ¼ in plates were displaced by ½ in towards the end nearest the chill viz. ¼ in, 1¼ in, 2¼ in etc. This does not affect the interpretation of the results since the shift only represents the taking of specimens from positions midway between the samples in the previous two series.

3.3.2 Density Measurements

The density of these test bars was measured before heat treatment. Some difficulty was encountered in obtaining a reference specimen from which the actual specimen porosities could be calculated. Two approaches were considered; one involved the casting of a thin, very heavily chilled, section from which a small specimen was machined. The second approach was to cast a series of flat plates which were lightly rolled and then density specimens were cut from each of them. By casting these reference specimens at the same time as the experimental series any error arising from variations in composition was eliminated. The heavily chilled thin section proved to be the more satisfactory technique resulting in negligible porosity in the areas adjacent to the chill.

3.3.3 Heat Treatment

There were two important departures from previous heat treatment cycles but these did not relate to the times or temperatures of each heating stage. The first departure from the original sequence was in the bulk of the material quenched. The removal of the bars from the cast plates, obviously, greatly reduced the weight of each item for quenching. Secondly, the delay time between removing the samples from the solution treatment furnace and quenching them was shortened to between 4 and 5 seconds.

3.3.4 Nomenclature used in Series III castings

The castings were precisely identified according to the system laid out in Series I. Owing to the fact that no variation existed in the Iron content the first letter was replaced in all the castings by two letters (SM) signifying the originating foundry.

Specimens for mechanical properties were again labelled sequentially 1 – 7, although the ½in displacement of the test bars has to be taken into account.

3.4 Mechanical Test Results As-cast and Heat Treated

Round test bars were machined from the series of cast ½in, 3/8in and ¼in plates with dimensions that satisfy the formula, gauge length = 5.65 $\sqrt{S_o}$ where S_o = the original cross-sectional area, found in B.S.18. The dimensions of the test lengths of these bars are listed below:

Original plate thickness (ins.)	Test bar diameter (ins.)	Gauge length (ins.)
0.500	0.252	1.25
0.375	0.178	0.90
0.250	0.160	0.80

Flat test specimens were manufactured from the 1/8in cast plates with thicknesses of 0.10in, widths of 0.50in and gauge lengths of 1.0in.

The results of mechanical tests on the whole series of castings were considered in two ways. In the first, a sequence of histograms was produced by showing the number of specimens whose mechanical properties exceeded the properties as detailed in the Specifications for designated and undesignated locations. When the project began the relevant specification was D.T.D.5028 (Appendix II), but this has been recently superseded by Specification 2L99 (Appendix III) although, apart from some increase in the 'designated location' Proof Stress, little has been altered. The second level of consideration used regression analysis which assessed not only the "go", "no-go" situation shown in the histograms but also considered the amount by which a value exceeded a specific level. This not only provided quantitative information regarding variables which appear to have similar effects in the visual display but also the effects of varying alloy composition. There was evidence of effective feeding provided by the improvement in mechanical properties of the last specimen (No. 7) in each of the ½in (12.5mm), 3/8in (9.5mm) and ¼in (6mm) plates. As a result it was thought advisable to remove these results from the regression analysis so that a better fit may be obtained but the results were retained in the histograms. Also, because of the small specimen size and the length of time involved only one proof stress value was determined from each of the ¼in (6mm) and 1/8in (3mm) plates. The regression equations, containing all variables significant at the 5% level, and regression coefficients are recorded in Tables VII, VIII and IX. Results were examined first for each section size independently and then all results were combined to reveal any influence of section thickness.

Key to the Nomenclature used in the Histograms.

UN. refers to Unchilled sections.

BL. refers to Block chilled sections.

S.T. refers to Single Taper chilled sections.

D.T. refers to Double Taper chilled sections.

D.T.S.T. refers to Double Thickness Single Taper chilled sections.

T.P. refers to Tapered Plate chilled sections.

C.I. refers to Cast Iron chill materials.

Alum. refers to Aluminium chill materials.

 refers to Designated Area results.

 refers to Undesignated Area results.

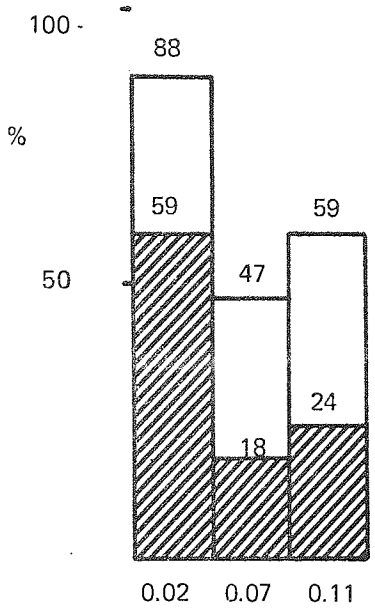

(a) Effect of Iron Content (%)

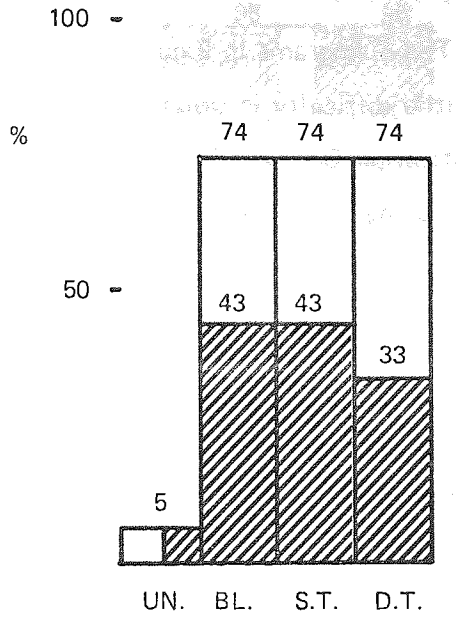

(b) Influence of Chill Technique.

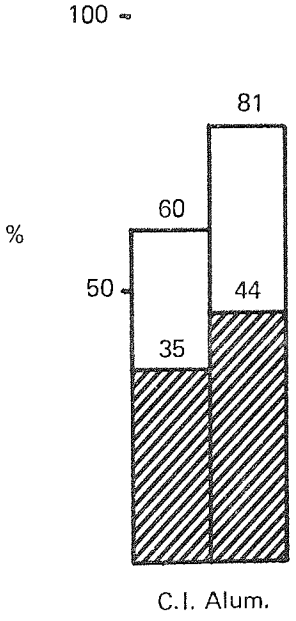

(c) Effect of Chill Material.

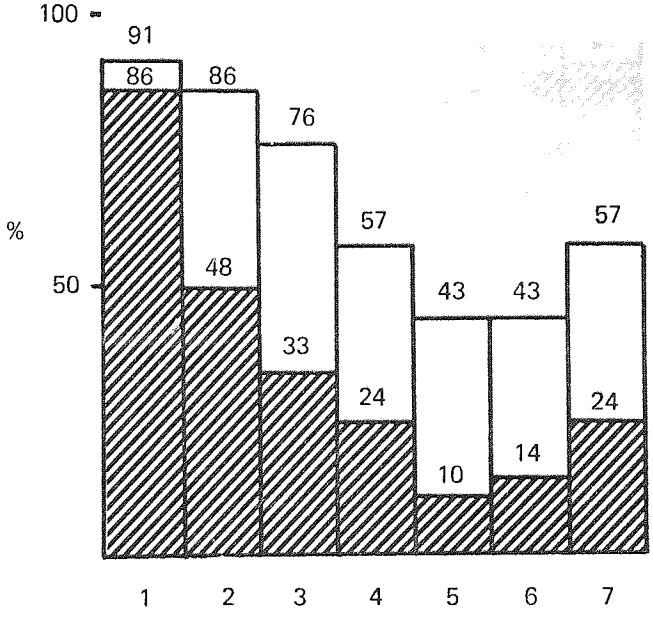

(d) Effect of Position - numbers referred to in text.

Figure 25.—*The influence of the 4 main variables on the % of Series I samples, from the ½in plates, which exceed the specified Elongation (D.T.D.5028) in Undesignated (clear) and Designated (shaded) locations.*

Series I: ½in Section - Elongation Results

There was general agreement between the regression analysis results (Table VII) and the histograms (Figure 25). If one considers the factors in the order of their visual presentation it is evident that there was a definite downward trend in the number of satisfactory samples with the higher Iron contents. This result was borne out by the regression equation in which a high Iron value produced a greater negative term. The reversal of the trend shown by the 0.07% Iron specimens could be attributable to variations in heat treatment and porosity. For meeting minimum standards at designated locations, the histograms indicated block and single taper chilling techniques were the most satisfactory but no conclusion could be made on the best chilling method for standards at undesignated regions. The most favourable chill shape revealed by the regression analysis was the block. There was no doubt as to which was the most effective chill material; both analysis approaches showed that Aluminium chills produced the better properties. Both approaches also indicated the unfavourable trend of the results with increased distance from the chilled end. But, as mentioned above, evidence did exist to suggest a feeding effect. This was displayed in the histogram by the increase in the number of satisfactory results (designated and undesignated) at distances close to the feeder end.

Series I: ½in Section - 0.2% Proof Stress Results

The histograms in Figure 26 were included to illustrate that there was little difficulty in obtaining the prescribed 0.2% Proof Stresses in Specification D.T.D.5028. However, under the experimental conditions at this stage of the investigation the 0.2% Proof Stress results did not comply quite as favourably with the increased values found in Specification 2L99 (Appendix III), (Figure 27).

SERIES I
½in SECTIONS
PROOF STRESS (D.T.D.5028)

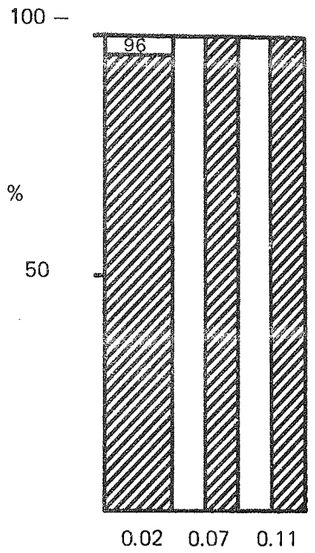

(a) Effect of Iron Content (%)

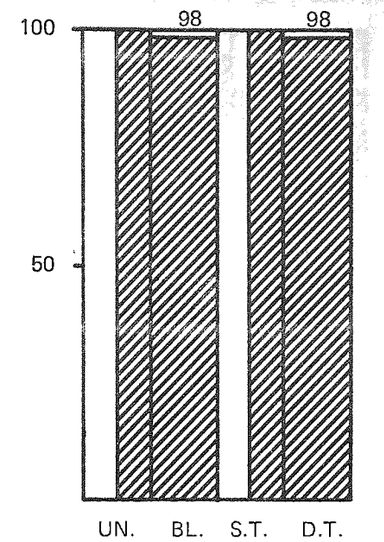

(b) Influence of Chill Technique

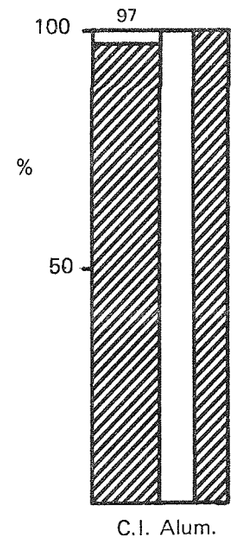

(c) Effect of Chill Material.

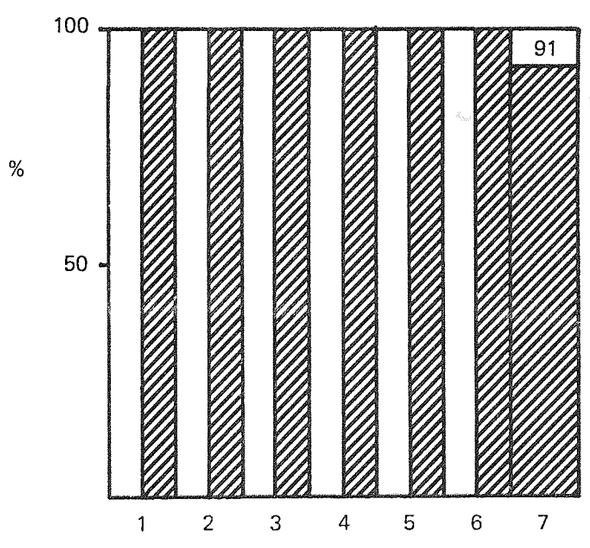

(d) Effect of Position - numbers referred to in text.

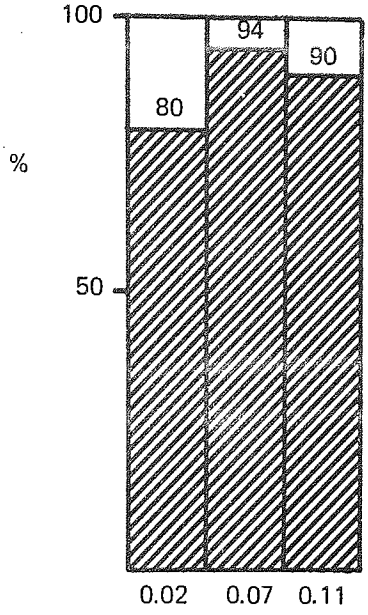

(a) Effect of Iron Content (%)

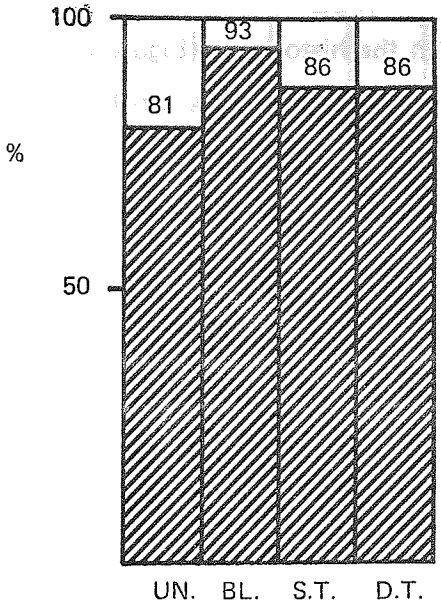

(b) Influence of Chill Technique.

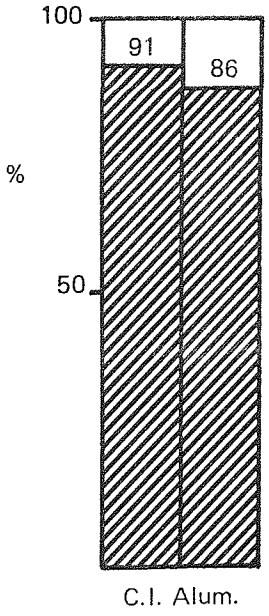

(c) Effect of Chill Material.

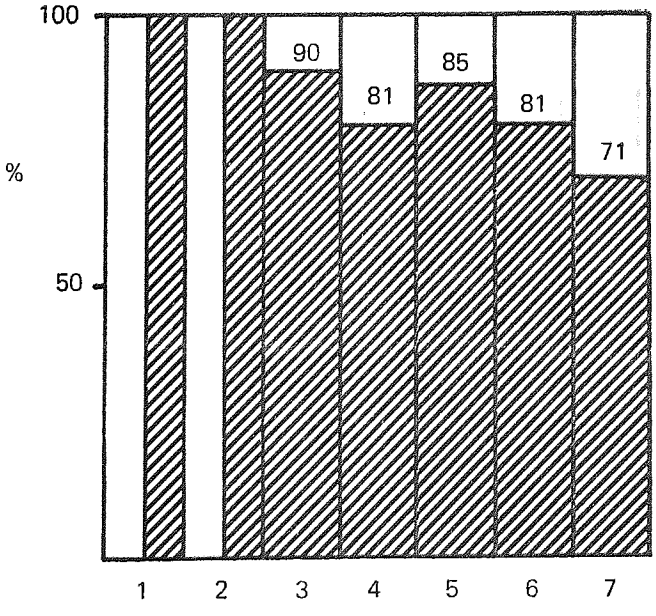

(d) Effect of Position - numbers referred to in text.

Figure 27.—*The influence of the 4 main variables on the % of Series I samples, from ½in plates which exceed the specified 0.2% Proof Stress (B.S.S. 2L99) in Undesignated (clear) and Designated (shaded) locations.*

Series I: ½in Section - Tensile Strength Results

In the histograms (Figure 28) very little can be derived from the undesignated location results but some indications of the conditions that favour designated area results can be made. The regression equation in Table VII defined which chill shape and material was most beneficial; it also included factors that revealed the influences of chemical composition and the interactions between some of the constituents. Again both techniques showed Iron to be detrimental. Figure 28 indicates a slight preference for single taper chilling but the regression equation favours block chilling, while both methods agree that better properties were obtained when Aluminium chills were used. The effect that sample positions had on tensile properties was similar to that of elongation but there was no evidence of feeding causing a rise in values at the feeder end. Finally, the regression equation revealed that higher levels of Magnesium and Silicon increased the tensile strength.

SERIES I
½in SECTIONS
TENSILE STRENGTH

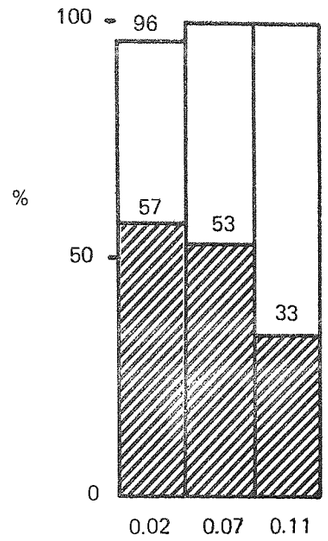

(a) Effect of Iron Content (%).

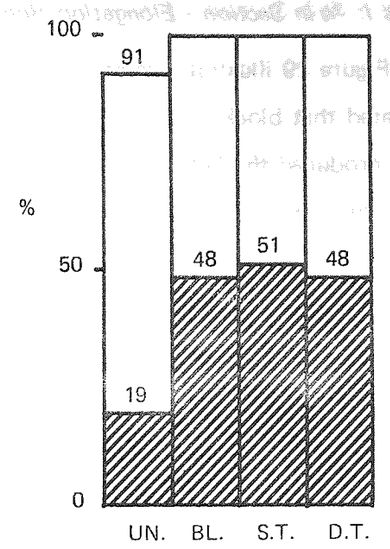

(b) Influence of Chill Technique.

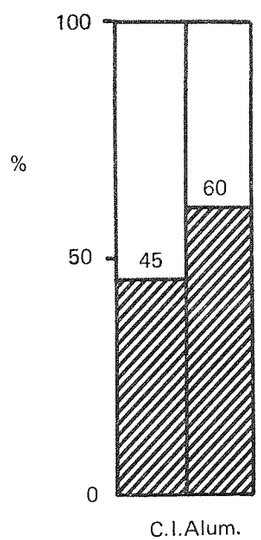

(c) Effect of Chill Material.

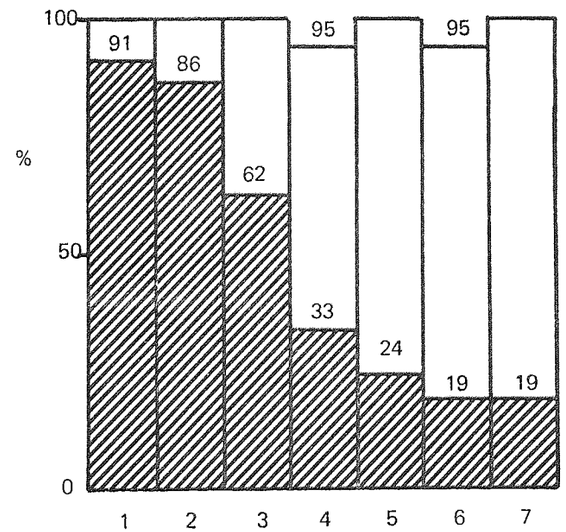

(d) Effect of Position - numbers referred to in text.

Series I: 3/8 in Section - Elongation Results

Figure 29 illustrates some conclusive results in that the histograms indicated that block chilling was the most advantageous and that Aluminium chills produced the better mechanical properties. Again the trend was for a reduction in properties as the sample position moved away from the chilled end. There was, however, evidence of the feeding effect in the improvement in number of specimens exceeding the prescribed properties at the feeder end. The regression analysis selected the block chill as the first choice for chilling but it did indicate that single taper chilling was a second practical method. Further agreement was noted regarding the effect increased Iron content had on the mechanical properties, both techniques suggesting a reduction in properties with increase in Iron level. The regression analysis also predicted a decrease in the value of properties with increased distance from the chilled end.

SERIES I
3/8 in SECTIONS
% ELONGATION

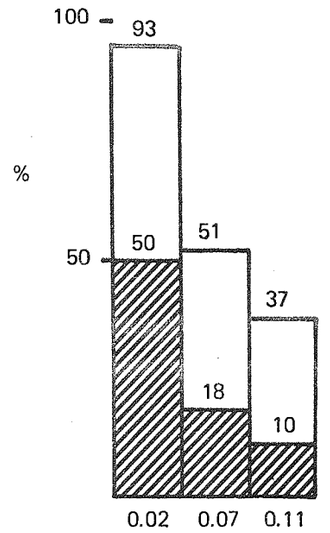

(a) Effect of Iron Content (%).

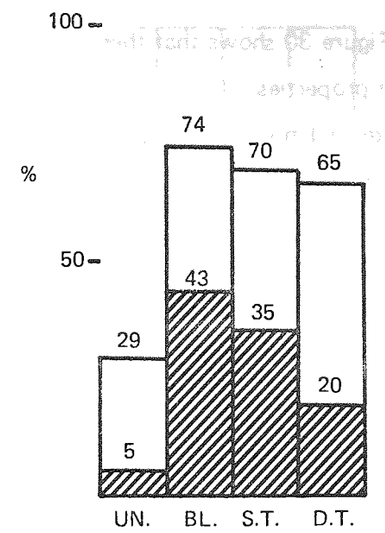

(b) Influence of Chill Technique.

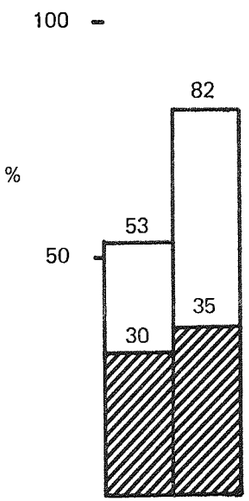

(c) Effect of Chill Material.

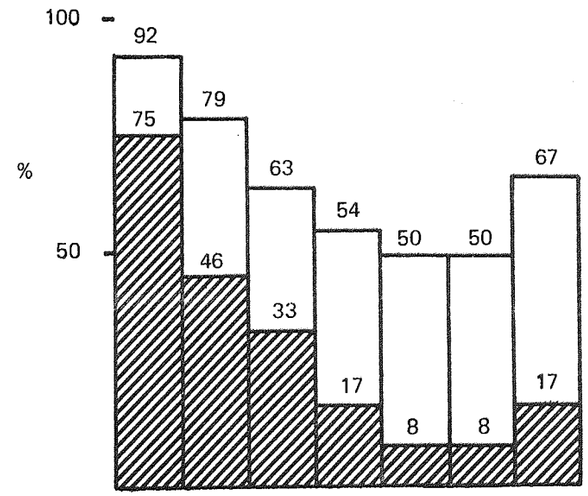

(d) Effect of Position - numbers referred to in text.

Series I: 3/8 Section - Tensile Strength Results

Figure 30 shows that there was no difficulty in producing undesignated tensile properties. To achieve designated area properties the histograms indicate that the most satisfactory chilling technique was the single taper method. However, the regression equation showed no evidence for any particular chill shape (Table VII). Both methods suggest Aluminium as the better chill material, and both detect a downward trend in mechanical properties with increasing distances from the chill end. The effects of chemical composition were similar to those revealed in the previous tensile regression, an increased Iron content produced a lowering of mechanical properties, whereas, an increase in the other two elements (Magnesium and Silicon) elevated the tensile strength values.

The results of all the samples exceeding the designated location specification were sorted and two additional regression analyses performed on the data. The analyses showed:

(a) Aluminium chills were more satisfactory in producing designated elongations.

(b) The block chill was the most successful chill technique for elevating tensile properties.

SERIES I
3/8 in SECTIONS
TENSILE STRENGTH

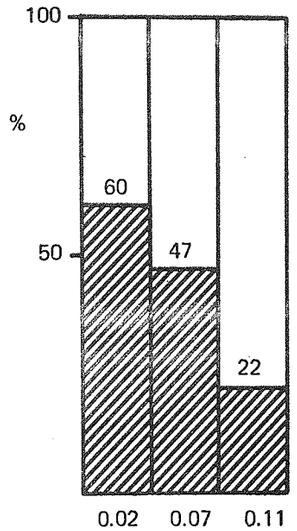

(a) Effect of Iron Content (%).

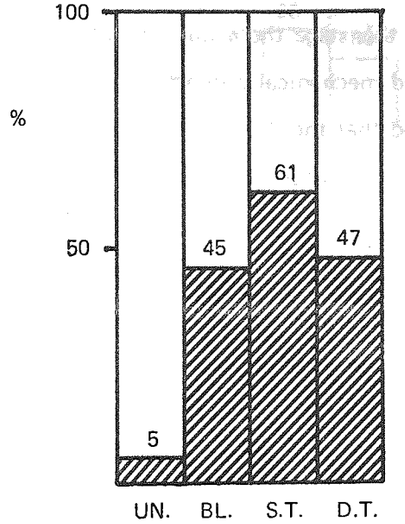

(b) Influence of Chill Technique.

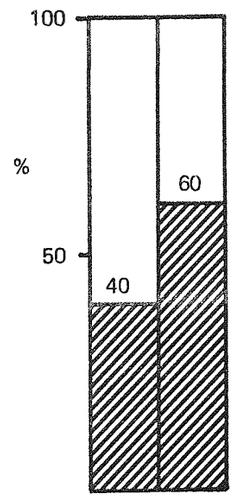

(c) Effect of Chill Material.

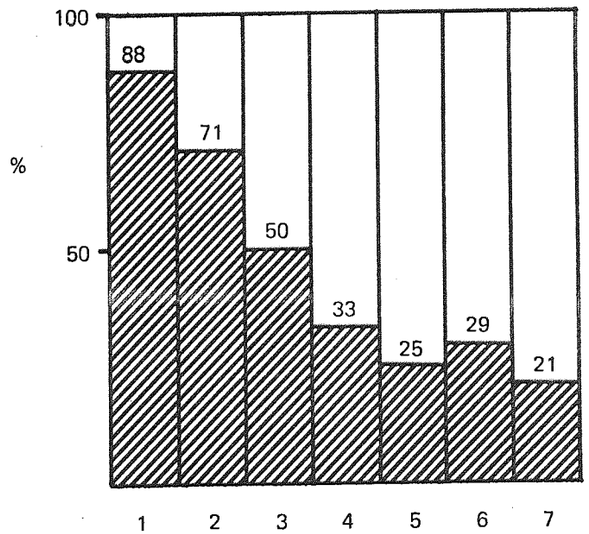

(d) Effect of Position - numbers referred to in text.

Series I: ¼ in Section - Elongation Results

At this stage there was a significant change in the conditions favouring increased mechanical properties. The results in the previous two sections indicated that the Aluminium block chill method was the one most likely to produce satisfactory results. This system, however, appeared less suitable for thinner cast sections where the taper chill shape was preferred. In the histograms (Figure 31) both of the taper chill techniques produced better results than the block chill. This observation, relating to chill shape, was also evident in the regression analysis which showed the single taper chill to be best. Both the histograms and the regression equations suggested that Cast Iron was superior to Aluminium as the chill material. The two methods again showed that mechanical properties decreased with increasing distances from the chilled end. There was evidence of some degree of feeding from the improvement in elongation of the samples nearest the feeder. The trend of reduced mechanical properties with increased Iron contents was maintained although it did appear from the histograms that the effect was less pronounced.

SERIES I
¼ in SECTIONS
% ELONGATIONS

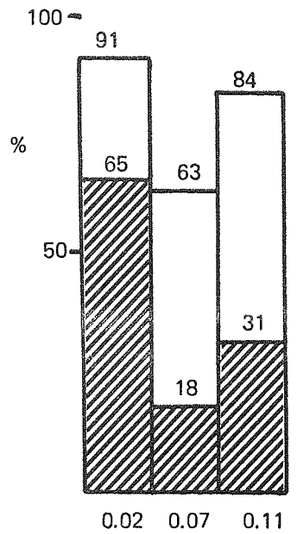

(a) Effect of Iron Content (%)

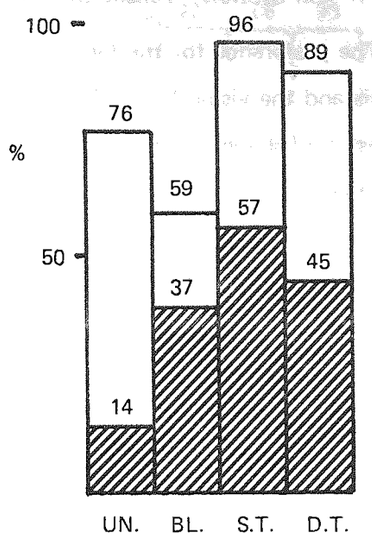

(b) Influence of Chill Technique.

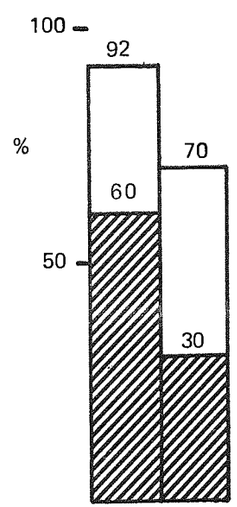

(c) Effect of Chill Material.

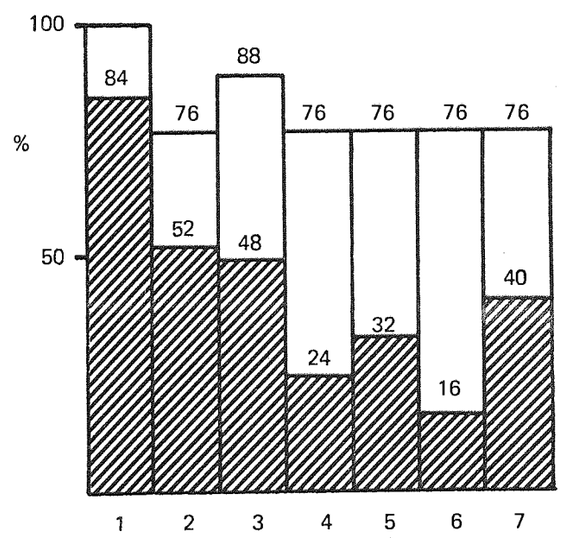

(d) Effect of Position - numbers referred to in text.

Series I: ¼in Section - Tensile Strength Results

The preference for the taper chill method was continued. The regression analysis and the visual form (Figure 32) both indicated the double taper as the best chill shape. While the histogram indicated that designated area properties were more easily achieved using Aluminium chills, the regression analysis suggested Cast Iron as the more satisfactory material. The effect of specimen location was evident in the histogram and the regression equation. Increased Iron content produced a reversal of previous observations in that the histogram and the regression equation both indicated a slight improvement in tensile properties. A similar conclusion was made concerning increased Magnesium contents.

SERIES I
¼in SECTIONS
TENSILE STRENGTH

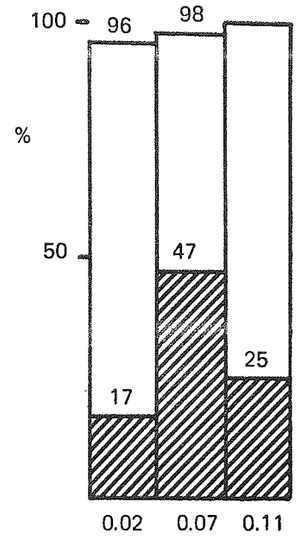

(a) Effect of Iron Content (%)

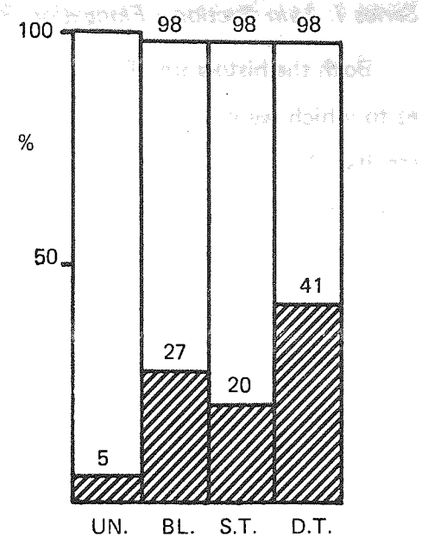

(b) Influence of Chill Technique.

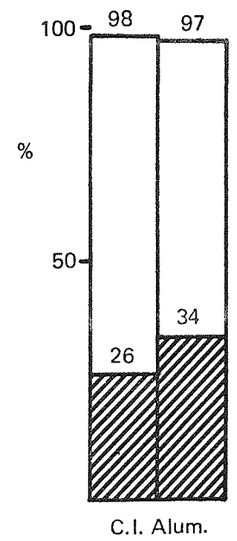

(c) Effect of Chill Material.

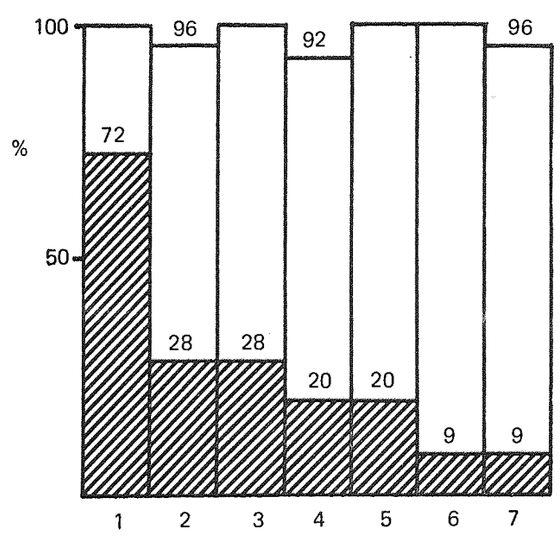

(d) Effect of Position - numbers referred to in text.

Series I: 1/8in Section - Elongation Results

Both the histograms (Figure 33) and regression equation were in agreement as to which were the important factors and in what way they influenced the results. Aluminium was favoured as the chill material and the chill shape suggested was the single taper. Neither analytical technique, however, took into consideration the fact that the total number of mis-runs when Aluminium chills were used was approximately 25% greater than for Cast Iron chilling, thus greatly diminishing the advantage of an Aluminium chill. The influence of Iron content on elongations was similar to the previous observations, an increase in Iron level resulted in a decrease in the number of samples exceeding both designated and undesignated area values. The influence of sample location on the properties obtained was not quite so clear. It was expected that feeding difficulties would be encountered in such thin sections resulting in a less pronounced trend in the results. This was certainly the case for designated properties. In the undesignated results the decrease in elongation with increase in specimen distance was again observed but there was a remarkable reduction in properties in specimens taken approximately 4in (102mm) from the chilled end.

SERIES I
1/8 in SECTIONS
% ELONGATION

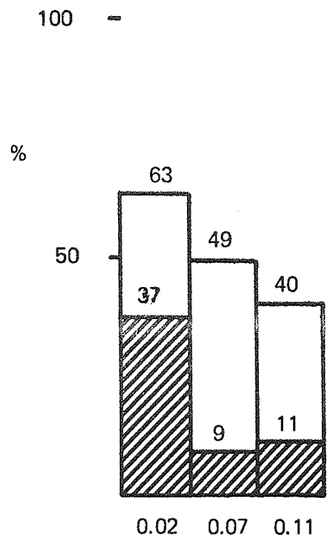

(a) Effect of Iron Content (%).

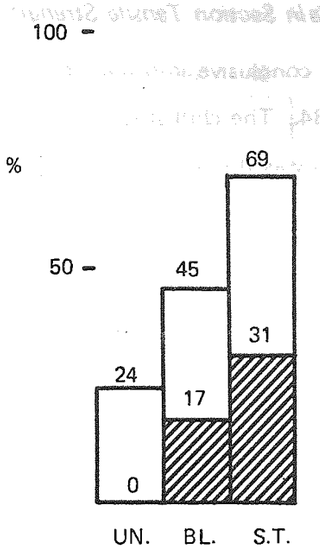

(b) Influence of Chill Technique.

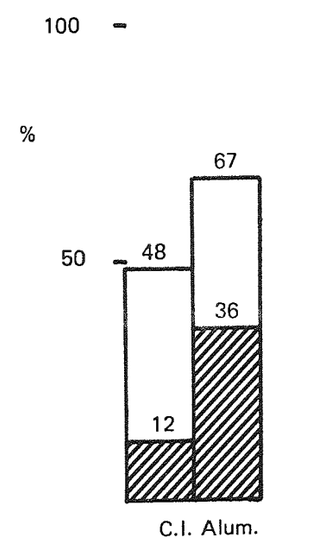

(c) Effect of Chill Material.

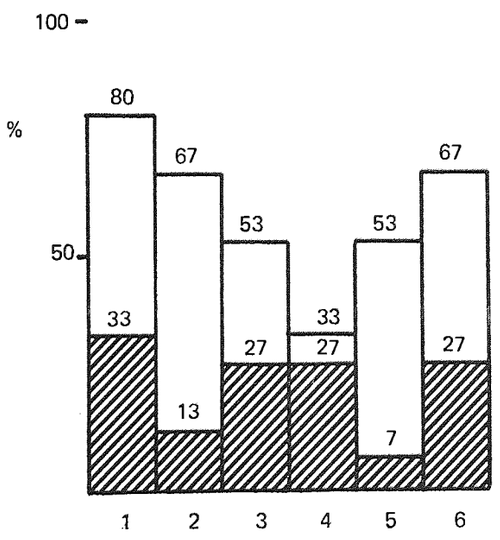

(d) Effect of Position - number referred to in text.

Series I: 1/8in Section Tensile Strength Results

Little conclusive information was gained from the histograms illustrated in Figure 34. The chill shape favoured by examination of the designated area results was the block although there was very little difference between the two techniques tried. The chill material preferred was Cast Iron. No information was available from the regression analysis concerning chill shape but the equation did indicate an advantage if Cast Iron was used as the chill material. A similar trend, to that first noted in the tensile results from the ¼in (6mm) section, was noticed where the mechanical properties were improved by increased Iron contents. This observation was reinforced by the regression analysis. The results obtained from variations in specimen locations were similar to those determined in the previous three sections.

SERIES I
1/8 in SECTIONS
TENSILE STRENGTH

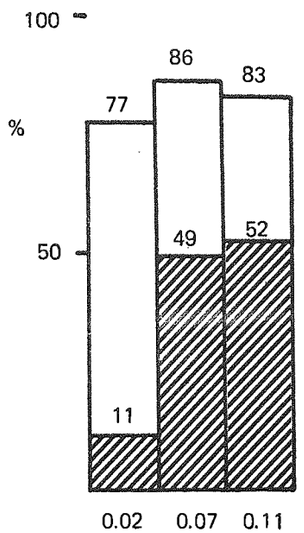

(a) Effect of Iron Content (%).

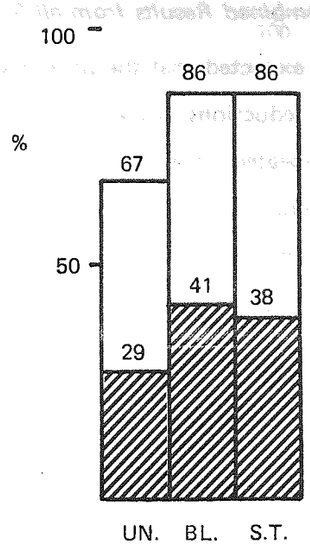

(b) Influence of Chill Technique.

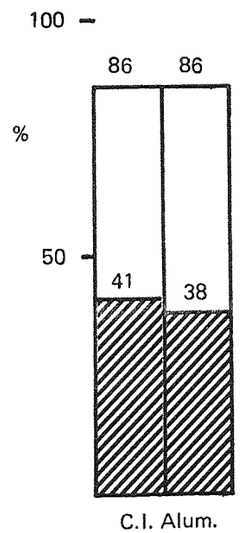

(c) Effect of Chill Material.

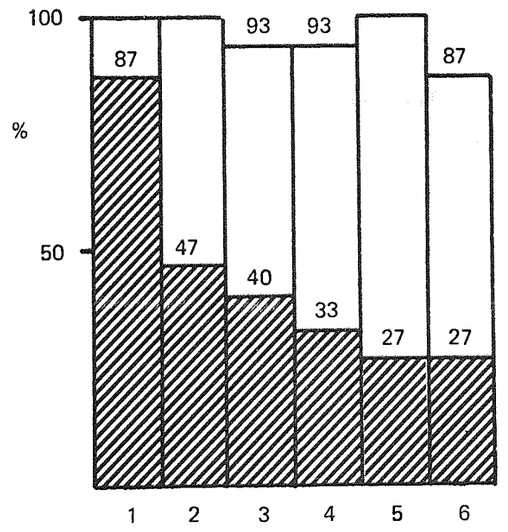

(d) Effect of Position - numbers referred to in text.

Series I: Combined Results from all Sections - Elongation Results

It was expected that the phenomenon of increasing Iron contents resulting in reductions in the elongations for the individual sections, would be repeated when the results were combined. This was evident in the histogram (Figure 35) but less pronounced in the regression analysis. There was, however, agreement between the two analytical techniques as to the best chill shape; both agreed that the single taper produced the best overall results. There was on the other hand, disagreement about the better chill technique, the regression suggested the block chill and the histogram the double taper. The histogram showed for the designated area results, Aluminium as the better chill material, whereas, Cast Iron was slightly more favourable for the undesignated region results. No definite conclusion was revealed by the regression analysis but as the results from each decreasing cast section were added a distinct swing was noted away from favouring Aluminium chills for the thicker sections (above ¼in) to Cast Iron with the thinner sections.

The regression equation also provided information regarding analysis (in addition to Iron). Silicon had no effect upon elongation but increased Magnesium contents did tend to reduce elongation slightly. With the well defined behaviour of mechanical properties with distance away from the most chilled end in the separate sections it was not surprising that it was also expressed in this equation.

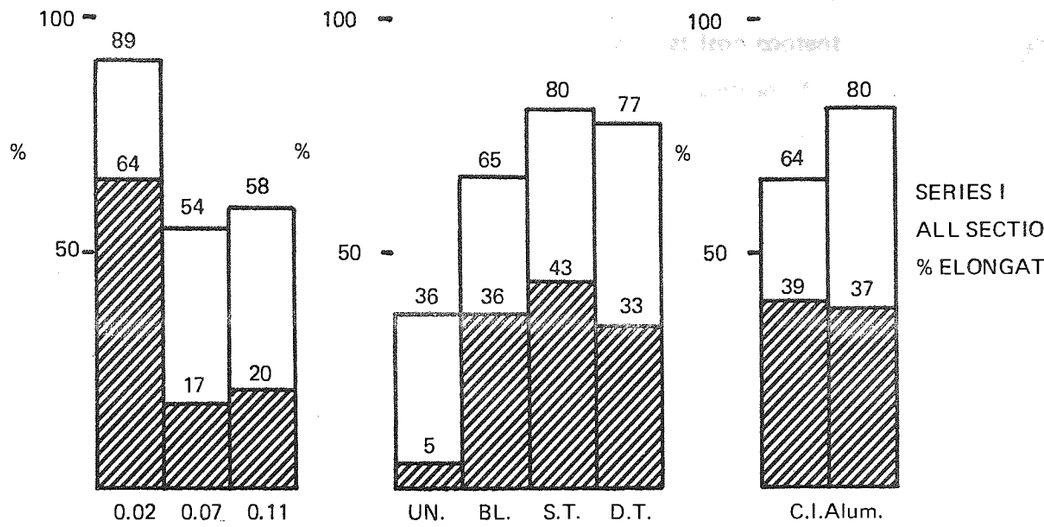

Figure 35.—*The influence of a, b and c on the % of all Series I samples which exceed the specified Elongation (D.T.D.5028) in the Undesignated (clear) and Designated (shaded) locations.*

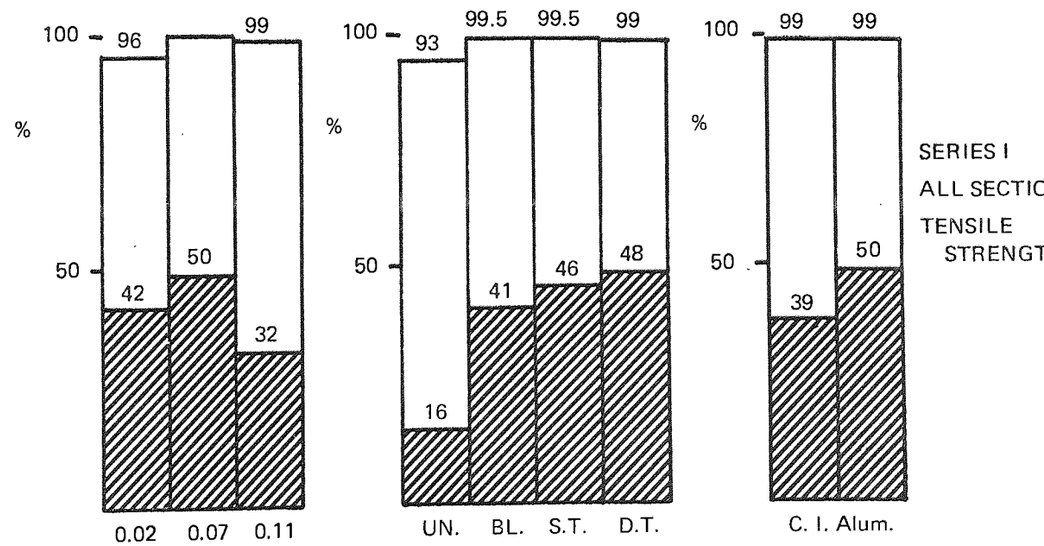

Series I: Combined Results from all Sections - Tensile Results

Although a reversal, in the trend showing the effect that Iron content had on the tensile properties, was experienced during the comparison of separate cast sections, both the regression analysis and the designated area histogram (Figure 36) indicated an overall reduction in mechanical properties with increased Iron contents. For designated area tensile properties the histogram indicated a preference for taper chills, particularly the double taper. There was little difference between any of the chill techniques when undesignated properties were considered. Aluminium was favoured as the chill material by both the regression equation and the designated area histogram.

In addition, the equation provided information on chemical analysis and section. The tensile properties were slightly improved with increased section, Silicon and Magnesium.

Series II

The visual presentation of the Series II results was made to illustrate the effect that two additional chill shapes (in the form of tapered plates and double thickness single tapers) had on the mechanical properties of all the cast sections. Both chill materials were again examined but the number of castings was reduced by adopting a partial replicate. The designated location tensile results were particularly disappointing and this is attributed to an unplanned variation in heat treatment.

Combined Results from all Sections - Elongation Results

The histograms in Figure 37 illustrate some conclusive results. For good elongation values the double thickness taper chill was preferred to the taper plate. The regression analysis, Table VIII, supported this selection but it did not reveal any preference for the chill material whereas the histograms indicated Aluminium to be the better choice of chill metal. Additional information from the regression equation appertaining to section thickness, specimen location, Iron and Silicon contents was also available. An increase in either Iron or Silicon contents or a decrease in section thickness was accompanied by a reduction in elongation. Finally, the further the test-piece was away from the more chilled end of the plate the smaller the elongation.

Combined Results from all Sections - Tensile Strength Results

The illustrations (Figure 38) for improvements to designated tensile properties show that increased strengths were achieved using the taper plates. Only a marginal difference was noted between the chill techniques for undesignated location results. Neither regression analysis nor histograms revealed any significant difference in the effect of chill material. For un-designated location tensile strength results Aluminium was favoured as the chill material but Cast Iron was preferred for the designated location results. The analysis, Table VIII, preferred taper plate chilling. Infor-

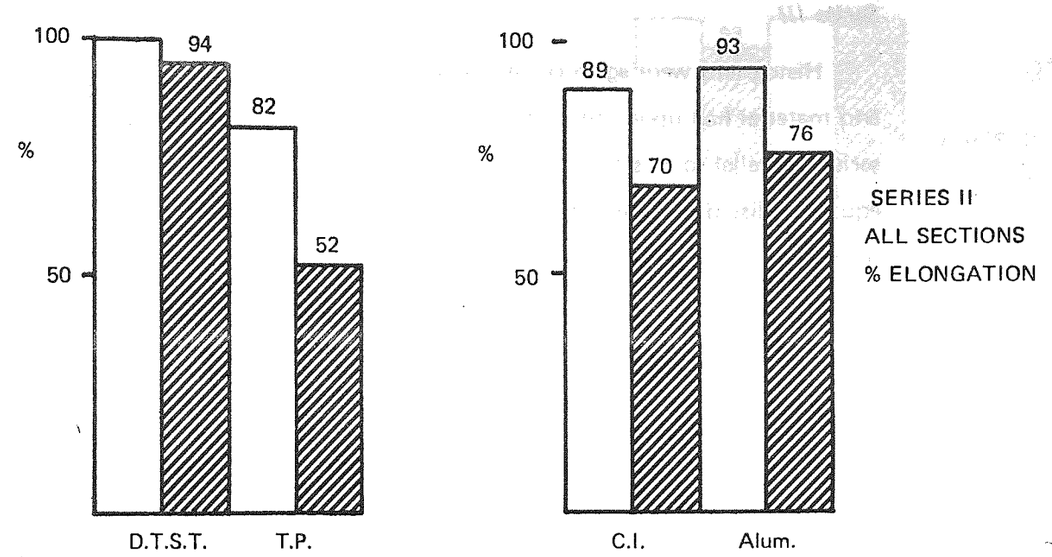

(a) Influence of Chill Technique. (b) Effect of Chill Material.

Figure 37.—*The influence of Chill Shape and Material on the % of all Series II samples which exceed the specified Elongation (D.T.D.5028) in the Undesignated (clear) and Designated (shaded) locations.*

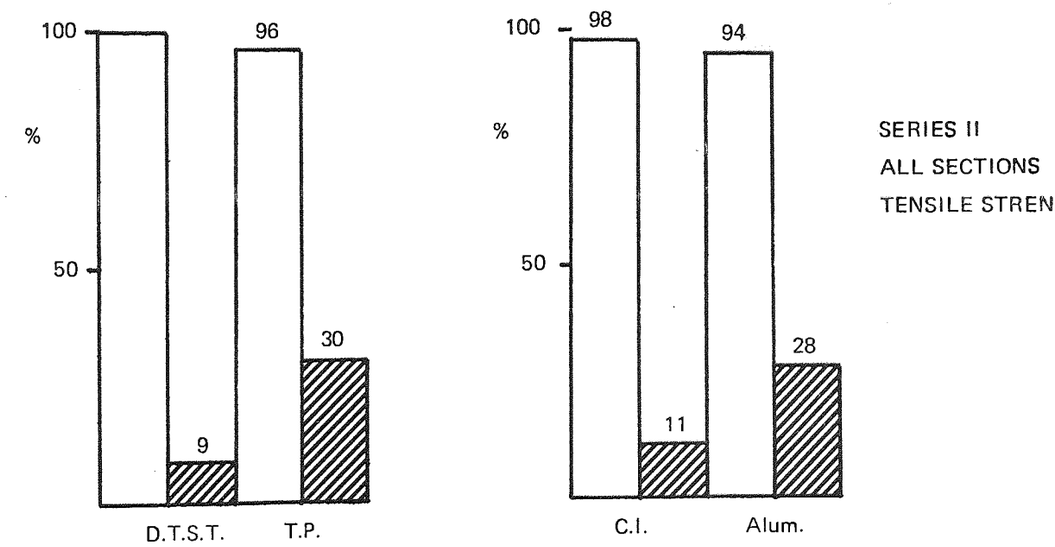

(a) Influence of Chill Technique. (b) Effect of Chill Material.

Series III

Histograms were again constructed to illustrate the effects chill shape and material had upon the mechanical properties achieved in this casting series. Parallel to this form of presentation was a sequence of regression equations listed in Table IX. The first conclusion prompted by the histograms is the degree of improvement in mechanical properties in this series, particularly in the designated area results. Because of this development in properties it was not worthwhile to extract information from histograms which differentiate on the basis of specimen position.

Series III: ½in Section - Elongation Results

According to the histograms (Figure 39) there was very little, if anything, to choose between chill techniques or between chill materials.

The quantitative results shown by the regression analysis indicated a preference for Aluminium chills, but did not distinguish on the basis of chill shape. The equation did, however, detect a gradual decrease in properties away from the chilled end.

Series III: ½in Section - Tensile Strength Results

The histograms (Figure 40) showed that all variants in chilling technique produced the required mechanical properties. 100% undesignated location minima were achieved even in the unchilled section.

The regression equation (Table IX) recorded a preference for the block method of chilling but did not differentiate between the chill materials. Again, the properties were depressed in specimens with locations away from the more chilled end.

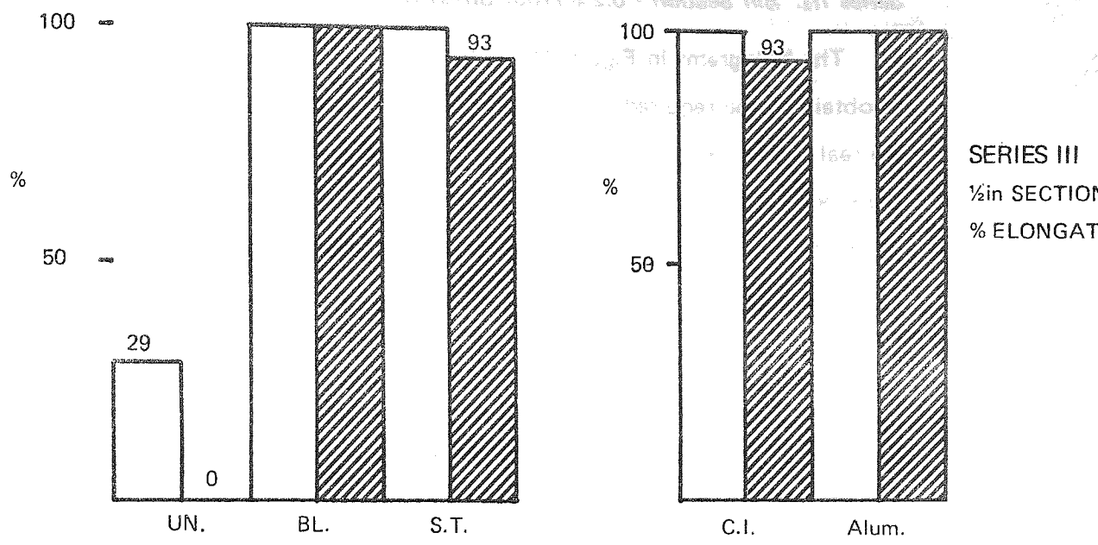

(a) Influence of Chill Technique.

(b) Effect of Chill Material.

Figure 39.—*The Influence of Chill Shape and Material on the % of Series III samples, from the ½in plates, which exceed the specified Elongation (D.T.D.5028) in the Undesignated (clear) and Designated (shaded) locations.*

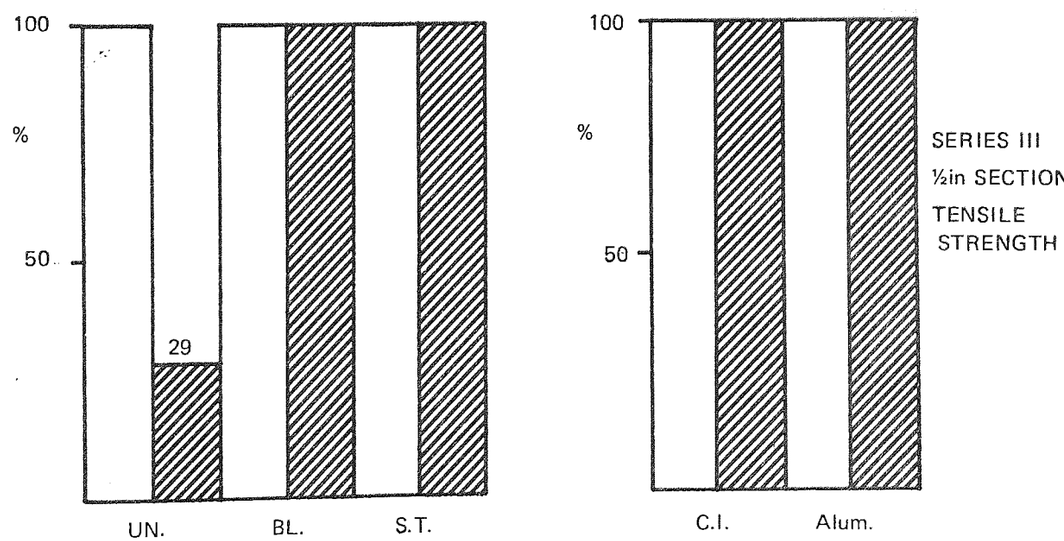

(a) Influence of Chill Technique.

(b) Effect of Chill Material.

Series III: ½in Section - 0.2% Proof Stress Results

The histograms in Figure 41 illustrate that there was little difficulty in obtaining the required 0.2% proof stresses in Specification D.T.D.5028. No real reason can be found as to why all the unchilled results satisfy the specification while single taper chilled specimens fail to produce 100% satisfactory designated location results. Similar histograms were obtained when the proof stress results were compared to Specification B.S.S.2L99 (Appendix III).

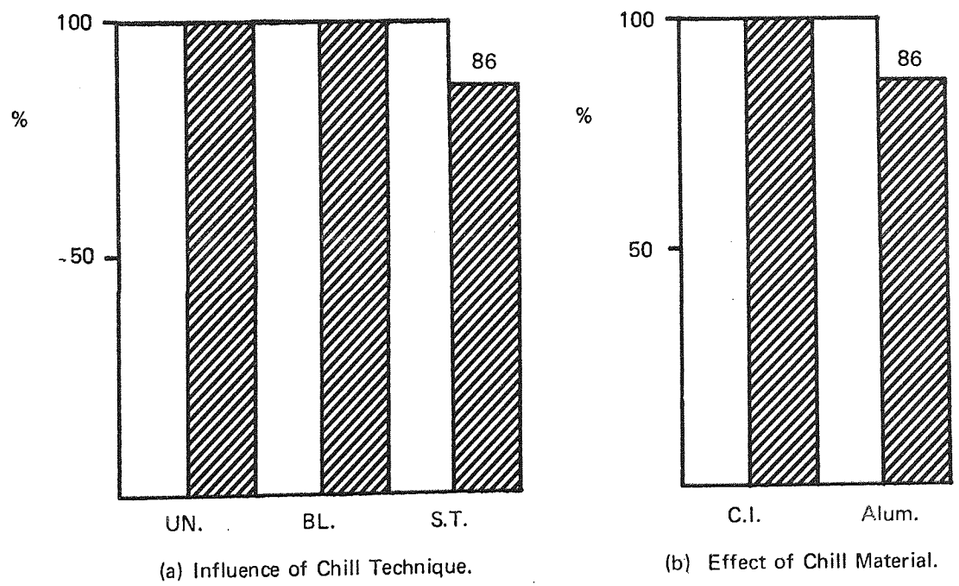

Figure 41.—*Influence of Chill Shape and Material on the % of Series III samples, from ½in plates, which exceed the specified 0.2% Proof Stress (D.T.D. 5028) in the Undesignated (clear) and Designated (shaded) locations.*

Series III: 3/8 in Section - Elongation Results

The regression analysis (Table IX) and histograms (Figure 42) failed to agree in predicting the better chill shapes. Nevertheless, the histogram method indicated that Cast Iron was favoured as the better chill material. The histogram suggested the single taper chill as the marginally better technique by virtue of the fact that it produced the slightly better undesignated area properties. The regression analysis, on the other hand, included weighting and predicted block chilling. The observation relating to specimen location was again apparent in the regression analysis.

Series III: 3/8 in Section - Tensile Strength Results

There was no problem in achieving the undesignated location properties (Figure 43). The chill technique showing the better results for the designated tensile strengths was the single taper. This was followed by the unchilled system. The linear regression analysis also favoured the taper chill. Both analytical methods suggested Aluminium as the better chill material and the equation repeated the effect of specimen location on mechanical properties.

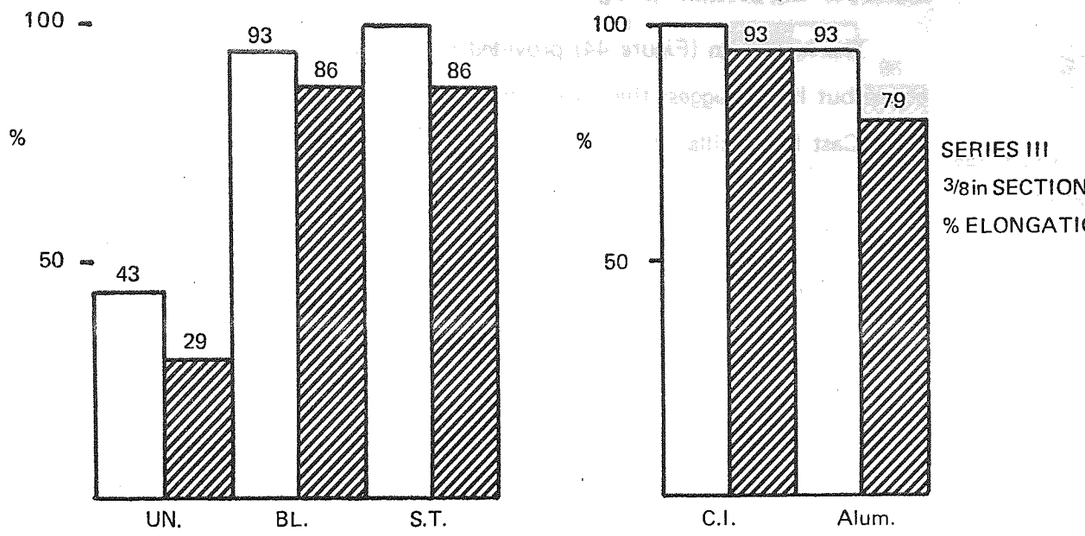

Figure 42.—*The Influence of Chill Shape and Material on the % of Series III samples, from the 3/8 in plates, which exceed the specified Elongation (D.T.D.5028) in the Undesignated (clear) and Designated (shaded) locations.*

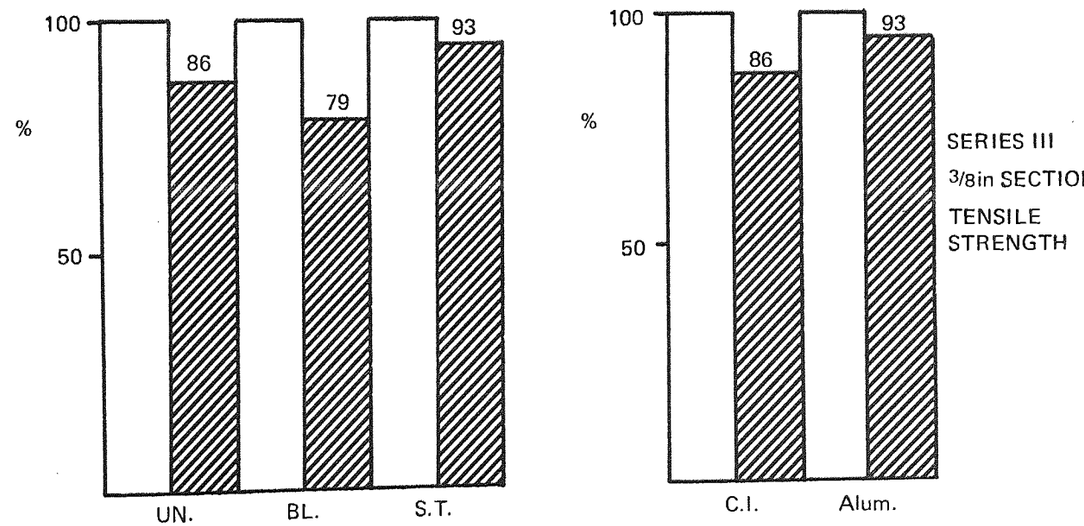

Series III: ¼in Section - Elongation Results

The histogram (Figure 44) provided no indication as to the better chill shape but it did suggest that marginally higher properties would be achieved using Cast Iron chills. The regression equation favoured the block chill.

Series III: ¼in Section - Tensile Strength Results

Both techniques (Figure 45, Table IX) were in accord regarding chill material, Cast Iron being the first choice.

As with previous observation on results for this section thickness, the single taper chilling system was preferred although only marginally.

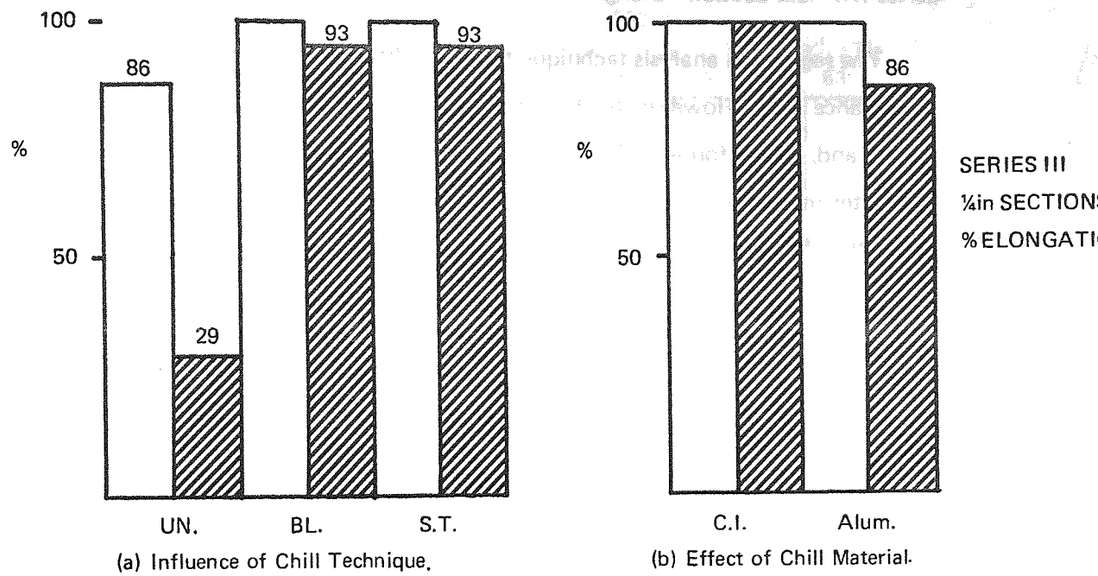

Figure 44.—*The Influence of Chill Shape and Material on the % of Series III samples, from the ¼in plates, which exceed the specified Elongation (D.T.D.5028) in the Undesignated (clear) and Designated (shaded) locations.*

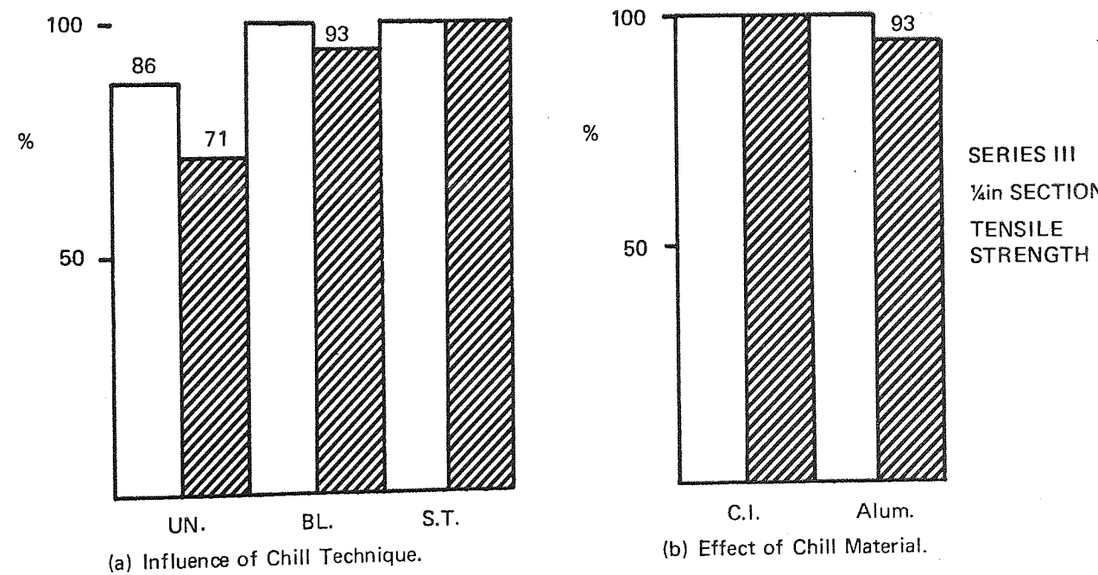

Series III: 1/8 in Section - Elongation Results

The regression analysis technique failed to obtain any factors at the 5% significance level. However, the histograms (Figure 46) favour a taper chill system and, as was found in Series I, Aluminium was observed to produce the better mechanical properties but neither analytical method accounted for plates that failed to run fully.

Series III: 1/8 in Section - Tensile Strength Results

No definite conclusions can be drawn from either set of results. From the histograms (Figure 47) it can be seen that it would be very unlikely if any factors were significant in the regression analysis. Any chilling technique appears to be successful.

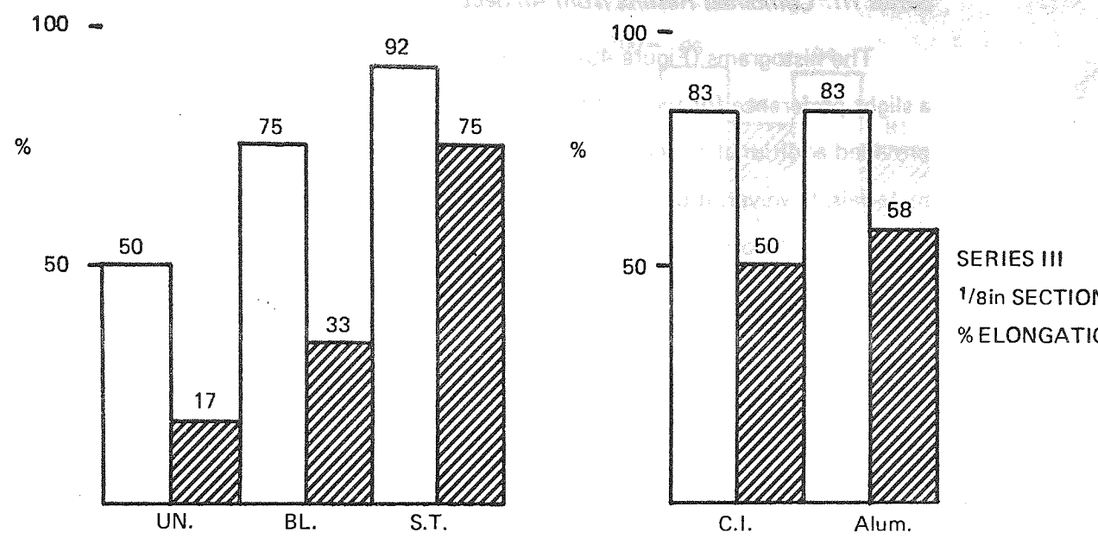

(a) Influence of Chill Technique.

(b) Effect of Chill Material.

Figure 46.—*The Influence of Chill Shape and Material on the % of Series III samples, from the 1/8 in plates, which exceed the specified Elongation (D.T.D.5028) in the Undesignated (clear) and Designated (shaded) locations.*

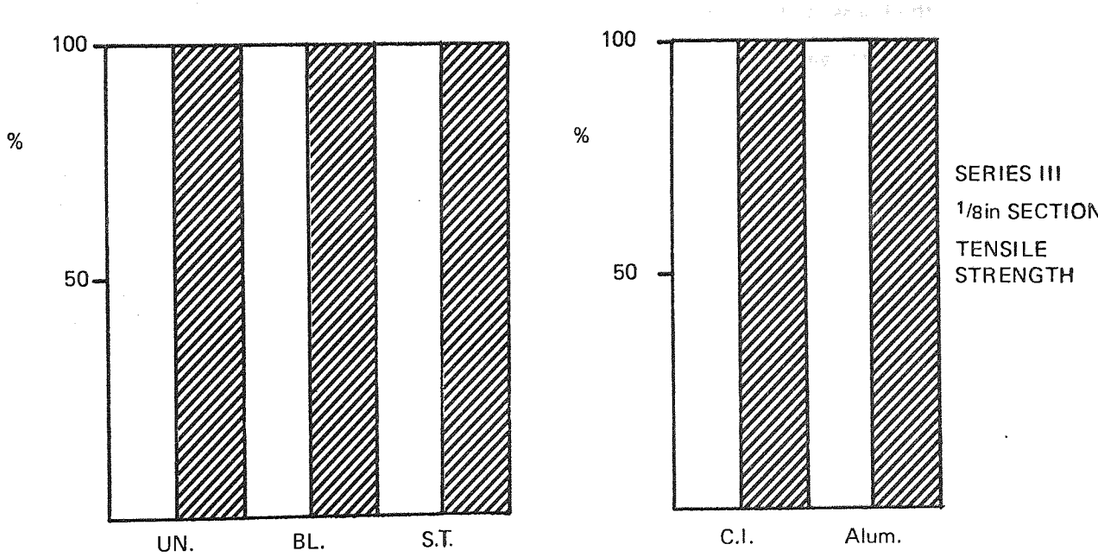

(a) Influence of Chill Technique.

(b) Effect of Chill Material.

Series III: Combined Results from All Sections - Elongation Results

The histograms (Figure 48) for the combined Series III results indicated a slight preference for the Cast Iron taper chill system. Thr regression analysis provided additional evidence for the small difference between the chill materials; however, it did conclude that Cast Iron was preferable. The analysis, on the other hand, disagreed with the histograms concerning the chill shape, it favoured the block chill. In addition, the regression equation indicated the influence that section and sample position had upon the elongation. Both increased distances and decreased section thicknesses reduced the elongation.

Series III: Combined Results from All Sections - Tensile Strength Results

The visual representations (Figure 49) of all the tensile results failed to point to any conclusion regarding the chill material. It did, however, indicate that the single taper chilling technique improved slightly, the designated properties. The regression analysis (Table IX) provided information on the chill material but not on the shape. The equation favoured Aluminium chills. Further information concerning the effect that section thickness, and distance away from the chilled end, had upon the tensile strength was also available from the regression. The equation indicated that increased sections and sample distances decreased the tensile strength.

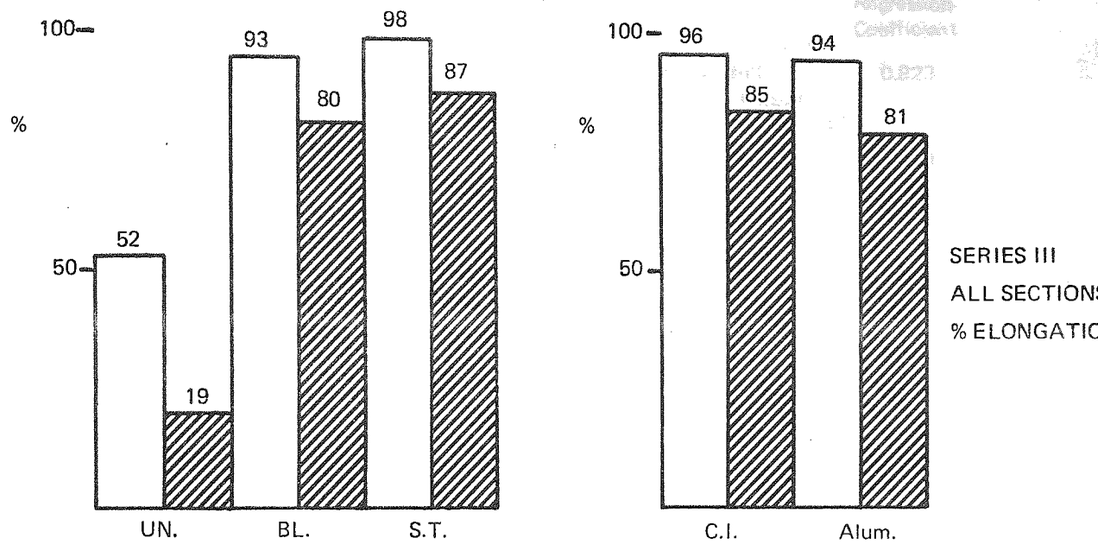

(a) Influence of Chill Technique.

(b) Effect of Chill Material.

Figure 48.—*The influence of Chill Shape and Material on the % of All Series III samples which exceed the specified Elongation (D.T.D.5028) in the Undesignated (clear) and Designated (shaded) locations.*

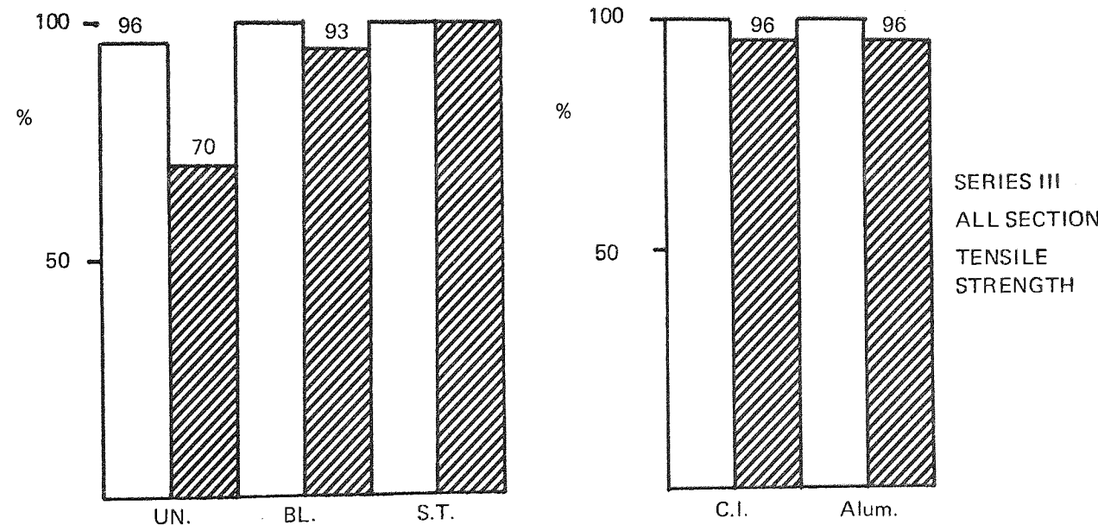

(a) Influence of Chill Technique.

(b) Effect of Chill Material.

TABLE VIII.—*Multiple Linear Regression Analysis of All Series II Experimental Results.*

Section	Dependent Variable	Regression Equation	Regression Coefficient
All combined	Elongation	4.20 x (log Section cast) + 3.55 x (2, if Double Thickness Single Taper chill) - 3.93 x (log Distance from most chilled end) - 0.06 x (log % Fe x (% Si)^2) + 1.82	0.785
All combined	Tensile Strength	-41.1 x (Section cast)^3 - 10.4 x (log Section cast) + 0.08 x (Distance from most chilled end)^2 - 0.72 x (Distance from most chilled end) + 0.44 x (2, if Tapered Plate chill) + 0.57 x (Section cast x (% Si)^2) + 4.22	0.742

TABLE IX.—*Multiple Linear Regression Equations for Series III Experimental Results.*

Section	Dependent Variable	Regression Equation	Regression Coefficient
½ in	Elongation	6.41 x (2, if Aluminium chill) + 5.14 x (2, if Cast Iron chill) - 0.66 x (Distance from most chilled end) - 7.28	0.828
½ in	Tensile Strength	2.51 x (2, if Block chill) + 1.75 x (2, if Single Taper chill) - 0.61 x (Distance from most chilled end) + 0.06 x (Distance from most chilled end)^2 + 13.3	0.935
½ in	Porosity	-0.39 x (2, if Aluminium chill) - 0.27 x (2, if Cast Iron chill) + 0.05 x (Distance from most chilled end) + 1.95	0.815
3/8 in	Elongation	6.69 x (2, if Block chill) + 4.21 x (2, if Single Taper chill) - 2.54 x (Distance from most chilled end)$^{1/2}$ - 3.03	0.714
3/8 in	Tensile Strength	0.72 x (2, if Single Taper chill) + 1.55 x (2, if Aluminium chill) + 0.81 x (2, if Cast Iron chill) - 0.99 x (Distance from most chilled end)$^{1/2}$ + 15.8	0.869
3/8 in	Porosity	-0.45 x (2, if Block chill) - 0.39 x (2, if Single Taper chill) + 0.11x(Distance from most chilled end)$^{1/2}$ + 1.91	0.780
¼ in	Elongation	5.89 x (2, if Block chill) + 3.48 x (2, if Single Taper chill) - 4.74	0.594
¼ in	Tensile Strength	1.24 x (2, if Aluminium chill) + 1.86 x (2, if Cast Iron chill) + 13.8	0.507
¼ in	Porosity	-0.21 x (2, if Block chill) -0.18 x (2, if Aluminium chill) + 1.1	0.713
1/8 in	Elongation	No variables found significant at the 5% level	
1/8 in	Tensile Strength		
1/8 in	Porosity	-0.34 x (2, if Single Taper chill) + 1.69	0.736
All combined	Elongation	50.5 x (Section cast) + 1.40 x (2, if Block chill) + 3.74 x (2, if Aluminium chill) + 3.76 x (2, if Cast Iron chill) -74.5 x (Section cast)^2 -1.38 x (Distance from most chilled end)$^{1/2}$ -10.2	0.668
All combined	Tensile Strength	-9.62 x (Section cast) + 1.49 x (2, if Aluminium chill) + 1.42 x (2, if Cast Iron chill) + 11.4 x (Section cast)^2 -0.58 x (Distance from most chilled end)$^{1/2}$ + 17.07	0.655
All combined	Porosity	-8.91 x (Section cast) -0.34 x (2, if Aluminium chill) -0.28 x (2, if Cast Iron chill) + 14.7 x (Section cast)^2 + 0.10 x (Distance from most chilled end)$^{1/2}$ + 2.72	0.785

4. EXPERIMENTAL WORK INVOLVING RADIOGRAPHY

This aspect of the work was prompted by the concept surrounding premium quality castings. That is, apart from the prescribed number of castings which are cut up for mechanical testing the remainder must be subjected to stringent non-destructive tests, particularly X-radiography. Thus, it would be of considerable advantage if additional quantitative information could be derived from the radiographs that already have to be produced, especially if the facts could be obtained at relatively little extra cost. To ensure that the investigations related to interior soundness rather than surface integrity the plates were machined, although castings to be inspected commercially would usually remain unmachined. It is appreciated that many sections exist within one commercial casting but for simplicity the work was restricted, in this limited enquiry, to the four separate sections already examined. In any technique developed from this investigation, standardized procedures would be needed to control the variables encountered in X-radiography for example, exposure time, developing time. Rigid control is exercised in this regard in the more enlightened organisations by radiographing standard samples periodically.

It was the intention of the work to compare observations obtained from the radiographs with the mechanical properties determined from the corresponding samples cut out of the plates. This necessitated the identification of strips of radiographic film within the radiograph of the complete plate which matched the locations of the mechanical test samples.

4.1 Experimental Work

With the limited time available the experimental work was restricted to the ½ in section but this did not prevent the determination of relationships between section density and mechanical properties in the other section thicknesses. No reason can be envisaged as to why any information extracted from the ½ in plates should be invalid for the remainder.

To derive extra facts from a radiograph the information must be presented in a more convenient form. By scanning a section of radiographic film using a Mark IIIc Joyce Automatic Recording Microdensitometer (Figure 50) a graphical interpretation of the information stored within a radiograph may be produced. Before microdensitometry experiments were performed on the film strips some convenient level of sensitivity to the features revealed by the densitometer was essential. A high degree of sensitivity, clearly, would produce the most graphical detail but too high a sensitivity setting would result in unwanted information such as from

grains and defects in the film itself. Throughout these investigations the optical wedge controlling the sensitivity within a film was set at 0.5 D i.e. a full scale graphical deflection was produced by a variation in the light intensity, through the film of 0.5 D. (The value of D is defined as the log. of the ratio of the light intensity incident upon a film to the intensity of the light transmitted through the film,

$$\text{i.e. } \log\left(\frac{I_o}{I_t}\right) \quad).$$

The overall density level of a particular radiograph was determined by means of comparisons between standard light filters and stepped radiographic standards. The following technique was used. With a wide range wedge (2.0D) and a light filter of say, 1.5D the pen recorder was adjusted to near the bottom of the scale. When an area of the stepped film, with a similar density to the density of the experimental plate radiograph, was installed under the objective a deflection was noted. The overall density of this section of the stepped film was the datum plus the deflection (in centimetres) times the slope (in D/cm) of the wedge. Once the value of this second datum density had been established it was moved to some convenient position, the 2.0D wedge was replaced by the 0.5D wedge and the 1.5D filter was also removed. The apparatus was then adapted to cope with high density radiographs over the limited range of sensitivity.

4.2 Results

A problem in measuring the density changes in the cast plates was that the overall density fluctuated considerably along the plate because of the varying degrees of chilling. This required the determination of a new datum D value for each radiographic strip. The variation in the datum caused considerably delays in determining areas under the radiographic curves, it also produced substantial scattering in the final curves of areas under the graphical plots against mechanical properties. This was not the case with the unchilled plate because little density variation existed along the plate length and one reference was sufficient for all the graphical plots from the film strips.

4.2.1 Relationship between Graphical Area and Specimen Porosity

Graphical representations of radiographs from the unchilled ½in section were obtained similar to the one in Figure 51. After an estimate of the datum D had been made, the areas bounded by the curves and this datum were measured using a Planimeter. The results for the unchilled ½in plate are shown in Figure 52.

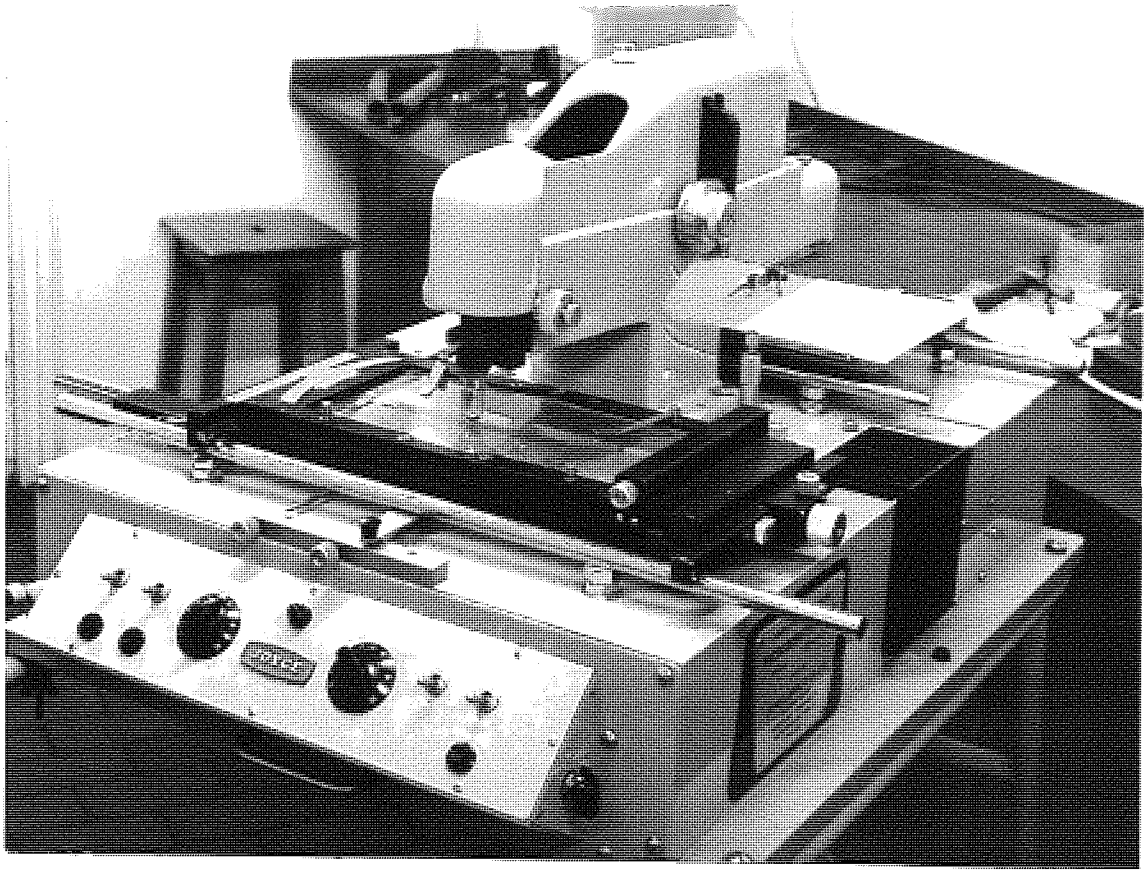

Figure 50.—*A Mk IIIc Joyce Automatic Recording Microdensitometer.*

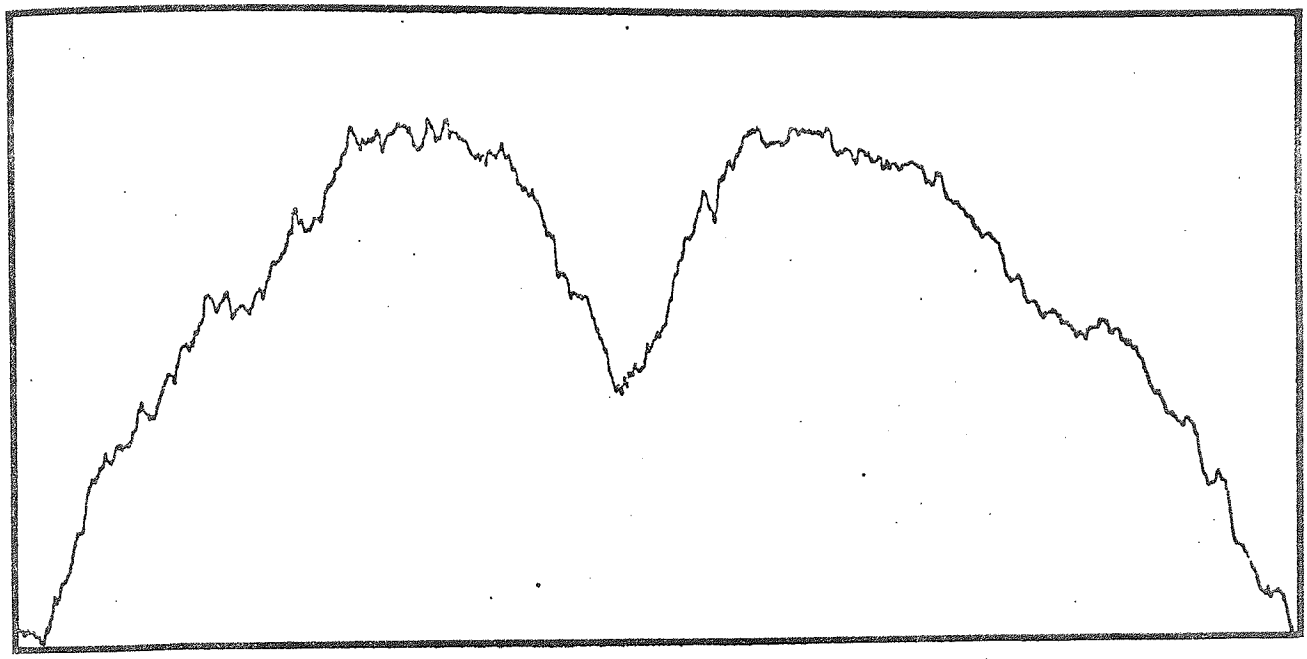

Figure 51.—*Graphical representation of a Radiographic Strip obtained from the ½in unchilled plate.*

4.2.2 *Relationship between Specimen Density and Elongation*

From the results obtained in Series III it was apparent that the elongation of a specimen was strongly correlated to its degree of unsoundness. Table X lists the linear regression equations correlating specimen elongation to porosity for all Series III results taken one section at a time. The degree of unsoundness, porosity, was measured using a displacement method. The relationship between elongation and percentage porosity for all the ½in sections is illustrated in Figure 53. A combination of Figure 52, for the unchilled ½in plate, and Figure 53 enables a direct estimate of elongation to be made from the original radiograph. The porosities obtained (Table XI) from the regression line in Figure 52 will be very similar to the experimentally determined results since a high correlation coefficient from such a small sample size excludes any large variations. The relationship between elongation and porosity in Figure 53 is drawn from a much larger population and the results obtained, Table XI, corresponding to the unchilled plate represent one small area at the end of the regression line. Error may have been introduced into this region by assuming a linear relationship over such a wide range of elongations.

The marked correlation between specimen porosity and elongation was further highlighted by Figures 54 and 55. The elongations from a range of Series I plates, chilled by various methods, were compared to the percentage porosities obtained from a similar set of chilled plates cast in Series III. An additional plate chilled with double thickness single taper chills was included to complete the comparison.

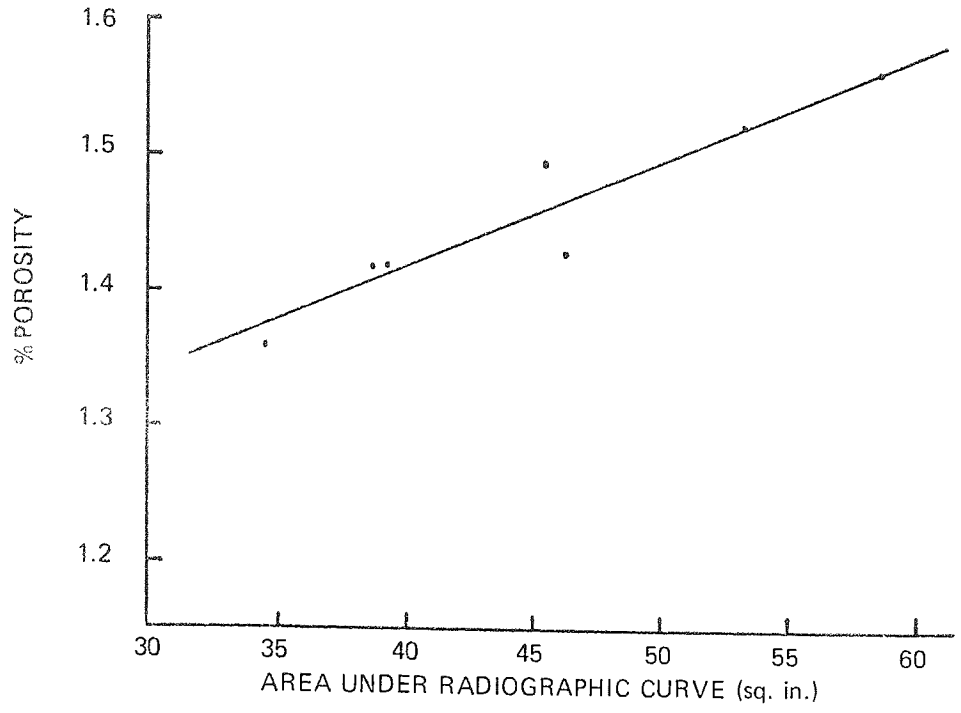

Figure 52.—*Relationship between Porosity and Area under the resulting Radiograph for the unchilled ½in plate.*

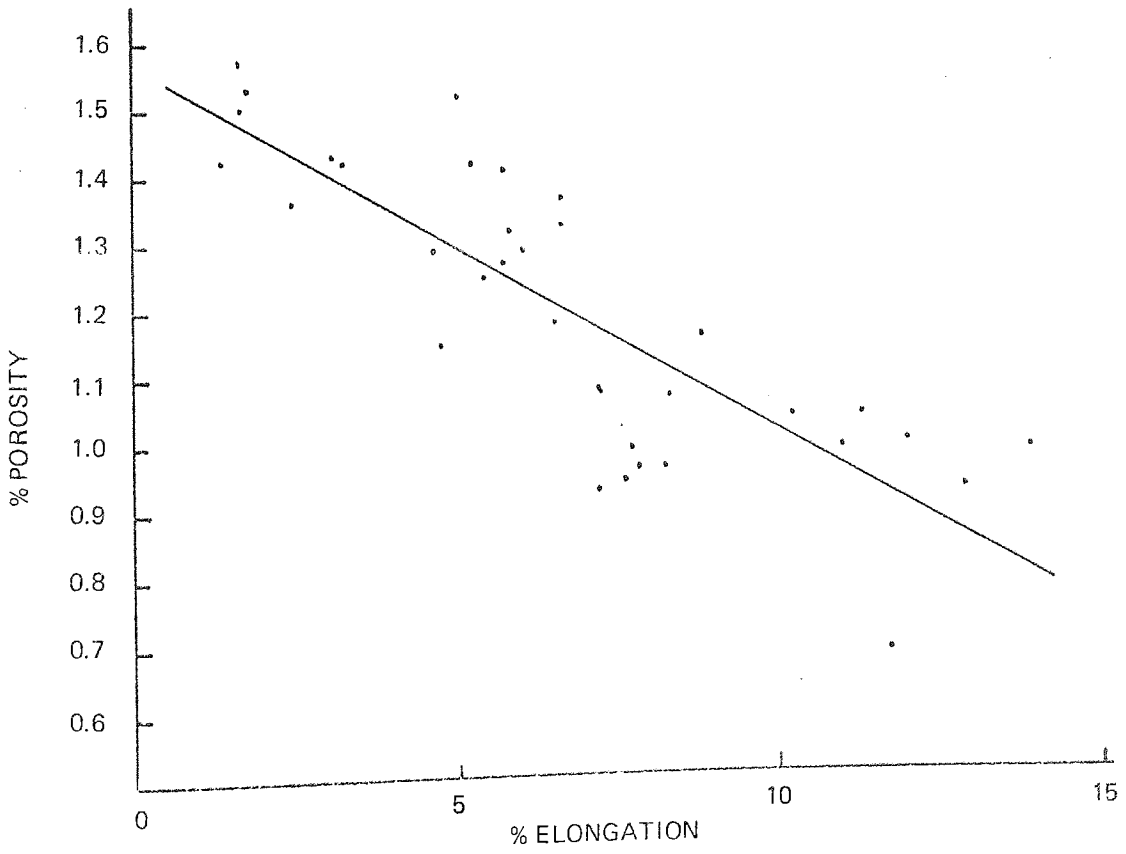

Figure 53.—*Relationship between Specimen Porosity and % Elongation.*

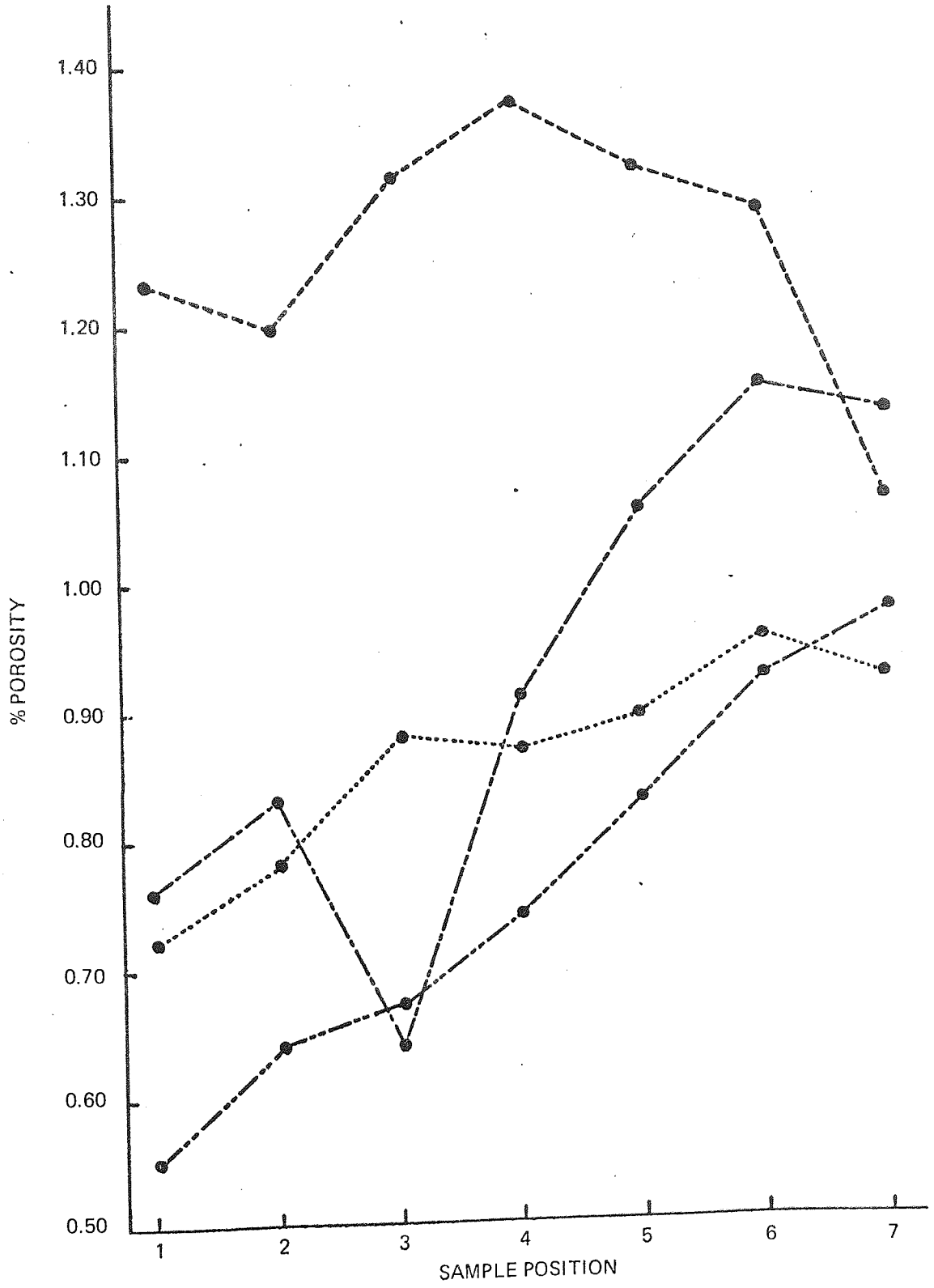

Figure 54.—*Some typical results of porosities determined at different sample positions from Series III castings chilled under similar conditions to those in Figure 55.*

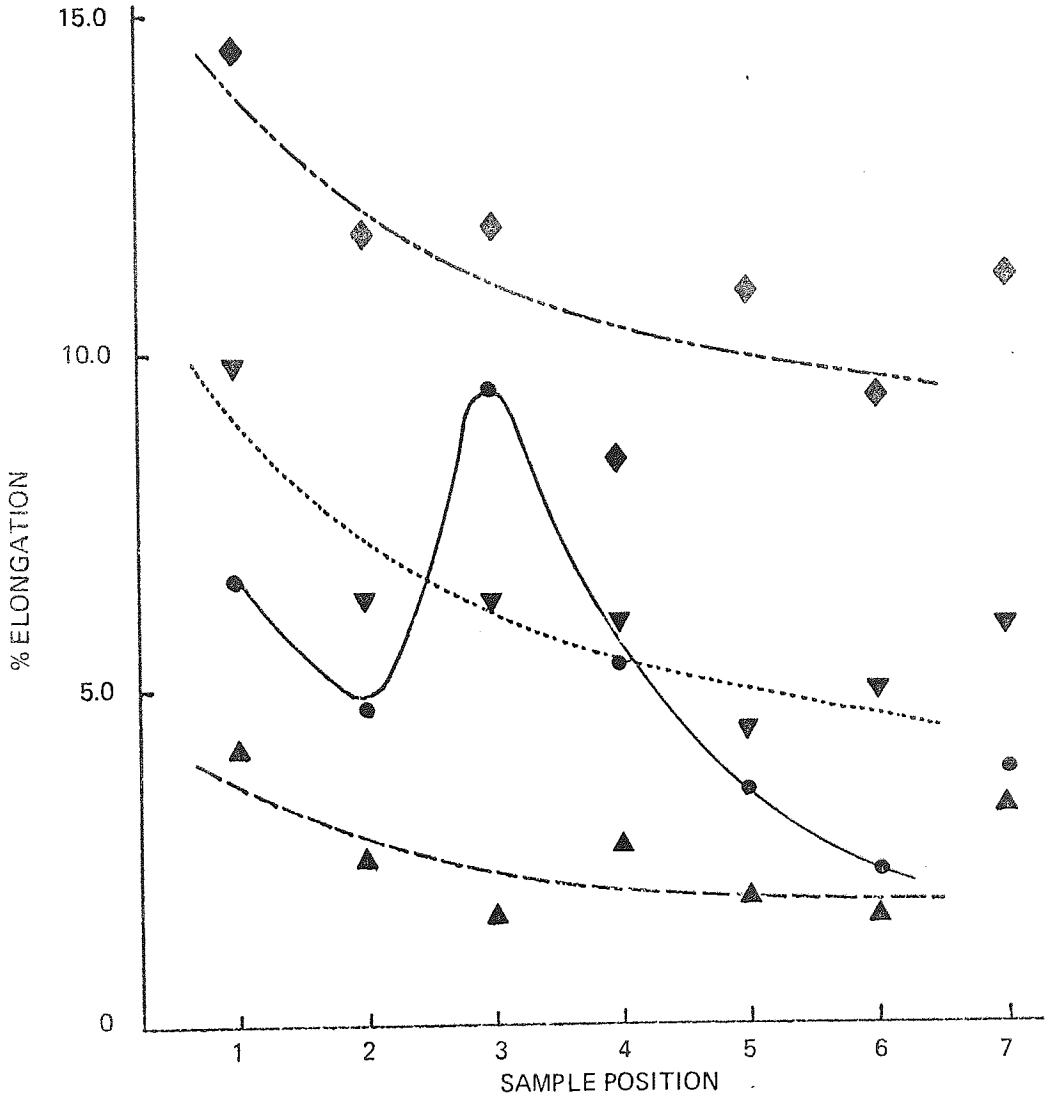

Figure 55.—*The effects different chilling techniques have on the trends of elongation values for specimens removed from Series I plates.*

TABLE X.—*Linear Regression Equations (y = a + bx) and Coefficients for all Series III results.*

Section	Dependent Variable (y)	Independent Variable (x)	a	b	Regression Coefficient
½ in	% Porosity	% Elongation	-0.055	1.57	-0.83
3/8 in	% Porosity	% Elongation	-0.042	1.26	-0.73
¼ in	% Porosity	% Elongation	-0.046	0.93	-0.80
1/8 in	% Porosity	% Elongation	-0.055	1.48	-0.50
All combined	% Porosity	% Elongation	-0.063	1.40	-0.66

TABLE XI.—*Showing interaction of Graphical Area, Porosity and Elongation for the unchilled ½ in plate.*

Area, in^2	Actual % Porosity	Calculated % Porosity	Actual % Elongation	Calculated % Elongation
38.6	1.42	1.41	3.20	2.90
34.4	1.36	1.38	2.40	3.40
39.2	1.42	1.42	1.30	2.70
45.4	1.50	1.47	1.60	1.90
53.3	1.53	1.53	1.70	0.70
58.6	1.57	1.58	1.60	0.00
46.2	1.43	1.47	3.00	1.80

5. HEAT FLOW AND SOLIDIFICATION

5.1 Mathematical Treatment

Analytical solutions for solidification problems are subject to many limitations and mathematical solutions may only be derived for simple assumed conditions often remote from the conditions encountered in practical castings. These idealised states involve such phenomena as semi-infinite masses of metal solidifying in contact with semi-infinite mould walls.

Attempts to produce more realistic solutions in practical circumstances necessitate simplifying assumptions such as a constant temperature at the mould/metal interface during solidification. In analytical solutions of this more practical nature it is essential to clarify the assumptions made and to estimate the errors incurred.

It was the purpose of this particular part of the work to attempt to remove some of the limiting assumptions in the analytical solutions provided the results remained within practical limits.

5.1.1 Basic Theory for Analytical Methods[63]

Solidification of a metal in any mould is a problem of unsteady heat flow and all mathematical attempts to find solutions to this problem are based on accepted theory of unsteady heat flow.

The change in temperature of an element of dimensions 2dx, 2dy and 2dz, in a homogeneous, isotropic solid through which heat is flowing is given by:

$$\delta\theta/\delta t = K/\rho c \left(\delta^2\theta/\delta x^2 + \delta^2\theta/\delta y^2 + \delta^2\theta/\delta z^2 \right) = K/\rho c . \nabla^2\theta \qquad \text{(i)}$$

where θ = temperature of the element;

t = time;

K = thermal conductivity of the homogeneous, isotropic, solid;

ρ = density of the solid and

c = specific heat of the solid.

The quantity $K/\rho c$ is referred to as the 'thermal diffusivity' and is represented by either α or κ. Heat conduction in one direction is derived from the equation as:

$$\delta\theta/\delta t = \alpha . \delta^2\theta/\delta x^2 \qquad \text{(ii)}$$

It is assumed in both equations that K, c and ρ are independent of temperature.

It may also be shown[64] that if the plane interface of a semi-infinite solid, initially at a uniform temperature, θ_o is instantaneously raised to a temperature θ_i at time t = o, then, after a lapse of time t the temperature, θ_m, of any point whose distance is x perpendicular from the interface is given by:

$$\theta_m = \theta_o + (\theta_i - \theta_o)\ \text{erfc}\left(\frac{x}{2\sqrt{\alpha t}}\right) \qquad \text{(iii)}$$

where:

$$\text{erfc}\left(\frac{x}{2\sqrt{\alpha t}}\right) = 1 - \text{erf}\left(\frac{x}{2\sqrt{\alpha t}}\right) \qquad \text{(iv)}$$

and $\text{erf}\left(\frac{x}{2\sqrt{\alpha t}}\right)$ is the error function defined by:

$$\text{erf}\left(\frac{x}{2\sqrt{\alpha t}}\right) = \frac{2}{\sqrt{\pi}}\int_0^{x/2\sqrt{\alpha t}} e^{-\beta^2}\, d\beta \qquad \text{(v)}$$

5.1.2 The Importance of Thermal Diffusivity in Heat Extraction Estimates

Equation (iii) is valuable in its application to sand mould walls, i.e. those of low conductivity. The small errors introduced, in spite of the assumptions, provide a useful basis for a simple solution to the problem of freezing castings. In this approach Chvorinov[65] and others have used equation (iii) to calculate the rate at which a mould removes heat from a casting and equated it to the heat loss when a casting freezes.

The assumptions made in this exercise of the mould wall absorbing the heat from the solidifying casting are:

(a) the temperature of the interface between the metal and the mould wall remains essentially constant throughout solidification,

(b) The thermal diffusivity, α, of the mould materials is independent of temperature,

(c) any non-homogeneity of the mould is unimportant,

(d) the error introduced by the finite size of the mould wall is not large.

Assuming the temperature distribution in a mould is given by equation (iii) for any time, t, after the casting has been poured, up to the end of solidification, the rate at which heat is removed from the casting per unit of area of mould wall, $\delta Q/\delta t$, is given by the equation:

$$\delta Q/\delta t = -K\left[\delta\theta/\delta x\right]_{x=o} \qquad \text{(vi)}$$

and by differentiation of equation (iii)

$$\delta Q/\delta t = K\frac{(\theta_i - \theta_o)}{\sqrt{\pi\alpha t}} = 0.564K\frac{(\theta_i - \theta_o)}{\sqrt{\alpha t}} \qquad \text{(vii)}$$

This is often written:

$$\delta Q/\delta t = \frac{0.564\,(\theta_i - \theta_o).b}{\sqrt{t}} \qquad \text{(viii)}$$

where $b = \sqrt{K.c.\rho}$ and is referred to as the 'heat diffusivity'.

The total heat absorbed in time t by a unit area of the mould wall is obtained by integrating equation (viii) between the time limits o and t:

$$Q = b\,(\theta_i - \theta_o) \cdot \int_o^t \frac{0.564}{\sqrt{t}} \cdot dt = 1.128b\,(\theta_i - \theta_o)\sqrt{t} \qquad \text{(ix)}$$

Equation (ix) may be shortened to:

$$Q = \xi\sqrt{t} \qquad \text{(x)}$$

where $\xi = 1.128b\,(\theta_i - \theta_o)$ and is called the 'mould constant' and is the measure of the chilling power of the mould.

In the derivation of equation (x) the assumptions are:-

(a) the mould wall is plane and

(b) the area under consideration is beyond the influence of any corners.

If one assumes that the metal solidifies by skin formation then the thickness, D, of the metal solidified in time, t, is proportional to the heat extracted by the mould in that time.

$$D = q\sqrt{t} \qquad \text{(xi)}$$

where q is the 'solidification constant' and is obtained from equations (ix) and (xi).

$$q = \frac{2K\,(\theta_i - \theta_o)}{L\rho'\sqrt{\pi\alpha}} = \frac{1.128b\,(\theta_i - \theta_o)}{L\rho'} \qquad \text{(xii)}$$

where L = the latent heat of the metal and ρ' its density. An additional assumption to those previously mentioned is the fact that the metal is presumed to be cast without superheat. This may be allowed for and is mentioned later. The most important aspect of equation (xi) is the fact that the skin formation of a metal solidifying against a plane mould wall is governed by a parabolic law, the thickness of the skin formed at a time, t, after casting is proportional to $\sqrt{t}$.

In instances where an alloy solidifies with a long freezing range a pasty region exists and it is necessary to solve for the complete solidification time rather than time to solidify to specific points but otherwise previous assumptions still apply.

If the latent heat of fusion of the metal be L and s is the estimated specific heat over the superheating and undercooling range, then the total heat extracted during complete solidification is:

$$W\,[L + s\,(\theta_c - \theta_f)] \qquad \text{(xiii)}$$

where W = weight of the casting,

θ_c = casting temperature,

θ_f = final solidification temperature.

If the time taken to complete solidification is 't' then this quantity of heat must be absorbed by the mould. Assuming a uniform heat extraction over the entire mould surface, then the heat absorbed by the mould is obtained by multiplying equation (ix) by the area of the mould A. This may be equated to expression (xiii) to produce the solidification time:

$$\sqrt{t} = \frac{W\,[L + s\,(\theta_c - \theta_f)]}{1.128\ A.b(\theta_i - \theta_o)} \qquad \text{(xiv)}$$

$$= \frac{\rho^{*} V\ [L + s\,(\theta_c - \theta_f)]}{A\ 1.128b\ (\theta_i - \theta_o)} \qquad \text{(xv)}$$

since $W = \rho^{*} V$ (where V is the volume of the casting) equation (xv) may be simplified and the solidification time for any alloy may be expressed as:-

$$t = \text{constant} \times (V/A)^2 \qquad \text{(xvi)}$$

The equation again assumes a constant interfacial temperature.

5.2 Practical Applications of Heat Flow and Solidification

Among the practical implications of this research there was need for quantitative information to describe the behaviour of chills. Although more complicated equations exist for the behaviour of metal chill materials inserted in moulding sands it was thought sensible to start with a relatively simple equation (iii) and use it as a basis of a mathematical model to predict the temperature distribution within a moulding material. It was also hoped that some of the boundary conditions relating to equation (iii) could be modified and their effects on the results estimated.

5.2.1 Determination of Thermal Diffusivity for Sand Moulds

Essentially, equation (iii) Carslaw and Jaeger's equation, is used to determine the temperature distribution within a mould material of known properties and with well defined boundary conditions. A source of error in the assumptions surrounding equation (iii) is the assumption that the interfacial temperature is raised instantaneously to the casting temperature. However, it is not unreasonable to assume that in a sand mould the mould/metal interface must very quickly reach a temperature approaching that of the melting point of the metal being cast particularly if the bulk of the casting is large.

A computer technique was developed to determine the thermal diffusivity of a moulding material (the importance of which has been previously explained) assuming the interface temperature is raised instantaneously to a value midway between the pouring and final solidification temperatures.

5.2.2. Additional Theory for Thermal Diffusivity Determinations

Equation (iii) may be expressed as follows:

$$\left(\frac{\theta_m - \theta_o}{\theta_i - \theta_o}\right) = 1 - \text{erf}\left(\frac{x}{2\sqrt{\alpha t}}\right) \qquad \text{(xvii)}$$

with substitutions the equation may be reduced to:

$$A\,I\,M = \text{erf}\ (X)$$

where:

$$AIM = 1 - \left(\frac{\theta_m - \theta_o}{\theta_i - \theta_o}\right) \qquad \text{and}$$

$$X = \left(\frac{x}{2\sqrt{\alpha t}}\right) .$$

5.2.3 Computer Program developed for Calculating Thermal Diffusivity

The program (see Appendix IV) is basically an Algol 60 equivalent of Carslaw and Jaeger's equation for unidirectional heat flow but there is a complication. The experiments performed to accumulate data for the program yield a numerical value, y, equal to the error function, erf, of an unknown figure, x. It was therefore necessary to evaluate the inverse error function using an iterative approach.

The iterative approach was started by supplying the program with two estimates of x (X1 and X2) and, from these, two corresponding values of y (Y1 and Y2) were determined. The calculated value of y for each set of results was designated the 'aim' and this value was the objective of the iterative approach. The curve joining the points (X1, Y1) and (X2, Y2) was assumed to be linear and a value of X corresponding to the AIM was obtained from the straight line produced and this figure was introduced into the equation y = erf (x) and a value of y calculated (Figure 56). The value of X was derived from a consideration of similar triangles (Figure 57) giving rise to the equation:

$$X := X1 + (AIM - Y1) * (X2 - X1) / (Y2 - Y1) \qquad \text{(xviii)}$$

By an updating procedure (Figure 58) the values of X and Y replace X2 and Y2 and the values of X2 and Y2 replace the values of X1 and Y1. From these newer estimates of x new values of y were derived and a further value of X was determined corresponding to the AIM on the ordinate. The figure for X was inserted into the error function equation and a more accurate value of Y deduced. This updating procedure was continued until the arithmetic difference between the AIM and Y was less than 0.0001.

The solution to any error function was produced in one of two Algorithmic procedures; the one being used depending upon the size of X. There was considerable overlap in the ranges of X that each procedure could handle and as a result of preliminary computer runs the value of X = 1.1 was chosen as the demarcation between the two procedures. The shape of the error function curve, asymptotic to unity, leads to two difficulties in the procedure for a large value of X (ERFL (X)). If one took the first two estimates of X with as large a range as possible the smaller figure was satisfactory. But, selection of an estimate of X over 2.75 resulted in a value of Y approaching unity. After successive iterations

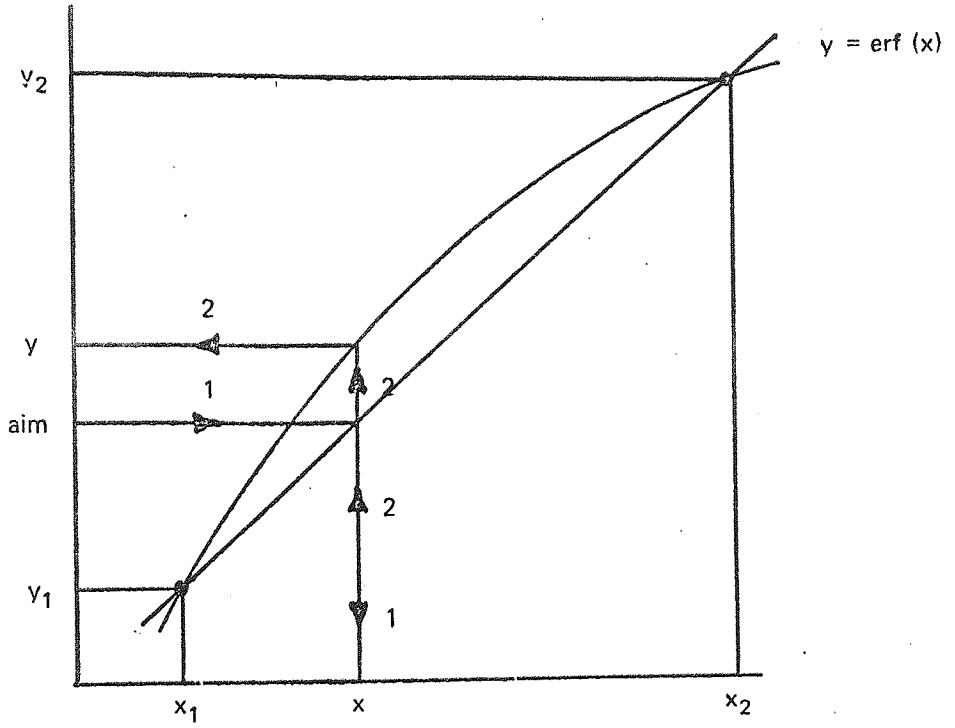

Figure 56.—*Initiation of the Iterative Approach.*

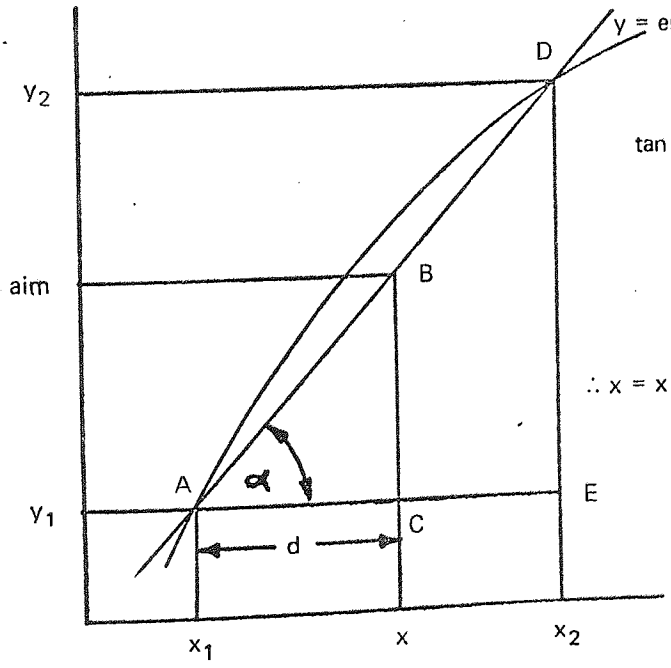

$$x = x_1 + d$$

$$\tan \alpha = \frac{\text{perpendicular}}{d}$$

$$= \frac{(\text{aim} - y_1)}{d} \quad (\text{in} \triangle ABC)$$

$$= (y_2 - y_1)/(x_2 - x_1) \quad (\text{in} \triangle ADE)$$

$$d = \frac{(\text{aim} - y_1) \times (x_2 - x_1)}{(y_2 - y_1)}$$

$$\therefore x = x_1 + (\text{aim} - y_1) \times (x_2 - x_1)/(y_2 - y_1)$$

Figure 57.—*Solution for x using similar triangles.*

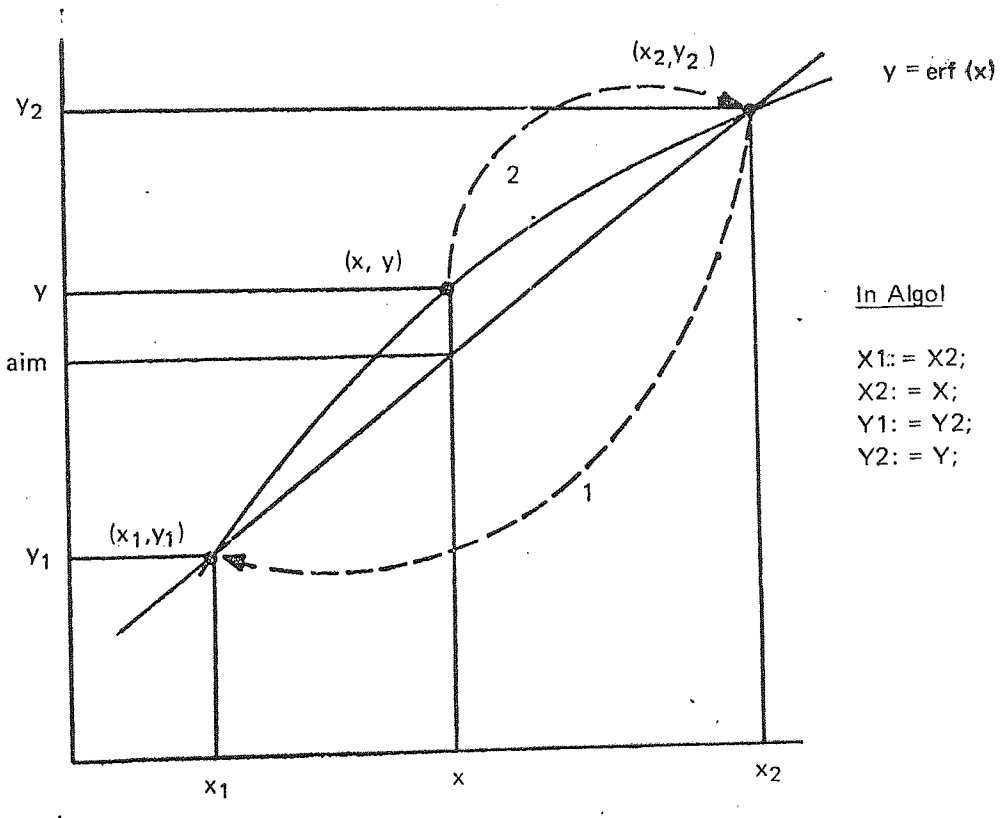

Figure 58.—*Updating procedure.*

the condition could arise in the determination of a new estimate of X that two values of Y (Y1 and Y2) both near unity were subtracted in the denominator causing overflow on entry into the procedure ERFL (X). An overflow was similarly encountered if the original AIM was too high. The problems were overcome as follows:

(1) although the iterative technique is correct for determining a value between two extreme choices, the estimates were restricted to the lower end of the large error function scale (i.e. X1 = 1.11 and X2 = 1.45). The updating procedure was capable of extrapolating outside the original choices up to the final answer.

(2) a ceiling on the value of the AIM, 0.9585, was introduced to prevent all values of y approaching unity. The value 0.9585 was selected after several program runs as the maximum figure possible for the AIM before the program failed.

5.2.4 Estimation of Interfacial Temperature

The technique previously described involved the determination of the thermal diffusivity from discrete data assuming a constant interfacial temperature. The errors arising from a constant interfacial temperature and independently calculated thermal diffusivities were unlikely to produce great variations in the values of thermal diffusivity in sand specimens. However, when investigating chills situated in sand moulds it would be better to use temperature readings obtained from various positions within the chill during each time cycle to give a better estimate of the properties of the chill and, simultaneously, of the real interface temperature. The assumption of a constant interfacial temperature must be erroneous under these more stringent conditions. It was hoped, therefore, to evolve a method by which the curve described by the experimental points could be fitted to a mathematical model defined by Carslaw and Jaeger's equation (iii); Figure 59. The degree of fit was measured by the sums of the squares of the differences between the observed and calculated results derived from equation (iii).

Solution for two Independent Variables by Successive Inverse Interpolations

With the problem defined, as above, it was necessary to assume some mathematical model relating the three variables under consideration, viz. sums of the squares, interfacial temperature and thermal diffusivity. The equation used was:

$$y = b_o + b_1 \alpha + b_2 \theta_i + b_3 \alpha^2 + b_4 \theta_i^2 + b_5 \alpha \theta_i \qquad \text{(xix)}$$

where y = sum of the squares of the differences between the five observed and calculated results ,

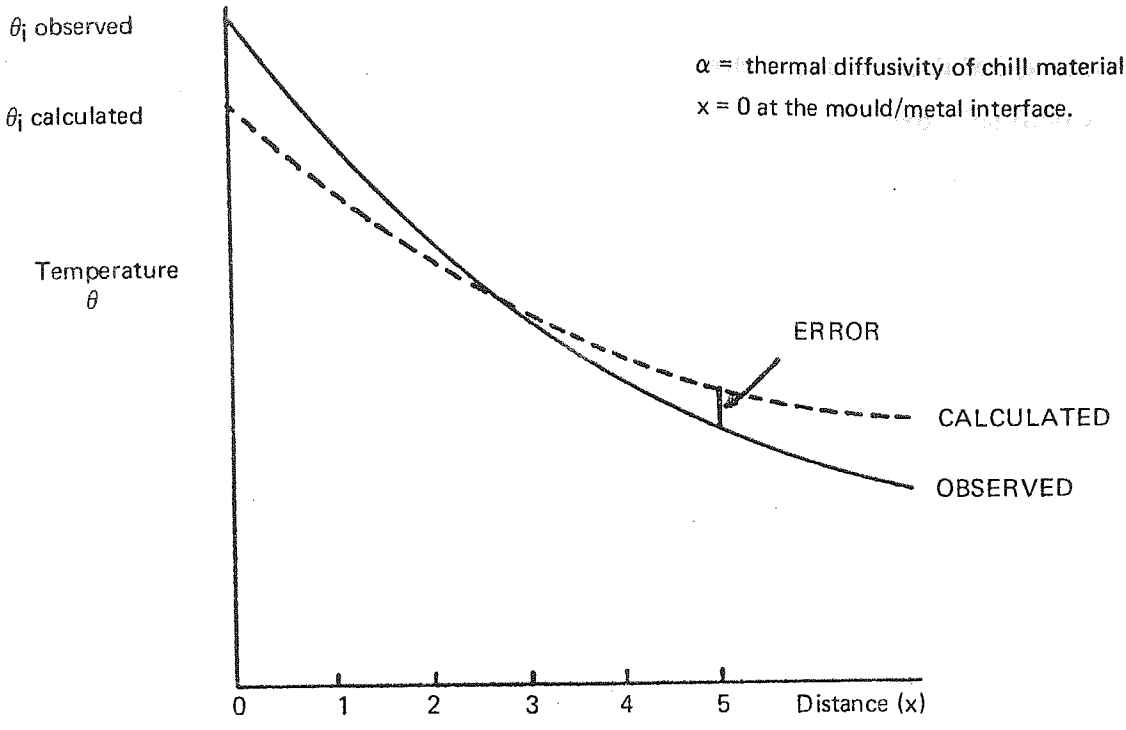

Figure 59.—*Diagramatic Representation of the Problem.*

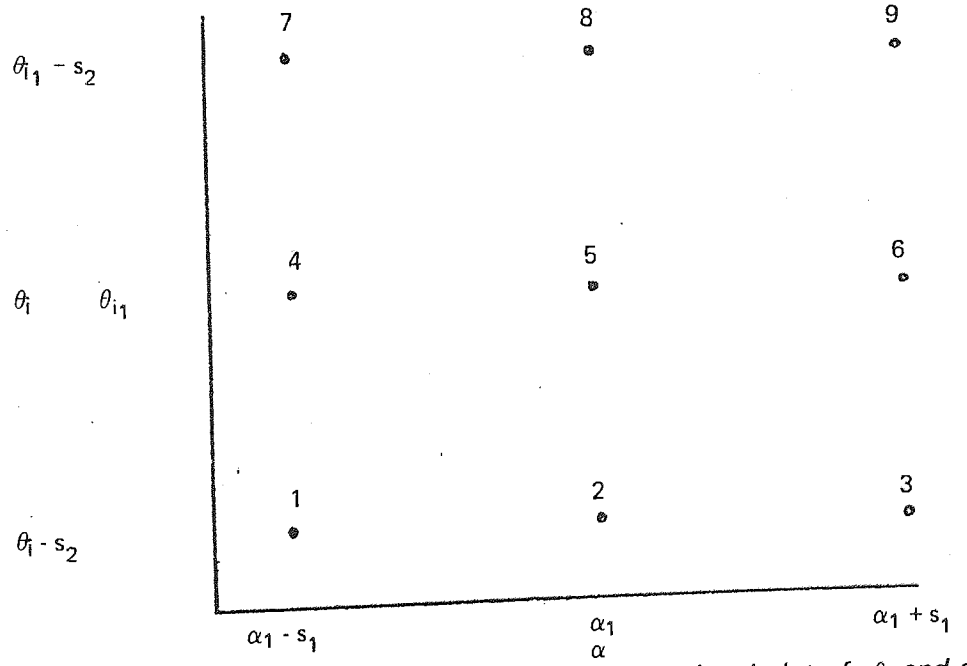

Figure 60.—*Represents plan view of the three dimensional plot of $\alpha\theta_i$ and sum of the squares, y. At each point(1-9) a value of y is produced defining the shape of the surface.*

α = thermal diffusivity and

θ_i = the interfacial temperature.

By differentiating the sum of the squares, y, with respect to each independent variable, a minimum is possible when the differential is equal to zero. The following relationships result:

$$\alpha = \frac{(-b_5\theta_i - b_1)}{2b_3} \qquad \text{(xx)}$$

and

$$\theta_i = \frac{(-b_5\alpha - b_2)}{2b_4} \qquad \text{(xxi)}$$

Substitution between equations (xx) and(xxi) results in the elimination of one of the independent variables, hence:

$$\alpha = \frac{(b_2b_5 - 2b_4b_1)}{(4b_3b_4 - b_5^2)} \qquad \text{(xxii)}$$

After the determination of α the interfacial temperature, θ_i, may be derived from equation (xxi). It is apparent from the theory previously explained that evaluation of the coefficients, b_1 to b_5, is necessary before any solution is forthcoming (see Appendix V). Primarily, the technique involves the supply of estimates for α (α_1) and θ_i (θ_{i_1}), see Figure 60. Around these initial values a 3 x 3 matrix is developed by adding to and substracting from them, factors proportional to the magnitudes of each of the original guesses. From the matrix, the nine combinations of α and θ_i were used to produce nine sets of calculated results which were in turn compared to the group of experimentally determined results. This procedure resulted in a matrix of sums of squares, derived from the original estimates of α and θ_i, and from this matrix the coefficients were calculated which were incorporated in factors employed to modify the original guesses. The equations using the factors to modify the original guesses were:

$$\alpha_2 = \alpha_i + (s_1 \times \alpha) \qquad \text{(xxiii)}$$

and

$$\theta_{i_2} = \theta_{i_1} + (s_2 \times \theta_i) \qquad \text{(xxiv)}$$

where: s_1 - the step size either side of the original estimate of thermal diffusivity, α_1,

s_2 = the step size either side of the original estimate of interfacial temperature, θ_{i_1},

α_2 = the new estimate of the thermal diffusivity, α, and

θ_{i_2} = the new estimate of interfacial temperature, θ_i .

Thus as the technique converged upon the ultimate solutions a cut off was established when α and θ_i fell below certain values which, if changed, made little difference to the previous results of α_2 and θ_{i_2}.

5.2.5 *Computer Program for the Solution of Interfacial Temperature*

The program included is essentially the Algol 60 equivalent of the theoretical solution for the technique developed to determine the thermal diffusivity and interfacial temperature. However, several practical points are explained in Appendix VI in order that cross reference between the theoretical solution and the program is simplified. A typical range of guesses for this program and a particular set of data is illustrated in Table XII. A reasonable estimate for the interfacial temperature may be obtained from plotting the observed temperatures after the first time interval.

With the good agreement between the observed and calculated results, bearing in mind the deficiencies of the practical arrangements, it was thought valuable to investigate further the behaviour of the chills employed. By determining the areas under the estimated curves, using an Algorithm of Simpsons rule, the quantity of heat absorbed during each experimental cycle could be predicted. This helped to explain such factors in chill behaviour as saturation.

5.3 Experimental Details

5.3.1 *Determination of Thermal Diffusivity of sand mould walls*

Figure 61 illustrates schematically the technique for determining the thermal diffusivity of a sand under practical conditions. The accurate positioning of the thermocouples within the block of sand is very important. The thermocouples were located in the sand at the required depths by cutting grooves in the sand corresponding to the grooves in the pattern equipment, Figure 62. It was hoped to reduce the disruption of the isotherms by the thermocouples, by staggering the grooves over a portion of the sand. The overall dimensions of the sand blocks were 7 in (178 mm) square by 3 in (76 mm) deep. The thermocouple grooves were spaced ¾ in (19 mm) apart and stepped in 5 x ¼ in (6.4 mm) steps beginning a ¼ in from the mould/metal interface, Figure 63.

Finally, it should be noted that the thermocouple beads were positioned so as to be uninfluenced by any effects the corners of the mould recess have on the unidirectional heat flow isotherms.

The mould cavity into which the metal was poured was 8 in (203 mm) square by 2 in (51 mm). As the cavity was 8 in deep it was necessary to modify the 16 in (406 mm) square by 4 in (102 mm) deep moulding boxes by having one side

TABLE XII.—*Illustrates the range of guesses acceptable for the solution of the variables shown.*

Thetages = 80

Alphages	No. of Iterations	Final Values θ_i °C	Final Values α cm^2/sec	Remarks
0.06	7	-	-	Failed
0.07	6	109.87	0.06938	OK
0.08	6	109.87	0.06938	OK
0.10	5	109.87	0.06938	OK
0.12	4	109.87	0.06938	OK
0.14	4	109.87	0.06938	OK
0.15	10	109.87	0.06938	OK
0.16	4	-	-	Failed

Alphages = 0.08

Thetages	No. of Iterations	Final Values θ_i °C	Final Values α cm^2/sec	Remarks
70	8	-	-	Failed
80	6	109.87	0.06938	OK
90	4	109.87	0.06938	OK
100	3	109.87	0.06938	OK
110	4	109.87	0.06938	OK
120	4	109.87	0.06938	OK
150	5	109.87	0.06938	OK
200	7	109.87	0.06938	OK
210	7	109.87	0.06938	OK
220	8	109.87	0.06938	OK
230	8	-	-	Failed

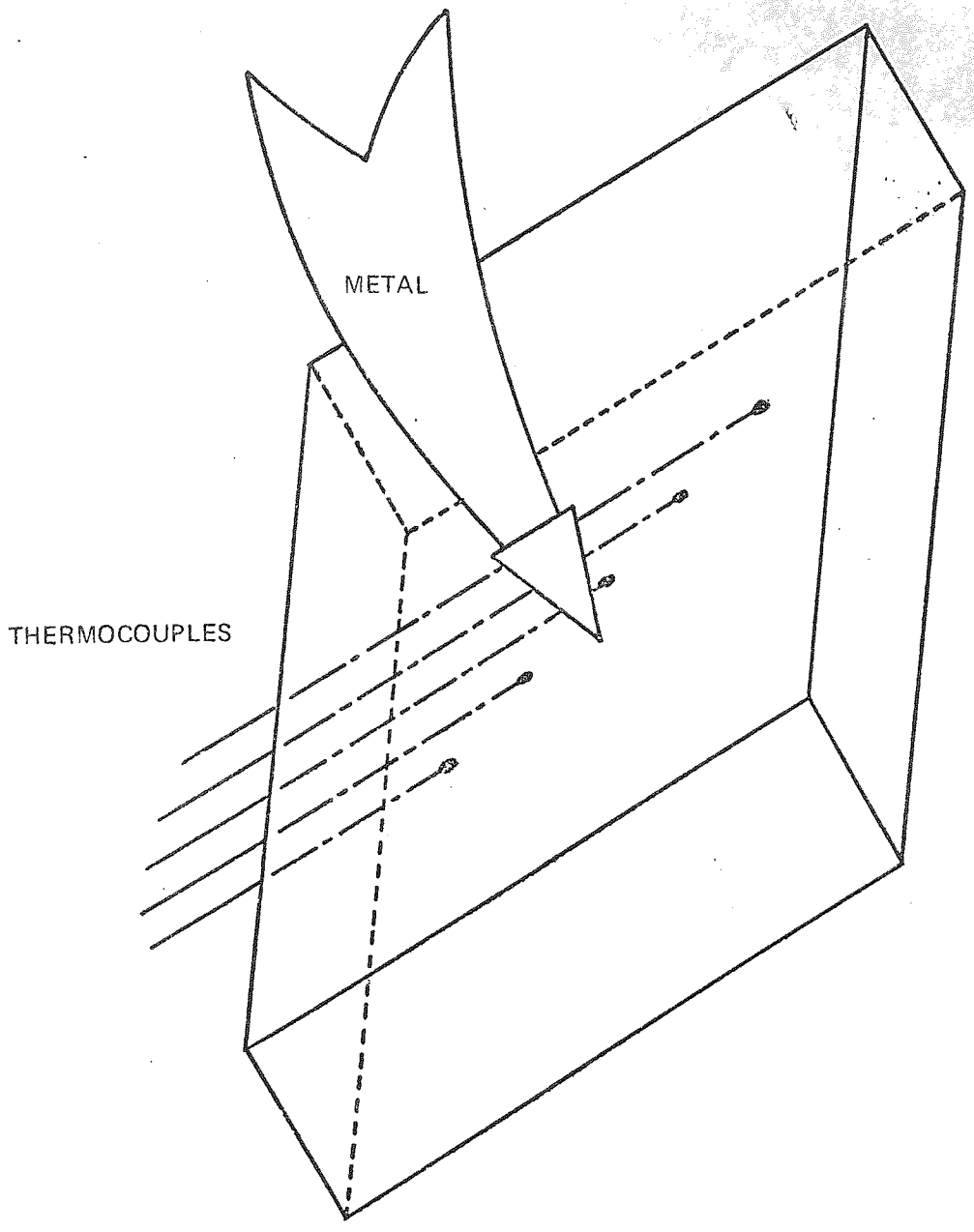

Figure 61 .—*Schematic Representation of Thermal Diffusivity Experiment.*

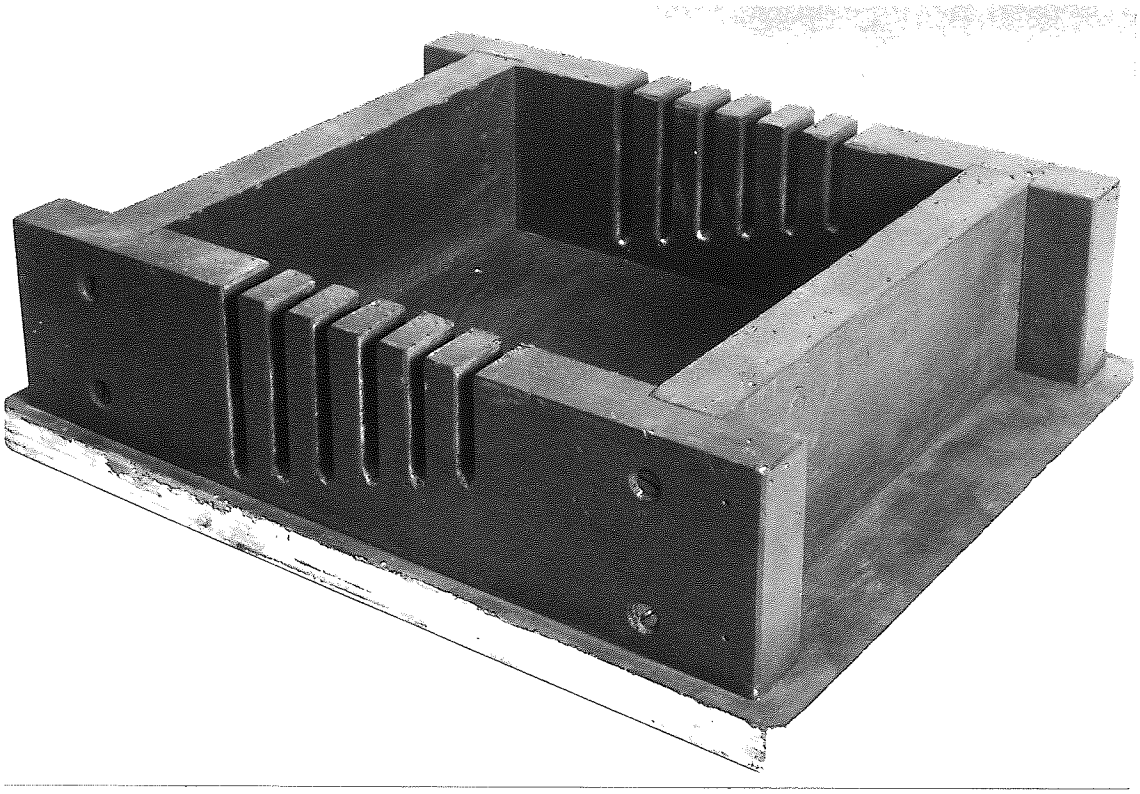

Figure 62.—*Moulding box to assist thermocouple location in the sand block.*

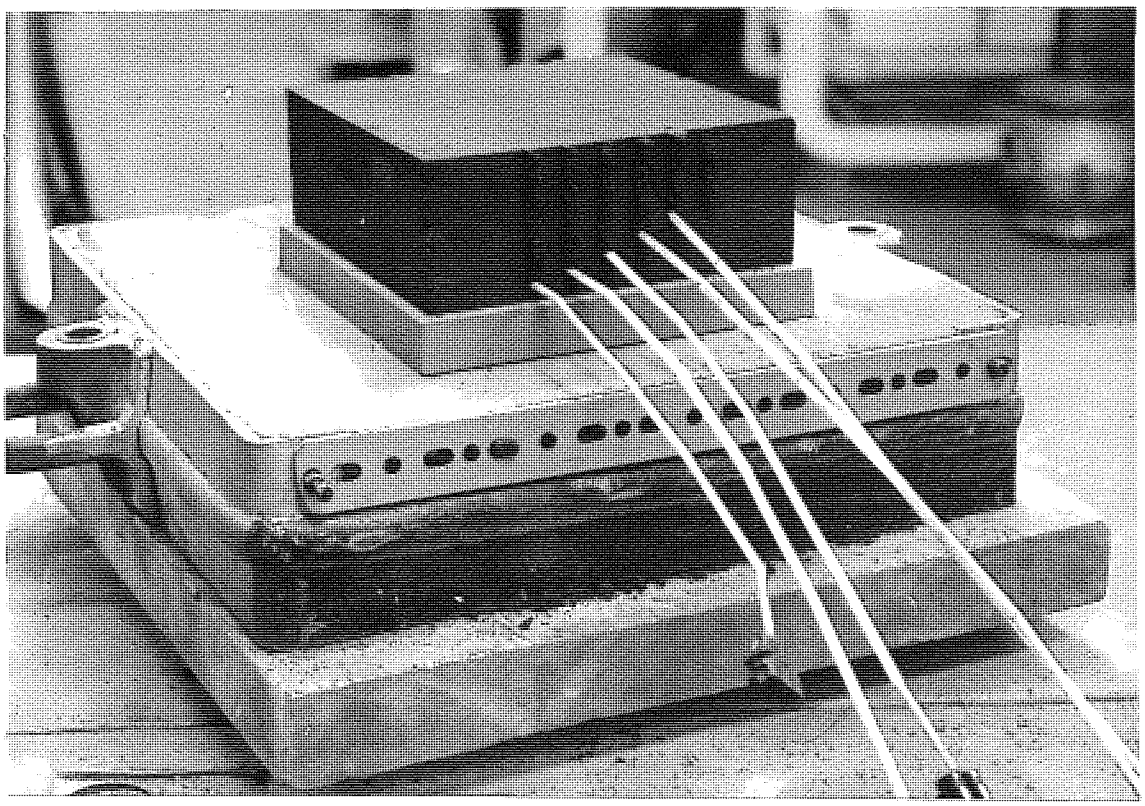

Figure 63.—*Second half of the slab pattern and sand block in position.*

removable to allow pouring in through that side. One half of the mould was rammed up in the experimental sand with the removable side in position. The pattern and box were inverted and the remaining half of the pattern was linked to the rammed portion. The plane surface of the sand block containing the thermocouples, the mould/metal interface, was placed on this half of the slab pattern, Figure 64. The second half of the moulding box was placed on the lower half and ramming completed. The box halves were separated (Figure 65), the slab pattern removed and the removable side released to allow for a pouring point. The box was placed on its edge, mouth uppermost, and plates clamped around the unsupported sand sides to restrain any possible breakout, Figure 66.

The thermocouples were connected to a digital voltmeter (Figure 67) which had electronic compensation for cold junction effects, and a mechanical printout. The mechanical printer, in fact, limited the speed at which the voltmeter could be set to measure potentials to a maximum of one reading per ½ second. However, this was generally sufficient.

5.3.2 Determination of Interfacial Temperature

The casting series was also intended to allow examination of the effect that deviations from semi-infinite conditions had on the temperature distribution that resulted under more practical foundry conditions. Other foundry conditions investigated were the influence of pouring temperature and of mould coatings on the chills. The technique is best explained by the sequence of photographs reproduced in Figures 68 to 70.

A series of parallel holes were drilled into each of the blockchills at varying distances, 1/8 in (3mm), 3/8 in (9.5mm), 5/8 in (16mm), 7/8 in (22mm) and 1 1/8 in (28.5mm) from the chill/metal interface in the plane perpendicular to the line joining the midpoints of the 2in (51mm) sides of the interface. For the same reason as in the determination of the thermal diffusivities for sand specimens, the depths of the holes were varied from 1½ in (38mm) in ½ in (12.5mm) intervals to 3½ in (89mm).

There were, however, several unavoidable limitations to the experimental procedure. The apparatus, previously described, for measuring thermocouple potentials was only capable of continuously logging single measurements or multiples of five separate measurements. Bearing in mind that one was attempting to investigate the behaviour of the chills during their most useful period of life, i.e. during the solidification of the casting, and that the minimum time for each item

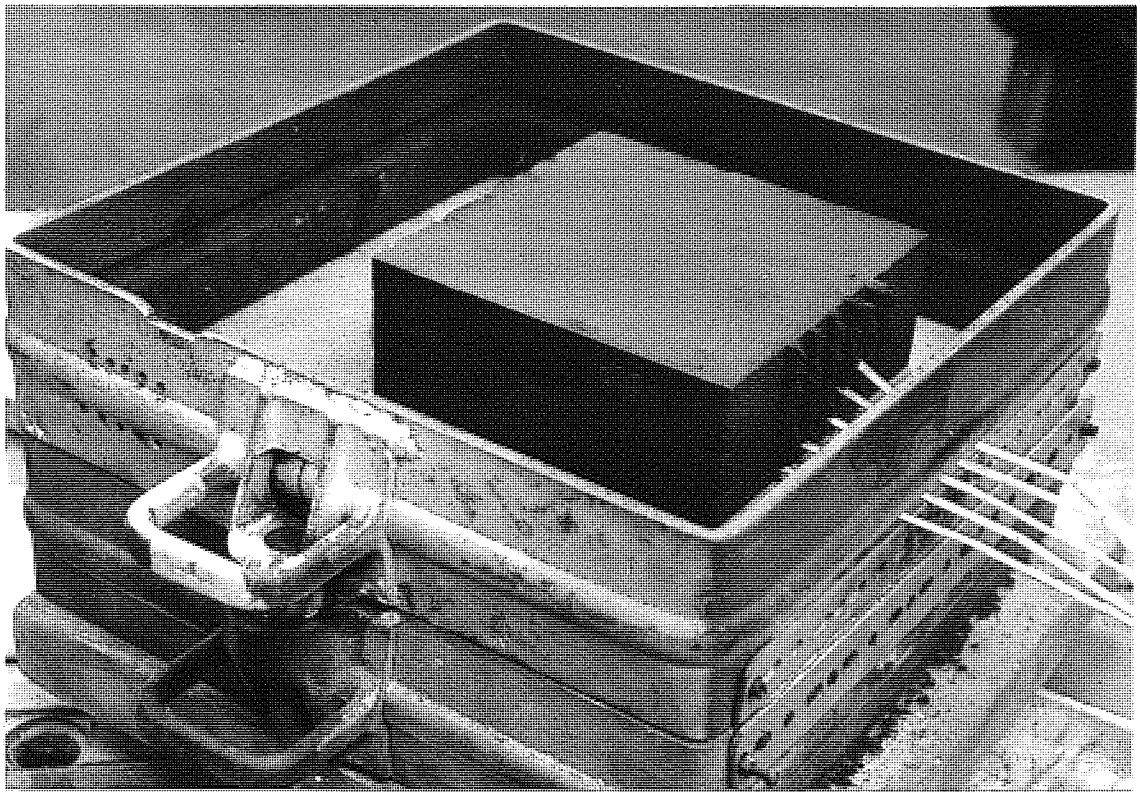

Figure 64.—*Showing the position of the thermocouples leaving the moulding box.*

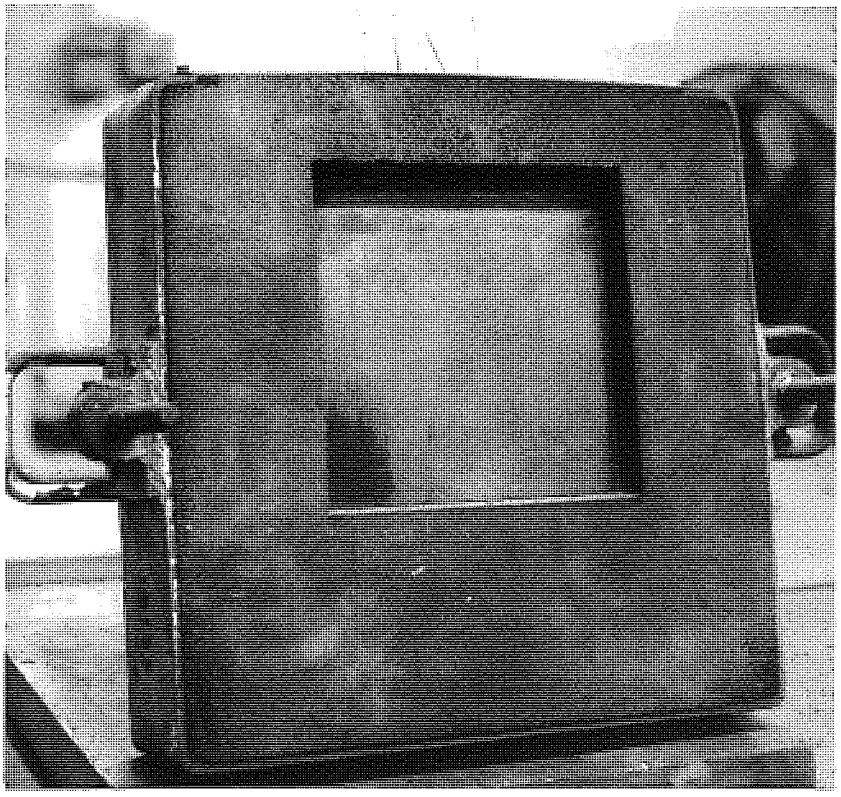

Figure 65.—*Inside of the slab cavity just revealing the outline of the experimental sand block. The mouth has yet to be cut.*

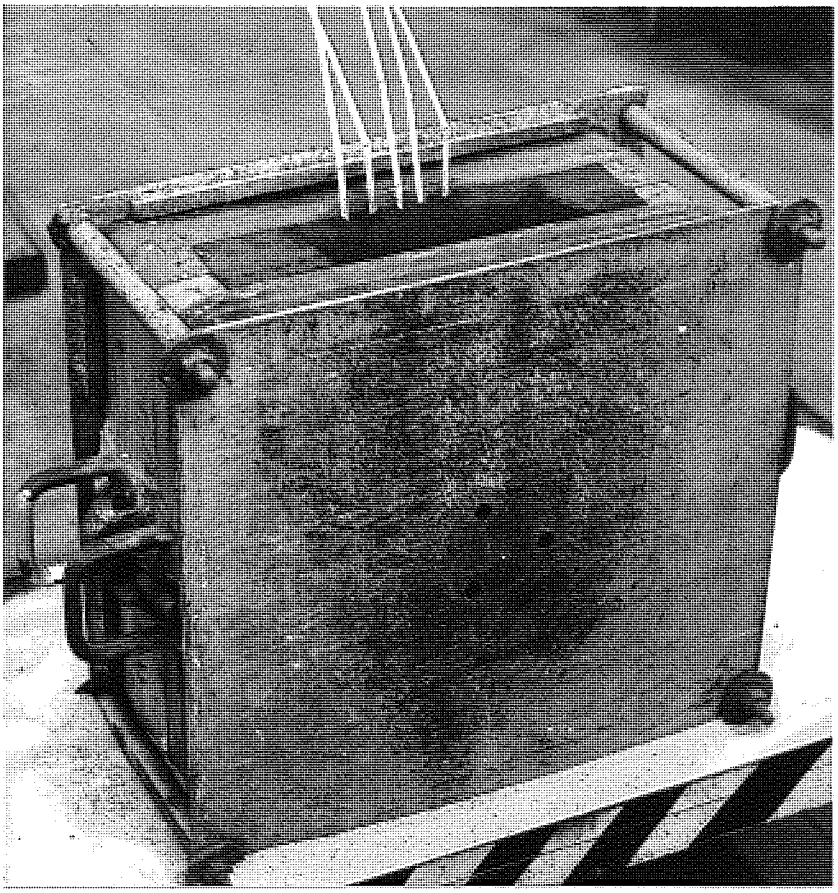

Figure 66 (left).—*The final assembly to ensure safety.*

Figure 67 (below).—*The complete experimental arrangement.*

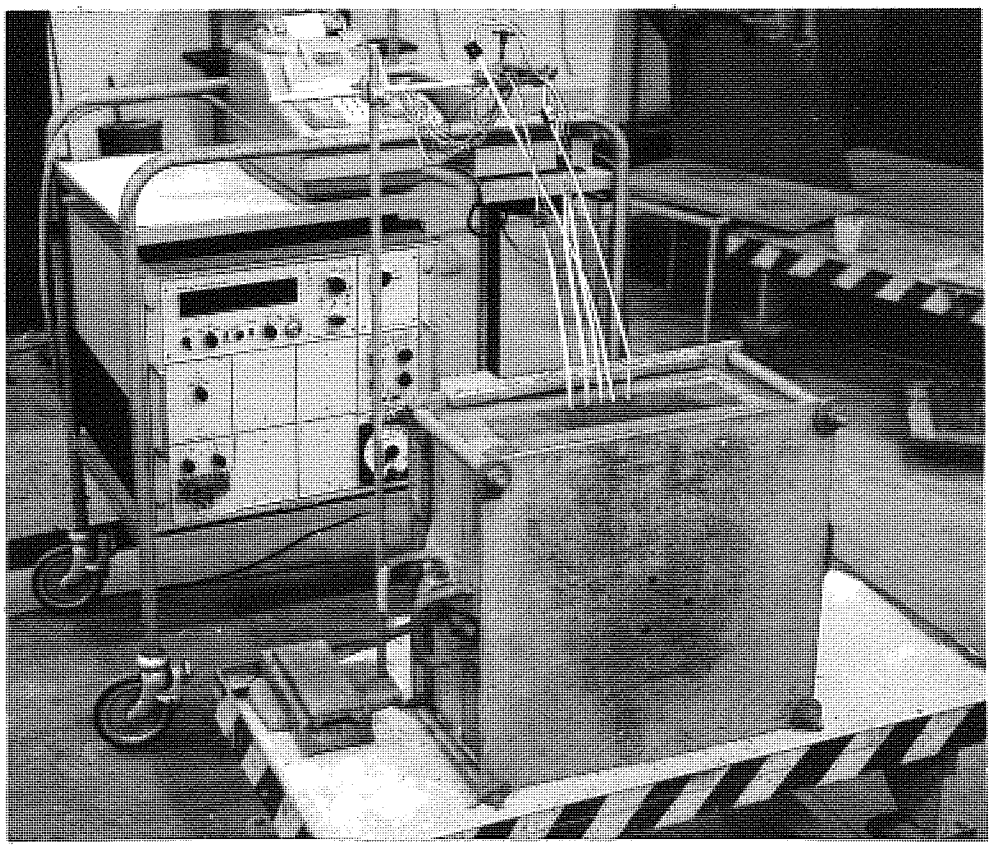

of data to be read was ½ second, then the optimum number of readings in a cycle was 5. This number of thermocouples only permitted investigation of the first half of the 2in (51mm) square section block chills during the short time intervals needed to solidify the sections concerned. Nevertheless, a good agreement between the calculated and observed readings would enable estimates to be made of the total behaviour of the chills with a high degree of confidence.

In addition to reducing the time intervals, in order to closely examine the initial stages of chill behaviour, the diameter of the holes drilled in the chills was chosen to disrupt the heat flow within the chills as little as possible but, also, to allow thermocouples to be introduced that were robust. The availability of 1/8in (3mm) diameter sheaths, long drills and the tight fit between the sheaths and 1/8in holes dictated the hole diameter. An added advantage of this close fit was the good mechanical contact that was achieved between the thermocouple bead and the base of the hole, produced by the drill point angle, when firm pressure was applied to the thermocouples during their installation.

5.3.3 Experimental Determination of the Influence of Chill Shape on Directional Solidification

The experimental pattern employed was that used in the previous investigations. To reduce the number of experiments three basic chilling techniques were examined, i.e. unchilled, block chilled and double thickness single taper chilled. The single and double taper chills with similar thickness to the section being chilled were omitted as it was concluded from previous experiments that the double thickness technique produced the most improved results for that particular shape. To develop a complete insight into the behaviour of the metal within the mould cavity it was essential to perform at least three experiments under identical conditions. It became obvious that investigations could not be carried out on all sections for two reasons. Firstly, too many intricate experiments were involved and secondly, the diameter of the thermocouple tubing would greatly restrict the metal flow in the mould cavity of the thinner sections. It was, therefore, decided to limit the investigations to the ½in (12.5mm) sections and predict the behaviour in thinner sections. Difficulty was encountered in obtaining fine silica tubing for the manufacture of the thermocouples, however, tubing with a maximum 0.040in (1mm) O.D. was available, resulting in an 8% reduction in the cavity's cross-sectional area.

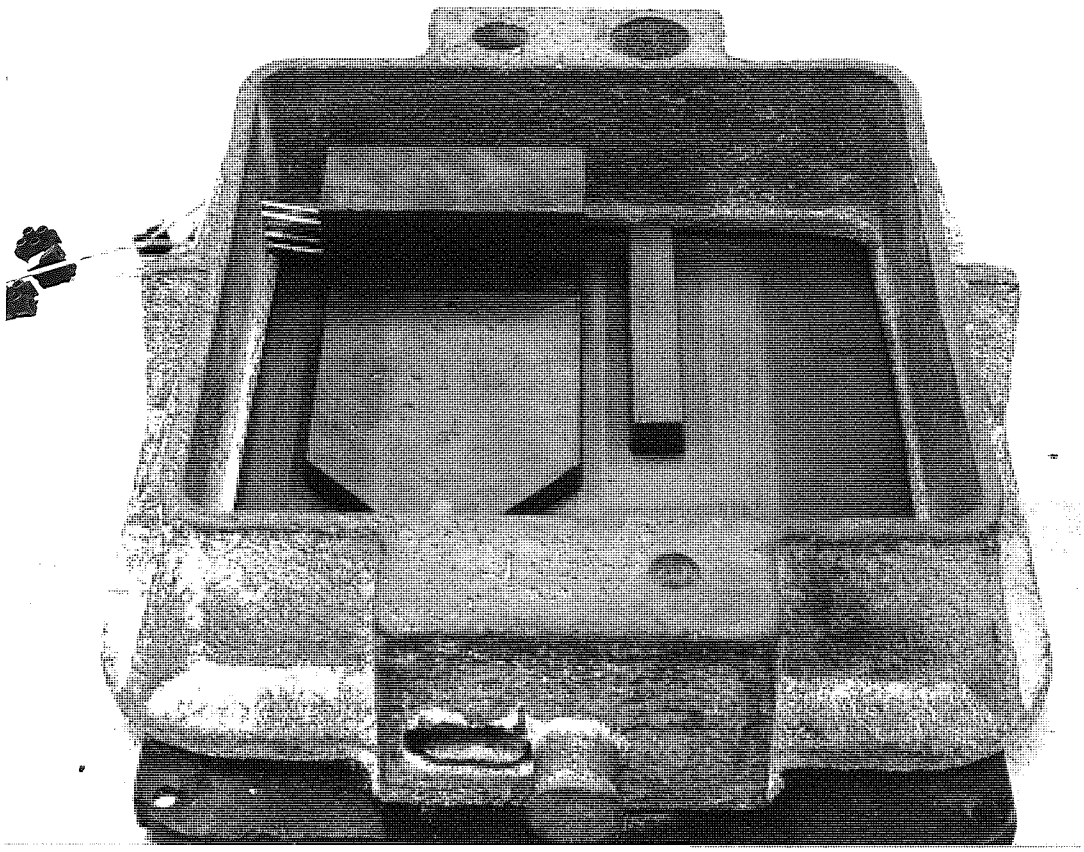

Figure 68.—*Illustrating the block chill in place above the plate pattern and the thermocouples fed in through the side of the moulding box.*

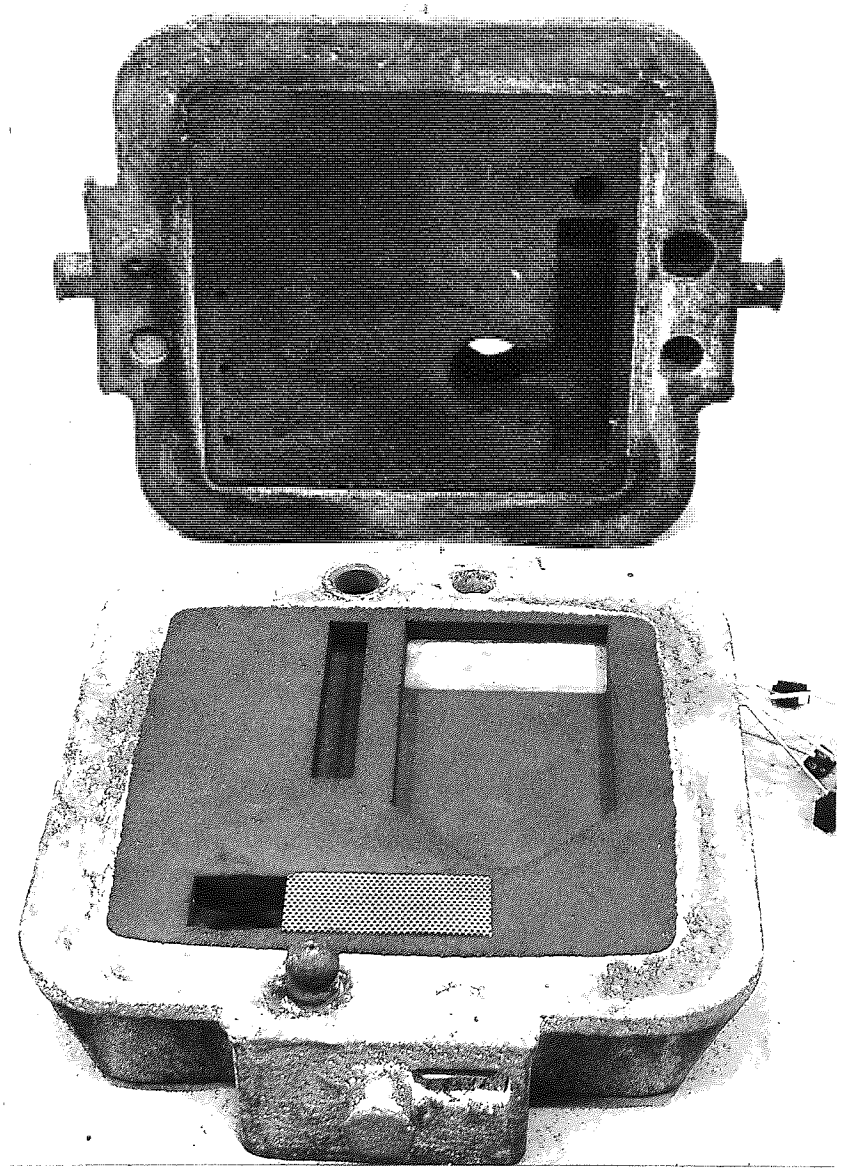

Figure 69.—*Both halves of the pattern rammed up showing the position of the chill. Note, also, the parting line screen in the running system.*

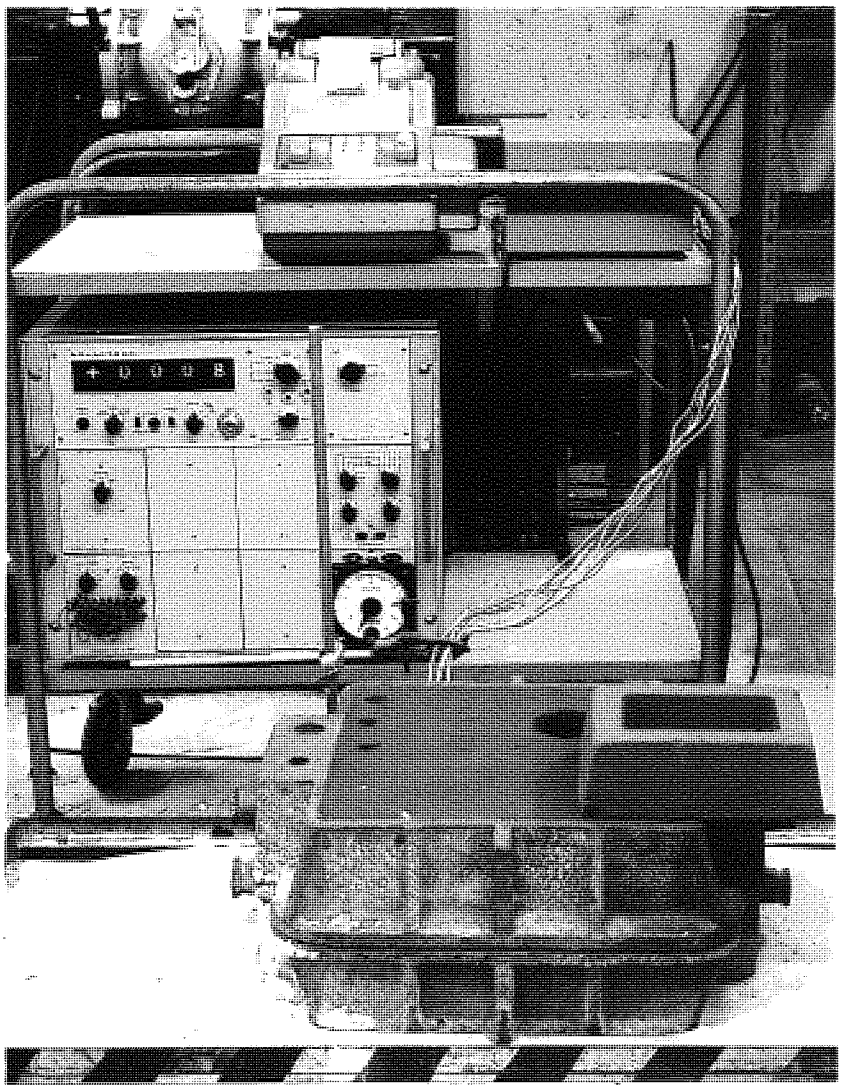

Figure 70.—*The final experimental arrangement.*

The experimental procedure is illustrated in Figures 71 and 72. In alternative experiments the thermocouple beads were placed on the centre line of the casting (viewed in plan, y = 0mm), 1¼in (32mm) from the centre line of the plate and the right hand edge (viewed from the chilled end, y = 32mm) and ½ in (12.5mm) from both the centre line of the plate and the right hand edge (in plan positions y = 12.5mm and y = 51mm), see Figure 81. The thermocouple heights were fixed at 6mm from the base of the plate cavity. The channel in the sand was to enable equal lengths of thermocouple wire to be accommodated within the mould and to be connected, by means of junction blocks, to the external voltmeter leads fed through five holes drilled in the moulding box flange. The thermocouple leads to the left of the plate pass through a similar set of holes drilled in the moulding box's left hand flange. However, these wires were doubly insulated by using lengths of silica sheath and heat resisting rubber sheathing before connection, via junction blocks, to the other set of voltmeter leads.

Several trial runs were carried out to determine:

(a) if there was any pronounced difference in the metal flow characteristics between the left and right hand half of the cavity,

(b) if the thermocouples lifted due to buoyancy and

(c) if the thermocouples were totally wetted by the metal.

These experiments also served to ascertain the reproducibility of the melting and casting technique previously employed. The results of these trial runs showed an exceptional degree of agreement. Thus, reproducibility was possible under foundry conditions provided an established procedure was laid down and that under such circumstances the data from four independent runs could be collated to produce the complete solidification front.

5.4 Experimental Results

5.4.1 Thermal Diffusivity Determinations

The experimental arrangement of the thermal diffusivity determinations gave the series of results shown in Table XIII. From each individual time and distance a value was obtained for the diffusivity of the sand. The gaps in the table indicate where the figure for the AIM in the computer program was greater than the cut off value. Once a casting has lost sufficient heat it becomes solid and the final role of the sand is to retain the original shape of the casting until it is self supporting. Thus, all the experimental results determined during the time interval before the casting was self sufficient were considered useful for a practical estimate of the

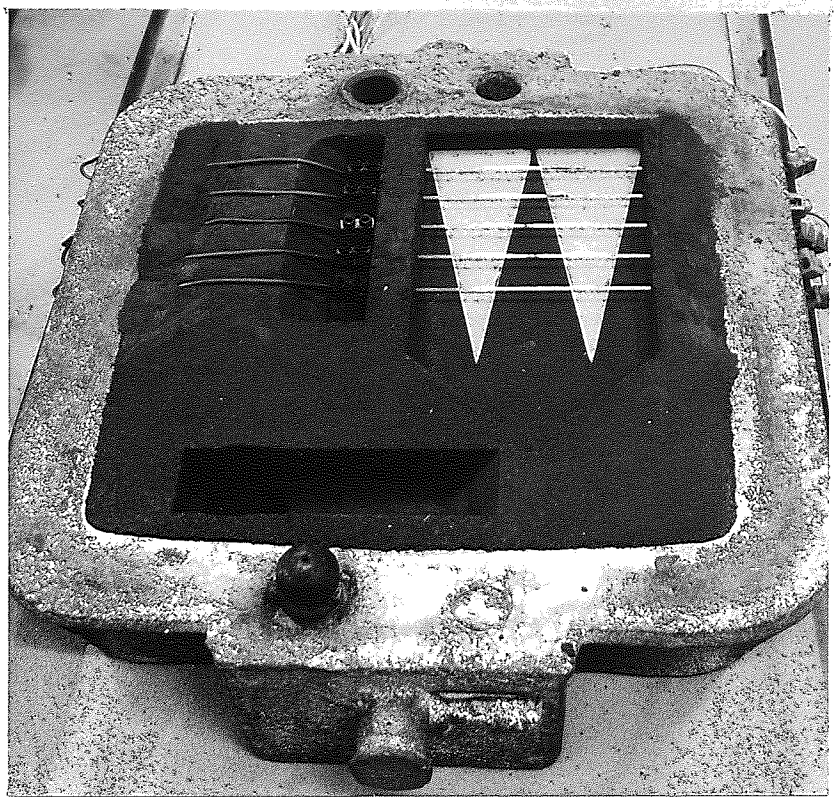

Figure 71.—*Depicting the complete thermocouple lay-out for one directional solidification experiment using taper chills.*

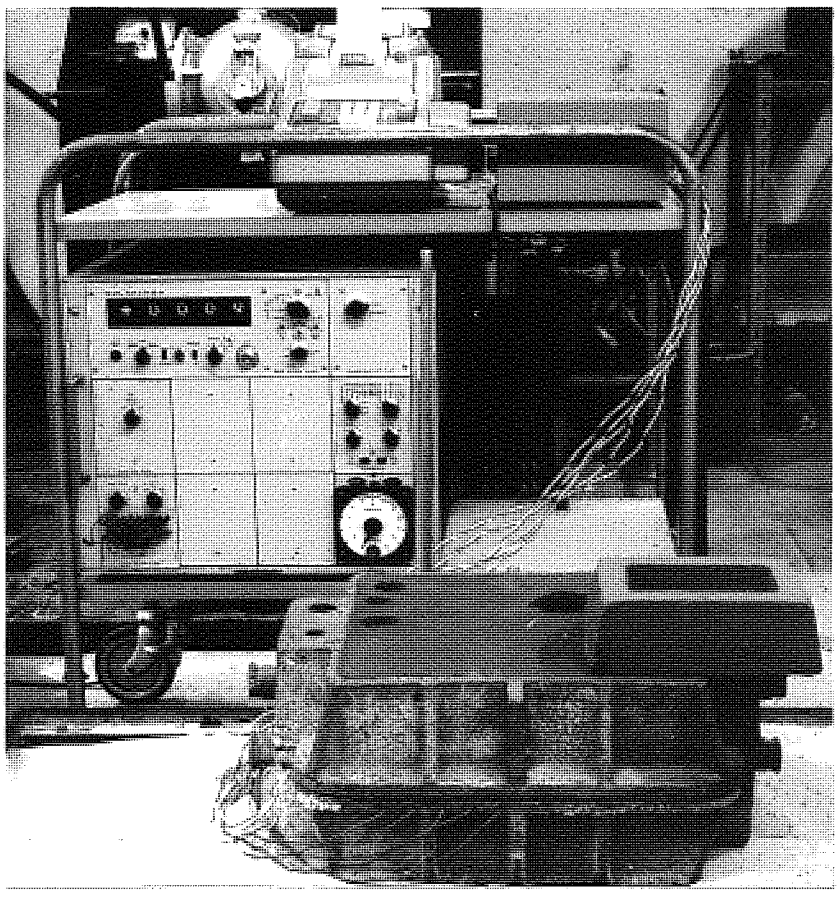

Figure 72.—*The final arrangement used in directional solidification experiments.*

thermal diffusivity. The solidification time interval was found by using the remaining channel in a five channel cycle, to measure the centre line temperature of the cooling slab. For this particular slab size the time elapsed was approximately 300 seconds. The mean thermal diffusivity that resulted was 0.00346 cm^2/sec.

TABLE XIII.—*A portion of the Individual Experimental Thermal Diffusivities obtained from a sand block using the Computer Program developed.*

Time secs	Distance ¼ in	½ in	¾ in	1 in
10	-	-	-	-
20	0.0033	-	-	-
30	0.0033	-	-	-
40	0.0035	0.0051	-	-
50	0.0032	0.0057	-	-
60	0.0034	0.0051	-	-
70	0.0033	0.0043	-	-
80	0.0032	0.0039	-	-
90	0.0032	0.0037	-	-
100	0.0031	0.0035	-	-
110	0.0031	0.0037	0.0041	-
120	0.0030	0.0037	0.0045	-
130	0.0029	0.0037	0.0042	-
140	0.0029	0.0037	0.0041	-
150	0.0028	0.0036	0.0039	-
160	0.0028	0.0038	0.0038	-
170	0.0027	0.0038	0.0037	0.0048
180	0.0027	0.0038	0.0035	0.0046

5.4.2 Interfacial Temperature Determinations

Table XIV reveals the good agreement between the results calculated from the computer program for determining interfacial temperatures, and the temperatures observed in a series of practical experiments. Further evidence of good agreement was provided by extrapolating plots of the experimentally observed data in the Cast Iron and Aluminium chills back to the interface (Figures 73 and 75). The influence of variations in pouring temperature on the interfacial temperatures of Cast Iron chills was examined. Aluminium chills were not examined because Aluminium has a much higher thermal diffusivity than Cast Iron, so there would be much less variation in the surface temperature distribution. The effect that a commercial chill coating had on the surface temperature variation of an Aluminium chill at a constant pouring temperature was also examined. The resulting two interfacial temperature distributions are shown in Figures 74 and 76.

TABLE XIV.—*Random examples of observed and calculated temperatures from several computer runs using experimental data for interfacial temperature determinations in both Aluminium and Cast Iron chills.*

Aluminium Chill

Positions	1	2	3	4	5	
Within chill	1/8 in	3/8in	5/8in	7/8in	11/8in	Sum of Squares
Observed	113.00	93.00	83.00	74.00	66.00	-
Calculated	109.59	97.91	84.93	73.67	63.44	38.05
Observed	202.00	198.00	196.00	194.00	190.00	-
Calculated	201.81	198.90	195.99	193.09	190.19	1.71
Observed	160.00	140.00	126.00	116.00	105.00	-
Calculated	156.99	142.75	128.84	115.46	102.79	29.88

Cast Iron chill

Positions	1	2	3	4	5	
Within chill	1/8 in	3/8in	5/8in	7/8in	11/8in	Sum of Squares
Observed	71.00	38.00	26.00	20.00	20.00	-
Calculated	70.74	39.16	24.17	19.84	19.09	5.64
Observed	186.00	145.00	110.00	82.00	64.00	-
Calculated	184.41	146.18	111.87	83.19	60.90	18.45
Observed	169.00	151.00	132.00	113.00	100.00	-
Calculated	169.26	150.31	132.00	114.69	98.69	5.11

It should be noted that the changes in the slopes of the curves A and B occur at approximately 10 and 17 seconds respectively.

Figure 73 illustrates the observed temperatures at the five equally spaced positions within the front half of the Cast Iron chill , i.e. nearest the cast metal. Extrapolations of these observations indicate a rise and fall in the interfacial temperature. These results compare favourably with those in Figure 74. Also shown in Figure 74 is the influence of different pouring temperatures on the interfacial temperature distributions of the Cast Iron chill. The peaks present in the curves become higher and occur earlier as the pouring temperature is increased.

Since the computer program provided an accurate estimate of the interfacial temperature it was thought worthwhile to determine the area under the derived curve and so calculate the heat absorbed by the chill during each cycle of temperature measurements. The incremental changes in heat content were added to produce a cumulative total heat content. Three sets of curves depicting heat contents are included (Figures 77 and 78). Two sets indicate the behaviour of uncoated Aluminium and Cast Iron chills in contact with metal poured at 720°C. The remaining set (in Figure 78) shows the behavioural change when a coating is applied to the Aluminium chill, the pouring temperature again being 720°C.

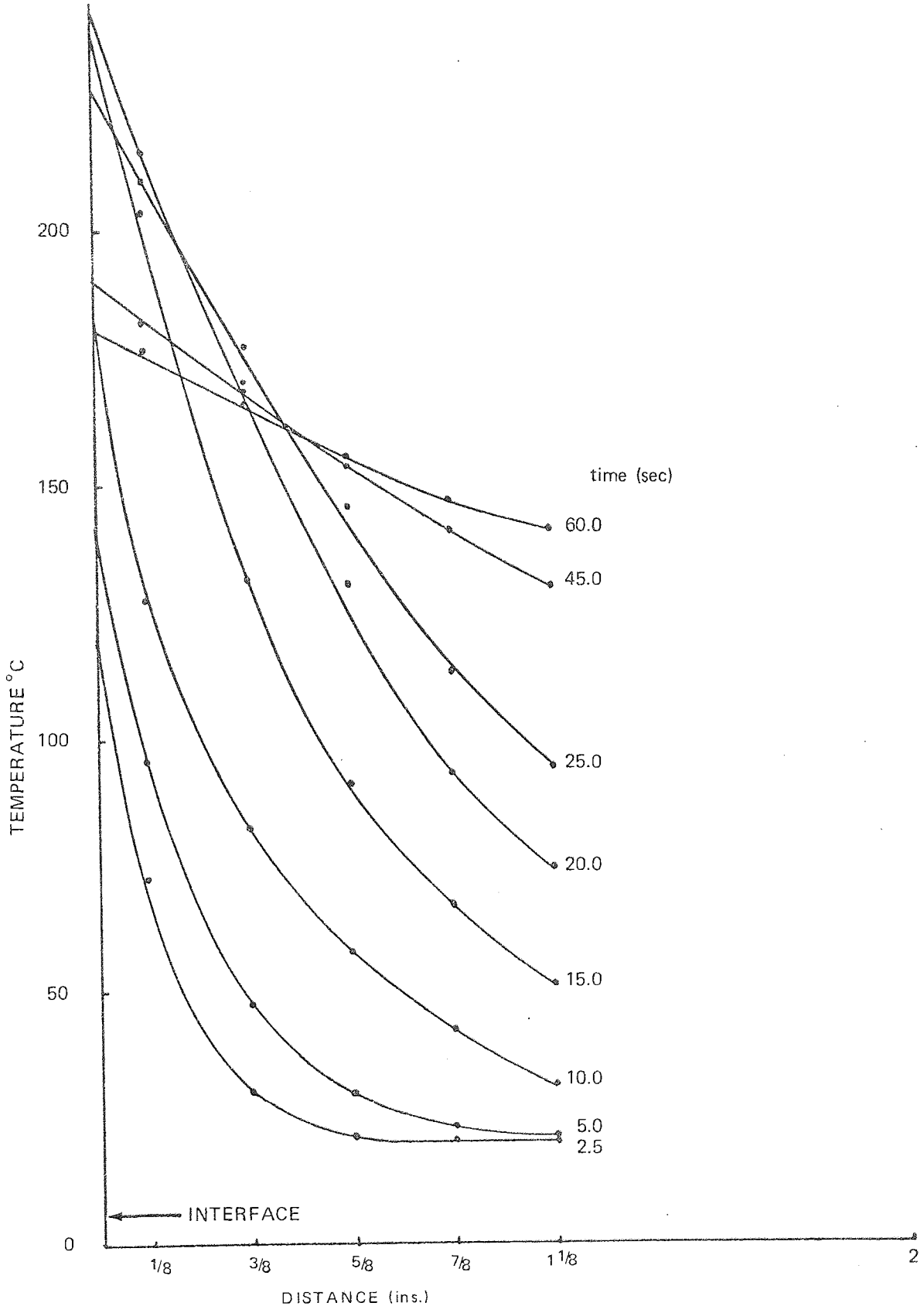

Figure 73.—*Observed Experimental Results for a Cast Iron chill showing Extrapolations to the Interface at various times (seconds).*

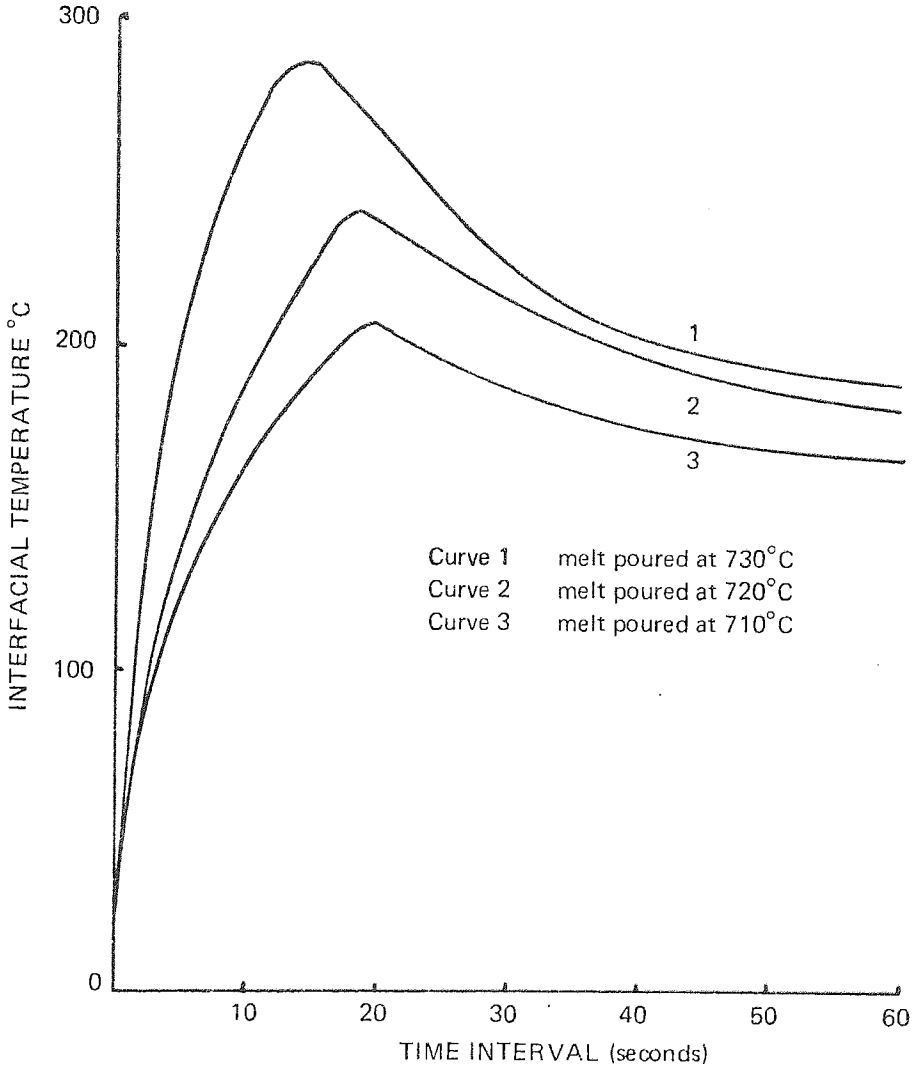

Figure 74.—*Interfacial Temperatures for Cast Iron Block chills.*

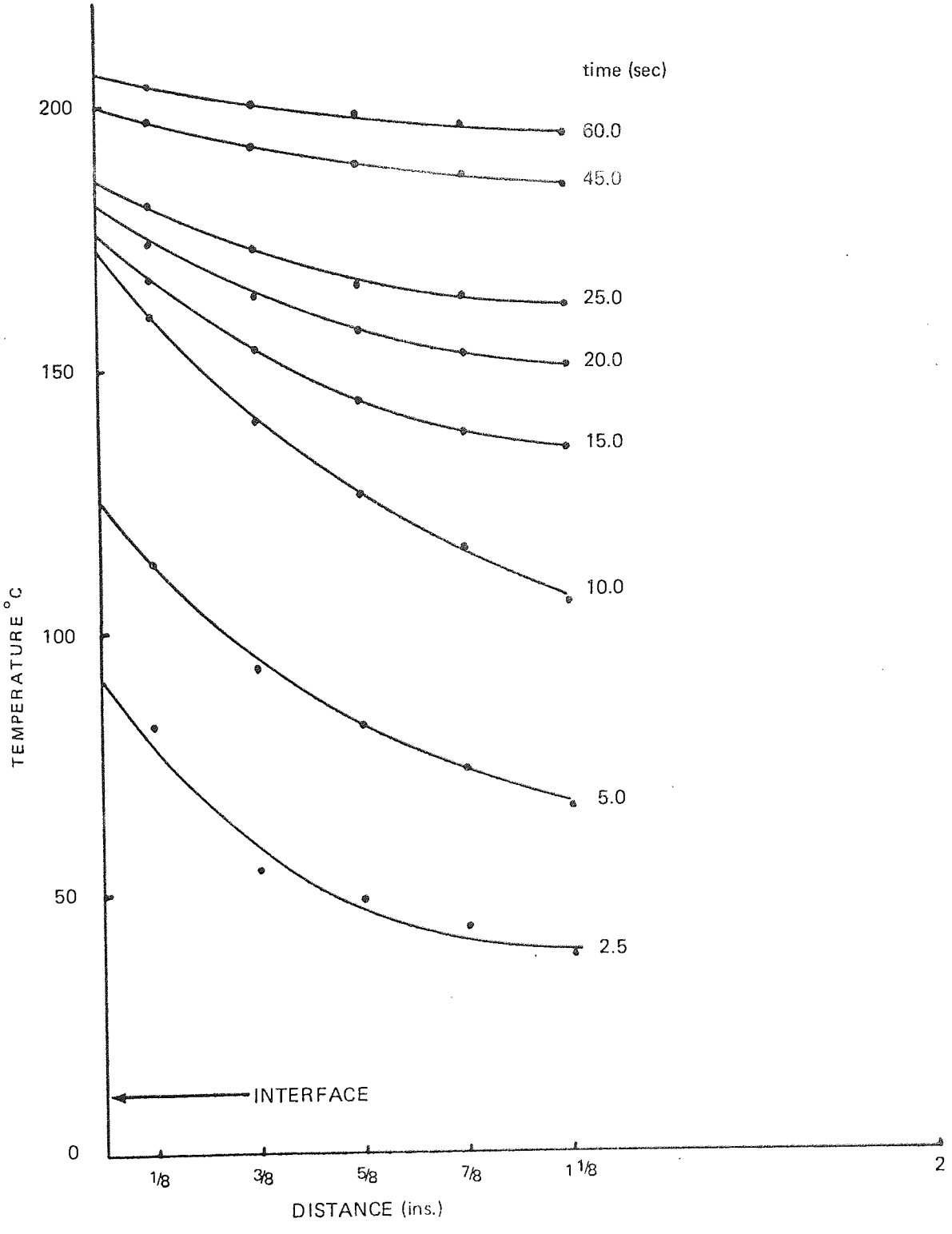

Figure 75.—*Observed Experimental Results for an Aluminium chill showing Extrapolations to the Interface at various times (seconds).*

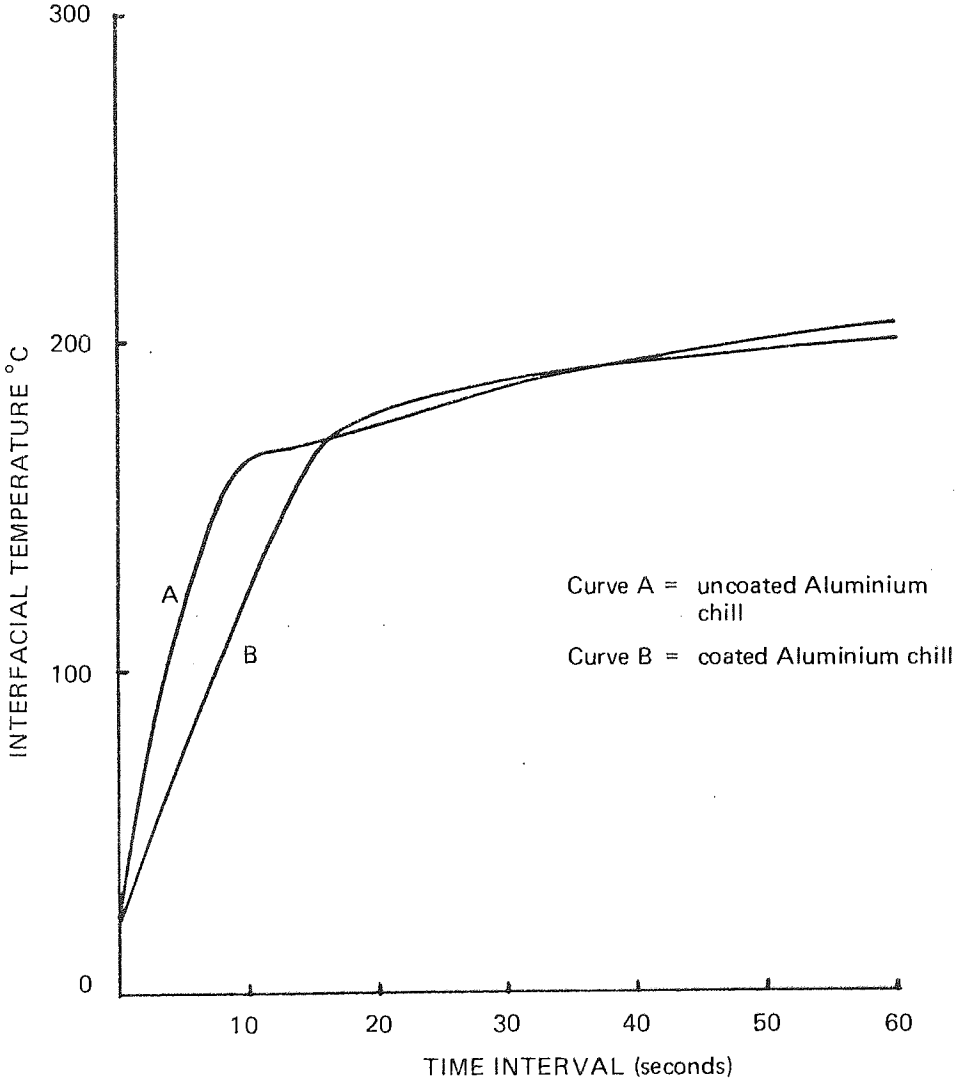

Figure 76.—*Interfacial Temperatures for Aluminium Block chills.*

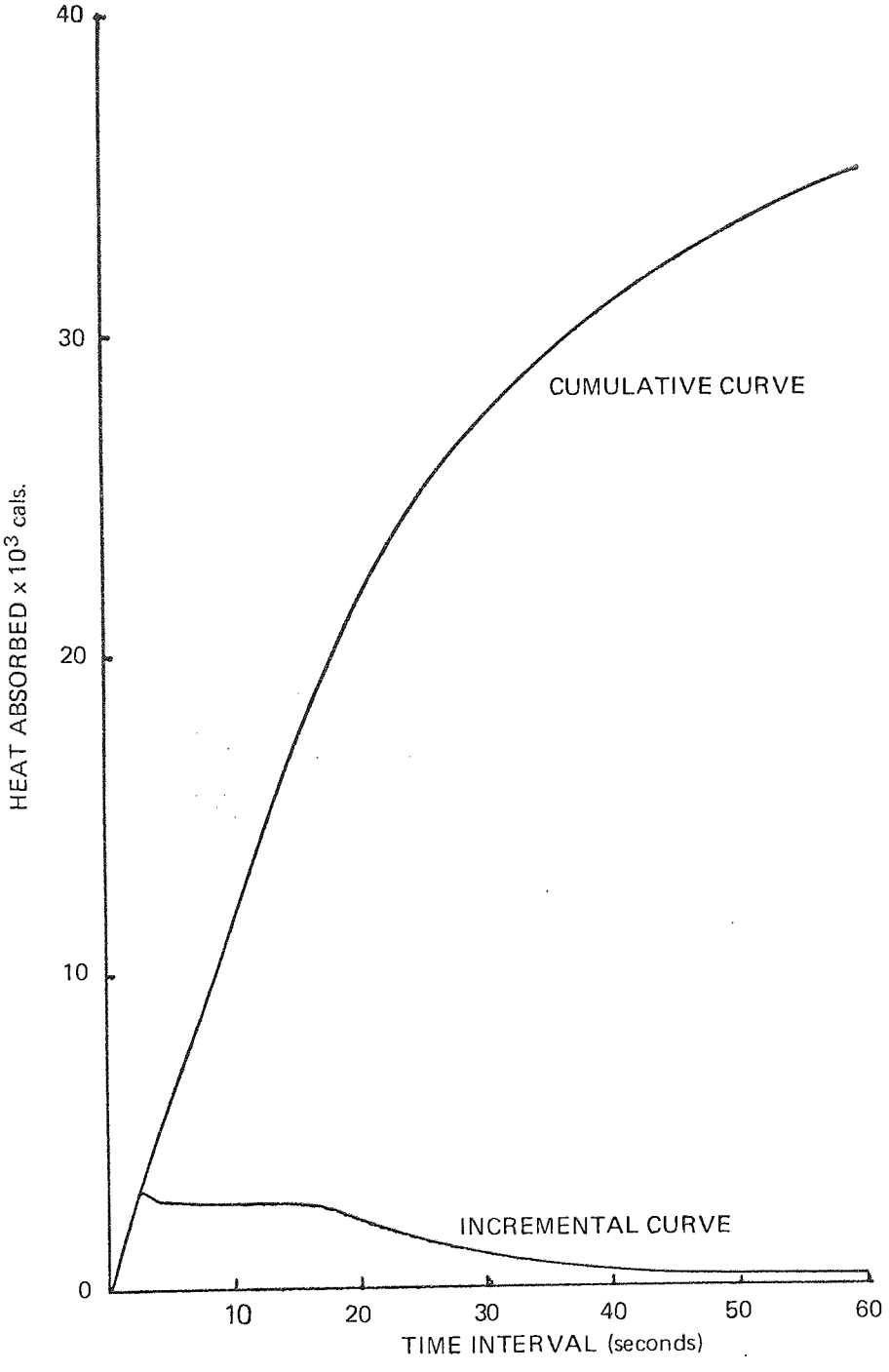

Figure 77.—*Cumulative and Incremental Heat Absorptions for an Uncoated Cast Iron Block chill.*

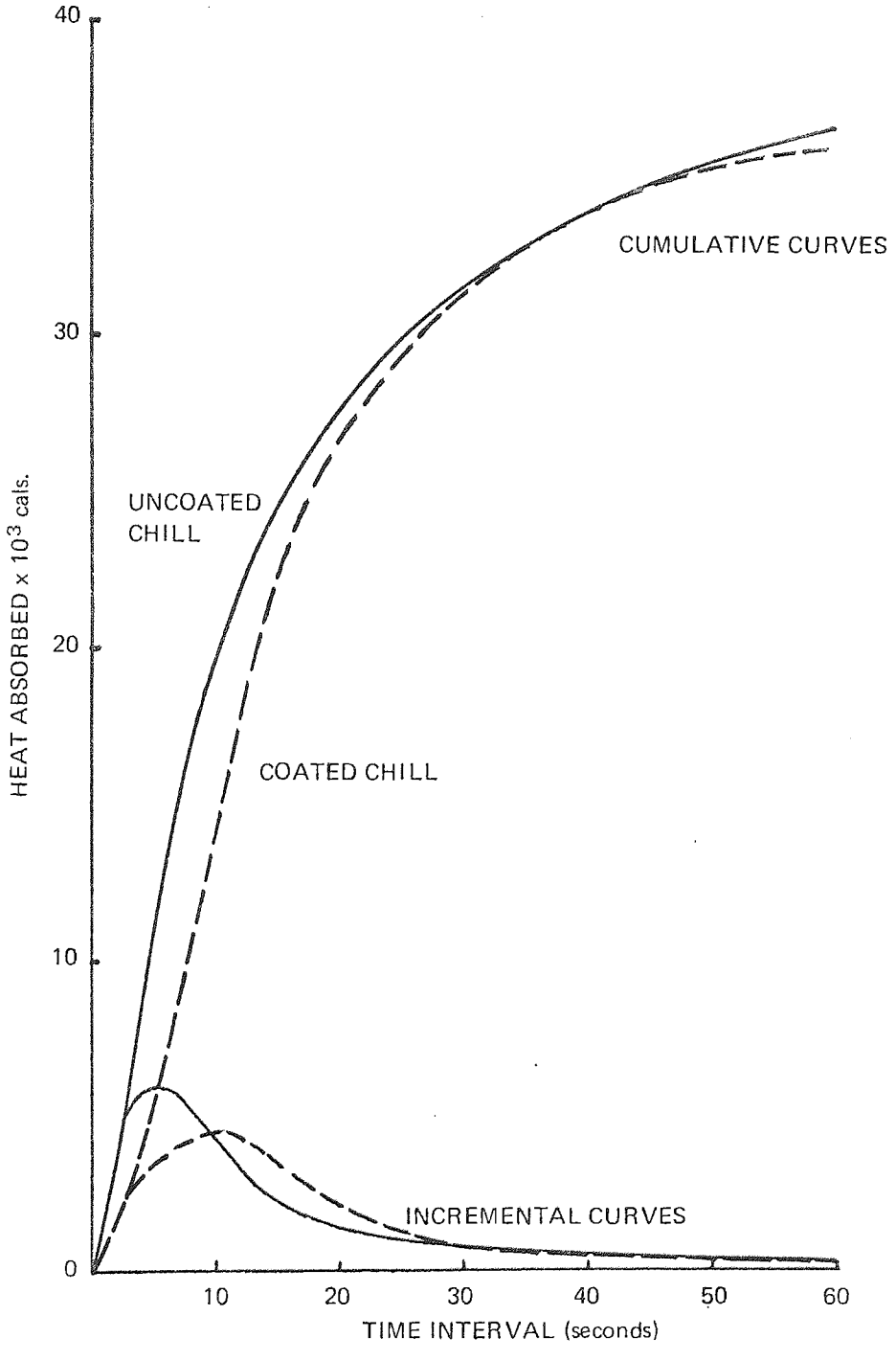

Figure 78.—*Cumulative and Incremental Heat Absorptions for a Coated (broken line) and Uncoated (solid line) Aluminium Block chill.*

5.4.3 *Influence of Chill Shapes on Directional Solidification*

Figure 81 represents a plan view of a complete plate casting and precedes Figures 82 to 101 which represent the isothermal distributions in the bottom half of the plan view. The time interval of five seconds between each isothermal distribution was selected because it represented a margin large enough to indicate the movement of the solidification fronts without too many diagrams.

Construction of Isothermal Diagrams

For each chilling technique four experiments were performed. These resulted in cooling curves for each thermocouple position in the matrix, down to 500°C, and hence temperature isotherms for every time interval. The temperature, in the diagrams (Figures 79 and 80) was assumed to vary linearly between each experimental point unless a smooth curve could be constructed through the points with certainty.

Unchilled Section

The first three illustrations, Figures 82 to 84, indicate that during pouring the metal flowed along the centre line of the cavity until it met the end opposite the feeder. Here the stream parted forming a triangular dead zone with its base along the edge away from the feeder and the apex pointing in the direction of the gate. There was some evidence of chilling in the front portion of the material entering the cavity, denoted by the closer spacing of the isotherms compared to the distances between isotherms in the metal which entered the mould later. The next three diagrams, Figures 85 to 87, illustrate the continued influence that the mould cavity sides had on the isotherms. The original metal flow along the cavity centre reduced the effectiveness of the sand as a heat sink, consequently, the isotherms lagged behind in the middle.

The final six diagrams in the series show that some mechanism was beginning to induce the forward movement of the isotherms along the plate centre line faster than at the centre of each half. This was more pronounced in the last three Figures (88 to 90) where the isothermal lag at the centre line was rapidly disappearing.

Aluminium Block Chilled Section

The most obvious detail in this series was the reduction in time taken for the thermocouple stations to fall to 500°C. The behaviour of the metal flow was apparent from Figure 91 where the metal stream parted in a similar fashion to the unchilled section. The flow back was arrested much more quickly in this technique, however, preventing the isotherms from advancing very far along the edges of the

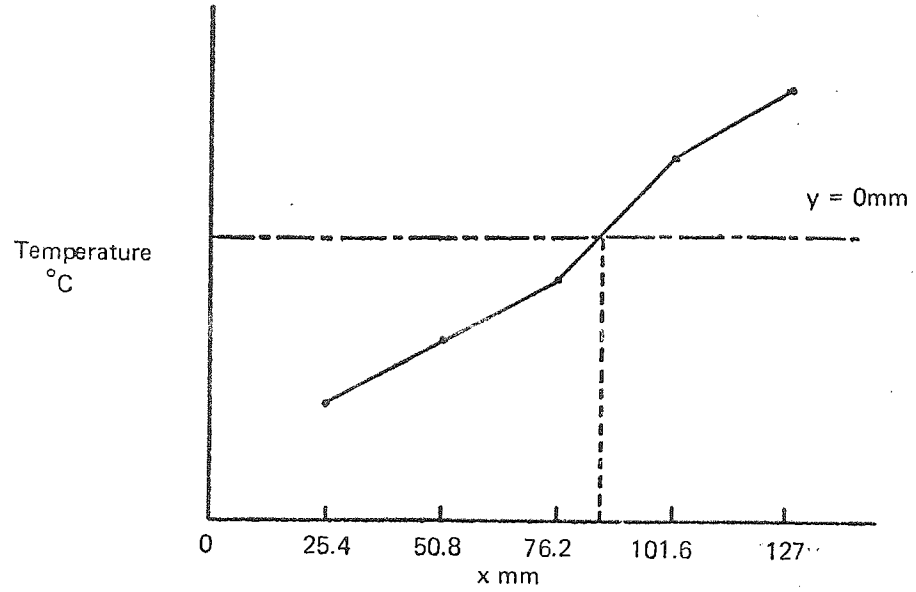

Figure 79.—*Determination of the point along the y = 0mm axis corresponding to a particular temperature for the construction of that isotherm.*

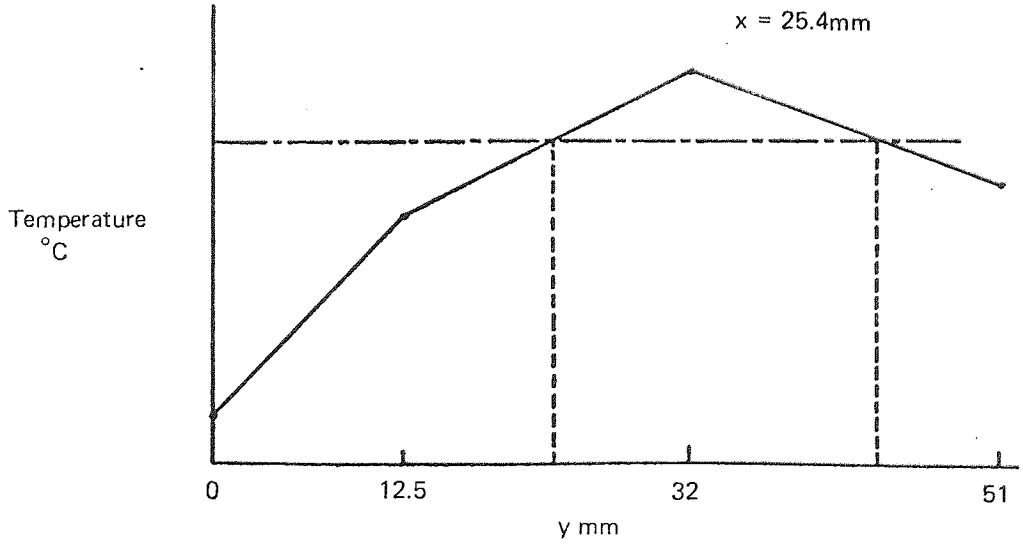

Figure 80.—*Determination of the points (or point) along the x = 25.4mm axis corresponding to a particular temperature for the construction of that isotherm.*

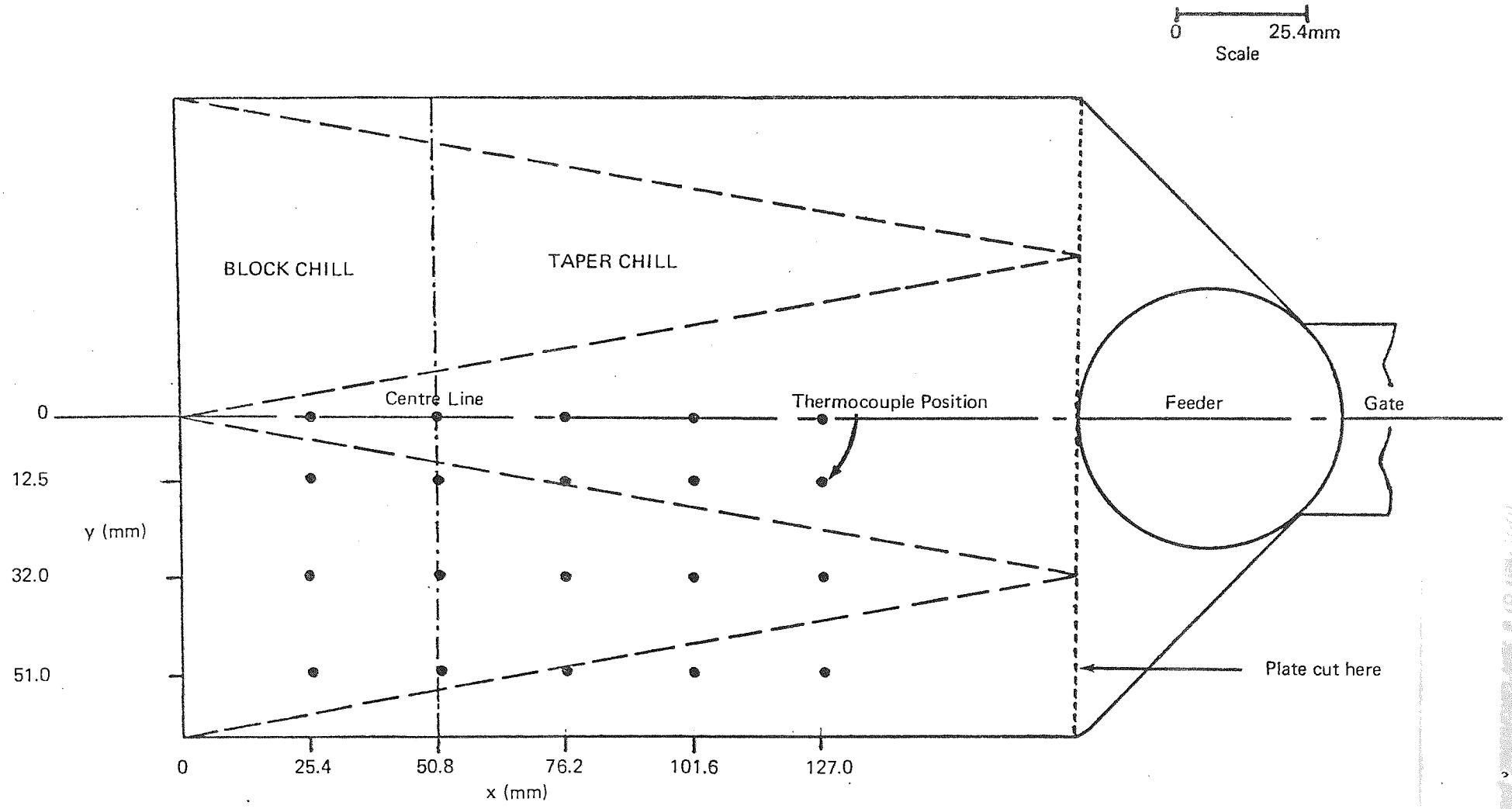

Figure 81.—*The plan view of plate, indicating chill and thermocouple positions.*

Distributions of Isotherms in the bottom half of a ½in Unchilled plate.

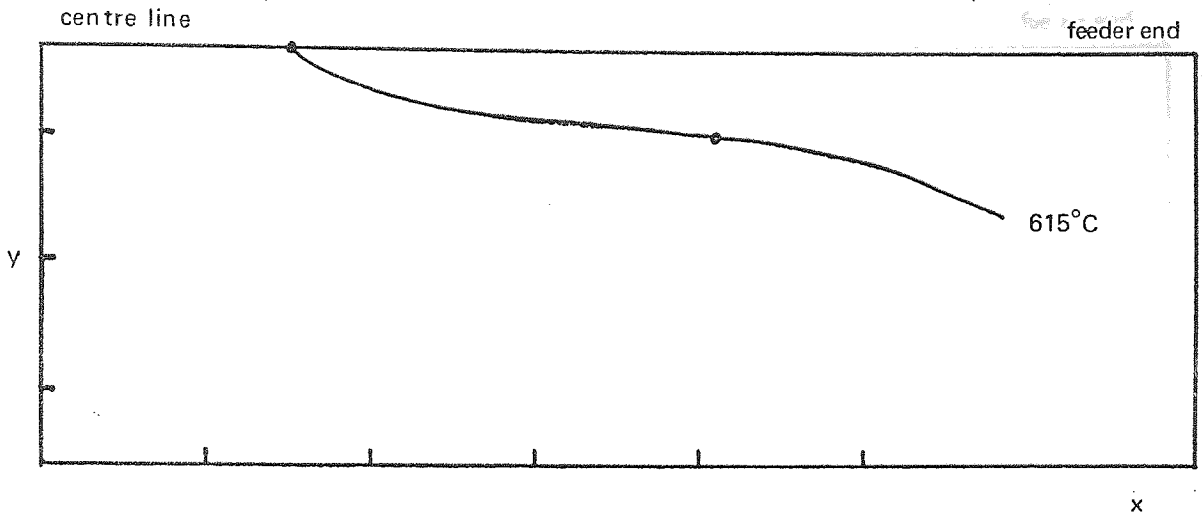

Figure 82.—*After 5 seconds.*

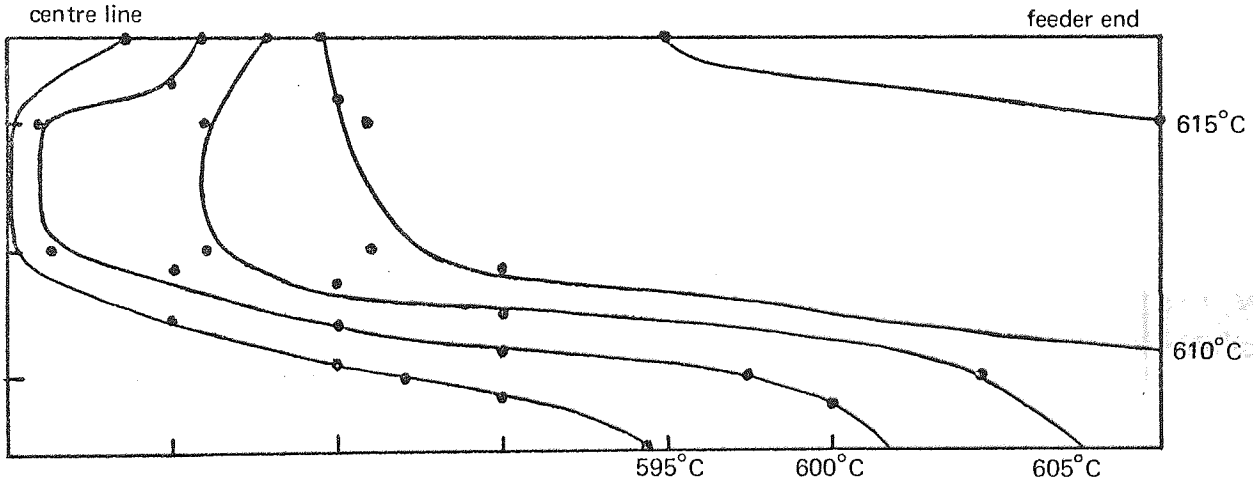

Figure 83.—*After 10 seconds.*

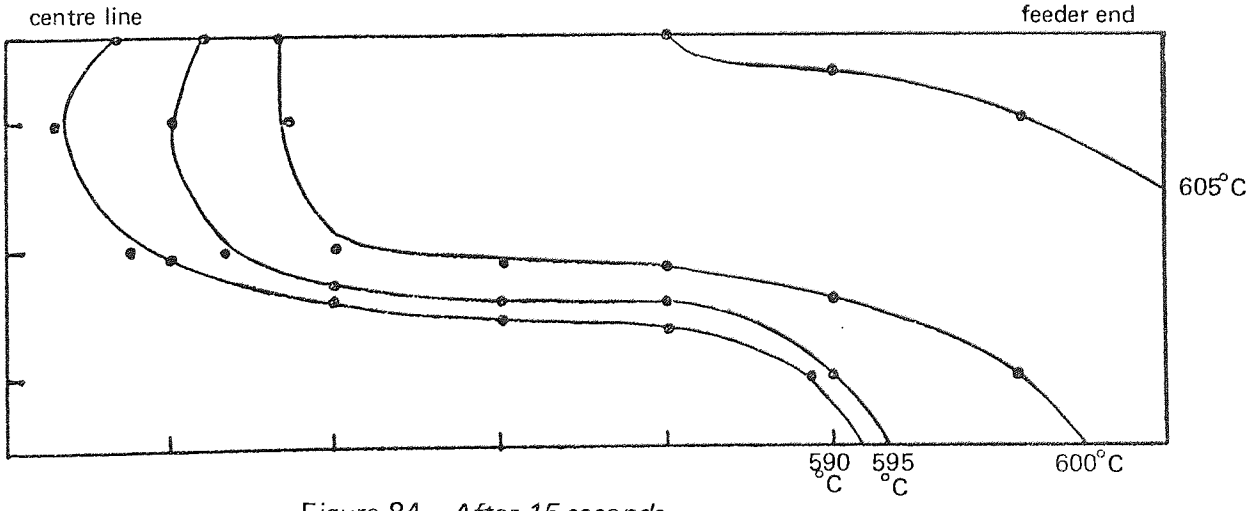

Figure 84.—*After 15 seconds.*

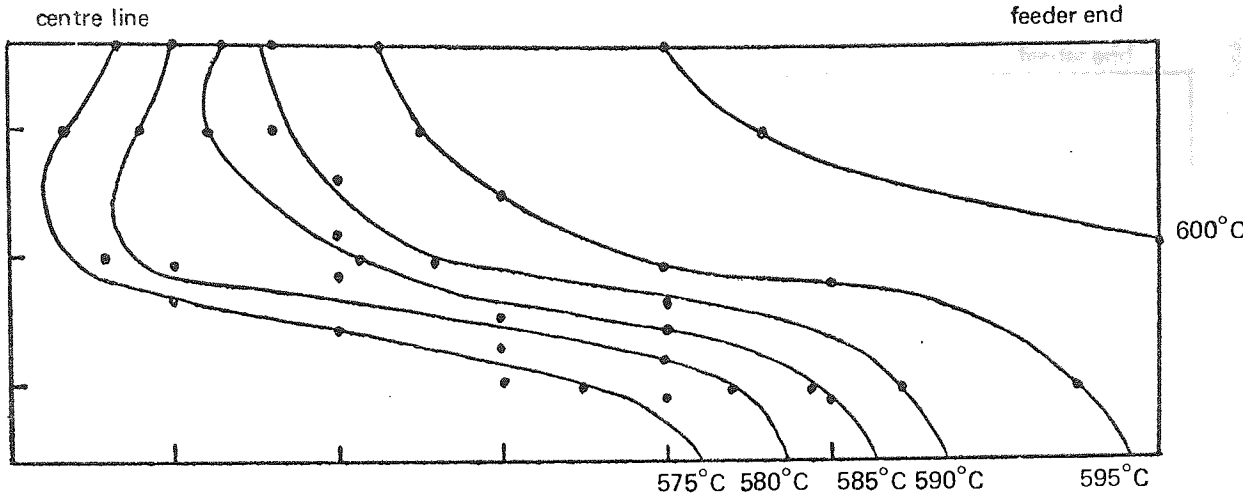

Figure 85.—*After 20 seconds.*

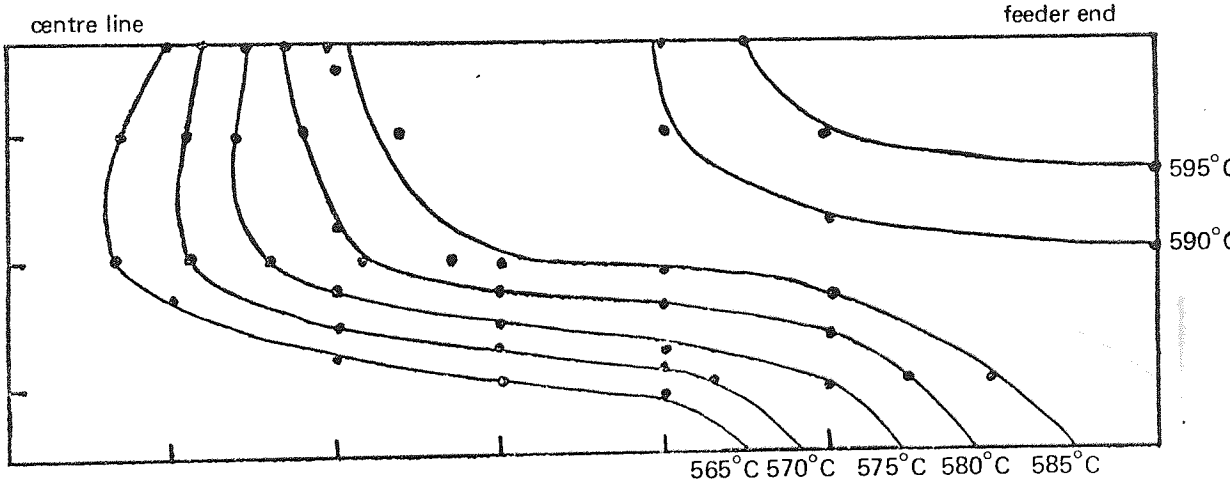

Figure 86.—*After 25 seconds.*

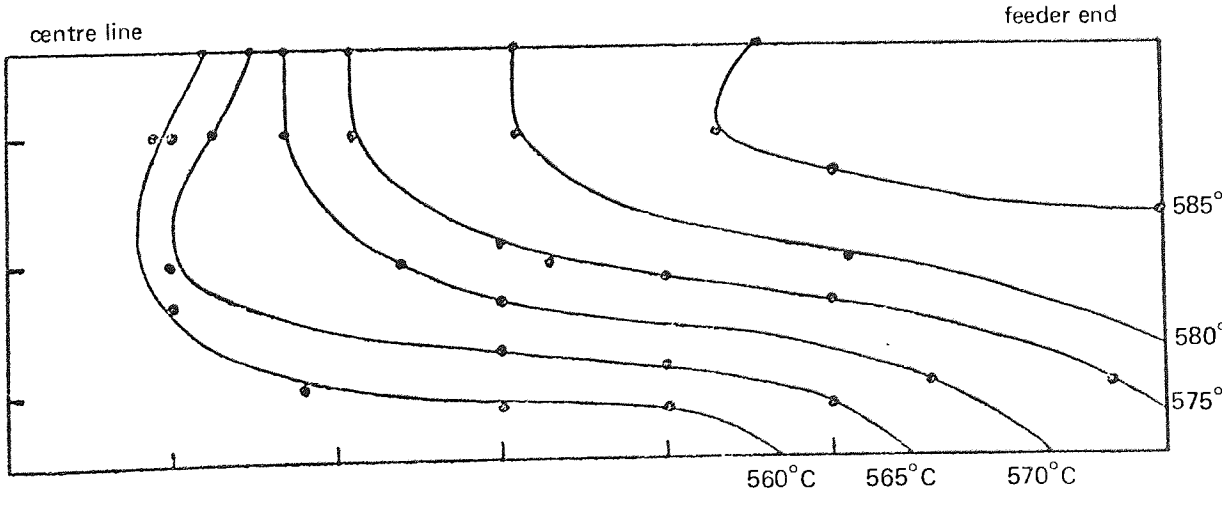

Figure 87.—*After 30 seconds.*

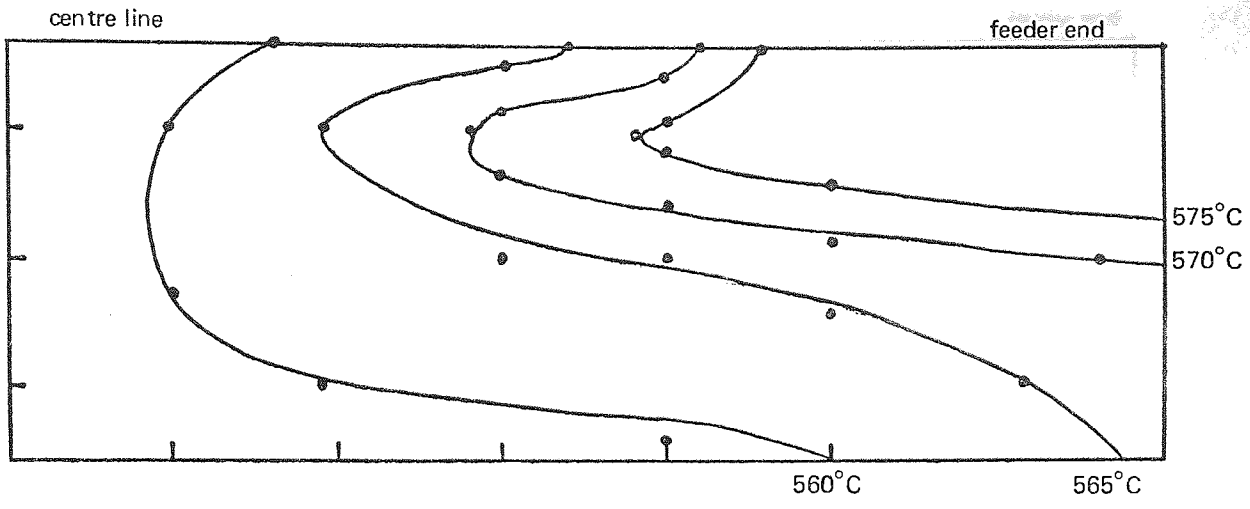

Figure 88.—*After 35 seconds.*

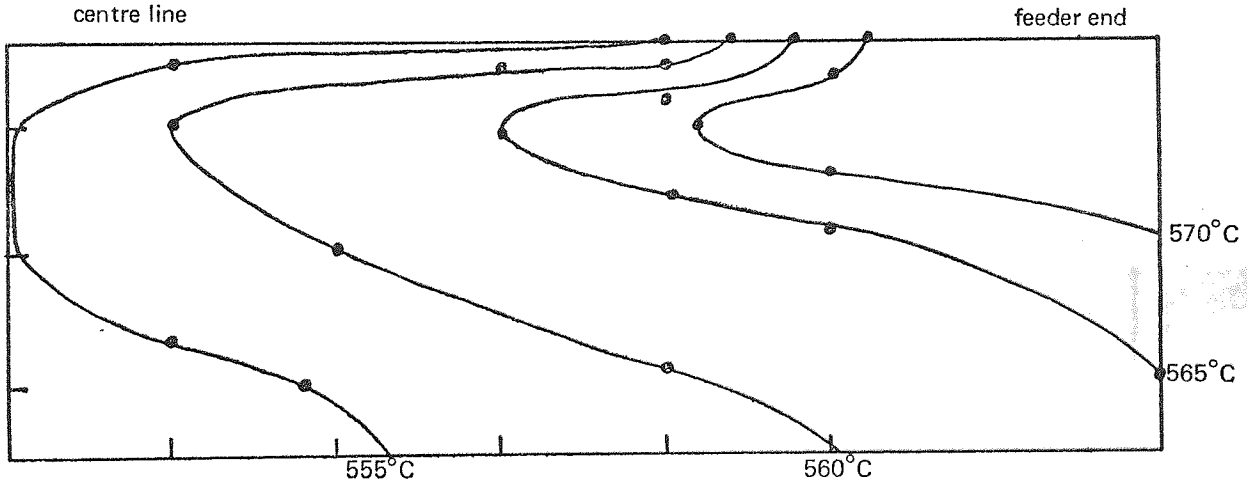

Figure 89.—*After 40 seconds.*

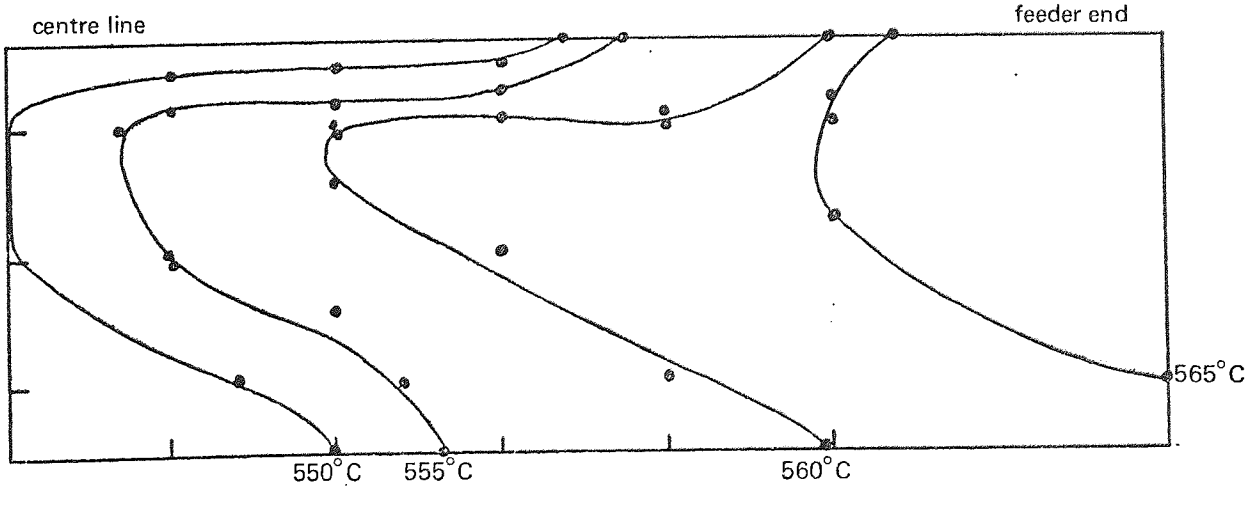

Figure 90.—*After 45 seconds.*

Distributions of Isotherms in an Aluminium Block chilled ½in plate.

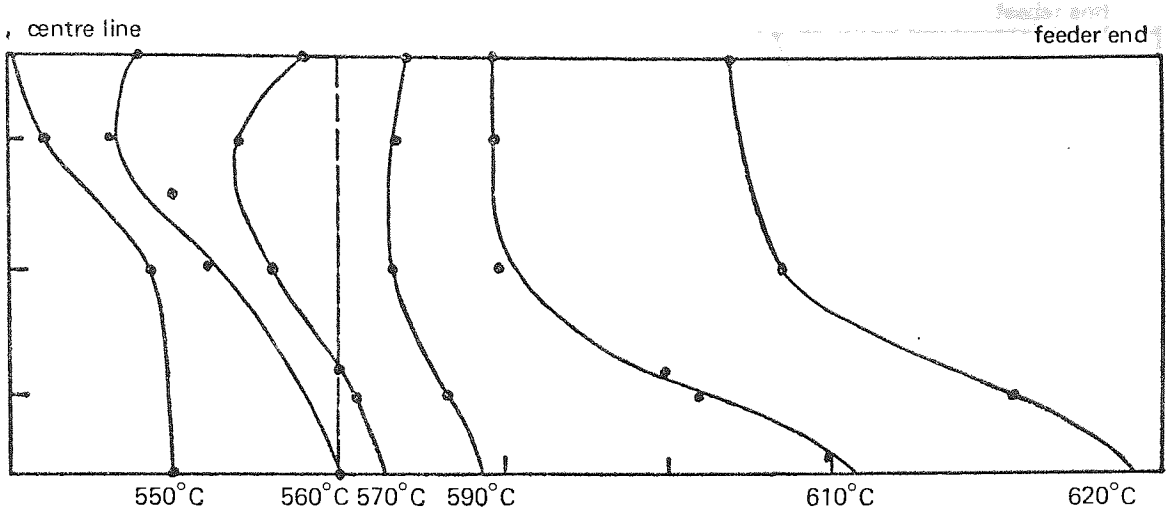

Figure 91.—*After 5 seconds.*

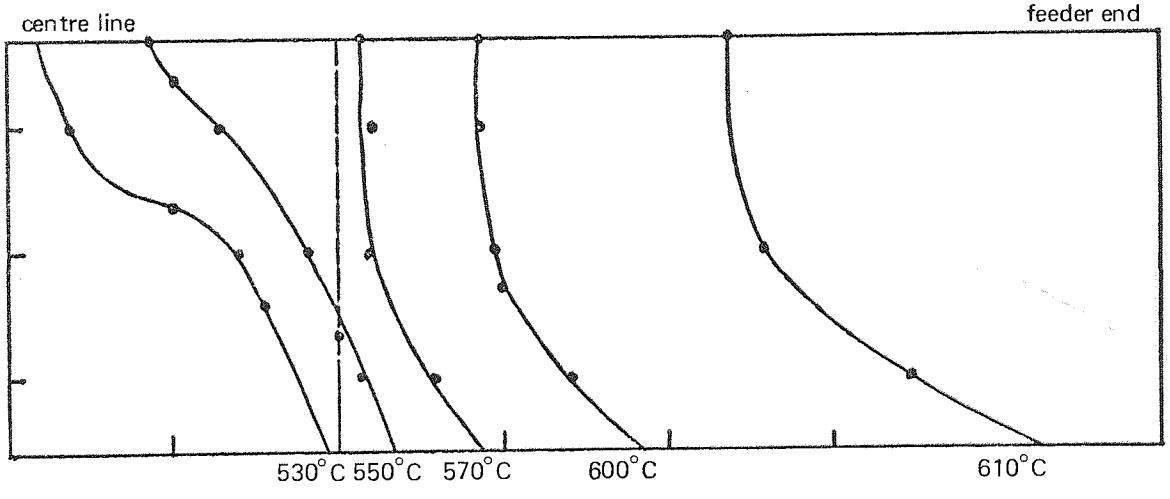

Figure 92.—*After 10 seconds.*

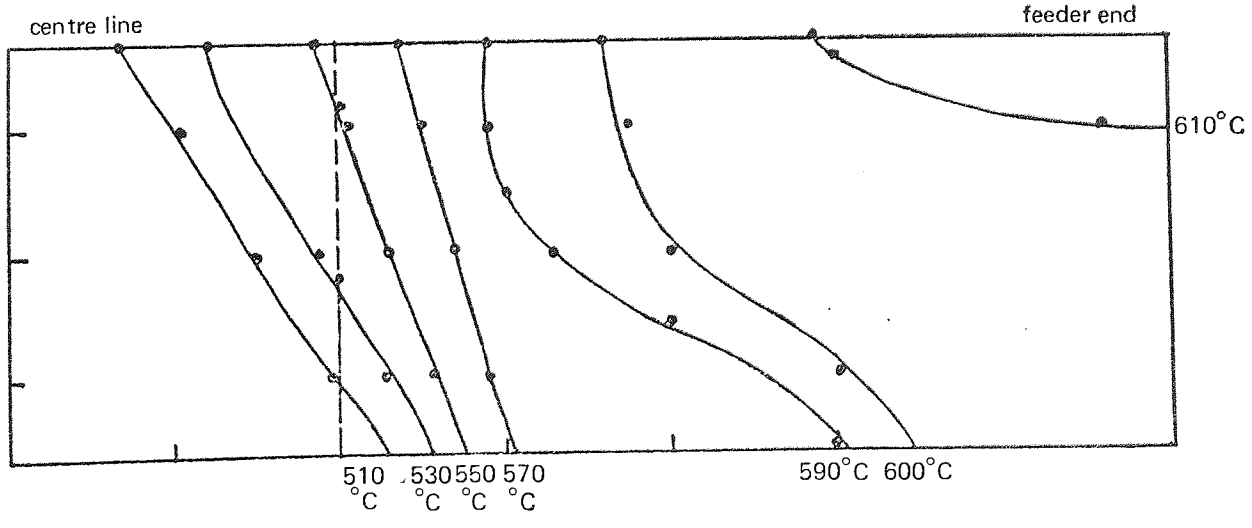

Figure 93.—*After 15 seconds.*

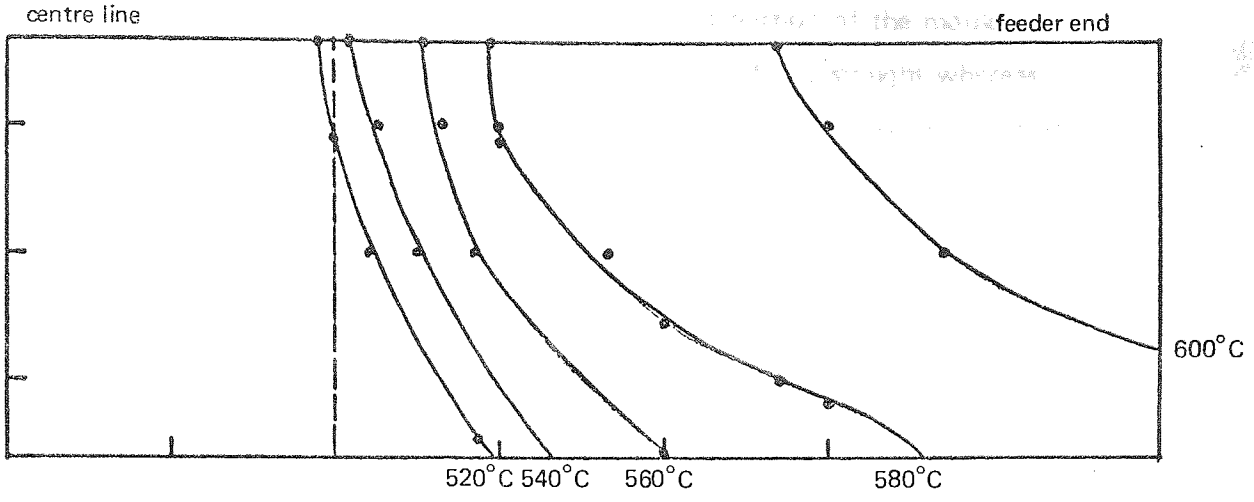

Figure 94.—*After 20 seconds.*

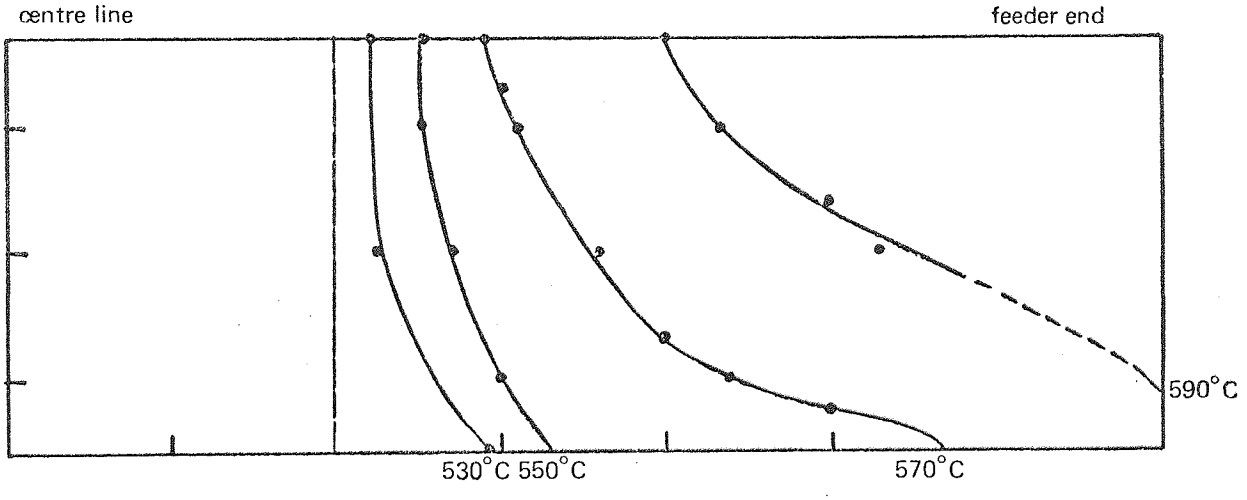

Figure 95.—*After 25 seconds.*

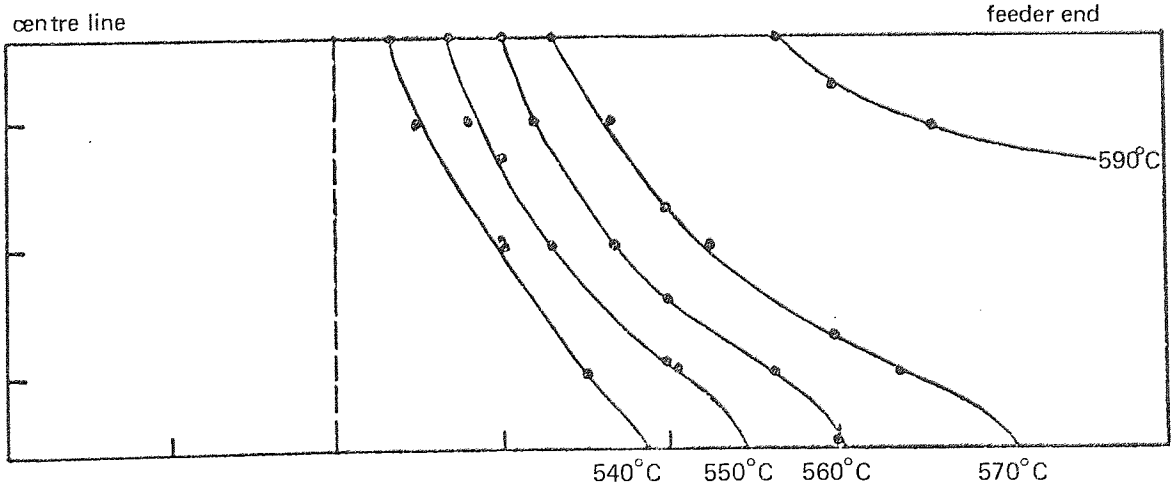

Figure 96.—*After 30 seconds.*

cavity. The spacing of the isotherms depicted steeper temperature gradients in the Aluminium above the chill compared to that in the sand portion of the mould. Isotherms within the influence of the chill block remained fairly straight whereas in the sand region away from the chill's effect they resemble the shape determined in the unchilled section.

Figures92 to 96 illustrate the progression of solidification away from the chill with the chill's effect manifested in steep thermal gradients away from the feeder. Shallow gradients were still found at the gate end.

Aluminium Double Thickness Single Taper Chilled Section

The results shown in Figures 97 to 101 represent a departure from those previously described. The isotherms are re-entrant along the axis of the taper chill and throughout the period of time investigated remained approximately equidistant.

5.4.4 Influence of Chill Shape on Porosity

Figures 102 to 104 illustrate micrographs of specimens taken from plates subjected to the following chill techniques:

(i) Unchilled,

(ii) Aluminium block chilled and

(iii) Aluminium double thickness single taper chilled.

The samples were taken from the centre of the plate (y = 0mm) at positions similar to where the thermocouples were placed.

Unchilled Plate

The micrographs show a reasonably constant level of porosity along the portion of the plate investigated. Although there was a scattering of density measurements a definite trend emerged leading to less dense specimens towards the feeder end (Figure 102).

Block Chilled Plate

The five micrographs reproduced in Figure 103 can be divided into two distinct groups. The first two pictures contain considerably less porosity than any of the remainder and they correspond to the region directly above the block chill. The remaining three photographs resemble the unchilled micrographs with the porosity increasing towards the gate. This again can be seen in Figure 103.

Double Thickness Single Taper

No different regions exist with this particular chilling method. The micrographs show that in a plate chilled by this technique an overall decrease in porosity was achieved compared to the previous chill methods and there is a pronounced increase in porosity from the more chilled end. This is in agreement with Figure 104 which

Distributions of Isotherms in an Aluminium Double Thickness Single Taper chilled ½in plate.

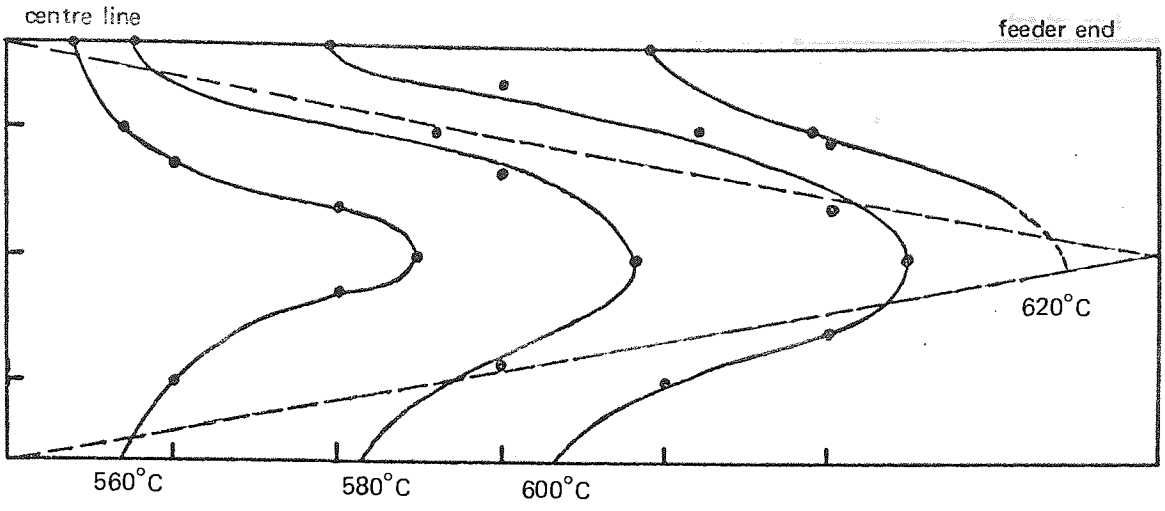

Figure 97.—*After 5 seconds.*

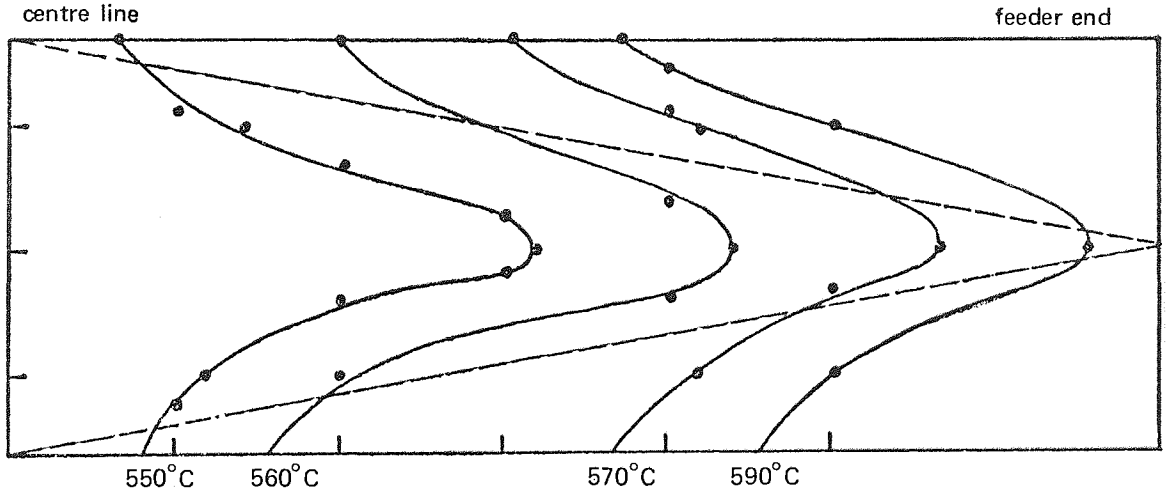

Figure 98.—*After 10 seconds.*

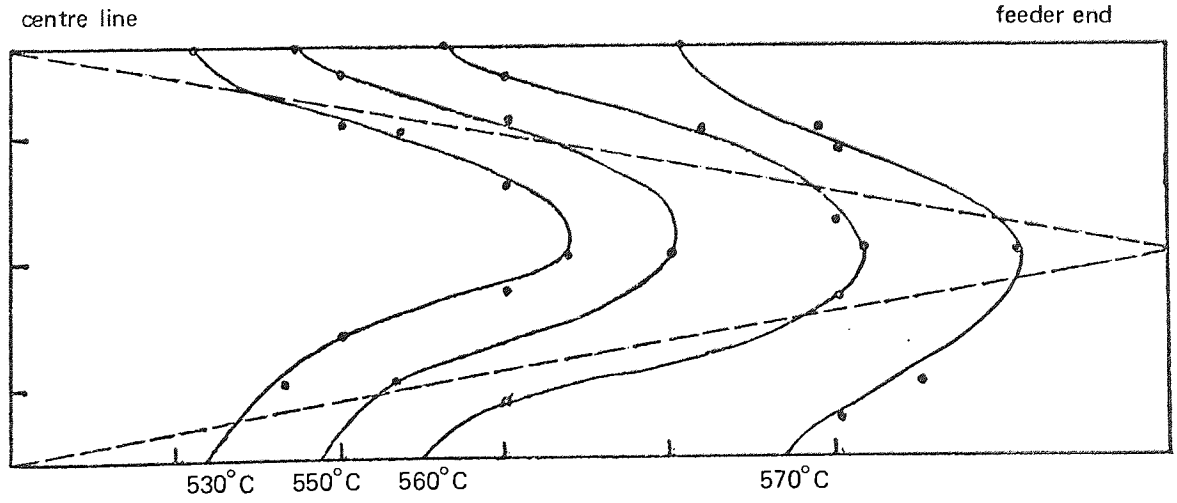

Figure 99.—*After 15 seconds.*

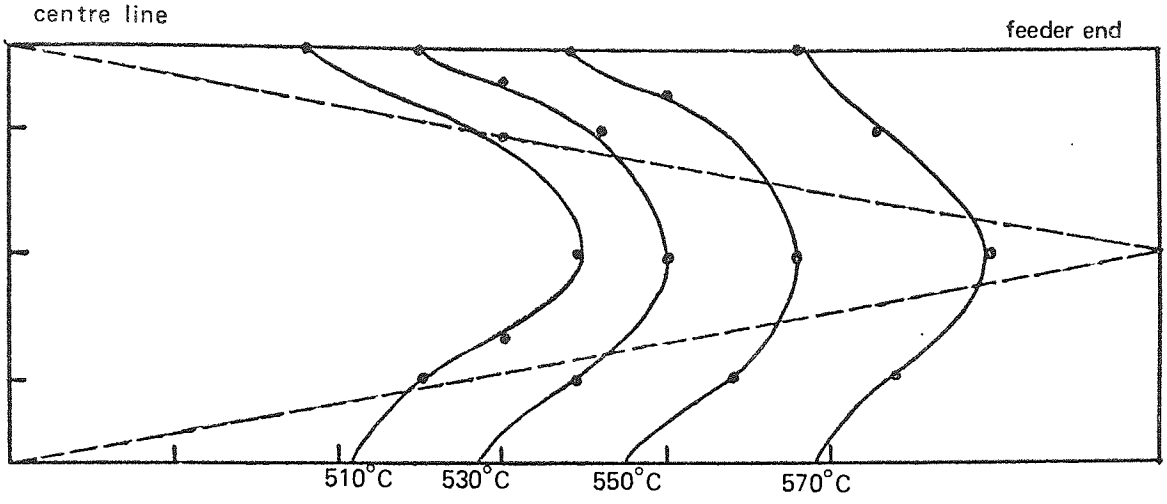

Figure 100.—*After 20 seconds.*

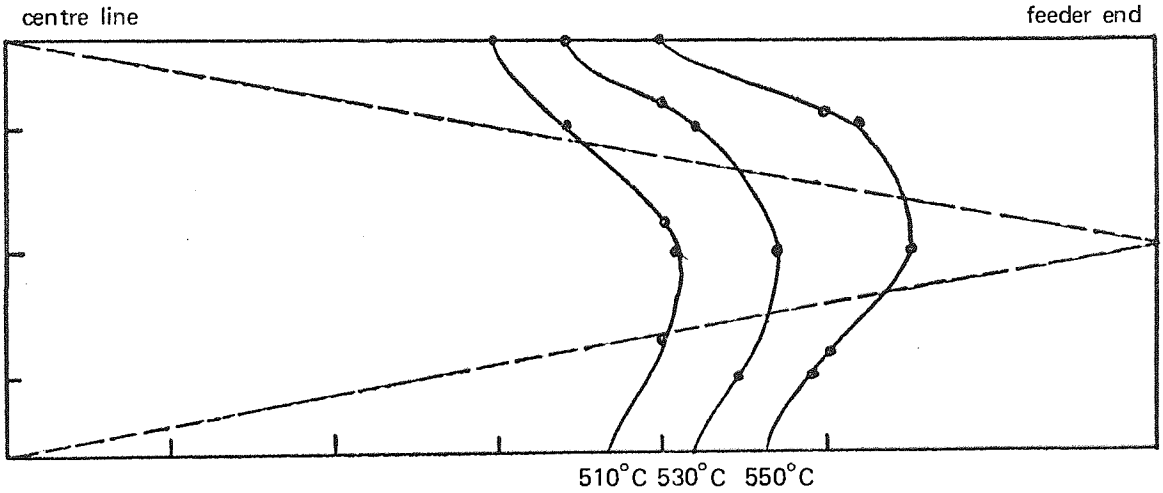

Figure 101.—*After 25 seconds.*

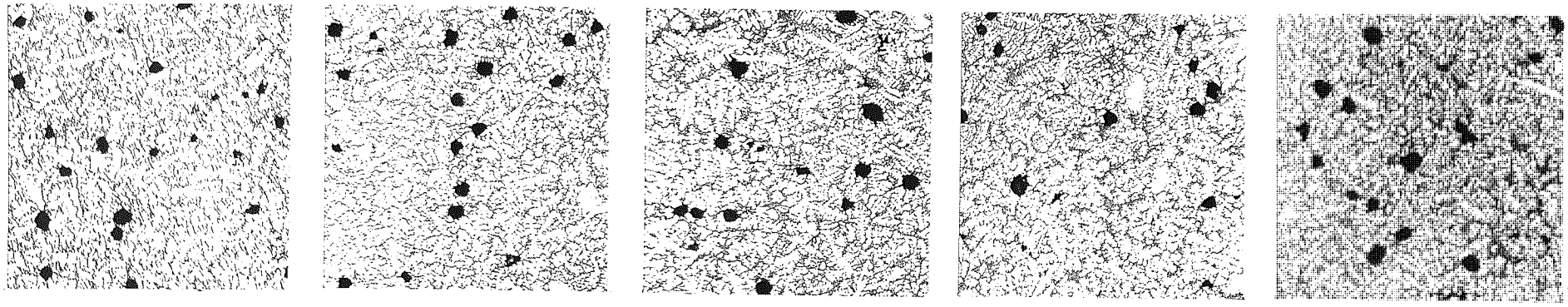

Figure 102.—*Sequence of specimens showing porosity from an Unchilled ½in plate.*

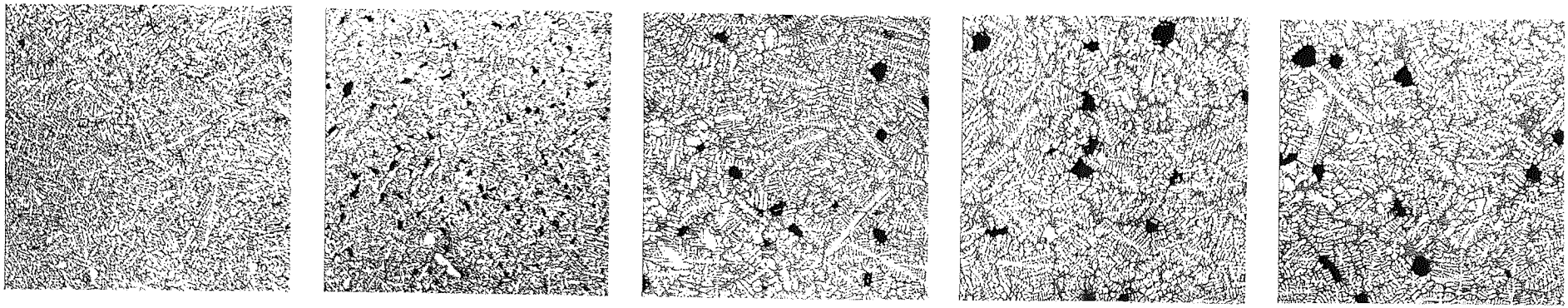

Figure 103.—*Sequence of specimens showing porosity from a Block chilled ½in plate.*

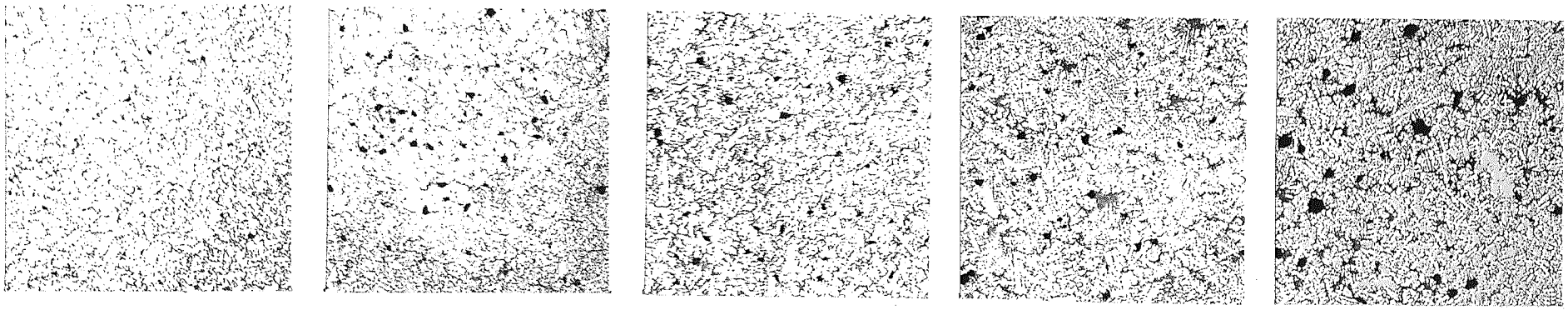

Figure 104.—*Sequence of specimens showing porosity from a Double Thickness Single Taper chilled ½in plate.*

illustrates the fact that this method of chilling produces the most consistently dense specimens.

5.4.5 *Influence of Solidification Rate on Cell Size*

Cells may be measured individually or in small lined up groups but this depends upon the observer establishing an overall idea of the structure before selecting separate cells for measurement. A safer method utilized the line intercept technique[66] where, after selection of a representative field, the field was traversed by a straight line of known length and the number of cell intercepts over this distance counted. The count provided information on the number of cells per inch and could be converted into length/cell.

The relationship between solidification rate and cell size was observed from results obtained directly from the isothermal determinations. As mentioned earlier the samples were removed from near the thermocouple beads to reduce any possible error. A relationship between average solidification rate and cell size was determined using linear regression where the average solidification rate used was produced by dividing the temperature interval between the liquidus and solidus by the time necessary for the sample to cool through it.

The relationship was:

$y = -5.697 - 2.828x$

where y = log (cell size, ins),

x = log (average solidification rate, °C/min),

and r = regression coefficient = 0.976.

6. DISCUSSION

6.1 Mechanical Properties

The most serious problem facing founders casting Aluminium 7% Silicon 0.3% Magnesium alloy is achieving the specified elongations. The mechanical properties data resulting from the research project may be devided into two main areas of interest. The first is the effect that varying foundry factors had on the mechanical properties of the final casting. The second concerns the additional factors that may influence the level of these mechanical properties.

6.1.1 Foundry Factors affecting Mechanical Properties

The foundry factors were investigated in the first two series of castings produced and chemical composition, chill shape and material, section thickness and sample position in the cast plate were considered. The general trends in the results are discussed below. The overall impression gained from the literature survey regarding high integrity Aluminium 7% Silicon 0.3% Magnesium alloy castings was that if one properly melted and degassed the alloy and poured it into a mould produced by current foundry practices the desired properties would result. Chilling techniques employed by the majority of the investigators in the more practical papers utilized Aluminium as the chill material. A disadvantage of this chill material in high volume casting production is its removal from the returned sand prior to remixing, so Cast Iron was also considered because of its ease of separation from the sand magnetically.

Composition also plays an important part in the production of high quality castings and private communications with several people involved in this field of work led the author to believe that reduction of impurity levels could produce significant improvements in the mechanical properties of the as-cast and heat treated alloy.

As mentioned previously improvements in ductility in this particular alloy were favoured by reduction in the porosity present in the castings. Several ways are open to the founder to reduce the interdendritic porosity. The basic purpose of a chill is to act as a heat sink and thereby impress upon the bulk of the solidifying metal a form of directional solidification that enables the front to proceed from one point to another while providing an adequate supply of warmer, still liquid, metal to that front. The sections chosen for this work were representative of the sections likely to be encountered in high integrity castings and the dimensions of the chills were related to section thickness. The relative merits of the different chill shapes and materials were analysed by the two techniques previously mentioned but, of the two, multiple regression analysis indicated an important changeover in the trends set by variations in chill shapes and materials. With the 3/8 in and ½ in cast sections

investigated in this work, corresponding to the thinner sections in Flemings[49] paper the regression favoured the use of block chills. Flemings' work supports this conclusion but indicated that the effect the block chill shape had upon levels of mechanical properties was greatly reduced with thinner cast sections. This was reinforced by the present work which showed the mechanical properties, particularly elongation, to be higher within a region extending 3T (where T is the section thickness) beyond the edge of the block chill. The chill material providing the better elongation results in these two sections was Aluminium. From the heat extraction curves it can be seen that Aluminium removes heat from a casting at a *greater* rate than Cast Iron, *before saturation*. This greater rate of heat removal would produce and maintain a more pronounced solidification front in a casting having a large heat capacity.

With the thinner cast sections (¼in and ⅛in) the optimum chill material selected was Cast Iron and the most advantageous chill shape was the single taper (in Series I). The explanation for the change in optimum chill material with change in cast section is the *slower* rate of heat removal over a *longer period* of time associated with the Cast Iron chill which allows the mould to be completely filled before any degree of chilling has occurred. This allows the formation of a smoother solidification front similar to those determined in thicker sections. The advantage of the taper chill is that with the reduction in the plate thickness, the block chill loses its effect while the taper chill maintains its influence by extending over the length of the plate; the degree of chilling at any point along the plate being represented by the contact area. The double taper chills were less effective due to the faster fall off in chill capacity or quicker saturation. The single taper chills produced the more consistent results with the thicker sections. The present author chose to investigate the taper chill system more fully because it was thought that the reason the regression analysis favoured the block chills was due to the much higher individual mechanical properties results in the region above the chill. The levels of the results are maintained for longer distances into the plates using the taper chills and the increased chill/feeder distance improves the effectiveness of the system. Flemings[52] refers to an optimum block chill to feeder distance of 2in, but the present work shows that this is greatly exceeded with taper chills. The ductility levels and the general trends of the property curves obtained from this project are similar to those obtained in Flemings[49] work. If any criticism is to be levelled at the latter's work it is, perhaps, of his choosing to take several test pieces from inside the first inch from the plate edge and neglecting completely samples more than 5in away (in sections below ½in for the chill technique similar to the one employed in this investigation). This might be the explanation for the omission of the plateau

or peak in the elongation properties above or adjacent to the block chill. The trends in mechanical properties are included in Figure 105, and the more rapid decline in results away from the block chills should be noted.

At this stage it was beneficial to examine the influence of composition on mechanical properties although from an economic view point it was hoped that the more commercially available alloys (0.1% Iron and above) could be made to produce the better properties. Of the elements present, without a doubt the most critical is Iron which severely reduces the elongation results in this alloy when present in quantities greater than 0.03%. However, if Iron is present and since it is untouched by heat treatment[67], any means of refining its structure during formation reduces its detrimental effect. Thus, controlled chilling not only results in better elongations due to reduced porosity levels, but also retards the formation of large needle-shaped Iron compounds that reduce the strength of the alloy. As would be expected in an age-hardening system, an increase in the quantities of the elements available (within the specified limits) for precipitation would give rise to an increased percentage of precipitates within the matrix for a particular heat treatment. This would show in reduced elongations, but the restricted specification analysis range would normally minimize this effect. Nevertheless, the regression analysis did indicate that increased percentages of Magnesium reduced the observed elongations.

In Series II, two additional chill techniques were investigated. The regression analysis of the Series II results supported the author's assumption that more chill capacity was required at the pointed ends of the taper chills used in Series I. The elongations obtained, from the cast plates chilled by the double thickness single taper chills with the increased heat capacities provided by the additional chill sections, were considerably better than the Series I results. Since Cast Iron was not favoured by the regression analysis it might be assumed that Aluminium should always be the preferred chill material, but for reasons explained above, it would be advantageous to employ Cast Iron chills against the thinner cast sections. Finally, the elongation results of Series I show a remarkable improvement in the test specimens near the feeder.

This is undoubtedly attributable to efficient feeding and observations from the four cast section thicknesses (1/8 in, ¼ in, 3/8 in and ½ in) lead to a feeding range relationship of 4T where:

(a) the feeding range is defined by Figure 106 and

(b) T is the section thickness.

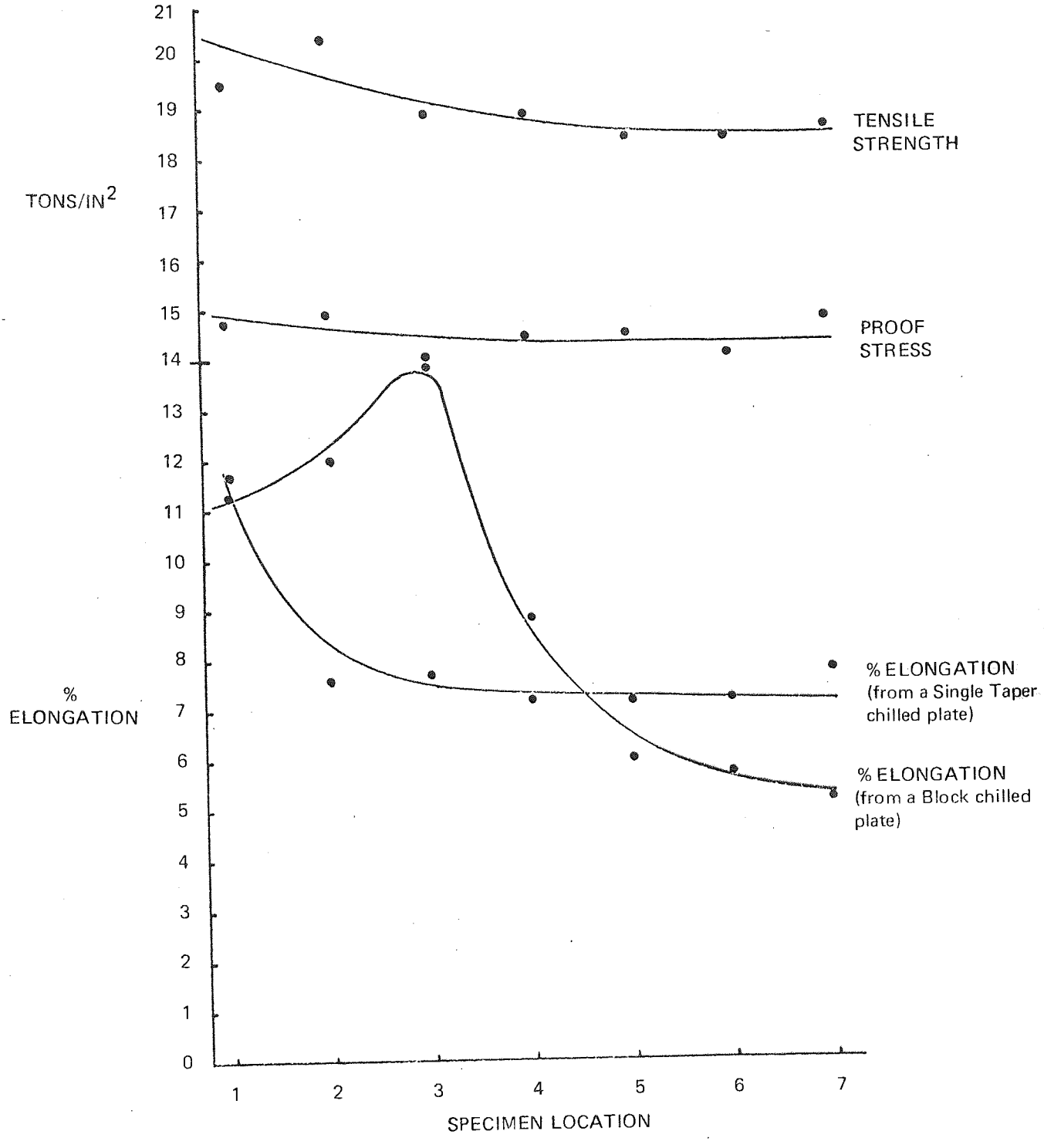

Figure 105.—*Trends in Mechanical Properties for typical Series III results - note the influence of chill shape on Elongation Trends.*

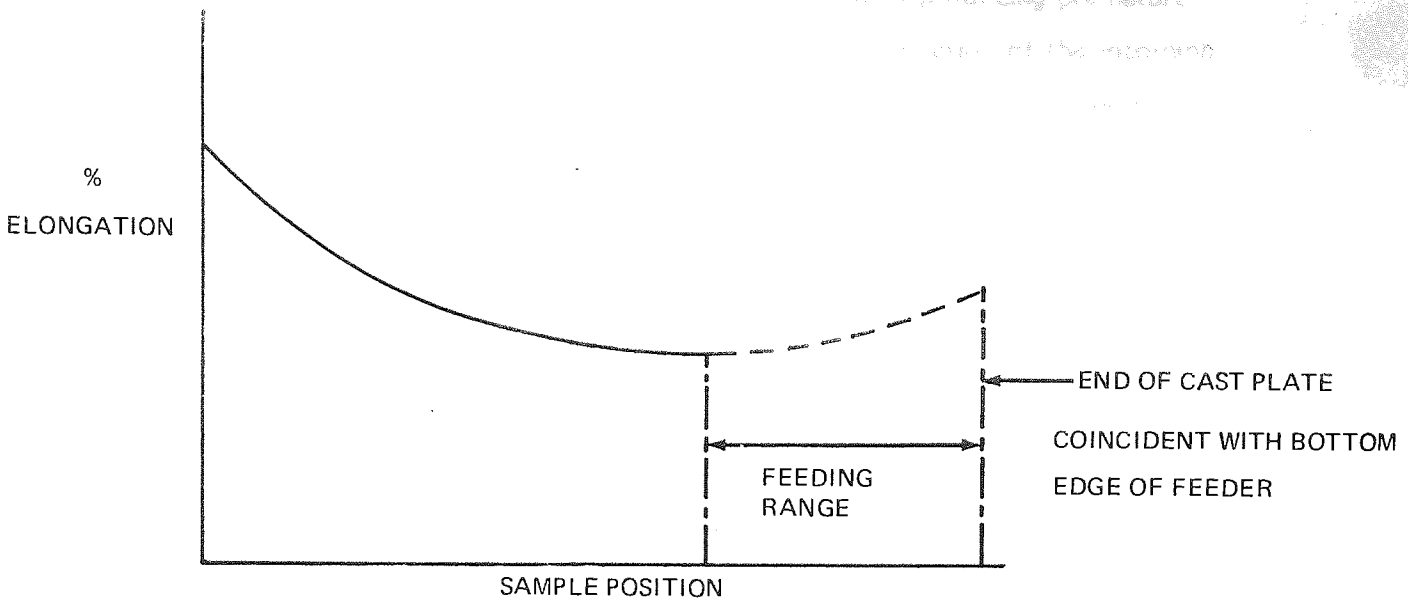

Figure 106.—*The Feeding Range defined as the region of improved Elongation results in the cast plate nearest the feeder.*

Although the U.T.S. results were generally less sensitive to variations in chilling technique there was some effect. This is probably associated with a refining of the 'as-cast' structure and even though heat treatment precedes the determination of tensile strength, some remnants of the original chilling behaviour exist. This would suggest some modification of the constituents formed that is relatively unaffected by heat treatment. Generally, the undesignated area properties responded to any form of chilling. The rate at which the U.T.S. falls away with distance from the chill is considerably less than for ductility (see Figure 105) again indicating the reduced dependence of U.T.S. upon porosity and greater dependence on the subsequent heat treatment. The designated area tensile results were most commonly achieved using Aluminium taper chills thus underlining the necessity for some form of direct chilling to enhance the properties. With these taper chills designated area results were achieved over the entire plate length. The insensitivity of the tensile strengths to the range of porosities encountered resulted in the taper plate, as used in the Series II castings, being particularly attractive although the unreliable metal flow, as detected by the radiographs, lead to erratic elongation results.

The effect that increased Iron contents have upon the tensile strength properties produced an unexpected trend. In the thicker cast sections (½in and 3/8in) the Iron is seen to be detrimental to strength as it was to ductility. However, in the 1/8in and ¼in sections an improvement in tensile strengths is noted with higher Iron contents. This might be related to the rate of cooling associated with these thin sections which could possibly change the morphology of some high melting point constituent.

This constituent, unaffected by the subsequent heat treatment, could elevate the tensile strength by assisting in dislocation pinning instead of producing premature fracture. Alternatively, in these thin sections the mechanical action of the incoming metal could possibly modify a constituent, which forms in the alloy as it cools between the liquidus and solidus, causing it to be less detrimental in service.

Finally, it must be stated that the designated area tensile results were rather poor in the Series II tests and when considered in conjunction with the rather low elongation results one must conclude that the heat treatment and/or degassing was not entirely satisfactory.

6.1.2 Effect of Heat Treatment on Mechanical Properties

Important though the chill shapes and materials are for producing improved mechanical properties the best results are definitely achieved, at this stage, by the low Iron alloys. However, the economics of low Iron alloys are not favourable and, therefore, other factors were investigated to improve the properties of the commercially available alloys. The possible improvements in mechanical properties as a result of optimizing heat treatment, were determined on a production run of plate castings using three of the chill techniques previously investigated block, single taper and unchilled. Flemings in his paper[52] suggests a maximum time interval between solution treatment and quenching of10 seconds. At present, this delay under industrial production conditions can be up to 45 seconds. In this investigation the time was comfortably reduced to between 4 and 5 seconds and the bulk of the castings was also reduced by removing the test bars from the cast plates.

The dramatic improvements in the mechanical properties as a result of reducing the pre-quench delay time are best shown by the histograms (Figures 39 to 49). The sample locations in Series III were no longer a *major* factor influencing the level of mechanical properties and consequently the variable, sample location, was removed from the histograms. Also, the effects that the chill shapes and materials had on the mechanical properties of the Series III cast plates, were small in comparison to chills' influences on the results of Series I and II plates (Figures 25 to 38). From the Series III results it appears that *any* one of the suggested chill methods, deduced from Series I and II results, *would be an acceptable* means of chilling the cast plates but *no one technique* would produce outstanding mechanical properties. The effect of this shorter delay time before quenching must be linked to the prevention of nuclei formation before the quenching action produces supersaturation.

6.2 Derivation of Additional Information from Radiographs

Having found the interaction between porosity and elongation the possibility of determining additional information from X-ray radiographs becomes increasingly attractive since the 'tightness' of a casting is automatically displayed in this method of examination. Time did not permit the author to carry out extensive investigations into the relationship but a more complete exploration with broader ranges of porosity and sections might permit radiography to be used to rate at least the potential ductility of cast sections *in situ* and non-destructively. A wider range of porosities would enable a datum sensitivity to be established for comparing the ductilities of similar section thicknesses which had undergone considerable variations in chilling. Once the radiographic sensitivity that satisfies the minimum requirements of the premium quality standard, for a particular section, has been established then comparisons may be made between the ductility derived from the area under the graphical representation of the radiograph and the datum from one casting section to the ductility calculated from the area derived from the radiograph of a similar section in another casting.

A strong correlation between porosity and percentage elongation has been demonstrated although some error was probably introduced by the methods of measurement. The Table (XI) comparing the observed and calculated porosities and elongations indicates the closeness of the estimated and determined porosity results, but this is to be expected from a small sample size exhibiting such a high correlation. The greater variation in the estimated and determined elongations illustrates the error of assuming a linear relationship between porosity and elongation over such an extensive range of elongation. The porosities of the unchilled ½ in cast section are restricted to a small section at one end of the regression line.

6.3 Relationship between Specimen Density and % Elongation

In all the sections investigated there was conclusive evidence of a strong relationship between specimen porosity and elongation. The first visual evidence for this phenomenon is the series of micrographs removed from plate samples variously chilled. This is further supported by the simple linear regression equations obtained from the Series III results, Table X and by Figures 54 and 55. The porosities of Series III castings were compared to Series I and II results to prove that the connection was not an isolated one. Most of the results for specimen position 7 showed the benefits of efficient feeding in both Figures 54 and 55.

The interdendritic nature of the porosity and its influence on the fracture mode is the most likely explanation for the relationship between density and ductility.

Although one would expect the U.T.S. properties to be affected by the quantity of voids present in the test bars it would appear that at the porosity levels encountered, the hardening mechanisms, which are influenced by additional variables in the heat treatment, outweigh the detrimental effects of the porosity.

6.4 Thermal Diffusivity

In an attempt to explain the trends in the thermal diffusivity results resulting from the computer analyses, several mathematical manipulations were carried out. These involved the calculation of thermal diffusivities under varying conditions. The effects on the thermal diffusivities at a fixed point and particular time were noted for instantaneous increases in the surface temperature, θ_i, and for the temperature θ_m at the specified experimental point. The results of these calculations help to explain the experimental thermal diffusivity results. The gradual decrease in the thermal diffusivity of the sand with time is almost certainly attributable to the increase in the interfacial temperature, between the sand and metal, with time. This underlines the weakness of the assumption that the surface temperature of even a sand mould is instantly raised to the melting point of the metal on casting. An explanation was also necessary for the series of increased thermal diffusivities determined for a position situated some distance from the casting/mould interface, Table XIII. Calculations using Carslaw and Jaegers' equation predicted a thermal diffusivity for a temperature higher than that expected at that distance after the time elapsed. A possible mechanism for this increased dissipation of heat over a limited range is the volatilizing of moisture adjacent to the metal/mould interface and its condensation some distance away from the interface; the heat as transported elevates the temperature in this region. The interaction of density and specific heat with increasing temperature also gives rise to a steady decline in thermal diffusivity although this is less evident in a material with a very low diffusivity such as sand.

6.5 Evaluation of Chill Saturation from Interfacial Temperature Determinations

The computer analysis produced accurate quantitative data concerning the behaviour of the chills and in conjunction with the experimentally determined temperature distributions, two distinct modes of chilling were indicated. The Aluminium chill rapidly extracts heat from the cast material in contact with it and this is represented by the steep portion of the incremental heat extraction curve. After reaching a maximum heat extraction per unit of time, the curve gradually falls denoting a reduction in the rate of heat absorbed from the still cooling cast plate. This reduction in heat absorption is associated with either the limited quantity of heat available for extraction from the cooling casting or the combination

of the Aluminium chill's thermal properties of low heat capacity, compared to Cast Iron, and high thermal diffusivity quickly reducing the temperature gradients within the chill. The reduction in temperature gradients is referred to as chill saturation. The saturation of the Aluminium chill is further highlighted by the interfacial temperature curve. The curve (Figure 76) has two regions; the first where the interface temperature gradually rises due to the hot material in contact with the chill, the second, shallower slope, shows the point where the temperature of the bulk of the cooling casting has been so reduced that the temperature differential between casting and chill, has been greatly diminished and the chill has become significantly saturated resulting in a small but steady increase in the surface temperature. The efficiency of the chill is marred by this rapid decrease in temperature gradient and can only be improved by the increase in chill dimensions away from the interface or by some other means of extracting the heat more rapidly from the back face of the chill. For the purposes of this investigation the sand was considered as an insulator surrounding five of the chill faces and although not exactly true this assumption was valid over the short time intervals examined.

The Cast Iron chill, on the other hand, exhibits a contrasting chilling mechanism. The diagram of the experimentally observed results shows a considerable temperature gradient within the half of the chill nearest the cooling casting. Assuming a high degree of contact between the chill and cast plate, the rate of heat extraction is initially governed by the heat content of the chill layer adjacent to the cast material. Further heat extraction is permitted by the thermal diffusivity of the Cast Iron removing the heat from the surface layers. The relatively low thermal diffusivity is the regulating factor in heat flow through Cast Iron and explains the slower mode of heat extraction exhibited by this material. This behaviour is shown by the small peak and plateau in the incremental heat extraction curve, Figure 77. Comparison of the cumulative total heat extraction curves for Aluminium and Cast Iron show the higher rates of heat removal in Aluminium chills. The interfacial temperature distribution for Cast Iron illustrates the fact that the Cast Iron chills do not become saturated under the experimental conditions involved. The fall in the incremental heat extraction curve is solely attributable to the reduction in heat content of the casting and coincides with the decrease in the interfacial temperature curve. The fall in the surface temperature further indicates the lack of saturation by suggesting that further heat could flow down the appreciable temperature gradients.

The trend for the peaks of the interfacial temperature curves to occur nearer the pouring time may be explained by considering the mould chilling power. The

chilling power of a mould may be regarded as being proportional to the temperature differential between the instantaneous interfacial temperature and the ambient temperature. The higher the pouring temperature the greater the instantaneous interfacial temperature difference and consequently the greater the heat extraction rate. Hence, the peak of the curve attains a *higher* maximum *earlier* with elevated pouring temperatures. The effects of pouring temperature variations on the surface temperature of an Aluminium chill would be less definite. Because of the Aluminium chills' higher thermal diffusivity coupled to its lower heat capacity the surface temperature could be particularly sensitive to the chill thickness.

The observation that Aluminium chills become saturated quicker than those of Cast Iron is supported by the results of Murthy *et al*[54]. These investigators related saturation to volumetric heat capacity and concluded that the total heat absorbed for a particular chill material in a given time interval was proportional to its heat capacity. However, they did not investigate the chill behaviour over the much shorter time intervals considered in the present work. The considerable difference between the casting size (2in x 2in x 12in) compared to the chill dimensions (2in x 2in x 1in) in Murthy's work and the chill to casting weights employed in this investigation explains the difference in the results obtained. Rapid saturation of the Aluminium chill by the vast heat content of the casting gives rise to the higher interfacial temperatures observed in Murthy's work. The higher heat content of the Cast Iron chill would explain the lower interfacial temperatures that he detected. In this present work the casting to chill weight ratios are considerably reduced and the thermal diffusivity factor is permitted to play a more important role. The lower heat content of the Aluminium chill results in an early saturation but the higher thermal diffusivity compared with Cast Iron causes a lower interfacial temperature. In Cast Iron the lower diffusivity explains the higher interfacial temperature.

The determination of the temperature distributions within the block chills over the short time intervals investigated is adequately handled by the basic Cawslaw and Jaeger equation. The more comprehensive equation adopted by Murthy *et al* is more acceptable to their experimental conditions where the time elapsed was an order of magnitude greater. The casting to chill weight ratio employed by Murthy *et al* (hardly commercially acceptable) requires the important additional factor of heat dissipation from the back face of the chill and this is more readily incorporated in the analytical technique they used. In the present small plate castings there is less 'thermal potential' to induce the chill to disperse heat to the surrounding sand.

Thus, while the computer program still maintains an accurate estimate of the interfacial temperature, the thermal saturation of the chill causes a gradual increase in the thermal diffusivity of the chill with time. The gradual increase depends upon the chill's dimensions and volumetric capacity and was observed after the initial high level of heat extraction during solidification.

6.5.1 Influence of Chill Coating

The incremental heat content curve of the coated chill (Figure 78) indicated a similar basic shape when compared to the uncoated Aluminium block but the *rate* of heat extraction was retarded. The time to maximum rate of heat removal was considerably delayed and when the maximum was achieved it was lower than for the untreated chill. The major difference in the rate of chilling is in the first ten seconds of the chill's useful life. Here the refractory coating acts as a barrier to heat flow when a rapid rate of heat removal would be the most advantageous.

6.6 Influence of Chill Shape on Solidification Mode

Several experimental castings were produced and the temperature distributions throughout both halves of the cast plates were similar. This was attributable to the influence of the sprue dimensions, runner-bar extension, screening system and finally gating through the riser which reduced the metal flow bias towards the half of the plate casting nearer the box side to an absolute minimum. Maintenance of a standard melting and pouring procedure enabled reproducibility between individual castings and so it was decided to investigate the temperature distribution in only the one half of the plate. The investigation was limited to determining the effect of the chill shapes on the solidification pattern. The double thickness single taper chill was selected from the taper chills as it would have the most pronounced effect.

6.6.1 Unchilled Section

Two particularly interesting phenomena, revealed without deliberate chilling, concern the metal and heat flows respectively. Regarding the metal flow, metal flowed in a stream along the floor of the mould cavity and then parted when the stream met an obstacle. Depending upon the nature of the barrier a dead zone of metal is produced. Since a considerable proportion of the early metal entering the mould will constitute the dead zone an area of cooler metal will be formed. The warmer material following will tend to run up the sides of the cavity giving rise to the observed trends in isothermal distributions. The explanation for the reduction in the dead zone with time is the conduction of heat through the sand and stabilization of the heat flow near the dead region. The second phenomenon, associated with heat flow, depended upon the influence of the original dead zone

not being completely removed. As solidification proceeded in the early formed dead zone it became the basis for a finger of solid metal progressing towards the feeder end. This growth of a third finger is evident in the graphical representation of the radiograph (Figure 51) showing three regions of more dense material, two at the edges and one along the centre line. The steeper temperature gradients in the centre and at the edges produce the more dense material but the low thermal gradients in the central regions of both half plates make feeding the alloy over such distances very difficult or impossible.

6.6.2 Block Chilled Section

In the early stages the dead metal zone is again evident with this chilling system. However, its life is restricted by the more rapid rate of heat removal by the chill such that all evidence of its existence soon disappears. The increased chilling rate produced by the block chill on the metal results in very little metal flow along the side walls of the cavity in the early stages. However, when the cavity above the chill is occupied, warmer metal following in does then flow along the side walls. The remainder of the casting, particularly beyond the influence of the chill, solidifies essentially as an unchilled sand casting, the centre of which lags behind the edges due to the sand being preheated by the metal entering the mould. No finger of cooler material is detected since the dead region is obliterated by the heat extraction by the chill.

6.6.3 Double Thickness Single Taper Chilled Section

The observations for this chill shape bear no resemblance to any previously encountered. The mode of solidification is amply explained by the diagrams with the chill shape superimposed. The slight lag in the temperature isotherms at the centre may be attributable to the sand being heated by the incoming metal.

6.7 Cooling Rate and Chill Influence on Porosity and Properties

Basically, the main purpose of employing chills is to vary temperature gradients within castings. By producing steep temperature gradients along the length of a casting one hopes to reduce the distance over which an alloy is required to feed itself. This depends upon rates of cooling at particular points particularly on the way the cooling rates vary with distance from the chill or from the feeder. The cooling rates obtained from thermocouple stations adjacent to the metallographic samples (Figures 102, 103 and 104) removed from the plates produced in the solidification experiments are illustrated in the table below.

TABLE XV.—*Cooling Rates (°C/second) for various chilling techniques.*

Chill Technique	Distance from chilled end				
	25.4mm	50.8mm	76.2mm	101.6mm	127.0mm
Unchilled	2.0	2.1	2.2	2.2	1.8
	+0.1	+0.1	0.0	-0.4	
Aluminium Block Chill used	6.8	3.7	2.2	1.4	1.5
	-3.1	-1.5	-0.8	+0.1	
Aluminium Double Thickness, Single Taper Chill used	5.8	4.2	3.6	3.0	3.1
	-1.6	-0.6	-0.6	+0.1	

Mechanical properties, likewise, do not rely solely upon the cooling rate at a particular point, they also depend on the soundness of the material which is greatly affected by the temperature gradients present. Within the practical foundry limitations of casting technology it is fair to assume that the greater the cooling rates and temperature gradients the higher the mechanical properties up to the theoretical maximum. The general trend in temperature gradients is similar to the trends in mechanical properties and porosities, the exception being in when the block chill was used and very low porosities were obtained in the cast plate approximately 1 in from the end of the block chill. This phenomenon is associated with the fact that the metal above the chill experiences very steep thermal gradients and is fed by metal from the sand chilled portion of the casting which contains low temperature gradients. From a study of the cooling rates, the variations in cooling rates with distance, and ductility, which is the critical property, the minimum cooling rate to produce satisfactory ductility results is 3.0°C/second and the minimum differential cooling rate is 0.6°C/second/25.4mm.

The limited time available for the project meant that most conclusions had to be drawn from the results of chilling ½in cast sections. Flemings[49] in his work on block chilled plates indicated that chills become less influential with reduction in cast section thickness. This was supported by the present work and the chill influence on the ½in cast plate extended some 3T (where T is the section thickness) beyond the edge of the chill block, i.e. 3½in from the end of the plate. From observations of mechanical properties in the remaining three sections it appears that the influence of the block chill, beyond the edge of the chill, remains approximately 3T, where T is the section thickness of the plate being cast. The influence of a taper chill upon a plate casting is more extensive.

The order of taper chill extensiveness is:

(a) double thickness single taper (Series II),

(b) single taper (Series I),

(c) double taper (Series I). The double thickness taper chill, in fact, affects

the entire casting, maintaining the mechanical properties above the specified minimum over the whole length of the plate.

6.8 Chill Shape and Size

6.8.1 Block Chills

In the present work the size of the Aluminium block chill was governed by the cast ½in section weight, on a 1:1 ratio basis, similar to Flemings *et al*[49]. A Cast Iron chill of similar dimensions to the Aluminium chill resulted in a chill to casting weight ratio of approximately 3:1. Thus, two chill weight to casting weight ratios were available for comparison. Flemings *et al*[49] and Chamberlain *et al*[53] favoured some overlap of the chill face in contact with the plate casting but this is rarely met in practice since the area of a chill in contact with a casting is determined by the casting area requiring local chilling. Because one is interested in the relationship between casting section and chill thickness no overlap was employed in the present work as this staggering of the chill and plate faces must certainly influence the region of casting affected by the chill.

For a chill to remain operative it must contain satisfactory thermal gradients. In the Aluminium block chill investigated a significant temperature distribution was set up over the *whole block depth* within 10 seconds but because of Aluminium's low specific heat content and higher thermal diffusivity the gradients were quickly reduced (Figure 75). On the other hand, the temperature gradients in the Cast Iron block chill *remained* considerably *steeper* for a *longer* period of *time* before the temperature gradients levelled out, see Figure 73, due to the material's much higher heat content per unit volume and considerably lower thermal diffusivity. It is these two factors, heat capacity per unit volume and thermal diffusivity, that affect the chills' performances, giving rise to the different outlines of the incremental heat absorption curves (Figures 77 and 78).

A marked change occurs in the curves once the plates have solidified (for ½in sections, after approximately 10 seconds) and examination of the experimentally determined temperatures show that the maximum temperature gradients coincide with the times (approximately 20 seconds in Cast Iron and 10 seconds in Aluminium) at which the slopes of the interfacial temperature curves (Figures 74 and 76) change and the temperature 16mm from the Cast Iron block/casting interface after 20 seconds was similar to the temperature of the back face of the Aluminium block chill after 10 seconds. Thus if one considers approximately 100°C to be the optimum temperature for the back of a chill to reach while still maintaining a significant temperature gradient within the chill, then an Aluminium block chill with a thickness

4 x that of the cast plate can be considered satisfactory, i.e. the chill weight to casting weight ratio being approximately 1:1. For a Cast Iron block chill the ratio of chill thickness to cast plate thickness of 1:1.25 appears ideal. If one considers a weight relationship similar to Aluminium the chill thickness should be 1.4 x the cast plate section.

6.8.2 Taper Chills

The reason for adopting taper chills is made clear if one considers the basic reason for chilling, viz. the promotion of directional solidification and the directing of solidification towards a riser in order to increase the distance over which feeding is effective. Johnson[48] investigated the influence of wedge shaped chills on mechanical properties employing 2 or 4 wedges depending upon the width of the cast plate. In the present work two were used, increasing the area of contact to 1.75 x that of the block chill. This increase in the contact area plus the variation in the degree of chilling provided by the contact of a tapered chill over the whole of the cast plate length reduced the necessity of having such deep chills. It also eliminated the need for heat to be conducted through large volumes of already solid material. The results show that the double taper chill was the least effective because of the absence of chill material at the feeder end. Of the two remaining systems the double thickness chills were better. This configuration was equivalent to a plate chilling a plate casting with the level of chilling varying from total chilling to none. With the area of contact increased proportionally it would be reasonable to expect a decrease in the chill depth from 4 x the cast section thickness employed when using an Aluminium block. The mechanical properties suggest that for Aluminium taper chills a depth of 2 x the section thickness is satisfactory. For Cast Iron chills a similar chill depth to section thickness relationship must be drawn from the information available.

The effects of large variations in chill base, length and depth had on directional solidification and mechanical properties were not studied and only one set of chill base, length and depth was used. The plate width permitted the same chill base to be used as in Johnson's work, but, unlike Johnson, the present author employed chills extending over the total length of the cast plate up to the edge of the feeder.

7. CONCLUSIONS

7.1

The most important factor in producing high integrity castings from the existing commercial A356 alloy (Aluminium 7% Silicon 0.3% Magnesium) is the delay time between solution treatment and quenching. Reducing this delay time to less than 5 seconds produces some significant changes in the mechanical properties. By comparison between the relevant results in Series I and the Series III results the quantitative changes produced by this short delay time may be highlighted; viz.the mean of the Series I elongation results is approximately 4% but the mean of the results with the short delay time, Series III, is above 7%.

No appreciable difference is noted in the 0.2% Proof Stresses, the means of both sets of results are just over 14 tons/in^2, but some difference is noted between the means of the Ultimate Tensile Strengths (U.T.S.): the mean of Series I results is 16.8 tons/in^2 and the mean of Series III results is 18.5 tons/in^2.

7.2

Although the heat treatment can produce the most significent advances in mechanical properties different chilling techniques affect the soundness of a casting and hence influence ductility, as illustrated by elongation results. As a result different chill shapes have varying uses, viz.

(a) block chills are more satisfactory for localized chilling since their influence extends beyond the edge of the chill about 1.5 x the cast section thickness. The mechanical properties obtained in these areas are better than those resulting from taper chills.

(b) the chill influence is greatly extended by using taper chills which create improved mechanical properties (particularly elongation) over large areas of the experimental castings. The promotion of directional solidification by this chill shape permits greater distances between the ends of the chills and the feeders.

7.3

Of the tapered chills, the double thickness single taper produces the greatest overall improvement in casting ductility.

7.4

The minimum thickness of an Aluminium block chill must be at least 4 x that of the cast section. The optimum relationship for a Cast Iron block would be 1.25 x the cast section. These factors both give rise to an approximate 1:1 casting/chill weight ratio.

7.5

From the limited data available on taper chills it is suggested that the chill thickness should be 2 x the casting thickness.

7.6

The best mechanical properties are not necessarily produced from the same chill material acting on different cast sections.

(a) With thicker cast sections (½in and ⅜in) the best improvements in the properties are achieved using Aluminium chills because of their more rapid heat absorption,

(b) Cast Iron chills are favoured with the thinner cast sections (¼in and ⅛in). The reason is associated with the reduced thermal properties and higher volume heat capacity of Cast Iron resulting in a slower rate of heat dissipation.

7.7

From the results obtained, % elongation is the property most sensitive to feeding efficiency which is, in turn, an indication of the damaging effect of porosity. The general trend of results suggests a distance of 4 x the cast section thickness as being within reasonable reach of the feeder.

7.8

While U.T.S. is affected by some form of chilling the increase in strength is not so sensitive to the chilling technique. Direct block chilling produces the greatest improvements.

7.9

Very little difficulty is experienced in obtaining Designated or Undesignated location 0.2% Proof Stresses if any form of chilling is employed.

7.10

The element most detrimental to good mechanical properties is Iron. This element severely reduces ductility and improvements to alloys containing in excess of 0.03% Iron can only be achieved by judicious chilling. Silicon and Magnesium combine to form a constituent that can also be instrumental in reducing ductility although beneficial to tensile properties.

7.11

The thermal behaviour of different chill materials vary and they should be carefully selected with regard to their most advantageous properties.

(a) Aluminium removes heat rapidly from a casting but its *high heat* removal *rate* is not allied with a commensurate heat *capacity* and as a result it quickly saturates. Aluminium chills are favoured for chilling heavy sections but a large enough chill must be present for it to remove sufficient heat to promote solidification before chill saturation.

(b) Cast Iron, on the other hand, possesses a high heat capacity but low thermal diffusivity and consequently this *slower rate* of *heat* dissipation is favoured for chilling thinner sections where a rapid heat extraction would cause difficulties in running.

7.12

The different thermal behaviour of different chills against cast sections produce considerable variations in the interfacial temperature.

7.13

A computer program was developed for the determination of thermal diffusivity and of interfacial temperature and is adequate for most practical considerations. The diffusivity determinations of the sand samples provide a useful quantitative estimate of the heat extracted by a sand mould. The calculated interfacial temperatures help to explain the thermal behaviour of the metal chills.

7.14

The interfacial temperature computer program also illustrated the effects of chill coatings manufactured from Jewellers Rouge in a suspension of Iso-propyl Alcohol.

7.15

Chill shape considerably influences the solidification mode of cast plates. Ideally the cooling rates for satisfactory mechanical properties are $>3.0^{\circ}C$/sec at any particular point and a temperature gradient of $>0.6^{\circ}C$/sec/25.4mm.

7.16

There was a strong inverse correlation between tensile elongation and porosity results obtained from the Series III cast plates.

7.17

X-Radiography is a possible method of non-destructively obtaining an estimate of ductility although further experimental evidence is required for a precise relationship. Unfortunately, no indication of U.T.S. and proof stress is obtainable from this method.

8. RECOMMENDATIONS FOR FUTURE WORK ON ALUMINIUM SILICON MAGNESIUM CAST ALLOYS

(i) Regarding the practical foundry aspects of chilling, further investigations should include variations in the dimensions of block and taper chills. For block chills, variations in the chill face area and chill depth may provide further improvements in mechanical properties by increasing the time before saturation, particularly in Aluminium chills. The variations in taper chill dimensions were limited in the present investigation but the improvements in tensile properties over the plate length employed in this project may be increased by attempting other combinations of chill taper, chill length and chill thickness.

Chill coatings appear to reduce the effectiveness of chills against cast sections thicker than ¼in. Some reappraisal of the use of a chill coating is therefore desirable since the application of a chill coat may nullify the effect of a chill. Again, the use of a chill coating may be essential if some chilling is required on a thin section (i.e. less than ¼in.).

(ii) No degassing technique was employed in this investigation. As most progressive foundries employ Nitrogen degassing on some alloys already, further improvements in mechanical properties may arise from use of this degassing method. Trials might also be carried out using the Nitrogen - Chlorine mixture. A further possible development might be vacuum degassing but little information is available on the effect of this particular technique on the mechanical properties of Aluminium - Silicon -Magnesium alloys.

(iii) Little information is available on the precise delay time between solution treatment and quenching that is critical to the tensile properties for Aluminium 7% Silicon 0.3% Magnesium alloys. An extensive investigation into the practical improvements in the mechanical properties and the possible physical explanations for the observations is important to achieve the maximum potential of this alloy system.

(iv) Another physical metallurgy aspect worthy of consideration is the derivation of some explanation for the observed reversal in the influence of Iron content on the U.T.S. properties of sections under ¼in.

(v) Appendix VIII covers some exploratory work on the use of compound chills. Very little information is available on the behaviour of these chills against cast sections or on their effect on the resulting soundness and mechanical properties of the cast product.

9. ACKNOWLEDGEMENTS

The author wishes to thank his Departmental Supervisors, originally Professor J. C. Wright and later Dr. J. T. Barnby for their guidance, encouragement and helpful discussions; also, thanks to his employer and Industrial Supervisor Mr. B. Haynes at Sterling Metals (Nuneaton) and Assistant Supervisor Mr. D. C. Hickson. He expresses his appreciation to Dr. S. S. Chang of the I.H.D. scheme for his advice.

Thanks also to his colleagues at Sterling Metals, particularly D.C.Critchley, J. Jarvis and M. Evans for their assistance in Casting, Radiography and Mechanical Testing and to D. Webb at Aston for his assistance in the experimental work.

Finally, a tribute to my wife for her continued encouragement and support.

10. REFERENCES

1. R. E. PAINE and W. D. STEWART. Mechanical Properties of Aluminium Alloy Castings. *Transactions American Foundryman's Society* 1955 **63** 745-751.
2. J. W. MEIER. Research on Premium Quality Castings in Light Alloys. *Modern Castings* 1965 **48** Dec. 49 - 64.
3. H. W. L. PHILLIPS. The Constitution of Alloys of Aluminium with Magnesium and Iron. *Journal of the Institute of Metals* 1941 **67** 275 - 287.
4. Aluminium Federation Information Bulletin No. 25. Equilibrium Diagrams of Aluminium Alloy Systems.
5. K. R. VAN HORN. *Aluminium* Vol1, p.116.
6. W. A. ANDERSON. Precipitation from Solid Solution. American Society of Metals.
7. H. CORDIER and W. GRUHL. A Contribution to the Question of Clustering in Al/Mg/Si Alloys based on Transmission Electron Microscopy. *Zeitachrift Für Metallkunde* 1965 **56** 669 - 674.
8. W. B. CORCORAN. High Quality Aluminium Castings. *Foundry* 1959 **87** Jan. 86 - 91.
9. R. H. HERRMANN. Rural Foundry Makes Premium Quality Castings. *Foundry* 1966 **94** July 56 - 61.
10. A. H. HINTON. How Melting Practice affects Aluminium Casting Quality. *Foundry* 1964 **92** July 48 - 51.
11. M. C. FLEMINGS. Premium Quality Aluminium Castings. *Foundry* 1963 **91** Part 1 July 60-63. Aug. 47 - 49.
12. W. A. KIRK. Melting Procedures for Aluminium and Magnesium Alloys. *Foundry* 1965 **93** Dec. 62 - 65.
13. R. C. LEMON and H. Y. HUNSICKER. New Aluminium Permanent Mould Casting Alloys C355 and A356. *Transactions of the American Foundryman's Society* 1956 **64** 255 - 266.
14. R. C. LEMON and C. R. HOWLE. Premium Strength Aluminium Alloys 354 and 359. *Transactions of the American Foundryman's Society* 1963 **71** 465 - 470.
15. R. J. KISSLING and J. F. WALLACE. Gas Porosity in Aluminium Castings. *Foundry* 1963 **91** Feb. 70 - 75.
16. J. P. MOEHLING. Aluminium Melting Practice in the Die Casting and Permanent Mould Fields. *Transactions of the American Foundrymen's Society* 1958 **66** 533 - 543.
17. E. E. LAYNE and H. F. BISHOP. Effect of Vacuum Degassing on Properties of Aluminium Alloys. *Foundry* 1956 **84** Sept. 118 - 123.
18. H. GREENEWALD. Develops Vacuum Casting Process for Aluminium. *Foundry* 1968 **96** Sept. 80 - 81.
19. R. F. BUDZIAK and F. W. RICHARDS. Degassing of Aluminium with Nitrogen-Chlorine Mixture.. *Foundry* 1962 **90** No. 150 - 152, 155.
20. L. M. ELIJAH. Aluminium Alloy Fluxes. *Foundry* 1964 **92** 88 - 90, 92, 94.
21. R. J. KISSLING and J. F. WALLACE. Fluxing to Remove Oxide from Alumium Alloys. *Foundry* 1963 **91** Mar. 76 - 81.
22. D. J. NEIL and A. C. BURR. Initial Bubble Test for Determination of Hydrogen Content in Molten Aluminium. *Transactions of the American Foundryman's Society* 1961 **69** 272 - 275.
23. E. L. ROOY and E. F. FISCHER. Control of Aluminium Casting Quality by Vacuum Solidification Tests. *Modern Castings* 1968 **54** July 97 - 100.
24. G. N. REINEMANN and L. E. MARSH. Mechanical Properties of A356 Aluminium Casting Alloy. *Metal Progress* 1959 **76** July 80 - 86.
25. B. OTANI. Silumen and its Structure. *Journal of the Institute of Metals* 1926 **36** 243.
26. R. S. ARCHER and L. W. KEMPF. Modification and Properties of Sand Cast Aluminium/Silicon Alloys. *Transactions American Institute of Mining and Metallurgical Engineers* 1926 **73** 581 - 621.
27. L. GUILLET. *Revue de Metallurgie* 1922 **19** 303.
28. Z. JEFFRIES. Aluminium Silicon Alloy. *Chemical and Metallurgical Engineering* 1922 **26** 16.
29. A. G. C. GWYER and H. W. L. PHILLIPS. Constitution and Structure of the Commercial Aluminium/Silicon Alloys. *Journal of the Institute of Metals* 1926 **36** 283 - 324.

30. C. E. RANSLEY and H. NEUFOLD. Solubility Relationships in Aluminium/Sodium and Aluminium/Silicon/Sodium Systems. *Journal of the Institute of Metals* 1950 **78** 25 - 46.

31. B. M. THALL and B. CHALMERS. Modification in Aluminium/Silicon Alloys. *Journal of the Institute of Metals* 1950 **77** 79 - 97.

32. C. MASCRÉ. Modification of High Silicon/Aluminium Alloy and the Corresponding Structures. *Foundry Trade Journal* 1953 **94** June 725 - 730.

33. V. KONDIC and H. J. KOZLUNSKI. Fundamental Characteristics of Casting Fluidity. *Journal of the Institute of Metals* 1949 **75** 665 - 678.

34. R. C. HARRIS, S. LIPSON and H. ROSENTHAL. Tensile Properties of Aluminium - Silicon - Magnesium Alloys and the Effects of Sodium Modification. *Transactions of the American Foundryman's Society* 1956 **64** 470 - 481.

35. R. A. ZUECH. Sodium Improves Aluminium 356. *The Iron Age* 1959 **183** Jan. 88 - 89.

36. A. CIBULA. The Grain Refinement of Aluminium Alloy Castings by the additions of Titanium and Boron. *Journal of the Institute of Metals* 1951/52 **80** 1 - 16.

37. R. J. KISSLING and J. F. WALLACE. Refinement of Aluminium/Silicon Alloys. *Foundry* 1963 **91** Part 1 Apr. 74 - 79; Part 2 May 142 - 144 and 146.

38. R. J. KISSLING and J. F. WALLACE. Grain Refinement of Aluminium Castings. *Foundry* 1963 **91** Part 1 June 78 - 82; Part 2 July 45 - 49.

39. M. C. FLEMINGS, S. Z. URAM and H. F. TAYLOR. Solidification of Aluminium Castings. *Transactions of the American Foundryman's Society* 1960 **68** 670 - 684.

40. L. W. EASTWOOD. Symposium on Principles of Gating. *American Foundryman's Society* 1951 pp. 25 - 30.

41. K. G. LATIMER. Running, Gating and Feeding of Sand Castings. Technical File No. R-1179 Alcan.

42. M. C. FLEMINGS and H. F. TAYLOR. Gating Aluminium Castings *Foundry* 1960 **88** Apr. 72-78.

43. R. F. POLICH, A. SAUNDERS and M. C. FLEMINGS. Gating Premium Quality Castings. *Modern Castings* 1963 **44** Aug. 418 – 426.

44. D. C. SWANSON. How to Improve Aluminium Casting Quality with Fibre Glass Sleeves. *Modern Castings* 1966 **50** Aug. 35 - 36.

45. M. C. FLEMINGS, H. F. CONRAD and H. F. TAYLOR. Aluminium Alloys Fluidity Test. *Transactions of the American Foundryman's Society* 1959 **67** 496 - 507.

46. M. R. SHESHRADRI and A. RAMACHANDRAN. Casting Fluidity and Fluidity of Aluminium and its Alloys. *Transactions of the American Foundryman's Society* 1965 **73** 292 - 304.

47. Symposium of Solidification. *American Foundryman's Society* 1961.

48. W. H. JOHNSON and J. G. KURA. Some Principles for Producing Sound Aluminium/7% Magnesium Alloy Castings. *Transactions of the American Foundryman's Society* 1959 **67** 535-552.

49. M. C. FLEMINGS, P. J. NORTON and H. F. TAYLOR. Performance of Chills on High Strength - High Ductility Sand-Mould Castings of Various Section Thicknesses. *Transactions of the American Foundryman's Society* 1957 **65** 259 - 266.

50. H. F. BISHOP, E. T. MYSKOWSKI and W. S. PELLINI. A Simplified Method for Determining Riser Dimensions. *Transactions of the American Foundryman's Society* 1955 **63** 271 - 281.

51. H. F. TAYLOR, M. C. FLEMINGS and T. S. PIWONKA. Risering Aluminium Castings. *Foundry* 1960 **88** May 216 - 226.

52. M. C. FLEMINGS and H. F. TAYLOR. *Aerospace Engineering* 1962 July 10 - 15.

53. B. CHAMBERLAIN and J. SULZER. Gas Content and Solidification Rate Effect on Tensile Properties and Soundness of Aluminium Casting Alloys. *Transactions of the American Foundryman's Society* 1964 **72** 600 - 607.

54. K. MURTHY, M. SESHADRI and A. RAMACHANDRAN. End Chills Thermal Behaviour and Effect on Casting Soundness. *Transactions of the American Foundryman's Society* 1965 **73** 502 - 508.

55. W. A. BAILEY, A.D.437102. Defense Documentation Center, Cameron Station, Alexandria, Virginia.

56. G. N. REINEMANN and L. E. MARSH. Mechanical Properties of A356 Aluminium Casting Alloy. *Metal Progress* 1959 **76** July 80 - 86.

57. MILITARY SPECIFICATION MIL-H-6088E. Heat Treatment of Aluminium Alloys.

58. AEROSPACE STRUCTURAL METALS HANDBOOK. Vol.II. Non Ferrous Alloys, Mar. 1963.

59. A. B. DEROSS. Aging Practices for High Strength Ductile Aluminium Alloy HP356. *Transactions of the American Foundryman's Society* 1957 65 565 - 569.

60. Private Communication. Aluminium Federation.

61. R. A. QUADT. The Effect of Room Temperature Intervals between Quenching and Aging of Aluminium Sand Castings. *Transactions of the American Foundryman's Society* 1947 55 351 - 356.

62. E. TOLEDO and B. CROCKER. February 1965. U.S. Army Material Command, Watertown Arsenal, Watertown, Massachusetts.

63. R. W. RUDDLE. The Solidification of Castings. Institute of Metals Monograph and Report Series No. 7, 1957.

64. H. S. CARSLAW and J. C. JAEGER. Conduction of Heat in Solids, 1947, Oxford University Press.

65. N. CHVORINOV. *Hutnicke Listy* 1951 6 549 and 594, 1953 8 7 and 64.

66. R. E. SPEAR and G. R. GARDNER. Dendrite Cell Size. *Transactions of the American Foundryman's Society* 1963 71 209 - 215.

67. Private Communication. D. James, Sterling Metals Ltd.

APPENDIX I

The Nomograms enable the founder to determine sprue dimensions and taper once the sprue height has been established. Below is a worked example using Latimer's[41] work to develop a design for the sprue in a running system once the pouring rate had been decided. All dimensions are in imperial units.

To calculate the sprue dimensions

(a) Connect the total height of sprue plus pouring basin in inches (h_1) on H scale to discharge coefficient on K scale, marking intersection with V reference line. (h_1 = 16.2in, K = 0.68).

(b) Connect intersection on the V reference line to flow-rate in lbs/sec. on the Q scale, extend to D scale to give the diameter at the bottom of the sprue (d_1). (Q = 3 lbs/sec., d_1 = 0.70in).

(c) Connect d_1 on D scale to h_1 on H scale to intersection on the A reference line.

(d) Connect height of pouring bush (h_2) on H scale to intersection on the A reference line, extend to D scale to give diameter at the top of the sprue (d_2). (h_2 = 4in, d_2 = 1.01in).

To calculate the sprue taper

(e) Connect d_1 on B scale through d_2 on C scale to intersect with the E reference line.

(f) Connect intersection on E reference line to the sprue height in inches (h_3) on G scale. The intersection with the F scale gives the angle, θ, in degrees. (h_3 = 12.2in, θ = 1.3°).

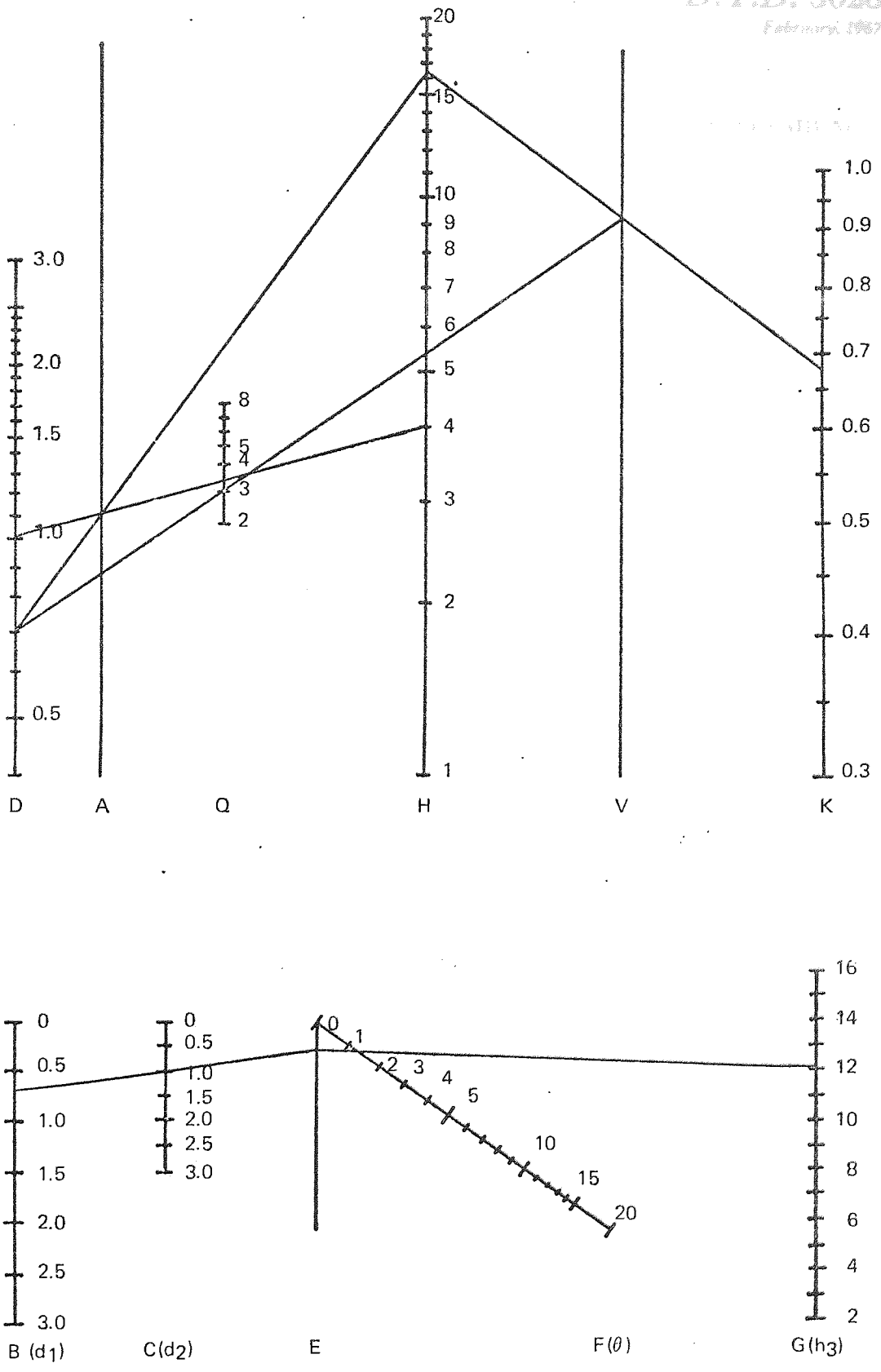

Figure 107.—*Latimer's Nomograph for Calculating Sprue Dimensions.*

APPENDIX II

MINISTRY OF TECHNOLOGY

D.T.D. 5028

February, 1967

Aircraft Material Specification

ALUMINIUM - SILICON - MAGNESIUM ALLOY INGOTS AND PREMIUM QUALITY CASTINGS

(Solution treated and precipitation treated)
(Si 7, Mg 0·3)

NOTE 1. This specification is one of a series issued by the Ministry of Technology, either to meet a limited requirement not covered by any existing British Standard for aircraft material, or to serve as a basis for inspection of materials the properties and uses of which are not sufficiently developed to warrant submission to the British Standards Institution for standardisation.

NOTE 2. This specification will normally be used only after prior consultation between the purchaser and the manufacturer at the earliest possible stage in design. British Standards in the "aircraft" series and D.T.D. specifications for castings draw attention to the fact that the tensile values specified for test pieces from separately cast test samples may not always be realised in certain portions of castings. In order that the intrinsic variation of strength in castings shall be minimised and the actual strengths optimised, it is essential that the design of each casting to this specification is such that engineering design requirements are compatible with foundry requirements.*

---

1. Inspection and testing procedure

The ingots and castings shall be inspected and tested in accordance with the following requirements:

Ingots .....British Standard L.101, Sections One and Two.

Premium quality castings .....British Standard L.101, Section One and Section Three or Four, and the additional requirements of this specification.

2. Quality of material

2.1 *Ingots.*

(*a*) The aluminium used shall comply with British Standard L.48.

(*b*) Approved scrap only may be used.

2.2 *Castings.* The castings shall be made from:

(*a*) Approved ingots, with or without approved scrap therefrom, or

(*b*) Aluminium complying with British Standard L.48 and alloying constituents.

3. Chemical composition

3.1 *Ingots.*

3.1.1 The chemical composition of the ingots shall be:

Element	Per cent	
	min.	max.
Copper	—	0·10
Magnesium	0·20	0·45
Silicon	6·5	7·5
Iron	—	0·15
Manganese	—	0·10
Nickel	—	0·10
Zinc	—	0·10
Lead	—	0·05
Tin	—	0·05
Titanium	—	0·20
Aluminium	The remainder	

3.1.2 The ingot shall be grain refined with titanium or with titanium and boron. The ingot maker shall declare the grain refining element(s) used.

3.2 *Castings.*

3.2.1 The manufacturer shall supply to the inspector, in respect of every cast, the results of analysis for the specified elements.

---

* The purchaser is responsible for securing the concurrence of the parent design firm.

3.2.2 The chemical composition of the castings shall be:

Element	Per cent	
	min.	max.
Copper	—	0·10
Magnesium	0·20	0·45
Silicon	6·5	7·5
Iron	—	0·20
*Manganese	—	0·10
*Nickel	—	0·10
*Zinc	—	0·10
*Lead	—	0·05
*Tin	—	0·05
†Titanium	—	0·20
Aluminium	The remainder	

* The proportion of casts in which this element is determined may be reduced, subject to the discretion of the Inspecting Authority, to not less than one in five.

† The determination of this element is not required by the Inspecting Authority when the castings have been produced from approved ingots with or without approved scrap therefrom.

4. Heat treatment

The castings and test samples shall be heated together at a temperature of 540° ± 5°C (1004° ± 9°F) for not less than 12 hours and quenched in water at a temperature of not less than 65°C (149°F). They shall then be reheated at a temperature of 155° ± 5°C (311° ± 9°F) for not less than 4 hours and cooled in air. Alternative heat treatments to give specific properties may be agreed between the purchaser and the manufacturer and stated on the drawing or order.

5. Mechanical properties

5.1 The mechanical properties obtained from chill cast test samples selected and prepared in accordance with the relevant requirements of B.S.L.101 shall be not less than the following values:

	0·2 per cent proof stress		Tensile strength		Elongation per cent
	tonf/in²	kgf/mm²	tonf/in²	kgf/mm²	
Chill cast test samples (Forms A, B, C or D)	13·0	20·4	18·0	28·3	5

(References to test sample forms are to those in British Standard L.101).

5.2 In addition to the mechanical testing required by Clause 5.1, castings are to be subjected to cut-up testing as follows:

(*a*) *Pattern approval cut-up test procedure from initial production castings; to be repeated after any significant change in manufacture.*

(i) The number of castings to be subjected to cut-up test shall be stated on the drawing or order.

(ii) The location, size and form of the test pieces to be taken from the highly stressed or otherwise important regions in each casting shall be stated on the drawing—these to be referred to as tests from designated locations.

(iii) Further test pieces shall be taken in typical undesignated locations at the discretion of the manufacturer, to demonstrate satisfactory strength in such locations.

(iv) Castings for test shall be heat treated in accordance with Clause 4, and shall not be further heat treated or mechanically worked before testing.

(v) The test results shall be made available to the purchaser.

and (*b*) *Routine cut-up tests as follows*:

(i) From each pattern of casting one casting shall be selected for test from every 50 castings passed by the founder's inspector, subject to a minimum of one casting per test in any period of six months when less than 50 castings have been passed by the inspector.

(ii) Unless otherwise agreed, tests shall be taken from designated locations as required by Clauses 5.2(a)(ii) and (iv).

(iii) When agreed between the manufacturer and the purchaser, and stated on the drawing or order, the number of test pieces cut from a production casting may be less than the number required for a pattern approval casting.

(iv) The castings selected for test may be those rejected for reasons which do not affect cut-up strength properties, e.g. faulty fettling.

5.3 The mechanical properties of test pieces cut from castings shall be not less than the following values:

	0·2 per cent proof stress		Tensile strength		Elongation per cent
	tonf/in²	kgf/mm²	tonf/in²	kgf/mm²	
Designated locations	12·5	19·7	17·0	26·7	5
Undesignated locations	11·5	18·1	14·5	22·8	3

6. Re-test procedure

6.1 *Chill cast test samples (Clause 5.1).* The re-test procedure shall be in accordance with the relevant requirements of British Standard L.101, except that if the additional samples tested fail to comply with the specified requirements, test pieces shall be machined from a casting selected from the batch represented, in accordance with Clause 5.2, and shall comply with the appropriate requirements of Clause 5.3.

6.2 *Test pieces cut from castings.* If any test piece cut from a casting fails to comply with the specified requirements, the test results shall be submitted to the purchaser and the Inspecting Authority, and a re-test procedure agreed.

Approved for issue,

E. W. RUSSELL,

Director of Materials Research and Development.

Printed in England for Her Majesty's Stationery Office
by Willsons (Printers) Ltd., Leicester

Dd. 133046 K11 2/67 WPL 455

UDC 629.7 : 669.715'782'721-412-14

2L. 99, March, 1972

(Superseding British Standard L.99 and D.T.D. 5028)

BRITISH STANDARDS INSTITUTION
2 PARK STREET, LONDON W1A 2BS

INCORPORATED BY ROYAL CHARTER
Telephone: 01-629 9000
Telex: 266933

BRITISH STANDARD : AEROSPACE SERIES

SPECIFICATION FOR

INGOTS AND CASTINGS OF ALUMINIUM-SILICON-MAGNESIUM ALLOY

(Solution treated and precipitation treated)

(Si 7, Mg 0.3)

1. INSPECTION AND TESTING PROCEDURE

The ingots and castings shall be inspected and tested in accordance with the relevant requirements of British Standard L.101 as follows:

Ingots	Sections 1 and 2
Castings not subject to cut-up testing	Sections 1 and 3
Castings subject to cut-up testing	Sections 1 and 4

2. CHEMICAL COMPOSITION

2.1 *Ingots*

2.1.1 The chemical composition of the ingots shall be:

Element	%	
	min.	max.
Copper	—	0.10
Magnesium	0.70	0.45
Silicon	6.5	7.5
Iron	—	0.15
Manganese	—	0.10
Nickel	—	0.10
Zinc	—	0.10
Lead	—	0.05
Tin	—	0.05
Titanium	—	0.20
Aluminium	—	The remainder

2.1.2 The ingot shall be grain refined with titanium or with titanium and boron. The ingot maker shall declare the grain refining element(s) used.

2.2 Castings. The chemical composition of the castings shall be:

Element	%	
	min.	max.
Copper	—	0.10
Magnesium	6.23	6.45
Silicon	6.5	7.5
Iron	—	0.20
*Manganese	—	0.10
*Nickel	—	0.10
*Zinc	—	0.10
*Lead	—	0.05
*Tin	—	0.05
*Titanium	—	0.20
Aluminium	—	The remainder

*The proportion of casts in which this element is determined may be reduced, subject to the discretion of the Inspecting Authority, to not less than one in five of those analysed.

3. HEAT TREATMENT

The castings and test samples shall be heat treated together as follows:

(1) Heat at a temperature of 540±5 °C for not less than 12 hours.

(2) Quench in water at a temperature of not less than 65 °C.

(3) Re-heat at a temperature of 155±5 °C for not less than 4 hours.

(4) Cool in air.

4. MECHANICAL PROPERTIES

NOTE. The tensile test values specified for test pieces machined from separately cast test samples may not be realized in certain portions of castings.

4.1 Separately cast test samples. The mechanical properties obtained from separately cast test samples, selected and prepared in accordance with the relevant requirements of British Standard L.101, shall be not less than the following values:

Test sample	0.2 % proof stress	Tensile strength	Elongation
	N/mm²	N/mm²	%
Sand cast	185	230	2
Chill cast	200	280	5

4.2 Cut-up test samples. Unless otherwise agreed between the supplier and the purchaser and stated in the Inspection Schedule in accordance with British Standard L.101, the mechanical properties obtained from cut-up test samples, selected and prepared in accordance with the relevant requirements of British Standard L.101, shall be not less than the following values:

Position of test samples	0.2 % proof stress	Tensile strength	Elongation
	N/mm²	N/mm²	%
Designated locations	200	260	5
Other locations	180	225	3

NOTE. 1 N/mm²=1 MN/m²=0.102 kgf/mm²=0.1 hbar=0.065 tonf/in². Information on SI units is given in BS 3763, 'The International System of units (SI)'; see also BS 350, 'Conversion factors and tables'.

This British Standard, having been approved by the Aerospace Industry Standards Committee, was published under the authority of the Executive Board of the Institution on 30 March 1972.

SBN: 580 07080 8

The Institution desires to call attention to the fact that this British Standard does not purport to include all the necessary provisions of a contract.

British Standards are revised, when necessary, by the issue either of amendment slips or of revised editions. It is important that users of British Standards should ascertain that they are in possession of the latest amendments or editions.

The following BSI references relate to the work on this standard:
Committee reference ACE/27 Draft for comment 70/16281

Printed in England by Gerald S. Sun Ltd., London, S.E.14
GP 432 2000 5.72

APPENDIX IV

COMPUTER PROGRAM FOR THE DETERMINATION OF THERMAL DIFFUSIVITY.

```
'BEGIN'
 'REAL'THETA,THETART,THETAMP,KAPPA,DIST,TIME,ATM,Y,Y1,Y2,X,X1,X2;
 'COMMENT'364;
 'REAL''PROCEDURE'ERF(X);
 'VALUE'X;
 'REAL'X;
 'COMMENT' FOR ERROR FUNCTIONS WITH X LESS THAN OR = TO 1.1;
      'BEGIN'
      'REAL'A,U,V,W,Y,Z,T;
      'INTEGER'N;
      Z:=0;
      CYMRU:'IF'X'NE'0.0000000000'THEN'
           'BEGIN'
           'IF'0.5'LT'ABS(X)'THEN'A:=-SIGN(X)*0.5'ELSE'A:=-X;
           U:=V:=1.12837917*EXP(-X↑2);
           Y:=T:=-V*A;
           N:=1;
           WALES:'IF'ABS(T)'GE'.0000000001'THEN'
                'BEGIN'
                N:=N+1;
                W:=-2*X*V-2*U*(N-2);
                T:=T*W*A/(V*N);
                U:=V;
                V:=W;
                Y:=Y+T;
                'GOTO'WALES;
                'END';
           Z:=Z+Y;
           X:=X+A;
           'GOTO'CYMRU;
           'END';
      ERF:=Z;
      'END'ERF;
      'REAL''PROCEDURE'ERFL(X);
      'VALUE'X;
      'REAL'X;
      'COMMENT' FOR ERROR FUNCTIONS WITH X GREATER THAN 1.1;
           'BEGIN'
          'INTEGER'M;
           'REAL'BMIN2,BMIN3,P,R,T,V,V2;
           V:=X*X;
           T:=-0.56418958*EXP(-V)/X;
           V:=0.5/V;
           P:=V*T;
           V2:=V*V;
           T:=T+1;
           M:=0;
           R:=BMIN3:=BMIN2:=1;
           'FOR'M:=M+2'WHILE'T'NE'R'DO'
                'BEGIN'
                P:=T;
                BMIN3:=V*(M-1)*BMIN3+BMIN2;
```

```
            T:=BMIN2;
            BMIN2:=V*M*BMIN2+BMIN3;
            T:=R-P/BMIN2/T;
            P:=M*(M+1)*V2*P;
            'END'WHILE;
        ERFL:=T;
        'END';
WRITETEXT('('('('5S')'THETA=THETA%R.T.%/')');
NEWLINE(1);
WRITETEXT('('('4S')'THETA%M.P.=THETA%R.T.'('9S')'X'('11S')'Y
'('11S')'X'('11S')'Y'('13S')'KAPPA')');
NEWLINE(1);
THETAMP:=READ;
THETART:=READ;
'FOR'DIST:=1.270'STEP'0.635'UNTIL'3.176'DO'
        'BEGIN'
        'FOR'TIME:=20'STEP'20'UNTIL'1550'DO'
            'BEGIN'
            THETA:=READ;
            AIM:=1-((THETA-THETART)/(THETAMP-THETART));
            SPACE(7);
            PRINT(AIM,2,8);
            'IF'AIM'GE'0.958500'THEN''GOTO'CASNEWYDD;
            'IF'AIM'LE'0.88021'THEN'
                'BEGIN'
                'COMMENT' IF AIM=ERF(X) WHEN X=1.1 AIM=0.88021;
                'COMMENT' ERF(X) FOR X LE 1.1;
                X1:=0.2;
                Y1:=ERF(X1);
                X2:=0.8;
                Y2:=ERF(X2);
                X:=X1+(AIM-Y1)*(X2-X1)/(Y2-Y1);
                SPACE(6);
                PRINT(X,2,6);
                Y:=ERF(X);
                PRINT(Y,2,6);
                    NEWLINE(1);
                'IF'ABS(Y-AIM)'GE'0.00001'THEN'
                    'BEGIN'
                    ABERTAWE:X1:=X2;
                    X2:=X;
                    Y1:=Y2;
                    Y2:=Y;
                    X:=X1+(AIM-Y1)*(X2-X1)/(Y2-Y1);
                    SPACE(52);
                    PRINT(X,2,6);
                    Y:=ERF(X);
                    PRINT(Y,2,6);
                    NEWLINE(1);
                    'IF'ABS(Y-AIM)'GE'0.00001'THEN''GOTO'ABERTAWE
                    'ELSE''GOTO'MYNWY;
                    'END';
                MYNWY:'END'
                'ELSE'
                'BEGIN'
                'COMMENT' AIM GT 0.88021 ERFL(X) SINCE X GT 1.1;
                X1:=1.11;
                Y1:=ERFL(X1);
                X2:=1.45;
```

```
                    Y2:=ERFL(X2);
                    X:=X1+(AIM-Y1)*(X2-X1)/(Y2-Y1);
                    SPACE(6);
                    PRINT(X,2,6);
                    Y:=ERFL(X);
                    PRINT(Y,2,6);
                    NEWLINE(1);
                    'IF'ABS(Y-AIM)'GE'0.00001'THEN'
                          'BEGIN'
                          BRYNBUGA:X1:=X2;
                          X2:=X;
                          Y1:=Y2;
                          Y2:=Y;
                          X:=X1+(AIM-Y1)*(X2-X1)/(Y2-Y1);
                          SPACE(52);
                          PRINT(X,2,6);
                          Y:=ERFL(X);
                          PRINT(Y,2,6);
                          NEWLINE(1);
                          'IF'ABS(Y-AIM)'GE'0.00001'THEN''GOTO'BRYNBUGA
                          'ELSE''GOTO'CAERDYDD;
                          'END';
                    CAERDYDD:'END';
                    KAPPA:=((DIST*DIST)/(4*X*X*TIME));
                    SPACE(80);
                    PRINT(KAPPA,2,6);
                    CASNEWYDD:NEWLINE(1);
              'END';
        'END';
'END';
```

APPENDIX V

SOLUTIONS FOR THE COEFFICIENTS REQUIRED IN THE FACTORS α AND θ_i

Considering the mathematical model:

$y = b_0 + b_1\alpha + b_2\theta_i + b_3\alpha^2 + b_4\theta_i^2 + b_5\alpha\theta_i$ and assuming

$\alpha = \theta_i = 0$ and $s_1 = s_2 = 1$ then a 3 x 3 design for the sums of the squares, y, may be represented by the matrix below:

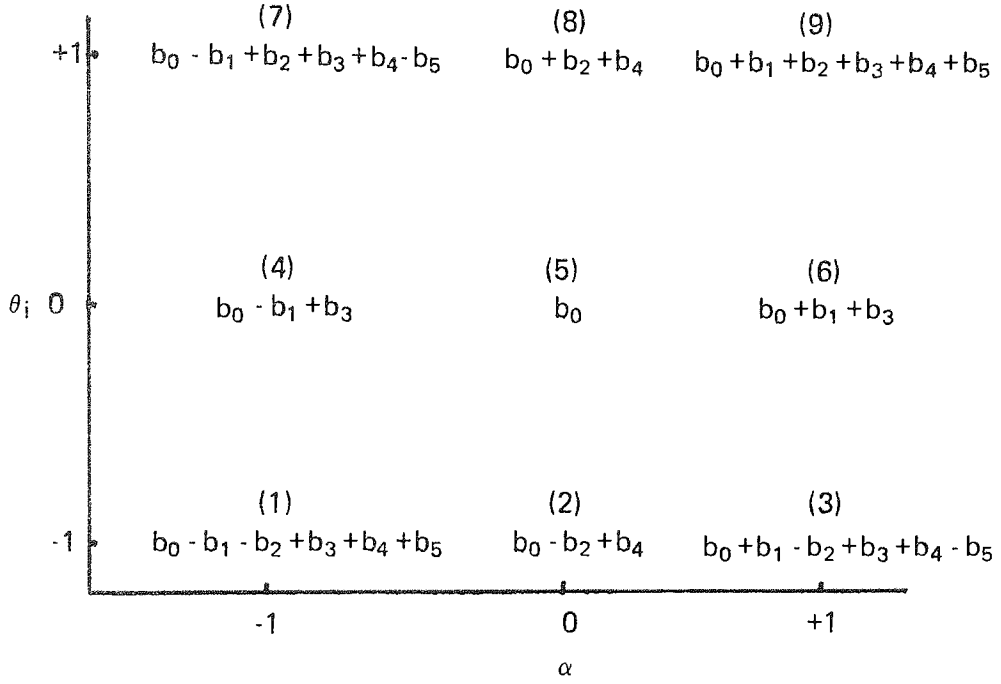

The matrix above can be expressed as follows:

$$[y] = \begin{bmatrix} y_7 & y_8 & y_9 \\ y_4 & y_5 & y_6 \\ y_1 & y_2 & y_3 \end{bmatrix}$$

To determine the individual coefficients it is necessary to eliminate the remainder by comparison of combinations of the equations representing the mathematical model at each point.

Solution for the coefficients b_1 and b_2

The equations for the nine points are

Point	Equation
1	$y_1 = b_0 - b_1 - b_2 + b_3 + b_4 + b_5$
2	$y_2 = b_0 - b_2 + b_4$
3	$y_3 = b_0 + b_1 - b_2 + b_3 + b_4 - b_5$
4	$y_4 = b_0 - b_1 + b_3$
5	$y_5 = b_0$

Point	Equation
6	$y_6 = b_0 + b_1 + b_3$
7	$y_7 = b_0 - b_1 + b_2 + b_3 + b_4 - b_5$
8	$y_8 = b_0 + b_2 + b_4$
9	$y_9 = b_0 + b_1 + b_2 + b_3 + b_4 + b_5$

If the equations for points 1, 4 and 7 are multiplied by -1 and the equations corresponding to points 3, 6 and 9 multiplied by +1, then:

$y_1 = b_0 - b_1 - b_2 + b_3 + b_4 + b_5 \quad x\,{-1} \quad -y_1 = -b_0 + b_1 + b_2 - b_3 - b_4 - b_5$

$y_4 = b_0 - b_1 + b_3 \quad x\,{-1} \quad -y_4 = -b_0 + b_1 - b_3$

$y_7 = b_0 - b_1 + b_2 + b_3 + b_4 - b_5 \quad x\,{-1} \quad -y_7 = -b_0 + b_1 - b_2 - b_3 - b_4 + b_5$

adding $-(y_1 + y_4 + y_7) = -3b_0 + 3b_1 - 3b_3 - 2b_4$ . . . A

$y_3 = b_0 + b_1 - b_2 + b_3 + b_4 - b_5 \quad x\,{+1} \quad y_3 = b_0 + b_1 - b_2 + b_3 + b_4 - b_5$

$y_6 = b_0 + b_1 + b_3 \quad x\,{+1} \quad y_6 = b_0 + b_1 + b_3$

$y_9 = b_0 + b_1 + b_2 + b_3 + b_4 + b_5 \quad x\,{+1} \quad y_9 = b_0 + b_1 + b_2 + b_3 + b_4 + b_5$

adding $(y_3 + y_6 + y_9) = +3b_0 + 3b_1 + 3b_3 + 2b_4$ . . . B

Adding equations A and B b_1 may be derived:

$$\frac{(y_3 + y_6 + y_9) - (y_1 + y_4 + y_7)}{6} = b_1$$

Diagramatically the solution can be represented as:

$$1/6 \begin{bmatrix} -1 & 0 & +1 \\ -1 & 0 & +1 \\ -1 & 0 & +1 \end{bmatrix} \times [y]$$

The solution for coefficient b_2 may be represented thus:

$$1/6 \begin{bmatrix} +1 & +1 & +1 \\ 0 & 0 & 0 \\ -1 & -1 & -1 \end{bmatrix} \times [y]$$

Solution for the coefficients b_3 and b_4

If the equations for points 1, 3, 4, 6, 7 and 9 are multiplied by +1 and the corresponding equations for points 2, 5 and 8 multiplied by -2, then:

$y_1 = b_0 - b_1 - b_2 + b_3 + b_4 + b_5 \quad x\,{+1} \quad y_1 = b_0 - b_1 - b_2 + b_3 + b_4 + b_5$

$y_3 = b_0 + b_1 - b_2 + b_3 + b_4 - b_5 \quad x\,{+1} \quad y_3 = b_0 + b_1 - b_2 + b_3 + b_4 - b_5$

$y_4 = b_0 - b_1 + b_3 \quad x\,{+1} \quad y_4 = b_0 - b_1 + b_3$

$y_6 = b_0 + b_1 + b_3 \quad x\,{+1} \quad y_6 = b_0 + b_1 + b_3$

$y_7 = b_0 - b_1 + b_2 + b_3 + b_4 - b_5 \quad x\,{+1} \quad y_7 = b_0 - b_1 + b_2 + b_3 + b_4 - b_5$

$y_9 = b_0 + b_1 + b_2 + b_3 + b_4 + b_5 \quad x\,{+1} \quad y_9 = b_0 + b_1 + b_2 + b_3 + b_4 + b_5$

adding $(y_1 + y_3 + y_4 + y_6 + y_7 + y_9) = 6b_0 + 6b_3 + 4b_4$ . . . C

$y_2 = b_0 - b_2 + b_4$ x -2 $-2y_2 = -2b_0 + 2b_2 - 2b_4$

$y_5 = b_0$ x -2 $-2y_5 = -2b_0$

$y_8 = b_0 + b_2 + b_4$ x -2 $-2y_8 = -2b_0 - 2b_2 - 2b_4$

adding $-2(y_2 + y_5 + y_8) = -6b_0 - 4b_4$ ... D

Adding equations C and D b_3 may be derived:

$$\frac{(y_1 + y_3 + y_4 + y_6 + y_7 + y_9) - 2(y_2 + y_5 + y_8)}{6} = b_3$$

Diagramatically the solution can be represented as:

$$1/6 \begin{bmatrix} +1 & -2 & +1 \\ +1 & -2 & +1 \\ +1 & -2 & +1 \end{bmatrix} \times [y]$$

The solution for coefficient b_4 may be represented thus:

$$1/6 \begin{bmatrix} +1 & +1 & +1 \\ -2 & -2 & -2 \\ +1 & +1 & +1 \end{bmatrix} \times [y]$$

Solution for the coefficient b_5

If the equations for points 1 and 9 are multiplied by +1 and the equations corresponding to points 3 and 7 are multiplied by -1, then:

$y_1 = b_0 - b_1 - b_2 + b_3 + b_4 + b_5$ x +1 $y_1 = b_0 - b_1 - b_2 + b_3 + b_4 + b_5$

$y_9 = b_0 + b_1 + b_2 + b_3 + b_4 + b_5$ x +1 $y_9 = b_0 + b_1 + b_2 + b_3 + b_4 + b_5$

adding $(y_1 + y_9) = 2b_0 + 2b_3 + 2b_4 + 2b_5$ ... E

$y_3 = b_0 + b_1 - b_2 + b_3 + b_4 - b_5$ x -1 $-y_3 = -b_0 - b_1 + b_2 - b_3 - b_4 + b_5$

$y_7 = b_0 - b_1 + b_2 + b_3 + b_4 - b_5$ x -1 $-y_7 = -b_0 + b_1 - b_2 - b_3 - b_4 + b_5$

adding $-(y_3 + y_7) = -2b_0 - 2b_3 - 2b_4 + 2b_5$ ... F

Adding equations E and F b_5 may be derived:

$$\frac{(y_1 + y_9) - (y_3 + y_7)}{4} = b_5$$

The solution for coefficient b_5 may be represented thus:

$$1/4 \begin{bmatrix} -1 & 0 & +1 \\ 0 & 0 & 0 \\ +1 & 0 & -1 \end{bmatrix} \times [y]$$

Solution for the coefficient b_0

Although the solution to this coefficient is superfluous to this particular problem it is displayed in this text to complete the technique. The equations for points 1, 3, 7 and 9 are multiplied by -1, equations for the points corresponding to 2, 4, 6 and 8 are multiplied by +2 and, finally, the centre point, 5, is multiplied by +5, then:

$y_1 = b_0 - b_1 - b_2 + b_3 + b_4 + b_5 \quad x\,{-1} \quad -y_1 = -b_0 + b_1 + b_2 - b_3 - b_4 - b_5$

$y_3 = b_0 + b_1 - b_2 + b_3 + b_4 - b_5 \quad x\,{-1} \quad -y_3 = -b_0 - b_1 + b_2 - b_3 - b_4 + b_5$

$y_7 = b_0 - b_1 + b_2 + b_3 + b_4 - b_5 \quad x\,{-1} \quad -y_7 = -b_0 + b_1 - b_2 - b_3 - b_4 + b_5$

$y_9 = b_0 + b_1 + b_2 + b_3 + b_4 + b_5 \quad x\,{-1} \quad -y_9 = -b_0 - b_1 - b_2 - b_3 - b_4 - b_5$

adding $-(y_1 + y_3 + y_7 + y_9) = -4b_0 - 4b_3 - 4b_4 \quad \ldots G$

$y_2 = b_0 - b_2 + b_4 \quad x\,{+2} \quad 2y_2 = 2b_0 - 2b_2 + 2b_4$

$y_4 = b_0 - b_1 + b_3 \quad x\,{+2} \quad 2y_4 = 2b_0 - 2b_1 + 2b_3$

$y_6 = b_0 + b_1 + b_3 \quad x\,{+2} \quad 2y_6 = 2b_0 + 2b_1 + 2b_3$

$y_8 = b_0 + b_2 + b_4 \quad x\,{+2} \quad 2y_8 = 2b_0 + 2b_2 + 2b_4$

$y_5 = b_0 \quad x\,{+5} \quad 5y_5 = 5b_0$

adding $2(y_2 + y_4 + y_6 + y_8) + 5y_5 = 13b_0 + 4b_3 + 4b_4 \quad \ldots H$

Adding equations G and H b_0 may be derived:

$$\frac{2(y_2 + y_4 + y_6 + y_8) + 5y_5 - (y_1 + y_3 + y_7 + y_9)}{9} = b_0$$

The solution for the coefficient b_0 may be represented thus:

$$1/9 \begin{bmatrix} -1 & +2 & -1 \\ +2 & +5 & +2 \\ -1 & +2 & -1 \end{bmatrix} \times [y]$$

The solution for b_0 can also be simply y_5, this, however, is less accurate than the method above.

APPENDIX VI

COMPUTER PROGRAM FOR THE SOLUTION OF INTERFACIAL TEMPERATURE AND THERMAL DIFFUSIVITY

The names of the variables b_1 to b_5 remain unchanged but the dialect Algol 60 uses upper register letters only. The step units s_1 and s_2 were labelled ALPHASTEP and THETASTEP respectively for ease of identification. α and θ_i, the factors which are multiplied by the step sizes (ALPHAGES and THETAGES) to produce the updated estimates, were referred to as ALPHA2 and THETA 2. Within the program, a mechanism was employed to stop the iterative steps when the changes in the factors controlling the new estimates were below a value, which made little improvement to the answer. In addition, should the first estimates be outside the range of the values the program can use the original size of s_1 may be reduced or the iterative loop broken and a new set of data read.

Finally, for simplification the expression within the error function was referred to as BIG X to avoid repetition of $\left(\frac{x}{2\sqrt{\alpha t}}\right)$.

APPENDIX VI

PRINT OUT OF COMPUTER PROGRAM FOR THE SOLUTION OF INTERFACIAL TEMPERATURE AND THERMAL DIFFUSIVITY

```
'BEGIN'
'REAL'THETART,THETAIGES,ALPHAGES,THETAI,ALPHA,DIST,TIME,BIGX,B1,B2
B3,B4,B5,ALPHA2,THETA2,THETASTEP,ALPHASTEP;
'REAL'MEANCP,LENGTH,WIDTH,DENSITY,TOTHEATCONT;
'INTEGER'X,N,T;
'ARRAY'THETAMOBS,THETAMCALC[1:5],SUMOFSQ[1:9];
'ARRAY'AREA[0:24],DHEATCONT[1:24];
'REAL''PROCEDURE'ERF(X);
'VALUE'X;
'REAL'X;
'COMMENT' FOR ERROR FUNCTIONS WITH X LESS THAN OR = TO 1.1;
'BEGIN'
'REAL'A,U,V,W,Y,Z,T;
'INTEGER'N;
Z:=0;
CYMRU:'IF'X'NE'0.0000000000'THEN'
'BEGIN'
'IF'0.5'LT'ABS(X)'THEN'A:=-SIGN(X)*0.5'ELSE'A:=-X;
U:=V:=1.1283791?*EXP(-X↑2);
Y:=T:=-V*A;
N:=1;
WALES:'IF'ABS(T)'GE'.0000000001'THEN'
'BEGIN'
N:=N+1;
W:=-2*X*V-2*U*(N-2);
T:=T*W*A/(V*N);
U:=V;
V:=W;
Y:=Y+T;
'GOTO'WALES;
'END';
Z:=Z+Y;
X:=X+A;
'GOTO'CYMRU;
'END';
ERF:=Z;
'END'ERF;
'REAL''PROCEDURE'ERFL(X);
'VALUE'X;
'REAL'X;
'COMMENT' FOR ERROR FUNCTIONS WITH X GREATER THAN 1.1;
'BEGIN'
'INTEGER'M;
'REAL'BMIN2,BMIN3,P,R,T,V,V2;
V:=X*X;
T:=-0.56418958*EXP(-V)/X;
'COMMENT' THE ABOVE LINE MAY BE USED AS AN ALTERNATIVE TO
              T:=-0.56418958/X/EXP(V) TO PREVENT OVERFLOW;
V:=0.5/V;
P:=V*T;
V2:=V*V;
T:=T+1;
M:=0;
```

```
   R:=BMIN3:=BMIN2:=1;
   'FOR'M:=M+2'WHILE'T'NE'R'DO'
   'BEGIN'
   R:=T;
   BMIN3:=V*(M-1)*BMIN3+BMIN2;
   T:=BMIN2;
   BMIN2:=V*M*BMIN2+BMIN3;
   T:=R-P/BMIN2/T;
   P:=M*(M+1)*V2*P;
   'END'WHILE;
   ERFL:=T;
   'END';
   'REAL''PROCEDURE'SIMPS(F,X,A,B,DELTA,V);
   'VALUE'A,B,DELTA,V;
   'REAL'F,X,A,B,DELTA,V;
   'BEGIN'
   'INTEGER'N,K;
   'REAL'H,J,I;
   'SWITCH'S:=J1;
   V:=(B-A)*V;
   N:=1;
   H:=(B-A)/2;
   X:=A;
   J:=F;
   X:=B;
   J:=(J+F)*H;
J1:B:=0;
   'FOR'K:=1'STEP'1'UNTIL'N'DO'
   'BEGIN'
   X:=(2*K-1)*H+A;
   B:=B+F;
   'END';
   I:=4*H*B+J;
   'IF'ABS(V)*DELTA<ABS(I-V)'THEN'
   'BEGIN'
   V:=I;
   J:=(I+J)/4;
   N:=2*N;
   H:=H/2;
   'GOTO'J1;
   'END';
   SIMPS:=I/3;
   'END'SIMPS;
   'COMMENT' END OF PROCEDURES;
   THETART:=READ;
   THETAIGES:=READ;
   ALPHAGES:=READ;
   MEANCP:=READ;
   LENGTH:=READ;
   DENSITY:=READ;
   WIDTH:=READ;
   THETASTEP:=5;
   AREA[0]:=0;
   TOTHEATCONT:=0;
   'FOR'T:=1'STEP'1'UNTIL'24'DO'
   'BEGIN'
   ALPHASTEP:=0.010;
   'FOR'X:=1'STEP'1'UNTIL'5'DO'
```

```
THETAMOBS[X]:=READ;
WRITETEXT('('OBSERVED%TEMPERATURES')');
NEWLINE(1);
'FOR'X:=1'STEP'1'UNTIL'5'DO'
PRINT(THETAMOBS[X],5,2);
NEWLINE(1);
N:=1;
LOOP:
'FOR'THETAI:=THETAIGES-THETASTEP'STEP'THETASTEP'UNTIL'THETAIGES+
THETASTEP'DO'
'BEGIN'
'FOR'ALPHA:=ALPHAGES-ALPHASTEP'STEP'ALPHASTEP'UNTIL'ALPHAGES+
ALPHASTEP'DO'
'BEGIN'
SUMOFSQ[N]:=0;
'FOR'X:=1'STEP'1'UNTIL'5'DO'
'BEGIN'
DIST:=(((0.25*X)-0.125)*2.54);
TIME:=(T*2.5);
BIGX:=(DIST/(2*SQRT(ALPHA*TIME)));
THETAMCALC[X]:=(THETART+((THETAI-THETART)*(1-('IF'BIGX'LE'1.1'THEN'
ERF(BIGX)'ELSE'ERFL(BIGX)))));
SUMOFSQ[N]:=SUMOFSQ[N]+((THETAMOBS[X]-THETAMCALC[X])*(THETAMOBS[X]
-THETAMCALC[X]));
'END';
N:=N+1;
'END';
'END';
WRITETEXT('('SUM%OF%SQUARES%FOR%POSITIONS%1%TO%9')');
NEWLINE(1);
'FOR'N:=1'STEP'1'UNTIL'9'DO'
PRINT(SUMOFSQ[N],5,4);
NEWLINE(1);
B1:=((-1*(SUMOFSQ[1]+SUMOFSQ[4]+SUMOFSQ[7]))+(+1*(SUMOFSQ[3]+SUMOFSQ
[6]+SUMOFSQ[9])))/6;
B2:=((-1*(SUMOFSQ[1]+SUMOFSQ[2]+SUMOFSQ[3]))+(+1*(SUMOFSQ[7]+SUMOFSQ
[8]+SUMOFSQ[9])))/6;
B3:=((-2*(SUMOFSQ[2]+SUMOFSQ[5]+SUMOFSQ[8]))+(+1*(SUMOFSQ[1]+SUMOFSQ
[4]+SUMOFSQ[7]+SUMOFSQ[3]+SUMOFSQ[6]+SUMOFSQ[9])))/6;
B4:=((-2*(SUMOFSQ[4]+SUMOFSQ[5]+SUMOFSQ[6]))+(+1*(SUMOFSQ[1]+SUMOFSQ
[2]+SUMOFSQ[3]+SUMOFSQ[7]+SUMOFSQ[8]+SUMOFSQ[9])))/6;
B5:=((-1*(SUMOFSQ[3]+SUMOFSQ[7]))+(+1*(SUMOFSQ[1]+SUMOFSQ[9])))/4;
ALPHA2:=(((B2*B5)-(2*(B1*B4)))/((4*(B3*B4))-(B5↑2)));
WRITETEXT('('ALPHA2')');
NEWLINE(1);
OUTPUT(ALPHA2);
NEWLINE(1);
THETA2:=(((-B5*ALPHA2)-B2)/(2*B4));
WRITETEXT('('THETA2')');
NEWLINE(1);
OUTPUT(THETA2);
NEWLINE(1);
THETAIGES:=THETAIGES+(THETA2*THETASTEP);
ALPHAGES:=ALPHAGES+(ALPHA2*ALPHASTEP);
WRITETEXT('('THERMAL%DIFFUSIVITY%AT%THIS%STAGE')');
NEWLINE(1);
OUTPUT(ALPHAGES);
WRITETEXT('('INTERFACIAL%TEMP%AT%THIS%STAGE')');
```

```
NEWLINE(1);
OUTPUT(THETAIGES);
NEWLINE(1);
'COMMENT' REDUCED ALPHA2*ALPHASTEP TO GT 0.001 FROM 0.0001;
'IF'ABS(THETA2*THETASTEP)'GT'0.40'OR'ABS(ALPHA2*ALPHASTEP)'GT'0.001
'THEN'
'BEGIN'
'IF'ALPHAGES'LT'ALPHASTEP+0.0001'THEN'
'BEGIN'
ALPHASTEP:=0.5*ALPHASTEP;
ALPHAGES:=ALPHASTEP+0.0001;
'IF'ALPHAGES'LT'0.001'THEN'
'BEGIN'
WRITETEXT('('OH%BOY%ARE%YOU%IN%TROUBLE')');
NEWLINE(1);
WRITETEXT('('APPROX%FINAL%INTERFACIAL%TEMP')');
NEWLINE(1);
PRINT(THETAIGES,4,2);
NEWLINE(1);
WRITETEXT('('APPROX%FINAL%THERMAL%DIFFUSIVITY')');
NEWLINE(1);
PRINT(ALPHAGES,2,5);
NEWLINE(10);
'GOTO'ABER;
'END'
'END';
N:=1;
'GOTO'LOOP;
'END'
'ELSE'
'BEGIN'
WRITETEXT('('FINAL%INTERFACIAL%TEMPERATURE')');
NEWLINE(1);
PRINT(THETAIGES,4,2);
NEWLINE(1);
WRITETEXT('('FINAL%THERMAL%DIFFUSIVITY')');
NEWLINE(1);
PRINT(ALPHAGES,2,5);
NEWLINE(1);
WRITETEXT('('FINAL%CALCULATED%TEMPERATURES')');
NEWLINE(1);
'FOR'X:=1'STEP'1'UNTIL'5'DO'
'BEGIN'
DIST:=(((0.25*X)-0.125)*2.54);
TIME:=(T*2.5);
BIGX:=(DIST/(2*SQRT(ALPHAGES*TIME)));
THETAMCALC[X]:=(THETART+((THETAIGES-THETART)*(1-('IF'BIGX'LE'1.1
'THEN'ERF(BIGX)'ELSE'ERFL(BIGX)))));
PRINT(THETAMCALC[X],3,2);
'END';
AREA[T]:=SIMPS(THETART+((THETAIGES-THETART)*(1-('IF'(DIST/(2*SQRT
(ALPHAGES*TIME)))'LE'1.1'THEN'ERF(DIST/(2*SQRT(ALPHAGES*TIME)))
'ELSE'ERFL(DIST/(2*SQRT(ALPHAGES*TIME)))))),DIST,0.5.08,0.05,10000)
-(THETART*5.08);
NEWLINE(1);
WRITETEXT('('AREA%UNDER%THE%CURVE')');
NEWLINE(1);
OUTPUT(AREA[T]);
```

```
NEWLINE(1);
DHEATCONT[T]:=((AREA[T]-AREA[T-1])*MEANCP*(LENGTH*2.54)*(WIDTH*2.54)
*DENSITY);
WRITETEXT('('CHANGE%IN%HEAT%CONT%OF%THE%CHILL')');
NEWLINE(1);
OUTPUT(DHEATCONT[T]);
NEWLINE(1);
TOTHEATCONT:=TOTHEATCONT+DHEATCONT[T];
WRITETEXT('('TOTAL%HEAT%CONT%OF%THE%CHILL')');
NEWLINE(1);
OUTPUT(TOTHEATCONT);
NEWLINE(10);
'END';
ABER;
'END';
'END';
```

APPENDIX VII IRON PICK-UP DURING MELTING OF THE LOW IRON ALLOY

During this study particular attention was paid to Iron pick-up. Precautions such as melting in Silicon Carbide crucibles and the use of coated foundry tools reduce the pick-up to a minimum but gradual contamination does occur. The graph below indicates the level of Iron impurities after the addition of recirculated scrap to virgin alloy (having been made up in one previous melt). The levels of recirculated scrap ran between 65% and 75% and were the products of two melts of pure alloy.

TWO MELTS EACH <0.01% Fe TO START

add scrap of one to the other: 65% - 75% recirculated (i.e. contaminated)
35% - 25% virgin alloy melted once.

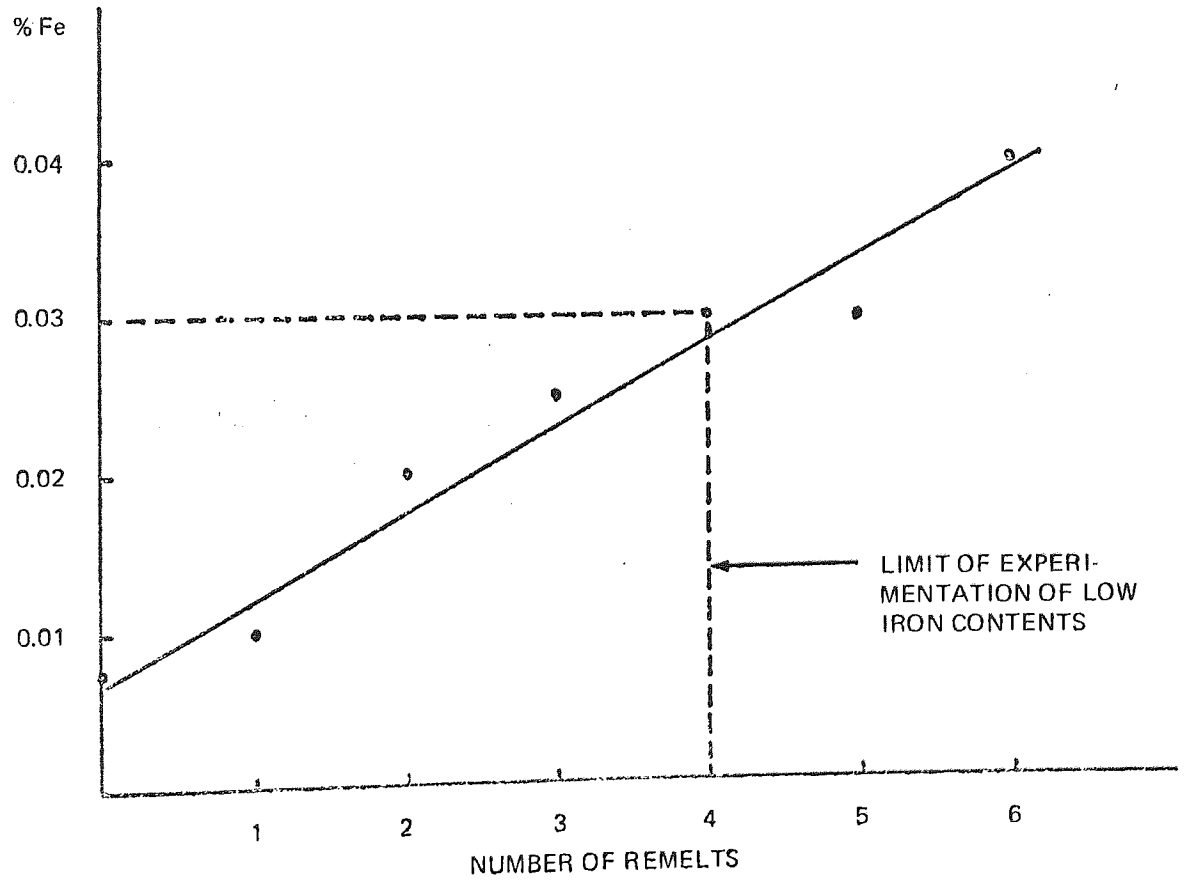

Figure 108.—*Iron pick-up during a sequence of remelts.*

APPENDIX VIII. COMPOUND CHILLS

The computer program included in this Appendix is an attempt to combine the advantages of both Aluminium and Cast Iron chills. The Cast Iron is placed nearest to the mould cavity in an attempt to absorb heat by virtue of its higher volume heat capacity. The backing material, Aluminium, is employed to rapidly extract the heat away from the Cast Iron layer. One, or two, thermocouples may be positioned in the Cast Iron layer, depending upon its thickness, the remainder (4 or 3) being spaced in the Aluminium. The program initially attempts to determine the interfacial temperature between the Aluminium and Cast Iron layers. Once this temperature has been calculated the program includes this result as one of the observed temperatures within the Cast Iron portion in an attempt to estimate the casting/chill interfacial temperature.

Several runs have been tried using dummy results and these have proved successful. This work is not entirely within the scope of the existing project but is included for completeness. The author envisages the practical problems of heat transfer across the metal interface and differential expansion causing operative and structural difficulties.

Alternatively, this technique could be employed as a means of overcoming the separation of Aluminium chills from sand. A strip of Cast Iron bolted to the back of an Aluminium chill would be convenient for magnetic sorting.

COMPUTER PROGRAM FOR THE SOLUTION OF INTERFACIAL TEMPERATURE AND THERMAL DIFFUSIVITY FOR COMPOUND CHILLS

```
'BEGIN'
'REAL'THETART,TETAIALGES,TETAICIGES,ALFAALGES,ALFACIGES,THETASTEP,
            ALFAALSTEP,TETAIAL,ALPHAAL,DISTAL,TIME,BIGXAL,A1,A2,A3,
A4,A5,ALPHA2,THETA2,ALFACISTEP,TETAICI,ALPHACI,DISTCI,BIGXCI,B1,B2,
B3,B4,B5,ALFA2,TETA2;
'REAL'WIDTH,DENSITYAL,DENSITYCI,MEANCPAL,MEANCPCI,LENGTH,TOTHTCONT;
'INTEGER'T,X,N,Y,M;
'ARRAY'TETAMALOBS,TETAMALCALC[1:4],SUMOFSQ,SUMOVSQ[1:9],TETAMCIOBS,
TETAMCICALC[1:2];
'ARRAY'AREAAL,AREACI[0:24],DALHTCONT,DCIHTCONT[1:24];
 'REAL''PROCEDURE'ERF(X);
 'VALUE'X;
 'REAL'X;
 'COMMENT' FOR ERROR FUNCTIONS WITH X LESS THAN OR = TO 1,1;
     'BEGIN'
     'REAL'A,U,V,W,Y,Z,T;
     'INTEGER'N;
     Z:=0;
     CYMRU:'IF'X'NE'0.0000000000'THEN'
         'BEGIN'
         'IF'0,5'LT'ABS(X)'THEN'A:=-SIGN(X)*0.5'ELSE'A:=-X;
         U:=V:=1.12837917*EXP(-X↑2);
         Y:=T:=-V*A;
         N:=1;
         WALES:'IF'ABS(T)'GE'.0000000001'THEN'
             'BEGIN'
             N:=N+1;
             W:=-2*X*V-2*U*(N-2);
             T:=T*W*A/(V*N);
             U:=V;
             V:=W;
             Y:=Y+T;
             'GOTO'WALES;
             'END';
         Z:=Z+Y;
         X:=X+A;
         'GOTO'CYMRU;
         'END';
     ERF:=Z;
     'END'ERF;
     'REAL''PROCEDURE'ERFL(X);
     'VALUE'X;
     'REAL'X;
     'COMMENT' FOR ERROR FUNCTIONS WITH X GREATER THAN 1,1;
         'BEGIN'
        'INTEGER'M;
         'REAL'BMIN2,BMIN3,P,R,T,V,V2;
         V:=X*X;
         T:=-0,56418958*EXP(-V)/X;
         V:=0,5/V;
         P:=V*T;
         V2:=V*V;
         T:=T+1;
         M:=0;
```

```
            R:=BMIN3:=BMIN2:=1;
            'FOR'M:=M+2'WHILE'T'NE'R'DO'
                'BEGIN'
                R:=T;
                BMIN3:=V*(M-1)*BMIN3+BMIN2;
                T:=BMIN2;
                BMIN2:=V*M*BMIN2+BMIN3;
                T:=R-P/BMIN2/T;
                P:=M*(M+1)*V2*P;
                'END'WHILE;
            ERFL:=T;
            'END';
    'REAL''PROCEDURE'SIMPS(F,X,A,B,DELTA,V);
    'VALUE'A,B,DELTA,V;
    'REAL'F,X,A,B,DELTA,V;
    'BEGIN'
    'INTEGER'N,K;
    'REAL'H,J,I;
    'SWITCH'S:=J1;
    V:=(B-A)*V;
    N:=1;
    H:=(B-A)/2;
    X:=A;
    J:=F;
    X:=B;
    J:=(J+F)*H;
J1: B:=0;
    'FOR'K:=1'STEP'1'UNTIL'N'DO'
    'BEGIN'
    X:=(2*K-1)*H+A;
    B:=B+F;
    'END';
    I:=4*H*B+J;
    'IF'ABS(V)*DELTA<ABS(I-V)'THEN'
    'BEGIN'
    V:=I;
    J:=(I+J)/4;
    N:=2*N;
    H:=H/2;
    'GOTO'J1;
    'END';
    SIMPS:=I/3;
    'END'SIMPS;
    'COMMENT' END OF PROCEDURES;
    THETART:=READ;
    TETAIALGES:=READ;
    TETAICIGES:=READ;
    ALFAALGES:=READ;
    ALFACIGES:=READ;
    DENSITYAL:=READ;
    DENSITYCI:=READ;
    MEANCPAL:=READ;
    MEANCPCI:=READ;
    LENGTH:=READ;
    WIDTH:=READ;
    AREAAL[0]:=0;
    AREACI[0]:=0;
    TOTHTCONT:=0;
    THETASTEP:=5;
    'FOR'T:=1'STEP'1'UNTIL'24'DO'
```

```
'BEGIN'
ALFAALSTEP:=0.010;
'FOR'X:=1'STEP'1'UNTIL'4'DO'
TETAMALOBS[X]:=READ;
WRITETEXT('('OBSERVED%TEMPERATURES%IN%MATERIAL%B')');
NEWLINE(1);
'FOR'X:=1'STEP'1'UNTIL'4'DO'
PRINT(TETAMALOBS[X],3,2);
NEWLINE(1);
N:=1;
LOOP:
'FOR'TETAIAL:=TETAIALGES-THETASTEP'STEP'THETASTEP'UNTIL'TETAIALGES+
THETASTEP'DO'
'BEGIN'
'FOR'ALPHAAL:=ALFAALGES-ALFAALSTEP'STEP'ALFAALSTEP'UNTIL'ALFAALGES+
ALFAALSTEP'DO'
'BEGIN'
SUMOFSQ[N]:=0;
'FOR'X:=1'STEP'1'UNTIL'4'DO'
'BEGIN'
DISTAL:=(((0.25*X)-0.125)*2.54);
TIME:=(T*2.5);
BIGXAL:=(DISTAL/(2*SQRT(ALPHAAL*TIME)));
TETAMALCALC[X]:=(THETART+((TETAIAL-THETART)*(1-('IF'BIGXAL'LE'1.1
'THEN'ERF(BIGXAL)'ELSE'ERFL(BIGXAL)))));
SUMOFSQ[N]:=SUMOFSQ[N]+((TETAMALOBS[X]-TETAMALCALC[X])*(TETAMALOBS
[X]-TETAMALCALC[X]));
'END';
N:=N+1;
'END';
'END';
WRITETEXT('('SUM%OF%SQUARES%FOR%POSITIONS%1%TO%9')');
NEWLINE(1);
'FOR'N:=1'STEP'1'UNTIL'9'DO'
PRINT(SUMOFSQ[N],5,2);
NEWLINE(1);
A1:=((-1*(SUMOFSQ[1]+SUMOFSQ[4]+SUMOFSQ[7]))+(+1*(SUMOFSQ[3]+SUMOFSQ
[6]+SUMOFSQ[9])))/6;
A2:=((-1*(SUMOFSQ[1]+SUMOFSQ[2]+SUMOFSQ[3]))+(+1*(SUMOFSQ[7]+SUMOFSQ
[8]+SUMOFSQ[9])))/6;
A3:=((-2*(SUMOFSQ[2]+SUMOFSQ[5]+SUMOFSQ[8]))+(+1*(SUMOFSQ[1]+SUMOFSQ
[4]+SUMOFSQ[7]+SUMOFSQ[3]+SUMOFSQ[6]+SUMOFSQ[9])))/6;
A4:=((-2*(SUMOFSQ[4]+SUMOFSQ[5]+SUMOFSQ[6]))+(+1*(SUMOFSQ[1]+SUMOFSQ
[2]+SUMOFSQ[3]+SUMOFSQ[7]+SUMOFSQ[8]+SUMOFSQ[9])))/6;
A5:=((-1*(SUMOFSQ[3]+SUMOFSQ[7]))+(+1*(SUMOFSQ[1]+SUMOFSQ[9])))/4;
ALPHA2:=(((A2*A5)-(2*(A1*A4)))/((4*(A3*A4))-(A5↑2)));
WRITETEXT('('ALPHA2')');
NEWLINE(1);
OUTPUT(ALPHA2);
NEWLINE(1);
THETA2:=(((-A5*ALPHA2)-A2)/(2*A4));
WRITETEXT('('THETA2')');
NEWLINE(1);
OUTPUT(THETA2);
NEWLINE(1);
TETAIALGES:=TETAIALGES+(THETA2*THETASTEP);
ALFAALGES:=ALFAALGES+(ALPHA2*ALFAALSTEP);
WRITETEXT('('THERMAL%DIFFUSIVITY%AT%THIS%STAGE')');
NEWLINE(1);
OUTPUT(ALFAALGES);
```

```
NEWLINE(1);
WRITETEXT('('INTERFACIAL%TEMP%AT%THIS%STAGE')');
NEWLINE(1);
OUTPUT(TETAIALGES);
NEWLINE(1);
'IF'ABS(THETA2*THETASTEP)'GT'0.40'OR'ABS(ALPHA2*ALFAALSTEP)'GT'0.000
1'THEN'
'BEGIN'
'IF'ALFAALGES'LT'ALFAALSTEP+0.0001'THEN'
'BEGIN'
ALFAALSTEP:=0.5*ALFAALSTEP;
ALFAALGES:=ALFAALSTEP+0.0001;
'IF'ALFAALGES'LT'0.0001'THEN'
'BEGIN'
WRITETEXT('('OH%BOY%ARE%YOU%IN%TROUBLE')');
NEWLINE(1);
'GOTO'ABER;
'END';
'END';
N:=1;
'GOTO'LOOP;
'END'
'ELSE'
'BEGIN'
WRITETEXT('('FINAL%INTERFACIAL%TEMPERATURE%BETWEEN%MATERIAL%A'AND%
MATERIAL%B')');
NEWLINE(1);
PRINT(TETAIALGES,4,2);
NEWLINE(1);
WRITETEXT('('FINAL%THERMAL%DIFFUSIVITY%OF%MATERIAL%B')');
NEWLINE(1);
PRINT(ALFAALGES,2,5);
NEWLINE(1);
WRITETEXT('('FINAL%CALCULATED%TEMPERATURES%IN%MATERIAL%B')');
NEWLINE(1);
'FOR'X:=1'STEP'1'UNTIL'4'DO'
'BEGIN'
DISTAL:=(((0.25*X)-0.125)*2.54);
TIME:=(T*2.5);
BIGXAL:=(DISTAL/(2*SQRT(ALFAALGES*TIME)));
TETAMALCALC[X]:=THETART+((TETAIALGES-THETART)*(1-('IF'BIGXAL'LE'
1.1'THEN'ERF(BIGXAL)'ELSE'ERFL(BIGXAL))));
PRINT(TETAMALCALC[X],3,2);
NEWLINE(1);
'END';
AREAAL[T]:=SIMPS(THETART+((TETAIALGES-THETART)*(1-('IF'(DISTAL/(2*
SQRT(ALFAALGES*TIME)))'LE'1.1'THEN'ERF(DISTAL/(2*SQRT(ALFAALGES*TIME
SQRT(ALFAALGES*TIME))))))),DISTAL,0.00,4.445,
)))'ELSE'ERFL(DISTAL/(2*SQRT(ALFAALGES*TIME))))))),DISTAL,0.00,4.445,
0.05,10000)-(THETART*4.445);
WRITETEXT('('AREAAL')');
NEWLINE(1);
OUTPUT(AREAAL[T]);
NEWLINE(1);
DALHTCONT[T]:=((AREAAL[T]-AREAAL[T-1])*MEANCPAL*(LENGTH*2.54)*
(WIDTH*2.54)*DENSITYAL);
WRITETEXT('('DALHTCONT')');
NEWLINE(1);
OUTPUT(DALHTCONT[T]);
NEWLINE(1);
NEWLINE(10);
```

```
'END';
TETAMCIOBS[1]:=READ;
TETAMCIOBS[2]:=TETAIALGES;
WRITETEXT('('OBSERVED%TEMPERATURE(S)%IN%MATERIAL%A%AND%INTERFACIAL%
TEMPERATURE%BETWEEN%MATERIALS%A%AND%B')');
NEWLINE(1);
'FOR'Y:=1'STEP'1'UNTIL'2'DO'
PRINT(TETAMCIOBS[Y],3,2);
NEWLINE(1);
ALFACISTEP:=0.010;
M:=1;
ARC:
'FOR'TETAICI:=TETAICIGES-THETASTEP'STEP'THETASTEP'UNTIL'TETAICIGES+
THETASTEP'DO'
'BEGIN'
'FOR'ALPHACI:=ALFACIGES-ALFACISTEP'STEP'ALFACISTEP'UNTIL'ALFACIGES+
ALFACISTEP'DO'
'BEGIN'
SUMOVSQ[M]:=0;
'FOR'Y:=1'STEP'1'UNTIL'2'DO'
'BEGIN'
DISTCI:=((0.125*Y)*2.54);
BIGXCI:=(DISTCI/(2*SQRT(ALPHACI*TIME)));
TETAMCICALC[Y]:=(THETART+((TETAICI-THETART)*(1-('IF'BIGXCI'LE'1.1
'THEN'ERF(BIGXCI)'ELSE'ERFL(BIGXCI)))));
SUMOVSQ[M]:=SUMOVSQ[M]+((TETAMCIOBS[Y]-TETAMCICALC[Y])*(TETAMCIOBS
[Y]-TETAMCICALC[Y]));
'END';
M:=M+1;
'END';
'END';
WRITETEXT('('SUM%OF%SQUARES%FOR%POSITIONS%1%TO%9')');
NEWLINE(1);
'FOR'M:=1'STEP'1'UNTIL'9'DO'
PRINT(SUMOVSQ[M],5,2);
NEWLINE(1);
B1:=((-1*(SUMOVSQ[1]+SUMOVSQ[4]+SUMOVSQ[7]))+(+1*(SUMOVSQ[3]+SUMOVSQ
[6]+SUMOVSQ[9])))/6;
B2:=((-1*(SUMOVSQ[1]+SUMOVSQ[2]+SUMOVSQ[3]))+(+1*(SUMOVSQ[7]+SUMOVSQ
[8]+SUMOVSQ[9])))/6;
B3:=((-2*(SUMOVSQ[2]+SUMOVSQ[5]+SUMOVSQ[8]))+(+1*(SUMOVSQ[1]+SUMOVSQ
[4]+SUMOVSQ[7]+SUMOVSQ[3]+SUMOVSQ[6]+SUMOVSQ[9])))/6;
B4:=((-2*(SUMOVSQ[4]+SUMOVSQ[5]+SUMOVSQ[6]))+(+1*(SUMOVSQ[1]+SUMOVSQ
[2]+SUMOVSQ[3]+SUMOVSQ[7]+SUMOVSQ[8]+SUMOVSQ[9])))/6;
B5:=((-1*(SUMOVSQ[3]+SUMOVSQ[7]))+(+1*(SUMOVSQ[1]+SUMOVSQ[9])))/4;
ALFA2:=(((B2*B5)-(2*(B1*B4)))/((4*(B3*B4))-(B5↑2)));
WRITETEXT('('ALFA2')');
NEWLINE(1);
OUTPUT(ALFA2);
NEWLINE(1);
TETA2:=(((-B5*ALFA2)-B2)/(2*B4));
WRITETEXT('('TETA2')');
NEWLINE(1);
OUTPUT(TETA2);
NEWLINE(1);
TETAICIGES:=TETAICIGES+(TETA2*THETASTEP);
ALFACIGES:=ALFACIGES+(ALFA2*ALFACISTEP);
WRITETEXT('('THERMAL%DIFFUSIVITY%AT%THIS%STAGE')');
NEWLINE(1);
OUTPUT(ALFACIGES);
```

```
NEWLINE(1);
WRITETEXT('('INTERFACIAL%TEMP%AT%THIS%STAGE')');
NEWLINE(1);
OUTPUT(TETAICIGES);
NEWLINE(1);
'IF'ABS(TETA2*THETASTEP)'GT'0.40'OR'ABS(ALFA2*ALFACISTEP)'GT'0.0001
'THEN'
'BEGIN'
'IF'ALFACIGES'LT'ALFACISTEP+0.0001'THEN'
'BEGIN'
ALFACISTEP:=0.5*ALFACISTEP;
ALFACIGES:=ALFACISTEP+0.0001;
'IF'ALFACIGES'LT'0.0001'THEN'
'BEGIN'
WRITETEXT('('BOY%ARE%YOU%IN%TROUBLE%AGAIN')');
'GOTO'ABER;
'END'
'END';
M:=1;
'GOTO'ARC;
'END'
'ELSE'
'BEGIN'
WRITETEXT('('FINAL%INTERFACIAL%TEMPERATURE%BETWEEN%MATERIAL%A%AND%
CASTING')');
NEWLINE(1);
PRINT(TETAICIGES,4,2);
NEWLINE(1);
WRITETEXT('('FINAL%THERMAL%DIFFUSIVITY%OF%MATERIAL%A')');
NEWLINE(1);
PRINT(ALFACIGES,2,5);
NEWLINE(1);
WRITETEXT('('FINAL%CALCULATED%TEMPERATURES%IN%MATERIAL%A')');
NEWLINE(1);
'FOR'Y:=1'STEP'1'UNTIL'2'DO'
'BEGIN'
DISTCI:=((0.125*Y)*2.54);
BIGXCI:=(DISTCI/(2*SQRT(ALFACIGES*TIME)));
TETAMCICALC[Y]:=THETART+((TETAICIGES-THETART)*(1-('IF'BIGXCI'LE'
1.1'THEN'ERF(BIGXCI)'ELSE'ERFL(BIGXCI))));
PRINT(TETAMCICALC[Y],3,2);
NEWLINE(1);
'END';
AREACI[T]:=SIMPS(THETART+((TETAICIGES-THETART)*(1-('IF'(DISTCI/(2*
SQRT(ALFACIGES*TIME)))'LE'1.1'THEN'ERF(DISTCI/(2*SQRT(ALFACIGES*TIME
)))'ELSE'ERFL(DISTCI/(2*SQRT(ALFACIGES*TIME))))))),DISTCI,0.00,0.635,
0.05,10000)-(THETART*0.635);
WRITETEXT('('AREACI')');
NEWLINE(1);
OUTPUT(AREACI[T]);
NEWLINE(1);
DCIHTCONT[T]:=((AREACI[T]-AREACI[T-1])*MEANCPCI*(LENGTH*2.54)*
(WIDTH*2.54)*DENSITYCI);
WRITETEXT('('DCIHTCONT')');
NEWLINE(1);
OUTPUT(DCIHTCONT[T]);
NEWLINE(1);
TOTHTCONT:=TOTHTCONT+DALHTCONT[T]+DCIHTCONT[T];
WRITETEXT('('TOTHTCONT')');
NEWLINE(1);
```

```
OUTPUT(TOTHTCONT);
NEWLINE(1);
NEWLINE(10);
'END';
ABER:
'END';
'END';
```

APPENDIX IX LISTING OF PRACTICAL RESULTS

Headings for Casting Series Results

The results of the casting series are reproduced from the cards employed in the multiple linear regression analysis program. The columns containing the integers (1 or 2) represent situations where the chill materials or shapes may or may not be included, 1 is equivalent to No, 2 equivalent to Yes.

Column Headings for Series I are from left to right

(a) Specimen Identification - see experimental details for nomenclature.

(b) Section thickness of original plate (ins.).

(c) % Iron content.

(d) % Magnesium content.

(e) % Silicon content.

(f) Cast Iron chill material present.

(g) Aluminium chill material present.

(h) Block chill shape present.

(i) Single Taper chill shape present.

(j) Double Taper chill shape present.

(k) Distance (ins.).

(l) % Elongation.

(m) Proof Stress (tons/in^2).

(n) Tensile Strength (tons/in^2).

Column Headings for Series II are as below, again from left to right

(a) Specimen Identification - see experimental details for nomenclature.

(b) Section thickness of original plate (ins.).

(c) % Iron content.

(d) % Magnesium content.

(e) % Silicon content.

(f) Cast Iron chill material present.

(g) Aluminium chill material present.

(h) Double Thickness Single Taper chill shape present.

(i) Tapered Plate chill shape present.

(j) Distance (ins.).

(k) % Elongation.

(l) Proof Stress (tons/in^2).

(m) Tensile Strength (tons/in^2).

Column Headings for Series III are as below, again from left to right

(a) Specimen Identification - see experimental details for nomenclature.

(b) Section thickness of original plate (ins.).

(c) Distance (ins.).

(d) Block chill shape present.

(e) Single Taper chill shape present.

(f) Aluminium chill material present.

(g) Cast Iron chill material present.

(h) % Elongation.

(i) Proof Stress (tons/in^2).

(j) Tensile Strength (tons/in^2).

(k) % Porosity.

SERIES I RESULTS

X41001	0.500	0.010	0.290	6.560	1	1	1	1	1	0.750	4.100	13.200	16.000
X41002	0.500	0.010	0.290	6.560	1	1	1	1	1	1.750	2.500	13.120	15.440
X41003	0.500	0.010	0.290	6.560	1	1	1	1	1	2.750	1.600	13.320	14.800
X41004	0.500	0.010	0.290	6.560	1	1	1	1	1	3.750	2.700	12.800	14.440
X41005	0.500	0.010	0.290	6.560	1	1	1	1	1	4.750	1.900	12.880	14.600
X41006	0.500	0.010	0.290	6.560	1	1	1	1	1	5.750	1.600	12.680	14.440
X41007	0.500	0.010	0.290	6.560	1	1	1	1	1	6.750	3.300	12.800	15.120
X42001	0.500	0.010	0.290	6.560	2	1	2	1	1	0.750	6.600	13.200	16.740
X42002	0.500	0.010	0.290	6.560	2	1	2	1	1	1.750	4.700	13.340	16.520
X42003	0.500	0.010	0.290	6.560	2	1	2	1	1	2.750	9.500	12.720	16.700
X42004	0.500	0.010	0.290	6.560	2	1	2	1	1	3.750	5.400	12.800	15.940
X42005	0.500	0.010	0.290	6.560	2	1	2	1	1	4.750	3.500	12.980	15.820
X42006	0.500	0.010	0.290	6.560	2	1	2	1	1	5.750	2.300	13.140	15.140
X42007	0.500	0.010	0.290	6.560	2	1	2	1	1	6.750	3.800	12.400	14.980
X43001	0.500	0.020	0.290	7.350	2	1	1	2	1	0.750	9.760	13.600	18.240
X43002	0.500	0.020	0.290	7.350	2	1	1	2	1	1.750	6.300	13.400	17.580
X43003	0.500	0.020	0.290	7.350	2	1	1	2	1	2.750	6.300	13.240	17.220
X43004	0.500	0.020	0.290	7.350	2	1	1	2	1	3.750	5.980	13.200	17.060
X43005	0.500	0.020	0.290	7.350	2	1	1	2	1	4.750	4.410	13.420	16.760
X43006	0.500	0.020	0.290	7.350	2	1	1	2	1	5.750	5.040	13.360	16.860
X43007	0.500	0.020	0.290	7.350	2	1	1	2	1	6.750	5.980	13.080	17.020
X44001	0.500	0.020	0.290	7.350	2	1	1	1	2	0.750	9.450	13.300	17.700
X44002	0.500	0.020	0.290	7.350	2	1	1	1	2	1.750	6.460	13.240	17.020
X44003	0.500	0.020	0.290	7.350	2	1	1	1	2	2.750	4.730	13.180	16.720
X44004	0.500	0.020	0.290	7.350	2	1	1	1	2	3.750	6.300	12.580	16.460
X44005	0.500	0.020	0.290	7.350	2	1	1	1	2	4.750	5.190	13.020	16.620
X44006	0.500	0.020	0.290	7.350	2	1	1	1	2	5.750	5.520	12.720	16.240
X44007	0.500	0.020	0.290	7.350	2	1	1	1	2	6.750	7.410	12.280	16.200
X46001	0.500	0.010	0.290	6.820	1	2	2	1	1	0.750	10.700	14.620	19.600
X46002	0.500	0.010	0.290	6.820	1	2	2	1	1	1.750	10.700	14.300	19.360
X46003	0.500	0.010	0.290	6.820	1	2	2	1	1	2.750	10.300	14.060	18.940
X46004	0.500	0.010	0.290	6.820	1	2	2	1	1	3.750	6.900	14.020	18.320
X46005	0.500	0.010	0.290	6.820	1	2	2	1	1	4.750	3.500	13.820	17.100
X46006	0.500	0.010	0.290	6.820	1	2	2	1	1	5.750	3.800	13.720	17.560
X46007	0.500	0.010	0.290	6.820	1	2	2	1	1	6.750	5.700	13.720	17.560

X47001	0.500	0.010	0.290	6.020	1	2	1	2	1	0.750	7.400	14.080	18.680
X47002	0.500	0.010	0.290	6.020	1	2	1	2	1	1.750	5.800	13.540	17.900
X47003	0.500	0.010	0.290	6.020	1	2	1	2	1	2.750	6.000	13.640	17.700
X47004	0.500	0.010	0.290	6.020	1	2	1	2	1	3.750	4.700	13.760	17.680
X47005	0.500	0.010	0.290	6.020	1	2	1	2	1	4.750	5.800	13.600	17.700
X47006	0.500	0.010	0.290	6.020	1	2	1	2	1	5.750	5.500	13.760	17.680
X47007	0.500	0.010	0.290	6.020	1	2	1	2	1	6.750	6.000	13.160	17.480
X48001	0.500	0.010	0.290	6.020	1	2	1	1	2	0.750	9.000	14.000	18.920
X48002	0.500	0.010	0.290	6.020	1	2	1	1	2	1.750	5.400	13.800	17.880
X48003	0.500	0.010	0.290	6.020	1	2	1	1	2	2.750	4.700	13.920	17.760
X48004	0.500	0.010	0.290	6.020	1	2	1	1	2	3.750	3.800	13.700	17.240
X48005	0.500	0.010	0.290	6.020	1	2	1	1	2	4.750	3.600	13.400	17.440
X48006	0.500	0.010	0.290	6.020	1	2	1	1	2	5.750	4.700	13.600	17.560
X48007	0.500	0.010	0.290	6.020	1	2	1	1	2	6.750	5.500	13.360	17.400
Y41001	0.500	0.080	0.550	7.150	1	1	1	1	1	0.750	2.520	15.280	18.400
Y41002	0.500	0.080	0.550	7.150	1	1	1	1	1	1.750	1.890	15.460	17.280
Y41003	0.500	0.080	0.550	7.150	1	1	1	1	1	2.750	1.730	15.160	17.080
Y41004	0.500	0.080	0.550	7.150	1	1	1	1	1	3.750	1.260	14.920	16.580
Y41005	0.500	0.080	0.550	7.150	1	1	1	1	1	4.750	1.100	15.100	16.500
Y41006	0.500	0.080	0.550	7.150	1	1	1	1	1	5.750	1.420	14.800	16.760
Y41007	0.500	0.080	0.550	7.150	1	1	1	1	1	6.750	2.050	14.200	16.380
Y42001	0.500	0.080	0.300	7.500	2	1	2	1	1	0.750	5.670	14.260	18.760
Y42002	0.500	0.080	0.300	7.500	2	1	2	1	1	1.750	3.930	14.540	18.020
Y42003	0.500	0.080	0.300	7.500	2	1	2	1	1	2.750	3.620	14.040	17.440
Y42004	0.500	0.080	0.300	7.500	2	1	2	1	1	3.750	1.890	14.380	16.960
Y42005	0.500	0.080	0.300	7.500	2	1	2	1	1	4.750	1.580	14.500	16.520
Y42006	0.500	0.080	0.300	7.500	2	1	2	1	1	5.750	1.260	14.400	16.040
Y42007	0.500	0.080	0.300	7.500	2	1	2	1	1	6.750	1.580	13.700	15.780
Y43001	0.500	0.080	0.550	7.150	2	1	1	2	1	0.750	8.040	14.840	19.220
Y43002	0.500	0.080	0.550	7.150	2	1	1	2	1	1.750	4.090	15.040	18.440
Y43003	0.500	0.080	0.550	7.150	2	1	1	2	1	2.750	2.990	14.600	17.740
Y43004	0.500	0.080	0.350	7.150	2	1	1	2	1	3.750	2.680	14.600	17.400
Y43005	0.500	0.080	0.550	7.150	2	1	1	2	1	4.750	2.520	14.580	17.200
Y43006	0.500	0.080	0.550	7.150	2	1	1	2	1	5.750	2.520	14.520	17.220
Y43007	0.500	0.080	0.550	7.150	2	1	1	2	1	6.750	2.680	14.120	16.980

Y44001	0.500	0.080	0.550	7.150	2	1	1	1	2	0.750	7.000	14.960	18.600
Y44002	0.500	0.080	0.550	7.150	2	1	1	1	2	1.750	4.250	14.740	18.380
Y44003	0.500	0.080	0.550	7.150	2	1	1	1	2	2.750	3.470	14.540	17.700
Y44004	0.500	0.080	0.550	7.150	2	1	1	1	2	3.750	2.680	14.720	17.600
Y44005	0.500	0.080	0.550	7.150	2	1	1	1	2	4.750	2.360	14.660	17.360
Y44006	0.500	0.080	0.550	7.150	2	1	1	1	2	5.750	1.260	14.460	16.740
Y44007	0.500	0.080	0.550	7.150	2	1	1	1	2	6.750	2.990	13.880	16.720
Y46001	0.500	0.080	0.240	7.260	1	2	2	1	1	0.750	7.900	13.340	18.100
Y46002	0.500	0.080	0.240	7.260	1	2	2	1	1	1.750	8.000	13.520	18.260
Y46003	0.500	0.080	0.240	7.260	1	2	2	1	1	2.750	5.700	13.160	17.340
Y46004	0.500	0.080	0.240	7.260	1	2	2	1	1	3.750	3.800	13.360	16.900
Y46005	0.500	0.080	0.240	7.260	1	2	2	1	1	4.750	1.900	13.200	15.840
Y46006	0.500	0.080	0.240	7.260	1	2	2	1	1	5.750	2.400	13.260	15.740
Y46007	0.500	0.080	0.240	7.260	1	2	2	1	1	6.750	2.400	12.760	15.380
Y47001	0.500	0.080	0.240	7.260	1	2	1	2	1	0.750	7.400	13.680	18.700
Y47002	0.500	0.080	0.240	7.260	1	2	1	2	1	1.750	5.200	13.460	17.980
Y47003	0.500	0.080	0.240	7.260	1	2	1	2	1	2.750	4.100	13.260	17.160
Y47004	0.500	0.080	0.240	7.260	1	2	1	2	1	3.750	2.800	13.520	16.700
Y47005	0.500	0.080	0.240	7.260	1	2	1	2	1	4.750	1.700	12.960	15.440
Y47006	0.500	0.080	0.240	7.260	1	2	1	2	1	5.750	3.200	13.160	16.580
Y47007	0.500	0.080	0.240	7.260	1	2	1	2	1	6.750	4.200	12.760	16.520
Y48001	0.500	0.080	0.240	7.260	1	2	1	1	2	0.750	7.400	13.720	19.060
Y48002	0.500	0.080	0.240	7.260	1	2	1	1	2	1.750	4.700	13.720	18.140
Y48003	0.500	0.080	0.240	7.260	1	2	1	1	2	2.750	4.100	13.160	17.100
Y48004	0.500	0.080	0.240	7.260	1	2	1	1	2	3.750	3.800	13.240	16.880
Y48005	0.500	0.080	0.240	7.260	1	2	1	1	2	4.750	1.900	13.280	16.000
Y48006	0.500	0.080	0.240	7.260	1	2	1	1	2	5.750	2.500	12.920	16.080
Y48007	0.500	0.080	0.240	7.260	1	2	1	1	2	6.750	2.800	12.540	15.960
Z41001	0.500	0.130	0.540	7.250	1	1	1	1	1	0.750	1.890	14.560	17.300
Z41002	0.500	0.130	0.540	7.250	1	1	1	1	1	1.750	1.580	14.720	16.800
Z41003	0.500	0.130	0.540	7.250	1	1	1	1	1	2.750	1.580	14.600	16.680
Z41004	0.500	0.130	0.540	7.250	1	1	1	1	1	3.750	1.260	14.480	16.620
Z41005	0.500	0.130	0.540	7.250	1	1	1	1	1	4.750	1.100	14.400	16.420
Z41006	0.500	0.130	0.540	7.250	1	1	1	1	1	5.750	1.260	13.940	15.900
Z41007	0.500	0.130	0.540	7.250	1	1	1	1	1	6.750	1.580	13.440	15.520

Z42001	0.500	0.130	0.550	6.530	2	1	2	1	1	0.750	5.830	14.400	18.120
Z42002	0.500	0.130	0.550	6.530	2	1	2	1	1	1.750	4.410	14.300	17.400
Z42003	0.500	0.130	0.550	6.530	2	1	2	1	1	2.750	6.300	13.800	17.420
Z42004	0.500	0.130	0.550	6.530	2	1	2	1	1	3.750	2.990	13.960	16.780
Z42005	0.500	0.130	0.550	6.530	2	1	2	1	1	4.750	1.730	14.200	16.300
Z42006	0.500	0.130	0.550	6.530	2	1	2	1	1	5.750	2.050	13.880	15.920
Z42007	0.500	0.130	0.550	6.530	2	1	2	1	1	6.750	2.520	13.300	15.600
Z43001	0.500	0.130	0.550	6.530	2	1	1	2	1	0.750	5.520	14.660	18.520
Z43002	0.500	0.130	0.550	6.530	2	1	1	2	1	1.750	4.730	14.200	17.680
Z43003	0.500	0.130	0.550	6.530	2	1	1	2	1	2.750	2.520	13.760	16.840
Z43004	0.500	0.130	0.550	6.530	2	1	1	2	1	3.750	2.210	14.160	16.460
Z43005	0.500	0.130	0.550	6.530	2	1	1	2	1	4.750	2.830	14.040	16.720
Z43006	0.500	0.130	0.550	6.530	2	1	1	2	1	5.750	2.520	14.120	16.580
Z43007	0.500	0.130	0.550	6.530	2	1	1	2	1	6.750	2.680	13.800	16.420
Z44001	0.500	0.130	0.550	6.530	2	1	1	1	2	0.750	5.670	14.360	18.100
Z44002	0.500	0.130	0.550	6.530	2	1	1	1	2	1.750	4.090	14.060	17.520
Z44003	0.500	0.130	0.550	6.530	2	1	1	1	2	2.750	2.520	14.040	16.700
Z44004	0.500	0.130	0.550	6.530	2	1	1	1	2	3.750	2.830	14.100	16.800
Z44005	0.500	0.130	0.550	6.530	2	1	1	1	2	4.750	2.520	14.120	16.320
Z44006	0.500	0.130	0.550	6.530	2	1	1	1	2	5.750	1.890	14.180	16.160
Z44007	0.500	0.130	0.550	6.530	2	1	1	1	2	6.750	2.050	13.920	15.940
Z46001	0.500	0.120	0.290	6.720	1	2	2	1	1	0.750	9.900	13.160	18.120
Z46002	0.500	0.120	0.290	6.720	1	2	2	1	1	1.750	8.200	13.110	17.700
Z46003	0.500	0.120	0.290	6.720	1	2	2	1	1	2.750	11.400	13.060	17.700
Z46004	0.500	0.120	0.290	6.720	1	2	2	1	1	3.750	7.600	13.380	17.660
Z46005	0.500	0.120	0.290	6.720	1	2	2	1	1	4.750	3.900	13.400	16.760
Z46006	0.500	0.120	0.290	6.720	1	2	2	1	1	5.750	3.000	13.520	16.500
Z46007	0.500	0.120	0.290	6.720	1	2	2	1	1	6.750	3.500	13.120	16.460
Z47001	0.500	0.120	0.290	6.720	1	2	1	2	1	0.750	8.200	13.200	17.920
Z47002	0.500	0.120	0.290	6.720	1	2	1	2	1	1.750	5.500	13.120	17.120
Z47003	0.500	0.120	0.290	6.720	1	2	1	2	1	2.750	4.600	12.920	16.600
Z47004	0.500	0.120	0.290	6.720	1	2	1	2	1	3.750	4.100	12.820	16.520
Z47005	0.500	0.120	0.290	6.720	1	2	1	2	1	4.750	3.600	12.580	16.220
Z47006	0.500	0.120	0.290	6.720	1	2	1	2	1	5.750	3.300	12.860	16.080
Z47007	0.500	0.120	0.290	6.720	1	2	1	2	1	6.750	4.100	12.540	16.280

Z40001	0.500	0.120	0.290	6.720	1	2	1	1	2	0.750	7.900	13.040	17.720
Z40002	0.500	0.120	0.290	6.720	1	2	1	1	2	1.750	6.100	13.000	17.160
Z40003	0.500	0.120	0.290	6.720	1	2	1	1	2	2.750	4.600	13.100	16.580
Z40004	0.500	0.120	0.290	6.720	1	2	1	1	2	3.750	3.500	13.220	16.520
Z40005	0.500	0.120	0.290	6.720	1	2	1	1	2	4.750	3.000	13.140	16.250
Z40006	0.500	0.120	0.290	6.720	1	2	1	1	2	5.750	3.500	13.140	16.240
Z40007	0.500	0.120	0.290	6.720	1	2	1	1	2	6.750	3.800	12.940	16.380
X31001	0.375	0.010	0.290	6.360	1	1	1	1	1	0.750	5.000	13.640	17.020
X31002	0.375	0.010	0.290	6.360	1	1	1	1	1	1.750	3.500	13.720	16.360
X31003	0.375	0.010	0.290	6.360	1	1	1	1	1	2.750	2.800	13.900	16.260
X31004	0.375	0.010	0.290	6.360	1	1	1	1	1	3.750	2.400	13.420	15.780
X31005	0.375	0.010	0.290	6.360	1	1	1	1	1	4.750	2.100	13.760	15.800
X31006	0.375	0.010	0.290	6.360	1	1	1	1	1	5.750	2.200	13.520	15.520
X31007	0.375	0.010	0.290	6.360	1	1	1	1	1	6.750	3.800	12.860	15.840
X32001	0.375	0.010	0.280	7.360	2	1	2	1	1	0.750	12.900	13.800	18.400
X32002	0.375	0.010	0.280	7.360	2	1	2	1	1	1.750	6.300	13.600	17.880
X32003	0.375	0.010	0.280	7.360	2	1	2	1	1	2.750	8.800	13.400	17.800
X32004	0.375	0.010	0.280	7.360	2	1	2	1	1	3.750	3.800	13.900	17.000
X32005	0.375	0.010	0.280	7.360	2	1	2	1	1	4.750	2.200	13.800	16.480
X32006	0.375	0.010	0.280	7.360	2	1	2	1	1	5.750	3.800	13.300	16.200
X32007	0.375	0.010	0.280	7.360	2	1	2	1	1	6.750	4.100	13.200	16.400
X33001	0.375	0.010	0.280	7.360	2	1	1	2	1	0.750	10.700	14.200	18.520
X33002	0.375	0.010	0.280	7.360	2	1	1	2	1	1.750	5.000	13.800	17.320
X33003	0.375	0.010	0.280	7.360	2	1	1	2	1	2.750	5.700	13.920	17.340
X33004	0.375	0.010	0.280	7.360	2	1	1	2	1	3.750	4.100	13.800	17.000
X33005	0.375	0.010	0.280	7.360	2	1	1	2	1	4.750	4.400	13.700	17.000
X33006	0.375	0.010	0.280	7.360	2	1	1	2	1	5.750	3.800	13.400	17.100
X33007	0.375	0.010	0.280	7.360	2	1	1	2	1	6.750	5.400	13.600	17.200
X34001	0.375	0.010	0.280	7.360	2	1	1	1	2	0.750	11.000	14.180	18.700
X34002	0.375	0.010	0.280	7.360	2	1	1	1	2	1.750	4.700	13.600	17.260
X34003	0.375	0.010	0.280	7.360	2	1	1	1	2	2.750	5.000	13.480	17.100
X34004	0.375	0.010	0.280	7.360	2	1	1	1	2	3.750	5.000	13.200	16.920
X34005	0.375	0.010	0.280	7.360	2	1	1	1	2	4.750	3.900	13.420	16.900
X34006	0.375	0.010	0.280	7.360	2	1	1	1	2	5.750	3.200	13.720	16.700
X34007	0.375	0.010	0.280	7.360	2	1	1	1	2	6.750	7.200	12.880	16.720

X36001	0.375	0.020	0.270	7.060	1	2	2	1	1	0.750	12.900	12.760	17.220
X36002	0.375	0.020	0.270	7.060	1	2	2	1	1	1.750	10.200	12.240	16.700
X36003	0.375	0.020	0.270	7.060	1	2	2	1	1	2.750	10.400	12.140	16.700
X36004	0.375	0.020	0.270	7.060	1	2	2	1	1	3.750	10.600	12.140	16.400
X36005	0.375	0.020	0.270	7.060	1	2	2	1	1	4.750	7.900	12.600	16.700
X36006	0.375	0.020	0.270	7.060	1	2	2	1	1	5.750	6.500	12.150	16.350
X36007	0.375	0.020	0.270	7.060	1	2	2	1	1	6.750	7.900	11.630	15.500
X37001	0.375	0.020	0.270	7.060	1	2	1	2	1	0.750	10.100	12.900	17.500
X37002	0.375	0.020	0.270	7.060	1	2	1	2	1	1.750	10.100	12.680	17.300
X37003	0.375	0.020	0.270	7.060	1	2	1	2	1	2.750	8.800	12.960	16.940
X37004	0.375	0.020	0.270	7.060	1	2	1	2	1	3.750	10.300	12.150	16.880
X37005	0.375	0.020	0.270	7.060	1	2	1	2	1	4.750	6.800	12.650	16.850
X37006	0.375	0.020	0.270	7.060	1	2	1	2	1	5.750	6.500	12.480	16.450
X37007	0.375	0.020	0.270	7.060	1	2	1	2	1	6.750	8.900	11.880	16.350
X50001	0.375	0.020	0.270	7.060	1	2	1	2	1	0.750	9.500	12.700	16.980
X50002	0.375	0.020	0.270	7.060	1	2	1	2	1	1.750	8.500	12.120	16.900
X50003	0.375	0.020	0.270	7.060	1	2	1	2	1	2.750	9.500	11.600	16.800
X50004	0.375	0.020	0.270	7.060	1	2	1	2	1	3.750	8.000	11.680	16.600
X50005	0.375	0.020	0.270	7.060	1	2	1	2	1	4.750	8.500	12.040	16.300
X50006	0.375	0.020	0.270	7.060	1	2	1	2	1	5.750	7.600	12.160	16.300
X50007	0.375	0.020	0.270	7.060	1	2	1	2	1	6.750	8.200	11.500	15.830
Y51001	0.375	0.080	0.280	6.990	1	1	1	1	1	0.750	2.500	13.400	16.020
Y51002	0.375	0.080	0.280	6.990	1	1	1	1	1	1.750	2.100	13.220	15.440
Y51003	0.375	0.080	0.280	6.990	1	1	1	1	1	2.750	1.700	13.160	15.000
Y51004	0.375	0.080	0.280	6.990	1	1	1	1	1	3.750	1.900	13.400	15.500
Y51005	0.375	0.080	0.280	6.990	1	1	1	1	1	4.750	1.100	13.320	15.200
Y51006	0.375	0.080	0.280	6.990	1	1	1	1	1	5.750	2.200	12.900	14.700
Y51007	0.375	0.080	0.280	6.990	1	1	1	1	1	6.750	1.900	12.540	14.560
Y52001	0.375	0.080	0.280	6.990	2	1	2	1	1	0.750	5.000	13.800	17.140
Y52002	0.375	0.080	0.280	6.990	2	1	2	1	1	1.750	1.600	13.540	15.580
Y52003	0.375	0.080	0.280	6.990	2	1	2	1	1	2.750	2.800	13.520	16.280
Y52004	0.375	0.080	0.280	6.990	2	1	2	1	1	3.750	2.800	13.560	15.740
Y52005	0.375	0.080	0.280	6.990	2	1	2	1	1	4.750	1.300	13.360	15.100
Y52006	0.375	0.080	0.280	6.990	2	1	2	1	1	5.750	1.300	13.700	15.340
Y52007	0.375	0.080	0.280	6.990	2	1	2	1	1	6.750	4.100	13.200	14.840

Y55001	0.575	0.080	0.500	7.500	2	1	1	2	1	0.750	6.620	14.400	18.400
Y55002	0.575	0.080	0.500	7.500	2	1	1	2	1	1.750	2.520	14.340	17.060
Y55003	0.575	0.080	0.500	7.500	2	1	1	2	1	2.750	2.210	13.940	16.700
Y55004	0.575	0.080	0.500	7.500	2	1	1	2	1	3.750	2.520	14.020	16.700
Y55005	0.575	0.080	0.500	7.500	2	1	1	2	1	4.750	2.210	13.920	16.620
Y55006	0.575	0.080	0.500	7.500	2	1	1	2	1	5.750	1.730	13.920	16.240
Y55007	0.575	0.080	0.500	7.500	2	1	1	2	1	6.750	2.520	13.360	15.980
Y54001	0.575	0.080	0.500	7.500	2	1	1	1	2	0.750	5.200	14.340	18.240
Y54002	0.575	0.080	0.500	7.500	2	1	1	1	2	1.750	2.800	13.960	17.020
Y54003	0.575	0.080	0.500	7.500	2	1	1	1	2	2.750	2.400	13.700	16.700
Y54004	0.575	0.080	0.500	7.500	2	1	1	1	2	3.750	2.500	13.860	16.600
Y54005	0.575	0.080	0.500	7.500	2	1	1	1	2	4.750	2.500	13.940	16.580
Y54006	0.575	0.080	0.500	7.500	2	1	1	1	2	5.750	1.700	14.050	16.380
Y54007	0.575	0.080	0.500	7.500	2	1	1	1	2	6.750	2.500	13.860	16.600
Y56001	0.575	0.070	0.280	7.110	1	2	2	1	1	0.750	9.150	14.280	19.280
Y56002	0.575	0.070	0.280	7.110	1	2	2	1	1	1.750	6.770	14.500	19.200
Y56003	0.575	0.070	0.280	7.110	1	2	2	1	1	2.750	9.150	14.040	18.980
Y56004	0.575	0.070	0.280	7.110	1	2	2	1	1	3.750	5.980	14.100	18.480
Y56005	0.575	0.070	0.280	7.110	1	2	2	1	1	4.750	3.150	14.460	17.920
Y56006	0.575	0.070	0.280	7.110	1	2	2	1	1	5.750	2.990	13.840	17.320
Y56007	0.575	0.070	0.280	7.110	1	2	2	1	1	6.750	3.150	12.880	16.580
Y57001	0.575	0.070	0.280	7.110	1	2	1	2	1	0.750	9.300	14.200	18.140
Y57002	0.575	0.070	0.280	7.110	1	2	1	2	1	1.750	5.670	13.600	17.960
Y57003	0.575	0.070	0.280	7.110	1	2	1	2	1	2.750	4.260	13.940	17.700
Y57004	0.575	0.070	0.280	7.110	1	2	1	2	1	3.750	4.880	13.900	17.600
Y57005	0.575	0.070	0.280	7.110	1	2	1	2	1	4.750	3.310	14.400	17.720
Y57006	0.575	0.070	0.280	7.110	1	2	1	2	1	5.750	3.630	14.200	17.400
Y57007	0.575	0.070	0.280	7.110	1	2	1	2	1	6.750	4.880	12.940	17.060
Y56001	0.575	0.070	0.280	7.110	1	2	1	1	2	0.750	4.420	14.040	18.280
Y56002	0.575	0.070	0.280	7.110	1	2	1	1	2	1.750	4.260	13.660	17.520
Y56003	0.575	0.070	0.280	7.110	1	2	1	1	2	2.750	3.470	14.640	18.000
Y56004	0.575	0.070	0.280	7.110	1	2	1	1	2	3.750	3.630	13.920	17.320
Y56005	0.575	0.070	0.280	7.110	1	2	1	1	2	4.750	4.090	13.160	16.820
Y56006	0.575	0.070	0.280	7.110	1	2	1	1	2	5.750	3.940	14.100	17.360
Y56007	0.575	0.070	0.280	7.110	1	2	1	1	2	6.750	3.780	13.240	16.820

Z51001	0.375	0.120	0.230	6.060	1	1	1	1	1	0.750	4.400	12.700	16.120
Z51002	0.375	0.120	0.230	6.060	1	1	1	1	1	1.750	3.500	12.940	15.900
Z51003	0.375	0.120	0.230	6.060	1	1	1	1	1	2.750	2.700	12.880	15.700
Z51004	0.375	0.120	0.230	6.060	1	1	1	1	1	3.750	2.500	12.780	15.380
Z51005	0.375	0.120	0.230	6.060	1	1	1	1	1	4.750	2.500	12.760	15.420
Z51006	0.375	0.120	0.230	6.060	1	1	1	1	1	5.750	2.300	12.500	14.820
Z51007	0.375	0.120	0.230	6.060	1	1	1	1	1	6.750	3.000	12.060	14.720
Z52001	0.375	0.120	0.230	6.060	2	1	2	1	1	0.750	8.400	13.080	17.360
Z52002	0.375	0.120	0.230	6.060	2	1	2	1	1	1.750	5.700	13.000	16.740
Z52003	0.375	0.120	0.230	6.060	2	1	2	1	1	2.750	5.400	12.660	16.340
Z52004	0.375	0.120	0.230	6.060	2	1	2	1	1	3.750	3.500	13.000	16.020
Z52005	0.375	0.120	0.230	6.060	2	1	2	1	1	4.750	2.500	13.040	15.680
Z52006	0.375	0.120	0.230	6.060	2	1	2	1	1	5.750	2.200	12.840	15.340
Z52007	0.375	0.120	0.230	6.060	2	1	2	1	1	6.750	3.000	12.000	14.800
Z53001	0.375	0.130	0.340	7.250	2	1	1	2	1	0.750	6.140	14.480	18.460
Z53002	0.375	0.130	0.340	7.250	2	1	1	2	1	1.750	3.600	14.140	17.560
Z53003	0.375	0.130	0.340	7.250	2	1	1	2	1	2.750	2.800	13.980	16.900
Z53004	0.375	0.130	0.340	7.250	2	1	1	2	1	3.750	2.200	13.940	16.740
Z53005	0.375	0.130	0.340	7.250	2	1	1	2	1	4.750	2.400	14.100	16.800
Z53006	0.375	0.130	0.340	7.250	2	1	1	2	1	5.750	2.500	14.020	16.800
Z53007	0.375	0.130	0.340	7.250	2	1	1	2	1	6.750	2.680	13.660	16.440
Z54001	0.375	0.130	0.340	7.250	2	1	1	1	2	0.750	6.700	14.530	18.800
Z54002	0.375	0.130	0.340	7.250	2	1	1	1	2	1.750	3.100	13.800	17.500
Z54003	0.375	0.130	0.340	7.250	2	1	1	1	2	2.750	2.600	14.040	17.110
Z54004	0.375	0.130	0.340	7.250	2	1	1	1	2	3.750	0.700	13.900	16.880
Z54005	0.375	0.130	0.340	7.250	2	1	1	1	2	4.750	2.350	13.880	16.690
Z54006	0.375	0.130	0.340	7.250	2	1	1	1	2	5.750	1.700	14.030	16.600
Z54007	0.375	0.130	0.340	7.250	2	1	1	1	2	6.750	2.400	13.350	16.300
Z50001	0.375	0.100	0.280	7.160	1	2	2	1	1	0.750	1.800	14.040	16.020
Z50002	0.375	0.100	0.280	7.160	1	2	2	1	1	1.750	3.400	14.350	18.500
Z50003	0.375	0.100	0.280	7.160	1	2	2	1	1	2.750	3.600	13.550	17.500
Z50004	0.375	0.100	0.280	7.160	1	2	2	1	1	3.750	1.700	13.780	16.650
Z50005	0.375	0.100	0.280	7.160	1	2	2	1	1	4.750	1.500	14.130	16.300
Z50006	0.375	0.100	0.280	7.160	1	2	2	1	1	5.750	1.500	13.580	15.880
Z50007	0.375	0.100	0.280	7.160	1	2	2	1	1	6.750	1.500	13.180	15.600

Z5F001	0.375	0.100	0.280	7.160	1	2	1	2	1	0.750	4.090	14.560	18.880
Z5F002	0.375	0.100	0.280	7.160	1	2	1	2	1	1.750	3.780	14.160	17.280
Z5F003	0.375	0.100	0.280	7.160	1	2	1	2	1	2.750	3.630	13.800	16.620
Z5F004	0.375	0.100	0.280	7.160	1	2	1	2	1	3.750	2.520	14.040	16.800
Z5F005	0.375	0.100	0.280	7.160	1	2	1	2	1	4.750	1.420	14.080	16.600
Z5F006	0.375	0.100	0.280	7.160	1	2	1	2	1	5.750	1.420	13.900	16.260
Z5F007	0.375	0.100	0.280	7.160	1	2	1	2	1	6.750	2.390	12.930	15.280
Z50001	0.375	0.100	0.280	7.160	1	2	1	1	2	0.750	3.940	13.860	17.720
Z50002	0.375	0.100	0.280	7.160	1	2	1	1	2	1.750	1.260	14.020	16.040
Z50003	0.375	0.100	0.280	7.160	1	2	1	1	2	2.750	2.370	13.960	16.500
Z50004	0.375	0.100	0.280	7.160	1	2	1	1	2	3.750	2.050	13.960	16.520
Z50005	0.375	0.100	0.280	7.160	1	2	1	1	2	4.750	1.580	13.400	15.660
Z50006	0.375	0.100	0.280	7.160	1	2	1	1	2	5.750	1.730	13.360	15.680
Z50007	0.375	0.100	0.280	7.160	1	2	1	1	2	6.750	1.540	12.800	14.750
X50001	0.375	0.020	0.270	7.060	1	2	2	1	1	0.750	8.200	15.200	19.300
X50002	0.375	0.020	0.270	7.060	1	2	2	1	1	1.750	6.500	15.420	19.000
X50003	0.375	0.020	0.270	7.060	1	2	2	1	1	2.750	6.000	15.000	18.400
X50004	0.375	0.020	0.270	7.060	1	2	2	1	1	3.750	3.500	15.180	18.020
X50005	0.375	0.020	0.270	7.060	1	2	2	1	1	4.750	3.700	15.120	17.540
X50006	0.375	0.020	0.270	7.060	1	2	2	1	1	5.750	3.200	14.880	17.380
X50007	0.375	0.020	0.270	7.060	1	2	2	1	1	6.750	3.800	14.260	17.180
X5F001	0.375	0.020	0.270	7.060	1	2	1	2	1	0.750	8.600	15.320	19.360
X5F002	0.375	0.020	0.270	7.060	1	2	1	2	1	1.750	6.200	15.180	19.020
X5F003	0.375	0.020	0.270	7.060	1	2	1	2	1	2.750	4.800	15.000	18.680
X5F004	0.375	0.020	0.270	7.060	1	2	1	2	1	3.750	3.800	14.880	18.200
X5F005	0.375	0.020	0.270	7.060	1	2	1	2	1	4.750	3.700	14.780	17.980
X5F006	0.375	0.020	0.270	7.060	1	2	1	2	1	5.750	3.400	14.500	17.540
X5F007	0.375	0.020	0.270	7.060	1	2	1	2	1	6.750	3.800	14.320	17.240
X50001	0.375	0.020	0.270	7.060	1	2	1	1	2	0.750	8.800	14.500	18.360
X50002	0.375	0.020	0.270	7.060	1	2	1	1	2	1.750	5.700	14.300	17.820
X50003	0.375	0.020	0.270	7.060	1	2	1	1	2	2.750	4.100	14.120	17.280
X50004	0.375	0.020	0.270	7.060	1	2	1	1	2	3.750	4.100	14.020	16.980
X50005	0.375	0.020	0.270	7.060	1	2	1	1	2	4.750	4.400	14.060	17.280
X50006	0.375	0.020	0.270	7.060	1	2	1	1	2	5.750	4.100	14.060	17.120
X50007	0.375	0.020	0.270	7.060	1	2	1	1	2	6.750	4.100	13.860	17.000

X21001	0.250	0.020	0.290	7.160	1	1	1	1	1	0.750	6.800	13.000	17.000
X21002	0.250	0.020	0.290	7.160	1	1	1	1	1	1.750	5.300	0.000	16.360
X21003	0.250	0.020	0.290	7.160	1	1	1	1	1	2.750	4.400	0.000	16.200
X21004	0.250	0.020	0.290	7.160	1	1	1	1	1	3.750	3.300	0.000	15.200
X21005	0.250	0.020	0.290	7.160	1	1	1	1	1	4.750	4.800	0.000	16.040
X21006	0.250	0.020	0.290	7.160	1	1	1	1	1	5.750	2.200	0.000	14.680
X21007	0.250	0.020	0.290	7.160	1	1	1	1	1	6.750	4.800	0.000	15.640
X22001	0.250	0.010	0.280	6.760	2	1	2	1	1	0.750	12.300	12.400	17.240
X22002	0.250	0.010	0.280	6.760	2	1	2	1	1	1.750	6.000	0.000	16.480
X22003	0.250	0.010	0.280	6.760	2	1	2	1	1	2.750	9.200	0.000	16.480
X22004	0.250	0.010	0.280	6.760	2	1	2	1	1	3.750	6.600	0.000	16.400
X22005	0.250	0.010	0.280	6.760	2	1	2	1	1	4.750	6.600	0.000	16.800
X22006	0.250	0.010	0.280	6.760	2	1	2	1	1	5.750	5.300	0.000	16.400
X22007	0.250	0.010	0.280	6.760	2	1	2	1	1	6.750	6.600	0.000	16.200
X23001	0.250	0.010	0.280	6.760	2	1	1	2	1	0.750	9.100	14.400	16.910
X23002	0.250	0.010	0.280	6.760	2	1	1	2	1	1.750	9.500	0.000	16.350
X23003	0.250	0.010	0.280	6.760	2	1	1	2	1	2.750	6.500	0.000	16.400
X23004	0.250	0.010	0.280	6.760	2	1	1	2	1	3.750	7.000	0.000	16.050
X23005	0.250	0.010	0.280	6.760	2	1	1	2	1	4.750	6.000	0.000	15.900
X23006	0.250	0.010	0.280	6.760	2	1	1	2	1	5.750	7.000	0.000	15.950
X23007	0.250	0.010	0.280	6.760	2	1	1	2	1	6.750	8.100	0.000	15.600
X24001	0.250	0.010	0.280	6.760	2	1	1	1	2	0.750	7.500	12.880	17.280
X24002	0.250	0.010	0.280	6.760	2	1	1	1	2	1.750	8.100	0.000	16.900
X24003	0.250	0.010	0.280	6.760	2	1	1	1	2	2.750	7.500	0.000	16.600
X24004	0.250	0.010	0.280	6.760	2	1	1	1	2	3.750	6.100	0.000	16.400
X24005	0.250	0.010	0.280	6.760	2	1	1	1	2	4.750	5.700	0.000	16.040
X24006	0.250	0.010	0.280	6.760	2	1	1	1	2	5.750	8.300	0.000	16.320
X24007	0.250	0.010	0.280	6.760	2	1	1	1	2	6.750	8.000	0.000	16.700
X20001	0.250	0.010	0.570	7.360	1	2	2	1	1	0.750	5.300	15.000	18.400
X20002	0.250	0.010	0.570	7.360	1	2	2	1	1	1.750	2.200	0.000	16.720
X20003	0.250	0.010	0.570	7.360	1	2	2	1	1	2.750	3.100	0.000	17.080
X20004	0.250	0.010	0.570	7.360	1	2	2	1	1	3.750	2.000	0.000	16.360
X20005	0.250	0.010	0.570	7.360	1	2	2	1	1	4.750	0.900	0.000	16.280
X20006	0.250	0.010	0.570	7.360	1	2	2	1	1	5.750	1.500	0.000	16.200
X20007	0.250	0.010	0.570	7.360	1	2	2	1	1	6.750	2.400	0.000	16.240

X27001	0.250	0.020	0.270	7.000	1	2	1	2	1	0.750	8.900	12.000	16.820
X27002	0.250	0.020	0.270	7.000	1	2	1	2	1	1.750	9.500	0.000	16.450
X27003	0.250	0.020	0.270	7.000	1	2	1	2	1	2.750	7.000	0.000	16.600
X27004	0.250	0.020	0.270	7.000	1	2	1	2	1	3.750	5.300	0.000	16.520
X27005	0.250	0.020	0.270	7.000	1	2	1	2	1	4.750	6.500	0.000	16.150
X27006	0.250	0.020	0.270	7.000	1	2	1	2	1	5.750	4.500	0.000	16.100
X27007	0.250	0.020	0.270	7.000	1	2	1	2	1	6.750	7.000	0.000	15.280
X28001	0.250	0.020	0.270	7.000	1	2	1	1	2	0.750	5.900	11.520	14.490
X28002	0.250	0.020	0.270	7.000	1	2	1	1	2	1.750	8.100	0.000	15.240
X28003	0.250	0.020	0.270	7.000	1	2	1	1	2	2.750	8.800	0.000	15.350
X28004	0.250	0.020	0.270	7.000	1	2	1	1	2	3.750	8.500	0.000	14.150
X28005	0.250	0.020	0.270	7.000	1	2	1	1	2	4.750	8.100	0.000	15.760
X28006	0.250	0.020	0.270	7.000	1	2	1	1	2	5.750	4.400	0.000	14.490
X28007	0.250	0.020	0.270	7.000	1	2	1	1	2	6.750	7.800	0.000	14.430
Y21001	0.250	0.080	0.280	6.990	1	1	1	1	1	0.750	4.400	13.480	16.720
Y21002	0.250	0.080	0.280	6.990	1	1	1	1	1	1.750	2.600	0.000	15.920
Y21003	0.250	0.080	0.280	6.990	1	1	1	1	1	2.750	1.800	0.000	15.760
Y21004	0.250	0.080	0.280	6.990	1	1	1	1	1	3.750	1.800	0.000	15.880
Y21005	0.250	0.080	0.280	6.990	1	1	1	1	1	4.750	3.100	0.000	16.320
Y21006	0.250	0.080	0.280	6.990	1	1	1	1	1	5.750	3.100	0.000	16.080
Y21007	0.250	0.080	0.280	6.990	1	1	1	1	1	6.750	2.800	0.000	15.360
Y22001	0.250	0.080	0.500	7.130	2	1	2	1	1	0.750	7.800	14.500	18.240
Y22002	0.250	0.080	0.500	7.130	2	1	2	1	1	1.750	2.000	0.000	15.400
Y22003	0.250	0.080	0.500	7.130	2	1	2	1	1	2.750	4.500	0.000	17.800
Y22004	0.250	0.080	0.500	7.130	2	1	2	1	1	3.750	2.800	0.000	17.150
Y22005	0.250	0.080	0.500	7.130	2	1	2	1	1	4.750	2.300	0.000	16.600
Y22006	0.250	0.080	0.500	7.130	2	1	2	1	1	5.750	2.800	0.000	16.770
Y22007	0.250	0.080	0.500	7.130	2	1	2	1	1	6.750	3.500	0.000	15.200
Y25001	0.250	0.080	0.500	7.130	2	1	1	2	1	0.750	9.000	15.120	19.560
Y25002	0.250	0.080	0.500	7.130	2	1	1	2	1	1.750	5.500	0.000	18.360
Y25003	0.250	0.080	0.500	7.130	2	1	1	2	1	2.750	5.500	0.000	17.920
Y25004	0.250	0.080	0.500	7.130	2	1	1	2	1	3.750	4.400	0.000	17.440
Y25005	0.250	0.080	0.500	7.130	2	1	1	2	1	4.750	4.400	0.000	18.000
Y25006	0.250	0.080	0.500	7.130	2	1	1	2	1	5.750	4.200	0.000	18.240
Y25007	0.250	0.080	0.500	7.130	2	1	1	2	1	6.750	3.500	0.000	17.630

Y240001	0.250	0.080	0.500	7.130	2	1	1	1	2	0.750	10.300	15.080	19.600
Y240002	0.250	0.080	0.500	7.130	2	1	1	1	2	1.750	5.900	0.000	18.080
Y240003	0.250	0.080	0.500	7.130	2	1	1	1	2	2.750	5.700	0.000	18.080
Y240004	0.250	0.080	0.500	7.130	2	1	1	1	2	3.750	4.800	0.000	17.720
Y240005	0.250	0.080	0.500	7.130	2	1	1	1	2	4.750	3.500	0.000	17.560
Y240006	0.250	0.080	0.500	7.130	2	1	1	1	2	5.750	4.600	0.000	17.520
Y240007	0.250	0.080	0.500	7.130	2	1	1	1	2	6.750	4.600	0.000	17.520
Y200001	0.250	0.110	0.510	7.300	1	2	2	1	1	0.750	4.600	14.200	18.000
Y200002	0.250	0.110	0.510	7.300	1	2	2	1	1	1.750	3.100	0.000	16.980
Y200003	0.250	0.110	0.510	7.300	1	2	2	1	1	2.750	2.500	0.000	16.260
Y200004	0.250	0.110	0.510	7.300	1	2	2	1	1	3.750	3.000	0.000	16.260
Y200005	0.250	0.110	0.510	7.300	1	2	2	1	1	4.750	2.000	0.000	16.140
Y200006	0.250	0.110	0.510	7.300	1	2	2	1	1	5.750	1.800	0.000	15.340
Y200007	0.250	0.110	0.510	7.300	1	2	2	1	1	6.750	2.500	0.000	16.080
Y270001	0.250	0.110	0.510	7.300	1	2	1	2	1	0.750	5.300	14.360	18.200
Y270002	0.250	0.110	0.510	7.300	1	2	1	2	1	1.750	3.500	0.000	16.880
Y270003	0.250	0.110	0.510	7.300	1	2	1	2	1	2.750	2.600	0.000	16.280
Y270004	0.250	0.110	0.510	7.300	1	2	1	2	1	3.750	3.600	0.000	16.520
Y270005	0.250	0.110	0.510	7.300	1	2	1	2	1	4.750	3.400	0.000	16.480
Y270006	0.250	0.110	0.510	7.300	1	2	1	2	1	5.750	3.500	0.000	15.760
Y270007	0.250	0.110	0.510	7.300	1	2	1	2	1	6.750	3.800	0.000	16.000
Y280001	0.250	0.090	0.280	7.070	1	2	1	1	2	0.750	4.600	14.500	18.440
Y280002	0.250	0.090	0.280	7.070	1	2	1	1	2	1.750	2.000	0.000	17.160
Y280003	0.250	0.090	0.280	7.070	1	2	1	1	2	2.750	3.100	0.000	16.960
Y280004	0.250	0.090	0.280	7.070	1	2	1	1	2	3.750	2.500	0.000	16.160
Y280005	0.250	0.090	0.280	7.070	1	2	1	1	2	4.750	1.300	0.000	16.000
Y280006	0.250	0.090	0.280	7.070	1	2	1	1	2	5.750	0.900	0.000	15.160
Y280007	0.250	0.090	0.280	7.070	1	2	1	1	2	6.750	2.600	0.000	0.000
Z210001	0.250	0.120	0.230	6.060	1	1	1	1	1	0.750	5.900	13.040	17.120
Z210002	0.250	0.120	0.230	6.060	1	1	1	1	1	1.750	4.400	0.000	16.440
Z210003	0.250	0.120	0.230	6.060	1	1	1	1	1	2.750	3.700	0.000	16.200
Z210004	0.250	0.120	0.230	6.060	1	1	1	1	1	3.750	3.100	0.000	15.960
Z210005	0.250	0.120	0.230	6.060	1	1	1	1	1	4.750	3.100	0.000	15.880
Z210006	0.250	0.120	0.230	6.060	1	1	1	1	1	5.750	3.300	0.000	15.840
Z210007	0.250	0.120	0.230	6.060	1	1	1	1	1	6.750	4.600	0.000	16.080

Z4[illegible]	0.450	0.120	0.230	6.920	2	1	2	1	1	0.750	11.100	13.200	17.280
Z4[illegible]	0.450	0.120	0.230	6.920	2	1	2	1	1	1.750	1.500	0.000	14.200
Z4[illegible]	0.450	0.120	0.230	6.920	2	1	2	1	1	2.750	7.200	0.000	16.190
Z4[illegible]	0.450	0.120	0.230	6.920	2	1	2	1	1	3.750	4.000	0.000	16.160
Z4[illegible]	0.450	0.120	0.230	6.920	2	1	2	1	1	4.750	2.900	0.000	15.600
Z4[illegible]	0.450	0.120	0.230	6.920	2	1	2	1	1	5.750	4.000	0.000	15.720
Z4[illegible]	0.450	0.120	0.250	6.920	2	1	2	1	1	6.750	2.900	0.000	14.880
Z4[illegible]	0.450	0.120	0.230	6.920	2	1	2	1	1	0.750	6.600	12.400	16.200
Z4[illegible]	0.450	0.120	0.230	6.920	2	1	2	1	1	1.750	5.500	0.000	16.200
Z4[illegible]	0.450	0.120	0.250	6.920	2	1	2	1	1	2.750	5.300	0.000	15.460
Z4[illegible]	0.450	0.120	0.230	6.920	2	1	2	1	1	3.750	4.300	0.000	15.400
Z4[illegible]	0.450	0.120	0.230	6.920	2	1	2	1	1	4.750	5.500	0.000	15.700
Z4[illegible]	0.450	0.120	0.230	6.920	2	1	2	1	1	5.750	4.800	0.000	15.500
Z4[illegible]	0.450	0.120	0.230	6.920	2	1	2	1	1	6.750	5.500	0.000	15.800
Z4[illegible]	0.450	0.120	0.230	6.920	2	1	2	1	2	0.750	8.300	12.920	17.440
Z4[illegible]	0.450	0.120	0.250	6.920	2	1	1	1	2	1.750	7.200	0.000	16.440
Z4[illegible]	0.450	0.120	0.230	6.920	2	1	1	1	2	2.750	5.300	0.000	16.160
Z4[illegible]	0.450	0.120	0.230	6.920	2	1	1	1	2	3.750	4.200	0.000	15.880
Z4[illegible]	0.450	0.120	0.230	6.920	2	1	1	1	2	4.750	4.200	0.000	16.280
Z4[illegible]	0.450	0.120	0.230	6.920	2	1	1	1	2	5.750	3.500	0.000	15.960
Z4[illegible]	0.450	0.120	0.230	6.920	2	1	1	1	2	6.750	4.400	0.000	16.040
Z4[illegible]	0.450	0.120	0.280	6.950	1	2	2	1	1	0.750	5.300	15.850	19.700
Z4[illegible]	0.450	0.120	0.280	6.950	1	2	2	1	1	1.750	2.600	0.000	16.680
Z4[illegible]	0.450	0.120	0.280	6.950	1	2	2	1	1	2.750	5.700	0.000	18.040
Z4[illegible]	0.450	0.120	0.280	6.950	1	2	2	1	1	3.750	3.100	0.000	17.360
Z4[illegible]	0.450	0.120	0.280	6.950	1	2	2	1	1	4.750	2.600	0.000	17.160
Z4[illegible]	0.450	0.120	0.280	6.950	1	2	2	1	1	5.750	1.300	0.000	16.320
Z4[illegible]	0.450	0.120	0.280	6.950	1	2	2	1	1	6.750	2.900	0.000	16.320
Z4[illegible]	0.450	0.120	0.280	6.950	1	2	2	1	2	0.750	6.000	14.000	17.910
Z4[illegible]	0.450	0.120	0.280	6.950	1	2	2	1	2	1.750	5.300	0.000	17.040
Z4[illegible]	0.450	0.120	0.280	6.950	1	2	2	1	2	2.750	3.500	0.000	16.200
Z4[illegible]	0.450	0.120	0.280	6.950	1	2	2	1	2	3.750	2.900	0.000	16.200
Z4[illegible]	0.450	0.120	0.280	6.950	1	2	2	1	2	4.750	3.900	0.000	16.200
Z4[illegible]	0.450	0.120	0.280	6.950	1	2	2	1	2	5.750	3.500	0.000	16.040
Z4[illegible]	0.450	0.120	0.280	6.950	1	2	2	1	2	6.750	3.300	0.000	15.160

Z28001	0.450	0.120	0.280	6.750	1	2	1	1	2	0.750	4.400	13.680	17.840
Z28002	0.450	0.120	0.280	6.750	1	2	1	1	2	1.750	3.700	0.000	17.280
Z28003	0.450	0.120	0.280	6.750	1	2	1	1	2	2.750	4.800	0.000	16.840
Z28004	0.450	0.120	0.280	6.750	1	2	1	1	2	3.750	3.700	0.000	16.960
Z28005	0.450	0.120	0.280	6.750	1	2	1	1	2	4.750	4.800	0.000	17.080
Z28006	0.450	0.120	0.280	6.750	1	2	1	1	2	5.750	3.100	0.000	16.880
Z28007	0.450	0.120	0.280	6.750	1	2	1	1	2	6.750	3.500	0.000	16.400
X22001	0.450	0.010	0.280	6.760	2	1	2	1	1	0.750	8.500	13.250	16.800
X22002	0.450	0.010	0.280	6.760	2	1	2	1	1	1.750	6.000	0.000	16.480
X22003	0.450	0.010	0.280	6.760	2	1	2	1	1	2.750	8.800	0.000	16.240
X22004	0.450	0.010	0.280	6.760	2	1	2	1	1	3.750	7.000	0.000	16.320
X22005	0.450	0.010	0.280	6.760	2	1	2	1	1	4.750	3.500	0.000	15.280
X22006	0.450	0.010	0.280	6.760	2	1	2	1	1	5.750	5.300	0.000	16.400
X22007	0.450	0.010	0.280	6.760	2	1	2	1	1	6.750	5.300	0.000	14.520
X25001	0.450	0.010	0.280	6.760	2	1	1	2	1	0.750	9.100	14.400	16.910
X25002	0.450	0.010	0.520	6.920	2	1	1	2	1	1.750	3.500	0.000	15.480
X25003	0.450	0.010	0.520	6.920	2	1	1	2	1	2.750	4.800	0.000	16.200
X25004	0.450	0.010	0.520	6.920	2	1	1	2	1	3.750	4.200	0.000	13.560
X25005	0.450	0.010	0.280	6.760	2	1	1	2	1	4.750	6.000	0.000	15.900
X25006	0.450	0.010	0.520	6.920	2	1	1	2	1	5.750	5.500	0.000	16.200
X25007	0.450	0.010	0.520	6.920	2	1	1	2	1	6.750	5.500	0.000	16.280
X24001	0.450	0.010	0.280	6.760	2	1	1	1	2	0.750	4.800	14.320	17.520
X24002	0.450	0.010	0.280	6.760	2	1	1	1	2	1.750	6.100	0.000	16.630
X24003	0.450	0.010	0.280	6.760	2	1	1	1	2	2.750	4.500	0.000	16.420
X24004	0.450	0.010	0.280	6.760	2	1	1	1	2	3.750	4.200	0.000	16.280
X24005	0.450	0.010	0.280	6.760	2	1	1	1	2	4.750	6.000	0.000	16.750
X24006	0.450	0.010	0.280	6.760	2	1	1	1	2	5.750	3.800	0.000	15.900
X24007	0.450	0.010	0.280	6.760	2	1	1	1	2	6.750	8.300	0.000	15.370
X26001	0.450	0.020	0.270	7.000	1	2	1	1	2	0.750	5.700	15.200	19.160
X26002	0.450	0.020	0.270	7.000	1	2	1	1	2	1.750	4.000	0.000	18.440
X26003	0.450	0.020	0.270	7.000	1	2	1	1	2	2.750	4.000	0.000	17.560
X26004	0.450	0.020	0.270	7.000	1	2	1	1	2	3.750	2.400	0.000	17.160
X26005	0.450	0.020	0.270	7.000	1	2	1	1	2	4.750	3.300	0.000	18.040
X26006	0.450	0.020	0.270	7.000	1	2	1	1	2	5.750	3.100	0.000	17.360
X26007	0.450	0.020	0.270	7.000	1	2	1	1	2	6.750	5.500	0.000	17.400

X11001	0.125	0.010	0.520	6.920	1	1	1	1	1	0.500	2.600	14.460	16.450	
X11002	0.125	0.010	0.520	6.920	1	1	1	1	1	1.630	2.000	0.000	15.370	
X11003	0.125	0.010	0.520	6.920	1	1	1	1	1	2.750	1.700	0.000	14.180	
X11004	0.125	0.010	0.520	6.920	1	1	1	1	1	3.880	1.400	0.000	13.100	
X11005	0.125	0.010	0.520	6.920	1	1	1	1	1	5.000	1.000	0.000	15.580	
X11006	0.125	0.010	0.520	6.920	1	1	1	1	1	6.130	0.900	0.000	14.270	
X12001	0.125	0.010	0.520	6.920	2	1	2	1	1	0.500	4.200	14.100	17.100	
X12002	0.125	0.010	0.520	6.920	2	1	2	1	1	1.630	3.100	0.000	16.500	
X12003	0.125	0.010	0.520	6.920	2	1	2	1	1	2.750	2.100	0.000	16.000	
X12004	0.125	0.010	0.520	6.920	2	1	2	1	1	3.880	1.400	0.000	16.300	
X12005	0.125	0.010	0.520	6.920	2	1	2	1	1	5.000	3.400	0.000	16.400	
X12006	0.125	0.010	0.520	6.920	2	1	2	1	1	6.130	4.400	0.000	16.600	
X13001	0.125	0.030	0.430	7.360	2	1	1	2	1	0.500	7.300	13.800	17.300	
X13002	0.125	0.030	0.430	7.360	2	1	1	2	1	1.630	4.900	0.000	16.400	
X13003	0.125	0.030	0.430	7.360	2	1	1	2	1	2.750	5.500	0.000	16.800	
X13004	0.125	0.030	0.430	7.360	2	1	1	2	1	3.880	6.000	0.000	16.600	
X13005	0.125	0.030	0.430	7.360	2	1	1	2	1	5.000	3.600	0.000	16.100	
X13006	0.125	0.030	0.430	7.360	2	1	1	2	1	6.130	6.000	0.000	17.000	
X10001	0.125	0.020	0.400	7.370	1	2	2	1	1	0.500	5.400	13.300	16.300	
X10002	0.125	0.020	0.400	7.370	1	2	2	1	1	1.630	4.200	0.000	16.180	
X10003	0.125	0.020	0.400	7.370	1	2	2	1	1	2.750	5.800	0.000	16.480	
X10004	0.125	0.020	0.400	7.370	1	2	2	1	1	3.880	5.000	0.000	16.090	
X10005	0.125	0.020	0.400	7.370	1	2	2	1	1	5.000	3.700	0.000	15.590	
X10006	0.125	0.020	0.400	7.370	1	2	2	1	1	6.130	5.300	0.000	15.930	
X17001	0.125	0.030	0.500	6.800	1	2	1	2	1	0.500	6.000	14.000	17.100	
X17002	0.125	0.030	0.500	6.800	1	2	1	2	1	1.630	5.800	0.000	16.800	
X17003	0.125	0.030	0.500	6.800	1	2	1	2	1	2.750	5.500	0.000	16.700	
X17004	0.125	0.030	0.500	6.800	1	2	1	2	1	3.880	5.300	0.000	16.400	
X17005	0.125	0.030	0.500	6.800	1	2	1	2	1	5.000	4.800	0.000	16.500	
X17006	0.125	0.030	0.500	6.800	1	2	1	2	1	6.130	5.800	0.000	16.900	
Y11001	0.125	0.080	0.540	7.420	1	1	1	1	1	0.500	3.600	15.400	18.200	
Y11002	0.125	0.080	0.540	7.420	1	1	1	1	1	1.630	3.000	0.000	17.100	
Y11003	0.125	0.080	0.540	7.420	1	1	1	1	1	2.750	1.900	0.000	16.900	
Y11004	0.125	0.080	0.540	7.420	1	1	1	1	1	3.880	2.300	0.000	17.200	
Y11005	0.125	0.080	0.540	7.420	1	1	1	1	1	5.000	3.600	0.000	17.900	

Y11006	0.125	0.080	0.340	7.420	1	1	1	1	1	6.130	3.000	0.000	16.200
Y12001	0.125	0.080	0.340	7.420	2	1	2	1	1	0.500	6.000	16.140	19.250
Y12002	0.125	0.080	0.340	7.420	2	1	2	1	1	1.630	3.400	0.000	17.800
Y12003	0.125	0.080	0.340	7.420	2	1	2	1	1	2.750	2.100	0.000	17.470
Y12004	0.125	0.080	0.340	7.420	2	1	2	1	1	3.880	1.200	0.000	17.060
Y12005	0.125	0.080	0.340	7.420	2	1	2	1	1	5.000	2.600	0.000	17.370
Y12006	0.125	0.080	0.340	7.420	2	1	2	1	1	6.130	2.800	0.000	17.850
Y13001	0.125	0.080	0.340	7.420	2	1	1	2	1	0.500	3.400	14.900	18.200
Y13002	0.125	0.080	0.340	7.420	2	1	1	2	1	1.630	2.800	0.000	16.800
Y13003	0.125	0.080	0.340	7.420	2	1	1	2	1	2.750	1.800	0.000	16.400
Y13004	0.125	0.080	0.340	7.420	2	1	1	2	1	3.880	1.500	0.000	16.700
Y13005	0.125	0.080	0.340	7.420	2	1	1	2	1	5.000	2.600	0.000	16.900
Y13006	0.125	0.080	0.340	7.420	2	1	1	2	1	6.130	2.300	0.000	16.600
Y16001	0.125	0.090	0.280	7.070	1	2	2	1	1	0.500	8.100	14.900	18.900
Y16002	0.125	0.090	0.280	7.070	1	2	2	1	1	1.630	5.700	0.000	18.300
Y16003	0.125	0.090	0.280	7.070	1	2	2	1	1	2.750	3.900	0.000	17.700
Y16004	0.125	0.090	0.280	7.070	1	2	2	1	1	3.880	2.800	0.000	16.800
Y16005	0.125	0.090	0.280	7.070	1	2	2	1	1	5.000	2.600	0.000	16.800
Y16006	0.125	0.090	0.280	7.070	1	2	2	1	1	6.130	4.200	0.000	16.900
Y17001	0.125	0.090	0.280	7.070	1	2	1	2	1	0.500	4.700	14.550	17.610
Y17002	0.125	0.090	0.280	7.070	1	2	1	2	1	1.630	4.300	0.000	17.500
Y17003	0.125	0.090	0.280	7.070	1	2	1	2	1	2.750	4.200	0.000	17.500
Y17004	0.125	0.090	0.280	7.070	1	2	1	2	1	3.880	3.400	0.000	16.720
Y17005	0.125	0.090	0.280	7.070	1	2	1	2	1	5.000	3.400	0.000	16.490
Y17006	0.125	0.090	0.280	7.070	1	2	1	2	1	6.130	3.900	0.000	15.330
Z11001	0.125	0.110	0.500	7.530	1	1	1	1	1	0.500	3.900	14.420	17.610
Z11002	0.125	0.110	0.500	7.530	1	1	1	1	1	1.630	2.600	0.000	20.050
Z11003	0.125	0.110	0.500	7.530	1	1	1	1	1	2.750	1.300	0.000	16.910
Z11004	0.125	0.110	0.500	7.530	1	1	1	1	1	3.880	1.600	0.000	14.690
Z11005	0.125	0.110	0.500	7.530	1	1	1	1	1	5.000	0.000	0.000	15.330
Z11006	0.125	0.110	0.500	7.530	1	1	1	1	1	6.130	1.300	0.000	12.760
Z12001	0.125	0.070	0.540	6.520	2	1	2	1	1	0.500	0.900	17.140	19.250
Z12002	0.125	0.070	0.540	6.520	2	1	2	1	1	1.630	1.600	0.000	19.820
Z12003	0.125	0.070	0.540	6.520	2	1	2	1	1	2.750	4.500	0.000	17.480
Z12004	0.125	0.070	0.540	6.520	2	1	2	1	1	3.880	2.100	0.000	16.730

Z12005	0.125	0.070	0.540	6.520	2	1	2	1	1	5.000	1.000	0.000	14.680
Z12006	0.125	0.070	0.540	6.520	2	1	2	1	1	6.130	4.200	0.000	16.730
Z15001	0.125	0.110	0.500	7.530	2	1	1	2	1	0.500	3.500	14.300	17.500
Z15002	0.125	0.110	0.500	7.530	2	1	1	2	1	1.630	4.200	0.000	16.900
Z15003	0.125	0.110	0.500	7.530	2	1	1	2	1	2.750	3.700	0.000	16.800
Z15004	0.125	0.110	0.500	7.530	2	1	1	2	1	3.880	2.800	0.000	17.100
Z15005	0.125	0.110	0.500	7.530	2	1	1	2	1	5.000	4.200	0.000	18.300
Z15006	0.125	0.110	0.500	7.530	2	1	1	2	1	6.130	4.500	0.000	19.200
Z10001	0.125	0.110	0.520	7.530	1	2	2	1	1	0.500	2.900	15.230	17.750
Z10002	0.125	0.110	0.520	7.530	1	2	2	1	1	1.630	3.500	0.000	18.230
Z10003	0.125	0.110	0.520	7.530	1	2	2	1	1	2.750	2.100	0.000	18.090
Z10004	0.125	0.110	0.520	7.530	1	2	2	1	1	3.880	1.800	0.000	17.720
Z10005	0.125	0.110	0.520	7.530	1	2	2	1	1	5.000	1.800	0.000	16.310
Z10006	0.125	0.110	0.520	7.530	1	2	2	1	1	6.130	1.300	0.000	15.600
Z17001	0.125	0.110	0.520	7.530	1	2	1	2	1	0.500	3.700	15.400	17.240
Z17002	0.125	0.110	0.520	7.530	1	2	1	2	1	1.630	1.600	0.000	14.930
Z17003	0.125	0.110	0.520	7.530	1	2	1	2	1	2.750	6.000	0.000	21.100
Z17004	0.125	0.110	0.520	7.530	1	2	1	2	1	3.880	5.200	0.000	18.720
Z17005	0.125	0.110	0.520	7.530	1	2	1	2	1	5.000	5.200	0.000	18.350
Z17006	0.125	0.110	0.520	7.530	1	2	1	2	1	6.130	7.900	0.000	18.250

SERIES II RESULTS

XC4001	0.500	0.030	0.270	7.130	2	1	2	1	0.750	14.500	11.620	16.280
XC4002	0.500	0.030	0.270	7.130	2	1	2	1	1.750	11.800	11.080	15.900
XC4003	0.500	0.030	0.270	7.130	2	1	2	1	2.750	12.000	11.260	15.900
XC4004	0.500	0.030	0.270	7.130	2	1	2	1	3.750	8.500	11.100	15.600
XC4005	0.500	0.030	0.270	7.130	2	1	2	1	4.750	11.000	11.180	15.780
XC4006	0.500	0.030	0.270	7.130	2	1	2	1	5.750	9.500	11.020	15.520
XC4007	0.500	0.030	0.270	7.130	2	1	2	1	6.750	11.300	11.040	15.680
XD4001	0.500	0.030	0.220	7.000	2	1	1	2	0.750	11.900	12.200	16.900
XD4002	0.500	0.030	0.220	7.000	2	1	1	2	1.750	9.800	11.900	16.400
XD4003	0.500	0.030	0.220	7.000	2	1	1	2	2.750	5.400	11.400	15.400
XD4004	0.500	0.030	0.220	7.000	2	1	1	2	3.750	5.200	10.500	15.700
XD4005	0.500	0.030	0.220	7.000	2	1	1	2	4.750	4.600	12.000	15.700
XD4006	0.500	0.030	0.220	7.000	2	1	1	2	5.750	4.700	12.100	15.600
XD4007	0.500	0.030	0.220	7.000	2	1	1	2	6.750	11.000	11.500	16.000
ZA4001	0.500	0.130	0.230	7.060	1	2	2	1	0.750	10.400	11.520	16.280
ZA4002	0.500	0.130	0.230	7.060	1	2	2	1	1.750	6.800	11.340	15.740
ZA4003	0.500	0.130	0.230	7.060	1	2	2	1	2.750	6.000	11.380	15.520
ZA4004	0.500	0.130	0.230	7.060	1	2	2	1	3.750	4.300	11.420	15.160
ZA4005	0.500	0.130	0.230	7.060	1	2	2	1	4.750	4.600	11.420	15.260
ZA4006	0.500	0.130	0.230	7.060	1	2	2	1	5.750	5.200	11.320	15.200
ZA4007	0.500	0.130	0.230	7.060	1	2	2	1	6.750	6.800	10.940	15.400
ZB4001	0.500	0.110	0.240	6.060	1	2	1	2	0.750	7.200	12.200	16.700
ZB4002	0.500	0.110	0.240	6.060	1	2	1	2	1.750	5.000	12.100	15.900
ZB4003	0.500	0.110	0.240	6.060	1	2	1	2	2.750	5.000	12.000	15.600
ZB4004	0.500	0.110	0.240	6.060	1	2	1	2	3.750	1.300	10.900	12.100
ZB4005	0.500	0.110	0.240	6.060	1	2	1	2	4.750	1.300	12.200	13.800
ZB4006	0.500	0.110	0.240	6.060	1	2	1	2	5.750	2.500	12.000	14.400
ZB4007	0.500	0.110	0.240	6.060	1	2	1	2	6.750	6.300	12.300	15.500
XA5001	0.375	0.050	0.290	7.200	1	2	2	1	0.750	12.000	12.700	17.400
XA5002	0.375	0.050	0.290	7.200	1	2	2	1	1.750	11.000	12.660	17.180
XA5003	0.375	0.050	0.290	7.200	1	2	2	1	2.750	8.800	12.360	16.820
XA5004	0.375	0.050	0.290	7.200	1	2	2	1	3.750	10.100	12.500	16.920
XA5005	0.375	0.050	0.290	7.200	1	2	2	1	4.750	11.300	12.640	17.080
XA5006	0.375	0.050	0.290	7.200	1	2	2	1	5.750	9.800	12.440	16.900
XA5007	0.375	0.050	0.290	7.200	1	2	2	1	6.750	9.600	11.760	16.380

XB3001	0.375	0.020	0.270	7.110	1	2	1	2	0.750	14.000	12.800	18.400
XB3002	0.375	0.020	0.270	7.110	1	2	1	2	1.750	9.800	12.800	17.300
XB3003	0.375	0.020	0.270	7.110	1	2	1	2	2.750	6.000	12.400	16.300
XB3004	0.375	0.020	0.270	7.110	1	2	1	2	3.750	7.500	12.600	17.300
XB3005	0.375	0.020	0.270	7.110	1	2	1	2	4.750	3.800	12.800	16.400
XB3006	0.375	0.020	0.270	7.110	1	2	1	2	5.750	3.900	12.600	16.300
XB3007	0.375	0.020	0.270	7.110	1	2	1	2	6.750	6.600	12.600	16.800
ZC3001	0.375	0.130	0.250	6.960	2	1	2	1	0.750	12.300	12.200	16.920
ZC3002	0.375	0.130	0.250	6.960	2	1	2	1	1.750	11.000	11.780	16.540
ZC3003	0.375	0.130	0.250	6.960	2	1	2	1	2.750	9.600	11.740	16.360
ZC3004	0.375	0.130	0.250	6.960	2	1	2	1	3.750	7.500	11.880	16.330
ZC3005	0.375	0.130	0.250	6.960	2	1	2	1	4.750	6.800	12.150	16.500
ZC3006	0.375	0.130	0.250	6.960	2	1	2	1	5.750	7.200	11.650	15.900
ZC3007	0.375	0.130	0.250	6.960	2	1	2	1	6.750	8.600	10.880	15.120
ZD3001	0.375	0.120	0.260	6.820	2	1	1	2	0.750	10.300	13.100	17.700
ZD3002	0.375	0.120	0.260	6.820	2	1	1	2	1.750	6.600	13.000	17.000
ZD3003	0.375	0.120	0.260	6.820	2	1	1	2	2.750	4.600	12.800	16.300
ZD3004	0.375	0.120	0.260	6.820	2	1	1	2	3.750	1.600	12.600	14.600
ZD3005	0.375	0.120	0.260	6.820	2	1	1	2	4.750	2.400	12.600	15.400
ZD3006	0.375	0.120	0.260	6.820	2	1	1	2	5.750	2.200	13.200	15.500
ZD3007	0.375	0.120	0.260	6.820	2	1	1	2	6.750	6.300	11.600	15.900
XA2001	0.250	0.030	0.290	7.200	1	2	2	1	0.750	12.700	11.960	16.760
XA2002	0.250	0.030	0.290	7.200	1	2	2	1	1.750	11.400	0.000	15.680
XA2003	0.250	0.030	0.290	7.200	1	2	2	1	2.750	12.300	0.000	16.000
XA2004	0.250	0.030	0.290	7.200	1	2	2	1	3.750	10.100	0.000	16.000
XA2005	0.250	0.030	0.290	7.200	1	2	2	1	4.750	10.900	0.000	15.880
XA2006	0.250	0.030	0.290	7.200	1	2	2	1	5.750	9.200	0.000	15.720
XA2007	0.250	0.030	0.290	7.200	1	2	2	1	6.750	9.500	0.000	15.600
XB2001	0.250	0.020	0.280	7.260	1	2	1	2	0.750	9.000	14.500	18.100
XB2002	0.250	0.020	0.280	7.260	1	2	1	2	1.750	10.000	0.000	17.800
XB2003	0.250	0.020	0.280	7.260	1	2	1	2	2.750	5.000	0.000	17.500
XB2004	0.250	0.020	0.280	7.260	1	2	1	2	3.750	3.800	0.000	16.800
XB2005	0.250	0.020	0.280	7.260	1	2	1	2	4.750	3.500	0.000	16.200
XB2006	0.250	0.020	0.280	7.260	1	2	1	2	5.750	5.000	0.000	17.100
XB2007	0.250	0.020	0.280	7.260	1	2	1	2	6.750	8.500	0.000	17.200

ZC2001	0.250	0.130	0.250	6.960	2	1	2	1	0.750	10.900	11.880	16.440
ZC2002	0.250	0.130	0.250	6.960	2	1	2	1	1.750	7.900	0.000	16.040
ZC2003	0.250	0.130	0.250	6.960	2	1	2	1	2.750	7.900	0.000	16.000
ZC2004	0.250	0.130	0.250	6.960	2	1	2	1	3.750	8.300	0.000	15.760
ZC2005	0.250	0.130	0.250	6.960	2	1	2	1	4.750	9.200	0.000	16.200
ZC2006	0.250	0.130	0.250	6.960	2	1	2	1	5.750	8.100	0.000	16.040
ZC2007	0.250	0.130	0.250	6.960	2	1	2	1	6.750	6.100	0.000	15.520
ZD2001	0.250	0.100	0.290	6.060	2	1	1	2	0.750	4.200	13.100	17.500
ZD2002	0.250	0.100	0.290	6.060	2	1	1	2	1.750	2.200	0.000	13.500
ZD2003	0.250	0.100	0.290	6.060	2	1	1	2	2.750	1.500	0.000	14.900
ZD2004	0.250	0.100	0.290	6.060	2	1	1	2	3.750	3.100	0.000	16.300
ZD2005	0.250	0.100	0.290	6.060	2	1	1	2	4.750	3.100	0.000	16.100
ZD2006	0.250	0.100	0.290	6.060	2	1	1	2	5.750	1.500	0.000	15.000
ZD2007	0.250	0.100	0.290	6.060	2	1	1	2	6.750	3.900	0.000	16.000
XC1001	0.125	0.030	0.290	7.200	2	1	2	1	0.500	5.800	14.200	16.920
XC1002	0.125	0.030	0.290	7.200	2	1	2	1	1.630	6.000	0.000	16.600
XC1003	0.125	0.030	0.290	7.200	2	1	2	1	2.750	5.600	0.000	15.900
XC1004	0.125	0.030	0.290	7.200	2	1	2	1	3.880	5.300	0.000	16.300
XC1005	0.125	0.030	0.290	7.200	2	1	2	1	5.000	5.800	0.000	15.900
XC1006	0.125	0.030	0.290	7.200	2	1	2	1	6.130	6.600	0.000	16.000
XD1001	0.125	0.020	0.280	7.260	2	1	1	2	0.500	5.300	14.140	18.200
XD1002	0.125	0.020	0.280	7.260	2	1	1	2	1.630	5.300	0.000	17.200
XD1003	0.125	0.020	0.280	7.260	2	1	1	2	2.750	3.200	0.000	15.600
XD1004	0.125	0.020	0.280	7.260	2	1	1	2	3.880	4.400	0.000	16.360
XD1005	0.125	0.020	0.280	7.260	2	1	1	2	5.000	4.000	0.000	16.050
XD1006	0.125	0.020	0.280	7.260	2	1	1	2	6.130	5.800	0.000	17.710
ZA1001	0.125	0.130	0.230	7.060	1	2	2	1	0.500	5.800	13.100	17.200
ZA1002	0.125	0.130	0.230	7.060	1	2	2	1	1.630	5.300	0.000	16.900
ZA1003	0.125	0.130	0.230	7.060	1	2	2	1	2.750	5.000	0.000	17.050
ZA1004	0.125	0.130	0.230	7.060	1	2	2	1	3.880	5.300	0.000	16.220
ZA1005	0.125	0.130	0.230	7.060	1	2	2	1	5.000	4.800	0.000	16.360
ZA1006	0.125	0.130	0.230	7.060	1	2	2	1	6.130	5.600	0.000	16.920
ZB1001	0.125	0.120	0.260	6.820	1	2	1	2	0.500	2.800	13.750	15.550
ZB1002	0.125	0.120	0.260	6.820	1	2	1	2	1.630	6.000	0.000	16.400
ZB1003	0.125	0.120	0.260	6.820	1	2	1	2	2.750	6.000	0.000	16.850

ZB1004	0.125	0.120	0.260	6.020	1	2	1	2	3.880	5.600	0.000	17.100
ZB1005	0.125	0.120	0.260	6.020	1	2	1	2	5.000	4.000	0.000	17.440
ZB1006	0.125	0.120	0.260	6.020	1	2	1	2	6.130	4.800	0.000	16.300

SERIES III RESULTS

SM2001	0.500	0.250	1	2	2	1	11.700	13.000	18.600	0.680
SM2002	0.500	1.250	1	2	2	1	7.600	12.900	18.200	0.940
SM2003	0.500	2.250	1	2	2	1	7.700	12.700	18.000	0.990
SM2004	0.500	3.250	1	2	2	1	7.200	12.800	18.300	1.080
SM2005	0.500	4.250	1	2	2	1	7.200	12.600	17.700	1.080
SM2006	0.500	5.250	1	2	2	1	7.200	11.900	17.030	0.930
SM2007	0.500	6.250	1	2	2	1	7.800	12.300	17.200	0.960
SM1901	0.500	0.250	2	1	2	1	11.300	14.700	19.500	1.040
SM1902	0.500	1.250	2	1	2	1	12.000	15.300	20.400	1.000
SM1903	0.500	2.250	2	1	2	1	13.900	15.900	18.900	0.990
SM1904	0.500	3.250	2	1	2	1	8.800	14.200	18.900	1.160
SM1905	0.500	4.250	2	1	2	1	6.000	14.200	18.400	1.290
SM1906	0.500	5.250	2	1	2	1	5.700	14.500	18.400	1.410
SM1907	0.500	6.250	2	1	2	1	5.200	14.800	18.600	1.420
SM1801	0.500	0.250	1	2	1	2	10.200	14.800	19.500	1.040
SM1802	0.500	1.250	1	2	1	2	6.500	14.500	18.600	1.180
SM1803	0.500	2.250	1	2	1	2	4.600	16.000	18.200	1.290
SM1804	0.500	3.250	1	2	1	2	5.400	13.800	17.900	1.250
SM1805	0.500	4.250	1	2	1	2	5.700	14.000	18.100	1.270
SM1806	0.500	5.250	1	2	1	2	5.800	14.300	18.400	1.320
SM1807	0.500	6.250	1	2	1	2	6.600	13.800	18.100	1.370
SM1701	0.500	0.250	2	1	1	2	11.000	14.700	19.600	0.990
SM1702	0.500	1.250	2	1	1	2	8.200	14.900	19.400	0.960
SM1703	0.500	2.250	2	1	1	2	12.900	13.900	18.900	0.930
SM1704	0.500	3.250	2	1	1	2	8.300	14.400	19.000	1.070
SM1705	0.500	4.250	2	1	1	2	4.700	14.500	18.200	1.150
SM1706	0.500	5.250	2	1	1	2	5.000	14.100	17.900	1.520
SM1707	0.500	6.250	2	1	1	2	6.600	14.100	18.400	1.330
SM1601	0.500	0.250	1	1	1	1	3.200	14.600	17.700	1.420
SM1602	0.500	1.250	1	1	1	1	2.400	14.600	17.500	1.360
SM1603	0.500	2.250	1	1	1	1	1.300	13.900	15.700	1.420
SM1604	0.500	3.250	1	1	1	1	1.600	14.500	15.900	1.500
SM1605	0.500	4.250	1	1	1	1	1.700	13.600	15.800	1.530
SM1606	0.500	5.250	1	1	1	1	1.600	13.400	15.700	1.570
SM1607	0.500	6.250	1	1	1	1	3.000	13.300	16.400	1.430

SM1501	0.375	0.250	1	2	2	1	11.300	17.600	20.700	0.620
SM1502	0.375	1.250	1	2	2	1	8.800	15.700	20.700	0.680
SM1503	0.375	2.250	1	2	2	1	5.500	14.700	18.700	0.780
SM1504	0.375	3.250	1	2	2	1	5.000	15.200	19.100	0.770
SM1505	0.375	4.250	1	2	2	1	4.900	15.000	19.000	0.700
SM1506	0.375	5.250	1	2	2	1	4.600	14.600	18.400	0.860
SM1507	0.375	6.250	1	2	2	1	5.700	14.600	18.700	0.830
SM1401	0.375	0.250	2	1	2	1	9.900	15.300	20.400	0.760
SM1402	0.375	1.250	2	1	2	1	9.500	14.900	19.700	0.780
SM1403	0.375	2.250	2	1	2	1	16.100	13.400	18.800	0.640
SM1404	0.375	3.250	2	1	2	1	13.600	14.300	19.500	0.910
SM1405	0.375	4.250	2	1	2	1	9.000	14.900	19.700	1.060
SM1406	0.375	5.250	2	1	2	1	5.200	14.300	18.200	1.160
SM1407	0.375	6.250	2	1	2	1	2.500	13.900	16.500	1.140
SM1301	0.375	0.250	1	2	1	2	10.700	14.600	19.500	0.880
SM1302	0.375	1.250	1	2	1	2	9.800	14.400	19.300	1.000
SM1303	0.375	2.250	1	2	1	2	8.500	14.100	18.800	1.040
SM1304	0.375	3.250	1	2	1	2	9.800	14.100	19.200	0.960
SM1305	0.375	4.250	1	2	1	2	9.000	14.400	19.200	1.020
SM1306	0.375	5.250	1	2	1	2	8.200	14.200	18.900	1.040
SM1307	0.375	6.250	1	2	1	2	7.600	13.400	17.800	0.980
SM1201	0.375	0.250	2	1	1	2	15.400	12.800	18.800	0.550
SM1202	0.375	1.250	2	1	1	2	11.700	12.800	18.500	0.620
SM1203	0.375	2.250	2	1	1	2	16.800	11.700	18.000	0.420
SM1204	0.375	3.250	2	1	1	2	13.500	12.500	18.300	0.750
SM1205	0.375	4.250	2	1	1	2	6.600	12.600	17.700	0.980
SM1206	0.375	5.250	2	1	1	2	6.700	12.500	16.900	0.840
SM1207	0.375	6.250	2	1	1	2	7.600	11.200	16.900	0.790
SM1101	0.375	0.250	1	1	1	1	5.000	14.800	18.700	1.230
SM1102	0.375	1.250	1	1	1	1	3.600	14.200	17.500	1.200
SM1103	0.375	2.250	1	1	1	1	2.500	14.100	17.200	1.320
SM1104	0.375	3.250	1	1	1	1	1.600	13.800	16.000	1.380
SM1105	0.375	4.250	1	1	1	1	2.100	14.400	17.000	1.330
SM1106	0.375	5.250	1	1	1	1	2.800	14.200	17.300	1.300
SM1107	0.375	6.250	1	1	1	1	7.600	12.100	17.000	1.070

SM1001	0.250	0.250	1	2	2	1	11.000	14.700	19.450	0.470
SM1002	0.250	1.250	1	2	2	1	7.500	0.000	19.000	0.480
SM1003	0.250	2.250	1	2	2	1	10.500	0.000	19.500	0.280
SM1004	0.250	3.250	1	2	2	1	8.500	0.000	19.450	0.570
SM1005	0.250	4.250	1	2	2	1	10.000	0.000	18.750	0.510
SM1006	0.250	5.250	1	2	2	1	4.500	0.000	17.900	0.490
SM1007	0.250	6.250	1	2	2	1	11.400	0.000	18.250	0.410
SM 901	0.250	0.250	2	1	2	1	13.000	13.200	18.700	0.270
SM 902	0.250	1.250	2	1	2	1	6.500	12.900	17.200	0.340
SM 903	0.250	2.250	2	1	2	1	16.000	12.100	17.450	0.110
SM 904	0.250	3.250	2	1	2	1	13.000	12.900	18.300	0.350
SM 905	0.250	4.250	2	1	2	1	9.000	12.500	17.600	0.540
SM 906	0.250	5.250	2	1	2	1	3.300	12.600	15.500	0.650
SM 907	0.250	6.250	2	1	2	1	10.700	12.300	17.000	0.380
SM 801	0.250	0.250	1	2	1	2	9.400	14.800	19.760	0.720
SM 802	0.250	1.250	1	2	1	2	7.400	0.000	18.760	0.830
SM 803	0.250	2.250	1	2	1	2	5.500	0.000	18.320	0.800
SM 804	0.250	3.250	1	2	1	2	5.300	0.000	18.160	0.820
SM 805	0.250	4.250	1	2	1	2	5.500	0.000	18.600	0.720
SM 806	0.250	5.250	1	2	1	2	5.700	0.000	18.120	0.740
SM 807	0.250	6.250	1	2	1	2	7.300	0.000	18.480	0.590
SM 701	0.250	0.250	2	1	1	2	13.000	15.000	19.850	0.190
SM 702	0.250	1.250	2	1	1	2	9.500	0.000	19.300	0.700
SM 703	0.250	2.250	2	1	1	2	16.500	0.000	19.250	0.230
SM 704	0.250	3.250	2	1	1	2	15.800	0.000	19.250	0.370
SM 705	0.250	4.250	2	1	1	2	6.800	0.000	18.850	0.530
SM 706	0.250	5.250	2	1	1	2	6.300	0.000	18.320	0.530
SM 707	0.250	6.250	2	1	1	2	9.900	0.000	17.760	0.420
SM 601	0.250	0.250	1	1	1	1	6.300	15.280	18.800	0.570
SM 602	0.250	1.250	1	1	1	1	5.900	0.000	12.600	0.860
SM 603	0.250	2.250	1	1	1	1	4.200	0.000	16.000	0.720
SM 604	0.250	3.250	1	1	1	1	2.100	0.000	16.400	0.930
SM 605	0.250	4.250	1	1	1	1	3.000	0.000	17.300	0.840
SM 606	0.250	5.250	1	1	1	1	4.500	0.000	17.500	0.730
SM 607	0.250	6.250	1	1	1	1	8.400	0.000	17.760	0.470

SM 501	0,125	0,500	1	2	2	1	2,000	16,500	18,640	1,100
SM 502	0,125	1,630	1	2	2	1	6,600	0,000	19,300	1,140
SM 503	0,125	2,750	1	2	2	1	5,000	0,000	19,940	1,070
SM 504	0,125	3,880	1	2	2	1	6,400	0,000	19,960	1,040
SM 505	0,125	5,000	1	2	2	1	5,800	0,000	20,640	1,020
SM 506	0,125	6,130	1	2	2	1	7,400	0,000	19,920	1,060
SM 401	0,125	0,500	2	1	2	1	4,600	16,400	19,400	1,050
SM 402	0,125	1,630	2	1	2	1	3,000	0,000	18,460	1,160
SM 403	0,125	2,750	2	1	2	1	9,200	0,000	20,720	1,220
SM 404	0,125	3,880	2	1	2	1	2,600	0,000	18,660	1,680
SM 405	0,125	5,000	2	1	2	1	3,200	0,000	18,980	1,620
SM 406	0,125	6,130	2	1	2	1	5,400	0,000	19,360	1,280
SM 301	0,125	0,500	1	2	1	2	5,000	16,300	18,660	0,770
SM 302	0,125	1,630	1	2	1	2	7,600	0,000	18,840	0,990
SM 303	0,125	2,750	1	2	1	2	6,800	0,000	19,660	0,860
SM 304	0,125	3,880	1	2	1	2	5,400	0,000	19,520	0,850
SM 305	0,125	5,000	1	2	1	2	4,600	0,000	18,420	1,060
SM 306	0,125	6,130	1	2	1	2	7,000	0,000	18,700	1,090
SM 201	0,125	0,500	2	1	1	2	2,600	16,000	18,600	1,310
SM 202	0,125	1,630	2	1	1	2	6,800	0,000	19,540	1,100
SM 203	0,125	2,750	2	1	1	2	7,600	0,000	20,520	1,190
SM 204	0,125	3,880	2	1	1	2	4,600	0,000	19,660	1,450
SM 205	0,125	5,000	2	1	1	2	2,200	0,000	18,840	1,520
SM 206	0,125	6,130	2	1	1	2	4,600	0,000	18,940	1,290
SM 101	0,125	0,500	1	1	1	1	2,000	16,200	19,400	1,460
SM 102	0,125	1,630	1	1	1	1	2,000	0,000	18,300	1,430
SM 103	0,125	2,750	1	1	1	1	3,600	0,000	18,700	1,550
SM 104	0,125	3,880	1	1	1	1	2,800	0,000	18,520	1,470
SM 105	0,125	5,000	1	1	1	1	3,400	0,000	18,920	1,360
SM 106	0,125	6,130	1	1	1	1	6,400	0,000	19,420	1,140